

A NOVEL REGULATOR OF COPPER HOMEOSTASIS, CCIT1, AND
SPL7 CONNECT COPPER HOMEOSTASIS WITH POLLEN FERTILITY, JASMONIC ACID
BIOSYNTHESIS AND CADMIUM RESISTANCE IN *ARABIDOPSIS THALIANA*

A Dissertation

Presented to the Faculty of the Graduate School

of Cornell University

in Partial Fulfillment of the Requirements for the Degree of

Doctor of Philosophy

by

Jiapei Yan

February 2016

© 2016 Jiapei Yan

A NOVEL REGULATOR OF COPPER HOMEOSTASIS, CCIT1, AND
SPL7 CONNECT COPPER HOMEOSTASIS WITH POLLEN FERTILITY, JASMONIC ACID
BIOSYNTHESIS AND CADMIUM RESISTANCE IN *ARABIDOPSIS THALIANA*

Jiapei Yan, Ph.D.

Cornell University 2016

The transition metal copper (Cu) is among the most important mineral nutrients and is essential for plant growth, development and fertility. However, Cu is toxic if it is accumulated in cells in excess. To maintain Cu homeostasis, plants have evolved transcriptional regulation of genes involved in Cu uptake, trafficking, tissue partitioning and reallocation among Cu requiring enzymes. SPL7 has been shown to play a central role in this transcriptional regulatory network and is the only transcription factor with a documented role in Cu homeostasis. We have found recently that a member of the bHLH family of TFs, that we designated CCIT1, is transcriptionally regulated by Cu availability, is essential for Cu acquisition and is required for plant growth under low Cu condition. Previous transcriptome analyses have identified *CCIT1* among the downstream targets of SPL7. However, the *ccit1spl7* double mutant exhibited infertility phenotype due to altered flower morphology, substantially reduced pollen production and viability. These results suggest that CCIT1 does not simply act downstream of SPL7, and this interactive regulatory pathway is rather more complex. Y1H and RNA-seq studies identified components of this pathway and the hierarchy of interactions which provide essential molecular evidences of the connection between Cu homeostasis, jasmonic acid biosynthesis and male fertility. On the other hand, cadmium (Cd) is a non-essential, toxic metal that causes plant growth retardation, disrupts micronutrient homeostasis and interferes with photosynthesis and redox balance. The components of the molecular machinery mediating the crosstalk between Cd and essential elements, however, are unknown. We have found recently that the central regulator of Cu homeostasis, SPL7, is

important for basal Cd tolerance. Here we show that CCIT1 is induced by Cd toxicity. Loss of CCIT1 function results in hypersensitivity to Cd, and compromised Cu accumulation which is essential for basal Cd tolerance. Transcript abundance comparison between wild-type and *ccit1* mutant identified two high-affinity Cu transporters among the targets of CCIT1. Together, the results herein expand the understanding of the interaction between the essential heavy metal Cu and the toxic heavy metal Cd, and might provide novel avenues for biofortification strategies to improve mineral nutrition while avoid toxic metal entry into the food crops.

BIOGRAPHICAL SKETCH

Jiapei Yan earned her Bachelor of Science degree in turfgrass management from Beijing Forestry University and Michigan State University in May 2010, and entered Cornell University that year. She earned her Doctor of Philosophy degree in Crop Science from Cornell University in February 2016. Jiapei was a member of the Department of Crop and Soil Sciences graduate student association, a teaching assistant for several courses, a mentor to undergraduate teaching assistants, and a research mentor to several members of the Vatamaniuk lab.

ACKNOWLEDGMENTS

I would like to thank my family, advisor, labmates and collaborators who helped me to keep my spirits up these past five and half years.

To my family, for support and encouragement when I met difficulties.

To my advisor, Drs. Olena Vatamaniuk, for guidance, encouragement and patience during my Ph.D.

To all of my labmates for sharing suggestions and providing a supportive and friendly environment in the lab. Particularly, thank Hail and Sheena who were the second mentors to me, and Ju-Chen for her contribution to my research project.

To my collaborators, Rong Huang, Arthur Woll and Louisa Smieska who are Cornell CHESS researchers, for working late and being patient on scanning my samples using SXRF technique; Mike Rutzke, Leon Kochian , Shree K. Giri and Eric Craft for ICP-MS analysis; Zhangjun Fei and Chen Jiao for helping with statistical analysis of RNA-seq data.

Lastly, I would like to thank my committee members, Tim Setter and Maria Harrison, for guidance.

TABLE OF CONTENTS

BIOGRAPHICAL SKETCH	iii
ACKNOWLEDGMENTS	iv
LIST OF FIGURES	ix
LIST OF TABLES.....	xi
CHAPTER I: PREFACE	1
1. OVERVIEW OF COPPER HOMEOSTASIS IN PLANTS	2
1.1. Copper uptake and long-distance transport in plants	3
1.2 Intracellular copper trafficking.	8
1.3 The transcriptional regulation of copper homeostasis.	10
1.4 Copper and plant fertility	12
2. OVERVIEW OF CADMIUM AND ITS TOXICITY IN PLANTS	14
2.1 Cadmium uptake and translocation in plants	15
2.2 Cadmium detoxification.....	16
2.3 Crosstalk between Cd and essential metals in the cell.....	18
REFERENCES	21
CHAPTER II: A NOVEL TRANSCRIPTION FACTOR, CCIT1, AND A MEMBER OF THE SPL-FAMILY, SPL7, MEDIATE CROSSTALK BETWEEN COPPER HOMEOSTASIS, POLLEN FERTILITY AND JASMONIC ACID SYNTHESIS IN <i>A. THALIANA</i>	30
ABSTRACT.....	30
1. INTRODUCTION	31
2. METHODS	35
2.1 Plant material	35
2.2 Growth Conditions and Experimental Treatments.....	36
2.3 RNA extraction and cDNA synthesis	38
2.4 Plasmid construction	38
2.5 Subcellular Localization and Fluorescent Microscopy	39
2.6 Quantitative real-time (qRT)-PCR and data analysis.....	39
2.7 Histochemical analysis.....	40
2.8 Analyses of copper concentrations	40
2.9 F3 Scanning X-ray Fluorescence Microscopy	40
2.10 Pollen viability assay	41

2.11 High-Throughput Sequencing of mRNA, Mapping Sequences and Differential Gene Expression Analysis	42
2.12 LC/MS Analysis of Jasmonic Acid.....	43
2.13 Accession Numbers	43
3. RESULTS	44
3.1 Identification and Domain Organization of CCIT1	44
3.2 CCIT1 Localizes to the Nucleus in <i>A. thaliana</i> Protoplasts.....	45
3.3 Expression of <i>CCIT1</i> is regulated by Cu availability.....	46
<i>CCIT1</i> is expressed mainly in roots, leaves and anthers in <i>A. thaliana</i>	47
3.4 Isolation of the <i>ccit1-1</i> and <i>ccit1-2</i> mutant alleles and CCIT1 complemented and overexpressing lines.....	48
3.5 The <i>ccit1</i> knock-out plants are sensitive to low Cu condition	50
3.6 <i>CCIT1</i> is essential for Cu accumulation in roots and shoots of <i>A. thaliana</i>	51
3.7 <i>CCIT1</i> and <i>SPL7</i> act in a parallel interacting pathway regulating Cu homeostasis.....	52
3.8 The <i>ccit1spl7</i> double has nonviable pollen and altered gynoecium morphology	55
3.9 Copper localizes to anthers in flowers and is essential for plant fertility.	57
3.10 Copper deficiency significantly alters transcriptome of <i>A. thaliana</i>	58
3.11 Transcriptional response of <i>CCIT1</i> to Cu limitation in flowers and roots is partially independent of <i>SPL7</i> , novel transcriptional regulator exists to control <i>CCIT1</i> expression.....	60
3.12 RNA-seq identified common and unique downstream targets of <i>SPL7</i> and <i>CCIT1</i> in flowers..	61
3.13 Jasmonic acid biosynthetic pathway is significantly changed in <i>spl7</i> and <i>ccit1</i> mutants	64
3.14 RNA-seq identified common and unique downstream targets of <i>SPL7</i> and <i>CCIT1</i> in roots and shoots.	65
3.15 JA synthesis is impaired in leaves of <i>spl7</i> and <i>ccit1</i> mutants.....	70
4. DISCUSSION	71
4.1 CCIT1 is a novel Cu-responsive transcription factor in <i>A. thaliana</i> that is mainly expressed in roots and flowers and is transcriptionally upregulated during Cu limitation in all tissues.	71
4.2 <i>CCIT1</i> is essential for plant growth and development under low Cu condition	72
4.3 <i>CCIT1</i> is essential for Cu accumulation in roots and shoots	73
4.4 CCIT1- and SPL7-dependent Cu homeostasis is indispensable for plants survival	73
4.5 Simultaneous knock-out of <i>CCIT1</i> and <i>SPL7</i> results in male sterility and seed set failure which can be partially reversed by Cu application	74
4.6 Cu deficiency significantly alters flower transcriptome in <i>A. thaliana</i>	75
4.7 RNA-seq analysis in roots and shoots identified targets of CCIT1 and SPL7 which are involved in Cu homeostasis and plant fertility.....	76
4.8 SPL7 and CCIT1 control jasmonic acid pathway which plays a critical role in male fertility	78

5. SUPPLEMENTAL DATA	81
REFERENCES	100
CHAPTER III: AREB3, ATHB2 AND BZIP53 ARE UPSTREAM REGULATORS OF CCIT1 TRANSCRIPTIONAL RESPONSE TO COPPER DEFICIENCY IN REPRODUCTIVE TISSUES OF <i>A. THALIANA</i>	106
ABSTRACT.....	106
1. INTRODUCTION	107
2. METHODS	109
2.1 Plant materials.....	109
2.2 Growth Conditions and Experimental Treatments.....	109
2.3 Plasmid Construction	110
2.4 Subcellular Localization and Fluorescent Microscopy	110
2.5 RNA extraction and cDNA synthesis	111
2.6 Quantitative real-time (qRT)-PCR and data analysis.....	111
2.7 Yeast-one-hybrid screen	112
2.8 Chromatin Immunoprecipitation.....	112
2.9 Accession Numbers	113
3. RESULTS	113
3.1 Y1H screen of a prey library of <i>Arabidopsis</i> transcription factors identified 14 putative regulators of <i>CCIT1</i>	113
3.2 SPL7 negatively regulates expression of the putative CCIT1 regulators in flowers of <i>A. thaliana</i> under Cu deficiency	116
3.3 Expression of <i>CCIT1</i> in flowers, in part depends on AREB3, ATHB2 and bZIP53	117
3.4 AREB3, ATHB2 and bZIP53 localize to the nucleus in <i>A. thaliana</i> protoplasts.....	118
3.5 AREB3, ATHB2 and bZIP53 directly regulate expression of <i>CCIT1</i>	120
4. DISCUSSION	121
5. SUPPLEMENTAL DATA	124
REFERENCES	127
CHAPTER IV: A MEMBER OF THE BHLH FAMILY OF TRANSCRIPTION FACTORS, CCIT1, CONTRIBUTES TO THE CROSSTALK BETWEEN COPPER HOMEOSTASIS AND BASAL CADMIUM RESISTANCE IN <i>A. THALIANA</i>	130
ABSTRACT.....	130
1. INTRODUCTION	130
2. METHODS	133
2.1 Plant materials.....	133
2.2 Growth Conditions and Experimental Treatments.....	134

2.3 Plasmid construction	134
2.4 RNA extraction and cDNA synthesis	135
2.5 Quantitative real-time (qRT)-PCR and data analysis.....	135
2.6 Histochemical analysis.....	136
2.7 Fluorescent microscopy	136
2.8 Analyses of cadmium and copper concentrations.....	136
2.9 Yeast-one-hybrid assay	136
2.10 Accession numbers for genes used in this study	137
3. RESULTS	137
3.1 Cadmium increases the transcript abundance of <i>CCIT1</i> in roots of <i>A. thaliana</i> in a partial SPL7-dependent manner	137
3.2 <i>ccit1</i> knock-out alleles are sensitive to cadmium toxicity.....	139
3.3 The genomic fragment of <i>CCIT1</i> partially complements the hypersensitivity of the <i>ccit1-1</i> mutant to Cd.....	140
3.4 <i>ccit1</i> mutant accumulates high Cd in shoots and has defect in Cu accumulation	142
3.5 Cadmium toxicity affects the expression pattern of <i>CCIT1</i> in <i>A. thaliana</i>	144
3.6 The effect of cadmium on the expression of <i>COPT2</i> depends, in part, on CCIT1	145
4. DISCUSSION	146
5. SUPPLEMENTAL DATA	150
CONCLUSIONS.....	156

LIST OF FIGURES

Figure 1.1 Overview of cellular Cu homeostasis in <i>A. thaliana</i>	9
Figure 1.2 Overview of SPL7-dependent transcriptional regulation in response to Cu deficiency in <i>A. thaliana</i>	10
Figure 1.3 Cu deficiency leads to infertility in <i>A. thaliana</i> and wheat.....	12
Figure 1.4 Overview of Cd transport in plants.....	17
Figure 2.1 Protein motif prediction of the putative <i>A. thaliana</i> bHLH transcription factor, CCIT1.....	45
Figure 2.2 Subcellular localization of CCIT1 in <i>A. thaliana</i> protoplasts.....	46
Figure 2.3 Expression of <i>CCIT1</i> is differentially regulated in response to Cu availability.....	47
Figure 2.4 Histochemical analysis of the expression pattern of <i>CCIT1</i> in <i>A. thaliana</i> transformed with the <i>CCIT1pro-GUS</i> construct.....	48
Figure 2.5 The <i>ccit1</i> mutant is hypersensitive to Cu deficiency.....	49
Figure 2.6 Cu concentration in roots and rosette leaves of 5-week-old wild-type, <i>ccit1-1</i> and <i>CCIT1-1</i> grown hydroponically.....	52
Figure 2.7 <i>CCIT1</i> and <i>SPL7</i> act in a parallel interacting pathways regulating Cu homeostasis.....	53
Figure 2.8 The altered morphology of the <i>ccit1spl7</i> double mutant.....	56
Figure 2.9 Pollen viability assay of wild-type, <i>spl7-1</i> , <i>ccit1-1</i> and <i>ccit1spl7</i> double mutant.....	57
Figure 2.10 Cu deficiency significantly affects the seed setting and pollen viability.....	58
Figure 2.11 Cu deficiency significantly affects the transcriptome profile in flowers.....	59
Figure 2.12 The transcriptional response of <i>CCIT1</i> to Cu limitation depends, in part, on <i>SPL7</i>	61
Figure 2.13 Comparison of the transcriptome profile in flowers from <i>ccit1</i> and <i>spl7</i>	62
Figure 2.14 SPL7 and CCIT1 dependent genes that are involved in the JA biosynthetic pathway.....	65
Figure 2.15 The CCIT1-dependent transcriptional profile and its comparison to wild-type and SPL7 according to RNA-seq data.....	66
Figure 2.16 qRT-PCR-based validation of RNA-seq results.....	68
Figure 2.17 JA concentration in rosette leaves of 5-week-old wild-type (Wt), <i>ccit1-1</i> (<i>ccit1</i>), <i>spl7-1</i> (<i>spl7</i>) and <i>ccit1 spl7</i> grown hydroponically.....	71
Figure 2.18 Model of the CCIT1- and SPL7-dependent pathway in response to Cu availability and their function in Cu homeostasis, JA signaling and plant fertility.....	79
Supplemental Figure 2.1 CCIT1 transcript abundance of the second <i>ccit1</i> mutant allele (<i>ccit1-2</i>), 2 additional independent complemented and overexpressing lines and their phenotypes in response to Cu status.....	81

Supplemental Figure 2.2 The phenotype of full set of rosette leaves from wild-type, <i>ccit1-1</i> , <i>CCIT1-1</i> and <i>35S-CCIT1-1</i>	83
Supplemental figure 2.3 Using pollens from wild-type or floral dipping with Cu solution to rescue the infertility of the <i>ccit1 spl7</i> double mutant.....	84
Supplemental figure 2.4 Validation by quantitative RT-PCR showing between-experiment reproducibility.....	84
Supplemental figure 2.5 Cu concentration in flowers of 8-week-old wild-type grown hydroponically....	85
Supplemental figure 2.6 Number of genes that were changed in response to Cu deficiency.....	85
Figure 3.1 Putative regulators of <i>CCIT1</i> that were identified in Y1H screens.....	115
Figure 3.2 Transcript abundance of genes identified in Y1H is induced by Cu deficiency in flowers of the <i>spl7</i> mutant.....	116
Figure 3.3 The transcriptional level of <i>CCIT1</i> to Cu deficiency depends, in part, on AREB3, ATHB2 and bZIP53.....	118
Figure 3.4 Subcellular localization of AREB3, ATHB2 and bZIP53 in <i>A. thaliana</i> protoplasts.....	119
Figure 3.5 AREB3, ATHB2 and bZIP53 bind to regulatory regions of <i>CCIT1</i> chromatin <i>in vivo</i>	120
Figure 3.6 The model of the upstream transcriptional regulatory pathway of <i>CCIT1</i>	123
Supplemental figure 3.1 Histochemical analysis of Cu-deficiency induced <i>CCIT1</i> expression using 1.5 kb full length (<i>CCIT1pro full</i>) and 0.7 kb promoter region (<i>CCIT1pro</i>).....	124
Supplemental figure 3.2 The phenotype of <i>areb3</i> , <i>athb2</i> and <i>bzip53</i> mutants under Cu deficient conditions	125
Figure 4.1 Expression of <i>CCIT1</i> is regulated by cadmium (Cd) in the SPL7-dependent manner.....	138
Figure 4.2 <i>ccit1</i> mutant is hypersensitive to Cd toxicity.....	140
Figure 4.3 Genomic <i>CCIT1</i> fragment partially complement the hypersensitivity of the <i>ccit1-1</i> mutant to Cd.....	142
Figure 4.4 <i>ccit1-1</i> contains higher Cd in shoots and lower Cu in roots compared to wild-type.....	143
Figure 4.5 The expression pattern of <i>CCIT1</i> in <i>A. thaliana</i>	145
Figure 4.6 The transcriptional response of <i>COPT1</i> and <i>COPT2</i> to Cd toxicity depends, in part, on <i>CCIT1</i>	146
Figure 4.7 The model depicting the role of <i>CCIT1</i> in Cd induced transcriptional regulation.....	149
Supplemental Figure 4.1 The phenotype of wild-type plants after Cd treatment.....	150
Supplemental Figure 4.2 Ectopic expression of <i>CCIT1</i> does not improve Cd tolerance of wild-type <i>A. thaliana</i>	151

LIST OF TABLES

Table 2.1 Transcripts that are involved in Cu deficiency response are also induced in <i>ccit1</i> mutant under Cu sufficient condition.....	63
Table 2.2 Transcripts are highly responsive to Cu deficiency in an CCIT1-dependent fashion.....	69
Table 2.3 Transcripts related to nitrate uptake specifically depend on CCIT1.....	70
Table 2.4 Transcripts related to jasmonic acid biosynthesis in a CCIT1- or SPL7-dependent fashion....	70
Supplemental table 2.1 Primers used for genotyping.....	86
Supplemental table 2.2 Primers used for cloning.....	86
Supplemental table 2.3 Primers used in qRT-PCR.....	86
Supplemental table 2.4 The sample summary of RNA-seq analysis in roots and shoots.....	87
Supplemental table 2.5 The sample summary of RNA-seq analysis in floral buds and mature flowers...88	88
Supplemental table 2.6 GO term enrichment analysis of the Cu deficiency upregulated genes in floral buds.....	89
Supplemental table 2.7 GO term enrichment analysis of the Cu deficiency downregulated genes in floral buds.....	91
Supplemental table 2.8 GO term enrichment analysis of the Cu deficiency upregulated genes in mature flowers.....	91
Supplemental table 2.9 GO term enrichment analysis of the Cu deficiency downregulated genes in mature flowers.....	94
Supplemental table 2.10 GO term enrichment analysis of the downregulated genes in mature flowers of <i>ccit1-1</i> mutant compared to wild-type under Cu replete condition.....	95
Supplemental table 2.11 GO term enrichment analysis of the downregulated genes in mature flowers of <i>ccit1-1</i> mutant compared to wild-type under Cu deficient conditions.....	98
Supplemental table 3.1 Primers used for genotyping.....	125
Supplemental table 3.2 Primers used for cloning.....	125
Supplemental table 3.3 Primers used in qRT-PCR.....	126
Supplemental table 4.1 Primers used in this study.....	152

CHAPTER I

Preface

ABSTRACT

Copper (Cu) is an essential micronutrient that is required for the growth, development and reproduction of all organisms including plants. Cu, however, can be toxic when it accumulates in cells in excess. The bioavailability of Cu in agricultural soils largely depends on the soil type and agricultural practices. For example, Cu deficiency develops in alkaline soils due to the low solubility of Cu at high pH, and in organic soils due to Cu binding to organic matter. While Cu deficiency can be remedied by the application of Cu-based fertilizers, this strategy is not environmentally friendly, and the repeated use of fertilizers, as well as Cu-containing pesticides, has led to the build-up of toxic levels of Cu in soils. To prevent Cu deficiency while avoiding toxicity, plants have evolved sophisticated regulatory mechanisms, including transcriptional regulation of genes involved in Cu uptake, trafficking, tissue partitioning and reallocation among Cu requiring enzymes. The relationship between these processes and plant fertility, however, is not well understood. For example, it has been recognized for decades that Cu deficiency in agricultural soils is associated with compromised fertility, low seed/grain set and, in acute cases, a crop failure. Nevertheless, the molecular components underlying the crosstalk between Cu homeostasis and plant fertility have not been fully identified. In contrast to Cu, cadmium (Cd) is a non-essential and highly toxic metal that is increasingly emitted into the environment from various agricultural, mining and industrial activities, and the exhaust gas of automobiles. Cd causes organ dysfunction in humans, growth retardation in plants by interfering with essential biochemical processes of living cells. It is also recognized that among the cellular mechanisms of Cd toxicity is the disruption of the homeostasis of micronutrients. The components of the molecular machinery mediating the crosstalk between Cd and essential elements are not well known as well. This dissertation discusses the identification and characterization of a novel transcription regulator of Cu homeostasis in *A. thaliana*, CCIT1, its interaction with the master regulator of Cu homeostasis, SPL7, and

the crosstalk of SPL7- CCIT1-dependent pathways with plant fertility, synthesis of the plant hormone jasmonic acid and basal Cd resistance in *A. thaliana*.

1. OVERVIEW OF COPPER HOMEOSTASIS IN PLANTS

Copper (Cu) is an essential micronutrient for all organisms including plants because it acts as a cofactor for enzymes participating in important biological processes such as respiration, photosynthesis, and oxidative stress scavenging (Burkhead et al., 2009b; Merchant, 2010; Ravet and Pilon, 2013). In plants, Cu is also important for the perception of ethylene, salicylic acid, nitrogen metabolism, molybdenum cofactor biosynthesis, pathogen response, lignin synthesis and reproduction (Marschner, 1995b, a; Kuper et al., 2004; Pilon et al., 2006; Burkhead et al., 2009b; Wu et al., 2014). This remarkable array of physiological functions of Cu is attributed to its ability to change the oxidation state ($\text{Cu}^{2+} \leftrightarrow \text{Cu}^+$) (Marschner, 1995a). The same property imposes toxicity when free Cu ions accumulate in cells in excess due to the ability of Cu to cause oxidative stress (Halliwell and Gutteridge, 1984; Burkhead et al., 2009b). Therefore, Cu concentration within the cell must be tightly regulated to prevent deficiency while at the same time avoiding toxicity. The most abundant Cu-binding protein in higher plants is plastocyanin (PC), which uses oxidation-reduction reactions of Cu to shuffle electrons during photosynthesis (Gross, 1993). Another two major Cu proteins are cytosolic and chloroplast-localized Cu/zinc (Zn) superoxide dismutases (CSDs), designated as CSD1 and CSD2 respectively. These enzymes scavenge reactive oxygen species (ROS) (Bowler et al., 1994; Kliebenstein et al., 1998). The reallocation of Cu between PC and CSDs, the so-called “Cu-economy model”, is among the strategies used by plants to regulate Cu homeostasis, and this process is transcriptionally regulated by a transcription factor (TF) SPL7. Another mechanism includes the SPL7-mediated transcriptional control of genes involved in Cu uptake and redistribution between tissues (Burkhead et al., 2009b). A concerted action of SPL7 downstream targets is responsible for adequate Cu uptake and tissue partitioning to support growth and reproduction of plants. Thus far, SPL7 is the only TF identified in vascular plants with the role in Cu homeostasis. During my Ph.D. work, I discovered that previously uncharacterized member of the basic helix-loop-helix (bHLH) family of TFs, CCIT1, is essential

for Cu homeostasis in *A. thaliana* as well. This section discusses current knowledge of major mechanisms that regulate Cu homeostasis in vascular plants.

1.1. Copper uptake and long-distance transport in plants

Copper (II) is a dominant form of Cu in soils where it exists in a complex with the organic matter, iron (Fe) and aluminum (Al) oxides, and thus, Cu must be mobilized prior uptake into plant roots (Flemming and Trevors, 1989). Cu mobilization strategies are largely unknown but based on studies in *A. thaliana*, it has been proposed that dicots and non-grass monocots reduce Cu(II) to Cu(I), and so Cu(I) is the main form of Cu absorbed by plant roots (Burkhead et al., 2009a). Further, it has been proposed that membrane-bound ferric chelate reductases from the *FRO* family in *A. thaliana* reduce Cu(II) to Cu(I) upon Cu deficiency (Bernal et al., 2012b; Jain et al., 2014). There are eight members in the *FRO* family in *A. thaliana* (Jeong and Connolly, 2009). *FRO2* localizes at the plasma membrane, serves as the primary ferric reductase for root Fe uptake. The loss of *FRO2* function abolishes Fe-inducible Cu-chelate reductase activity, suggesting that *FRO2* could also reduce Cu(II) to Cu(I) to facilitate Cu(I) uptake (Robinson et al., 1999). However, Cu concentrations are not reduced in the *frd1* mutant that is allelic to *FRO2*, suggesting the possibility that other FROs function to reduce Cu at the root surface (Robinson et al., 1999; Jain et al., 2014). *FRO3*, is expressed primarily in the vasculature in roots, is induced by Cu limitation in both roots and shoots, but due to localization to the mitochondria, it is unlikely that *FRO3* contributes to Cu(I) uptake (Mukherjee et al., 2006). *FRO4* and *FRO5* are strongly upregulated by Cu limitation and their function is essential for high-affinity Cu uptake suggesting that these proteins are the primary Cu reductases that function in Cu uptake (Figure 1; Bernal et al., 2012a), *FRO6* is highly expressed in leaves and is involved in light response (Feng et al., 2006). It is downregulated by Cu deficiency in shoots (Mukherjee et al., 2006), which indicates that *FRO6* may function in Cu redistribution in photosynthetic tissues.

After Cu(II) reduction at the root surface, Cu (I) enters the cytosol of root epidermal cells *via* plasma membrane localized transporters of the CTR/COPT family, which is represented by 6 members in *Arabidopsis thaliana*, 7 members in *Oryza sativa* and 5 members in *Brachypodium distachyon* (Sancenon

et al., 2003; Yuan et al., 2011; Jung et al., 2012; Jung et al., 2014). Studies in *A. thaliana* determined that genes encoding COPT1, COPT2, and COPT6 are transcriptionally regulated by Cu deficiency, the encoded proteins localize to the plasma membrane, mediate Cu uptake, and complement the growth defect of the *S. cerevisiae* Cu uptake mutant lacking functional Cu transporters, Ctr1p, Ctr2p, and Ctr3p (Figure 1 and (Kampfenkel et al., 1995; Sancenon et al., 2004; Jung et al., 2012; Perea-Garcia et al., 2013)). AtCOPT1 and AtCOPT2 function primarily in Cu uptake into the root, while AtCOPT6 also contributes to Cu partitioning in photosynthetic tissue (Sancenon et al., 2004; Gayomba et al., 2013). *AtCOPT1* is highly expressed in root tips, embryos, trichomes, stomata and pollen grain and is transcriptionally upregulated by Cu deficiency in shoots (Yamasaki et al., 2009a). In contrast to *AtCOPT1*, *AtCOPT2* is not expressed in the root tip but is strongly expressed in the main root, vasculature of leaves, stigma of siliques and pollen grains (Gayomba et al., 2013). The transcript abundance of *AtCOPT5* is not altered by Cu availability, however, the *copt5* mutant allele exhibits chlorosis, has impaired photosynthetic electron transfer, root elongation defects and compromised vegetative growth under severe Cu limitation. COPT5 localizes to the tonoplast and the pre-vacuolar compartment and functions in remobilizing Cu from these organelles during Cu deficiency (Figure 1; Garcia-Molina et al., 2011b; Klaumann et al., 2011a). *AtCOPT5* is mostly expressed in the root vasculature and siliques and is suggested to facilitate Cu remobilization from roots to reproductive tissues. This suggestion is based on finding that the *copt5* mutant accumulates Cu in roots and has decreased Cu concentration in siliques and seeds (Garcia-Molina et al., 2011a; Klaumann et al., 2011b). COPT6 resides at the plasma membrane, is expressed mainly in the vasculature and reproduction organs, and is up-regulated by Cu deficiency. The reduced Cu concentration in leaves and seeds of the *copt6* mutant under Cu deficiency highlights the contribution of COPT6 to Cu distribution in photosynthetic and reproductive tissues during Cu limited conditions (Jung et al., 2012; Garcia-Molina et al., 2013).

COPT family members in rice also mediate Cu transport but manifest slightly distinct properties than *A. thaliana* COPTs. For example, OsCOPT2, 3, 4 and 6 have to heteromerize to mediate high-affinity Cu uptake in the Cu-uptake deficient *ctr1Δctr2Δctr3Δ* mutant of *Saccharomyces cerevisiae*. OsCOPT7 itself is sufficient to rescue Cu uptake of the yeast mutant (Yuan et al., 2011). In contrast, *A. thaliana*

COPTs can function as homooligomers (Jung et al., 2012). Further, studies of OsCOPT1 and OsCOPT5 discovered the role of Cu in pathogen resistance (Yuan et al., 2010). OsCOPT2, 3 and 4 physically interact with OsCOPT6 and mediate high-affinity uptake in *ctr1Δctr3Δ*. OsCOPT7 itself is sufficient to mediate high-affinity uptake in *ctr1Δctr3Δ* (Yuan et al., 2011). Of five COPT proteins in *Brachypodium*, BdCOPT3, and BdCOPT4 localize to the plasma membrane and are transcriptionally upregulated in roots and leaves by Cu deficiency. Further, BdCOPT3, BdCOPT4, and BdCOPT5 confer low-affinity Cu transport, in contrast to their counterparts in *A. thaliana* that confer high-affinity Cu transport (Jung et al., 2014).

Genes encoding ZIP2 and ZIP4 (ZRT-IRT-like Proteins (ZIP) family of metal transporters) are also regulated by Cu availability: they are induced by Cu deficiency and are repressed by Cu access in roots of *A. thaliana* (Wintz et al., 2003; Bernal et al., 2012b). Based on studies of Wintz et al (2003) it has been suggested that ZIP2 and ZIP4 are low affinity Cu(II) transporters (Figure 1). However, Milner et al (2013) have shown that ZIP2 is involved in the transport of Zn and Mn but not Cu.

Members of the Heavy Metal P-type ATPases (HMAs) have been reported to play important role in Cu transport in various plant species. The *Arabidopsis* genome encodes 8 HMA members, denoted HMA1 to HMA8, which are clustered into 2 subgroups according to their metal specificity (Baxter et al., 2003; Mills et al., 2003; Hussain et al., 2004; Mills et al., 2005; Williams and Mills, 2005; Mills et al., 2012). HMA1 to HMA4 were suggested to play a role in Zn, Cd, Co and Pb transport, whereas HMA5 to HMA8 were predicted to transport Cu and Ag (Baxter et al., 2003; Mills et al., 2003; Hussain et al., 2004; Mills et al., 2005; Williams and Mills, 2005; Mills et al., 2012). AtHMA1 localizes at the chloroplast envelope and has a broad substrate specificity. It is implicated in Zn²⁺ export from chloroplast, functions as a Ca²⁺/heavy metal pump (Moreno et al., 2008; Kim et al., 2009), and Cu delivery to the stroma (Seigneurin-Berny et al., 2006). AtHMA5 is mainly expressed in roots and flowers and exhibits a dose-independent induction by Cu (Andres-Colas et al., 2006; Kobayashi et al., 2008). The T-DNA insertion alleles of *HMA5* are hypersensitive to Cu toxicity and accumulated Cu in their roots where *HMA5* is mostly expressed (Andres-Colas et al., 2006; Kobayashi et al., 2008). These findings suggested that HMA5 functions in Cu efflux from root symplasm into the xylem and plays a role in Cu partition and detoxification (Figure 1 and

(Andres-Colas et al., 2006; Kobayashi et al., 2008)). In addition, HMA5 interacts with ATX1-like Cu chaperones, ATX1 and CCH (Andres-Colas et al., 2006; Puig et al., 2007b). AtHMA6 (PAA1, P-type ATPase of *Arabidopsis* 1) localizes at the chloroplast inner envelope and delivers Cu to chloroplast-localized Cu/Zn SOD, whereas AtHMA8 (PAA2) localizes at the thylakoid and has been suggested to transport Cu into thylakoid lumen for supplying Cu to plastocyanin (Figure 1 and (Shikanai et al., 2003; Abdel-Ghany et al., 2005)). AtHMA7 (RAN1, Responsive-to-antagonist 1) functions in Cu delivery to ethylene receptor (Figure 1 and (Hirayama et al., 1999; Woeste and Kieber, 2000)). Seedlings carrying weak alleles of *ran1* had normal ethylene-binding activity but were hypersensitive to copper-chelating agents, suggesting a role of RAN1 (HMA7) in Cu homeostasis in seedlings (Binder et al., 2010). In contrast to *Arabidopsis*, rice HMAs family contains 9 members (Baxter et al., 2003). Among these members, OsHMA5 and OsHMA9 have been implicated in Cu transport. OsHMA5 localizes to the root pericycle cells and xylem region. Knock-out of *OsHMA5* function leads to the decrease of Cu concentration in shoots and an increase in roots, suggesting that OsHMA5 is involved in xylem loading of Cu (Deng et al., 2013). On the other hand, OsHMA9, localizes in plasma membrane, is mainly expressed in vascular tissues and anthers, the knockout lines accumulate more Zn, Cu and Cd in shoots but not in roots, suggesting its role in the efflux of these metals in the shoots (Lee et al., 2007).

Given the toxicity of Cu in ionic form, it must associate with a variety of cellular ligands. For example, a non-proteinogenic amino acid, nicotianamine (NA) has been identified as a Cu chelator in the xylem loading in tomato (Pich, 1994, 1996). The tomato *chloronerva* (*chl*) mutant, which bears a single base change in the NA synthase (*NAS*) gene, accumulates Cu in the root and has lower Cu concentration in leaves (Pich, 1994, 1996). Further, xylem exudates from the *chl* mutant have low Cu compared to wild-type. The NA-Cu complex has high stability constant, indicating that NA is the Cu chelator in xylem (Pich, 1994, 1996). Additionally, the inefficiency of Cu transport from roots to shoots in the *chl* mutant can be reversed by NA foliar application thereby further supported a role of NA in Cu translocation (Pich, 1996). The Yellow Stripe-Like (YSL) family of proteins in non-grass species, which are identified based on sequence similarity to maize Yellow Stripe1, have been suggested to transport metals complexed with NA

(Curie et al., 2001). The *Arabidopsis* YSL family has 8 members, AtYSL1, YSL2 and YSL3 are located in the plasma membrane and expressed in the vascular bundle parenchyma. The double mutant of *YSL1* and *YSL3* exhibited elevated Cu concentration in leaves and reduced Cu concentration in seeds, indicating the role of YSL1 and 3 in Cu delivery from senescing leaves to sinks (Waters et al., 2006). YSL2 can also transport Cu-NA, and its expression in *A. thaliana* is regulated by Cu availability in the growth media. Based on the fact that YSL2 localizes at the plasma membrane and is associated with vascular parenchyma cells, it was proposed that YSL2 mediates lateral movement of metals within the vasculature (DiDonato et al., 2004). Recently, in *Oryza sativa*, *OsYSL16* was found to be expressed at the phloem of nodes and vascular tissues of leaves and to transport Cu-NA (Zheng et al., 2012). Knock-out of this gene results in increased Cu concentration in old leaves and husks, but decreased Cu concentration in young leaves and panicles, and significantly reduced fertility (Zheng et al., 2012). These results suggest that OsYSL16 is required for transporting Cu-NA from source to sink *via* the phloem, and this OsYSL16-mediated Cu transport to grain is important for fertility.

Other putative Cu ligands contributing to the long distance transport of Cu include a **Cu chaperone**, CCH, and members of the small cysteine-rich proteins, metallothioneins (MTs). CCH in addition to its role in intracellular Cu trafficking to the secretory pathway (Lin et al., 1997) is proposed to be involved in the long distance transport of Cu. It has a unique C-terminal extension which is proposed to be involved in the translocation of proteins through the plasmodesmata to sieve elements for Cu redistribution (Mira et al., 2001b). CCH has been found mainly in the vasculature of senescing leaves and petioles, and CCH protein can be collected in the phloem exudates, suggesting a role in Cu mobilization from senescing tissues to reproductive structures (Mira et al., 2001a). Metallothionein 1a (MT1a), is expressed in the phloem (Guo et al., 2008). Lack of MT1a in *Arabidopsis* results in 30 % Cu reduction in roots under high Cu condition, suggesting that it functions as a Cu ligand in the phloem for Cu detoxification (Guo et al., 2008). Further, the role of MTs in source to sink partitioning of Cu was reported by finding that the quadruple-MT mutant (*mt1a/mt2a/mt2b/mt3*) has a lower concentration of Cu in seeds but higher concentration in old leaves when compared to wild-type plants (Benatti et al., 2014).

1.2 Intracellular copper trafficking

The intracellular Cu trafficking is achieved by Cu chaperones, which are small, soluble proteins that bind Cu with high affinity and deliver it *via* protein-protein interaction to Cu requiring enzymes in the cytosol and intracellular organelles, including chloroplast and mitochondria (Arguello et al., 2007; Gonzalez-Guerrero and Arguello, 2008). *A. thaliana* has at least three types of Cu chaperones, including Cu chaperone for SOD (CCS), Antioxidant protein 1 (ATX1) and CCH (Figure 1 and (Casareno et al., 1998; Himelblau et al., 1998; Chu et al., 2005; Puig et al., 2007b)). CCS so far is the only Cu chaperone that has been identified for delivering Cu to Cu/ZnSOD. The *ccs* mutant of *A. thaliana* loses the activity of all three isoforms of Cu/ZnSOD. This defect is rescued by introducing the *CCS* gene into the *ccs* mutant (Chu et al., 2005). CCS is also implicated in Cu delivery to PAA2 (HMA8) for subsequent PAA2-mediated Cu translocation into thylakoid lumen (Blaby-Haas et al., 2014)

CCH and ATX1 of *A. thaliana* are orthologues of the yeast antioxidant protein 1 (ATX1) (Himelblau et al., 1998; Puig et al., 2007b). Both CCH and ATX1 have the conserved Cu-binding motif and can complement the yeast *atx1* mutant (Puig et al., 2007b). The transcript level of *CCH* is upregulated by limited Cu and downregulated by excess Cu, whereas *ATX1* expression is induced by excess Cu, indicating that they may have divergent functions in regulating Cu delivery (Puig et al., 2007a). Yeast-two-hybrid experiments showed that ATX1 and CCH without its C-terminal extension interacts with RAN1 (HMA7) and HMA5 (Andres-Colas et al., 2006; Puig et al., 2007b). The *atx1* single mutant and the *cch atx1* double mutant are hypersensitive to Cu excess, whereas the *cch* mutant responds to high Cu similarly to the wild-type. Ectopic overexpression of ATX1 in *Arabidopsis* confers higher tolerance to Cu excess (Shin et al., 2012). These results suggest that in addition to intracellular Cu trafficking, ATX1 and CCH contribute to Cu sequestration and detoxification. Recently, a novel Cu chaperone has been identified in *A. thaliana* and has been designated as Plastid Chaperone 1 (PCH1) (Figure 1 and (Blaby-Haas et al., 2014)). PCH1 is a product of alternatively-spliced *Arabidopsis* PAA1 (HMA6) and is suggested to act as a Cu(I) chaperone to PAA1 (Blaby-Haas et al., 2014). This suggestion is supported by results of biochemical

experiments showing that PCH1 interacts with PAA1 *in vitro* and activates the ATPase activity of PAA1 (Blaby-Haas et al., 2014).

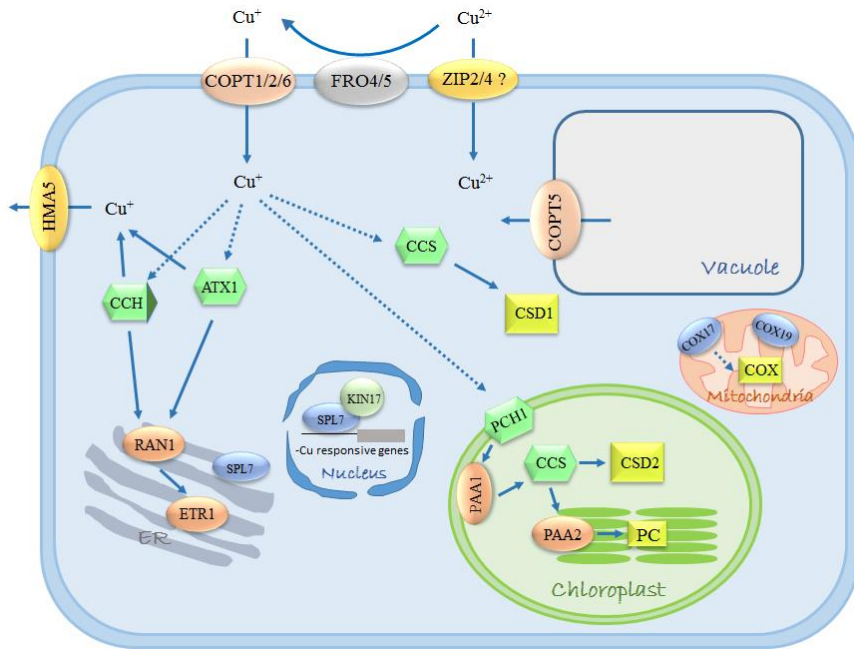


Figure 1. Overview of cellular Cu homeostasis in *A. thaliana*. Cu (II) in soil is reduced to Cu (I) by ferric reductase (FROs) and is transported into the cell primarily by high-affinity copper transporters of the COPT family. ZIP2 and ZIP4 may serve as low-affinity Cu transporter and transport Cu (II) into the cell. Once inside the cell, Cu chaperones mediate intracellular Cu delivery to specific apoproteins. For example, the cytosolic form of CCS provides Cu to cytosolic superoxide dismutase CSD1, whereas the CCS localized in chloroplast stroma transfers Cu to chloroplastic superoxide dismutase CSD2 and PAA2 for Cu delivery to plastocyanin. ATX1, and also CCH, provide Cu to P-type ATPase RAN1 that is located at the ER where Cu is acquired by the ethylene receptor (ETR1). Cu is sequestered into the vacuole by yet unidentified transporter, and effluxed via COPT5. The direction of Cu⁺ traffic is indicated by arrows. SPL7-, KIN17- dependence of Cu-responsive genes is also known, but is discussed in more details in section 1.3. AtYSL1, YSL2 and YSL3 that are located in the plasma membrane and transport Cu-NA via vasculature, are not shown in this figure.

Concerning chaperones for Cu delivery to the mitochondrial Cu-requiring proteins, the metallochaperone Cox17p has been found to be involved in the delivery of Cu for cytochrome c oxidase (COX) assembly in *Saccharomyces cerevisiae* (Glerum et al., 1996). *Arabidopsis* has two genes encoding ScCOX17 homologs, and both can rescue the yeast *cox17* null mutant (Attallah et al., 2007a). Another Cu chaperone in yeast, COX19p, is a soluble protein that is present in both cytoplasm and mitochondrial intermembrane space (Nobrega et al., 2002). The *Arabidopsis* genome also contains 2 yeast COX19 homologs, located to the inner mitochondrial membrane facing the intermembrane space. The short form of *AtCOX19-1* can complement the yeast *cox19* null mutant (Attallah et al., 2007b).

1.3 The transcriptional regulation of copper homeostasis

The transcriptional regulation of Cu homeostasis in plants has been thoroughly investigated in the *Chlamydomonas* model (Hill and Merchant, 1995; Quinn and Merchant, 1995). CRR1 (Cu responsive regulator 1), the Cu-sensing transcription factor containing the Squamosa promoter binding protein (SBP) domain (Kropat et al., 2005a; Sommer et al., 2010b), acts as the key regulator in activating the Cu assimilatory mechanisms under Cu deficiency. CRR1 binds to GTAC motifs (copper-response elements [(CuREs)]) in promoters of its targets (Quinn et al., 2000; Eriksson et al., 2004). CRR1 homolog in *A. thaliana*, SPL7 belongs to the *SQUAMOSA* promoter binding protein like (SPL) family of TFs (Kropat et al., 2005b). SPL7 has been found to play a central role in regulating Cu homeostasis under Cu limited condition (Yamasaki et al., 2009a) (Summarized in Figure 2). During Cu deficiency, SPL7 activates the transcription of its targets *via* CuRE in promoter regions of copper-responsive genes (Kropat et al., 2005b). There are at least two tiers of the SPL7-dependant regulation of the transcriptional response to limited Cu. One tier involves the regulation of Cu uptake and tissue partitioning.

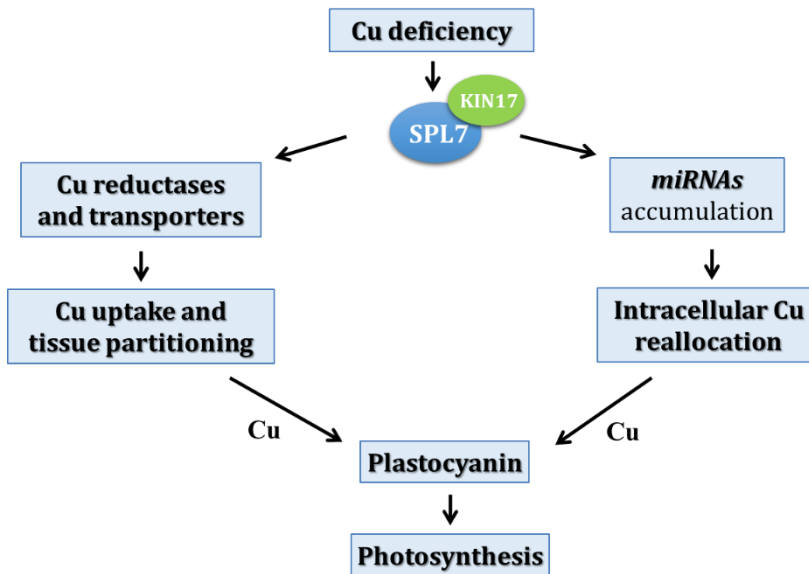


Figure 2. Overview of SPL7-dependent transcriptional regulation in response to Cu deficiency in *A. thaliana*. Under Cu limited condition, SPL7 induces the expression of Cu reductases, such as *FRO3*, *FRO4* and *FRO5*, and also Cu transporters, such as *COPT1*, *COPT2* and *COPT6* to increase Cu acquisition. SPL7 also triggers the accumulation of miRNAs that target the transcripts of abundant Cu binding proteins, such as *CSD1*, *CSD2* and *LACCASES*, to release Cu for plastocyanin, which serves as an essential electron carrier during photosynthesis. The function of

CSD1/2 is replaced by FSD1, which is also transcriptionally upregulated by SPL7 under Cu-deficient condition. KIN17 physically interacts with SPL7, and may be also involved in this transcriptional regulation pathway in response to Cu starvation.

For example, under Cu deficiency, SPL7 induces Cu reductases, such as *FRO3*, *4* and *5*, high-affinity Cu transporters, such as *COPT1*, *COPT2* and *COPT6*, and low-affinity Cu transporters, such as *ZIP2* and *ZIP4*, to increase the Cu acquisition. It is noteworthy that *COPT1* expression is induced by high Cu in the media in the *spl7* knock-out mutant, suggesting that SPL7 may also act as a repressor of Cu uptake under high Cu conditions (Yamasaki et al., 2009a). The second tier involves Cu reallocation among Cu-requiring functions. In this mechanism, SPL7 upregulates several miRNAs, which target the transcripts of abundant Cu-binding proteins to release Cu for plastocyanin to maintain its function in photosynthesis (Yamasaki et al., 2007; Abdel-Ghany and Pilon, 2008; Yamasaki et al., 2009a; Bernal et al., 2012a). For example, it has been determined that SPL7 induces the expression of *miRNA398* via direct binding to CuRE elements in the *miR398* promoter (Sunkar et al., 2006; Yamasaki et al., 2007; Yamasaki et al., 2009a). *miRNA398* then facilitates the degradation of the transcripts of less essential Cu-proteins, *CSD1*, *CSD2*, *CCS*, and the gene encoding *cytochrome c oxidase (COX-5b)*, to release Cu to plastocyanin for maintaining its function in photosynthesis. Meanwhile the expression of a gene encoding Fe-superoxide dismutase, *FSD1* is induced by SPL7 to replace the functions of *CSD1* and *CSD2* (Bowler et al., 1994; Kliebenstein et al., 1998; Cohu et al., 2009). *MiR408*, which is also upregulated by SPL7 under Cu deficiency, was shown to target plantacyanin (*ARPN*) and laccases, such as *LAC3*, *LAC12*, *LAC13* (Abdel-Ghany and Pilon, 2008). Additionally, a Cu chaperone, CCH, is also up-regulated under Cu starvation via SPL7 (Mira et al., 2002; Yamasaki et al., 2009b). Recently, a nuclear protein, KIN17 was found to physically interact with SPL7 and regulate the gene expression, such as *COPT2*, *COPT6*, *CCH* and *FSD1*, in response to Cu deficiency in *Arabidopsis* (Garcia-Molina et al., 2014). The double *spl7-2 kin17-1* mutant is more sensitive to Cu deficiency than *spl7-2* single mutant, providing evidence for KIN17's role during Cu deficiency (Garcia-Molina et al., 2014).

I note that SPL7 is the only TF with the characterized function in Cu homeostasis. My dissertation discusses the identification and characterization of a novel regulator of Cu homeostasis, CCIT1 and its relationship to the SPL7-dependant regulatory pathway.

1.4 Copper and plant fertility

It has been known for decades that Cu deficiency causes plant abortion and reduced grain set (Figure 3; Shorrocks and Alloway, 1988; Marschner, 1995a; Solberg et al., 1999). However, our knowledge of the underlying molecular determinants that link Cu with plant reproduction, is surprisingly limited. From what is known, COPT1, COPT2 and COPT6 are highly expressed in pollen grains and COPT1 was noted to have a role in pollen development (Sancenon et al., 2004; Jung et al., 2012; Gayomba et al., 2013). *COPT1* antisense plants exhibited nutritional induced pollen abnormalities that were specifically reversed by copper (Sancenon et al., 2004). In addition, a Cu chaperone, *AtCOX17*, is preferentially active in anthers (Attallah et al., 2007a), indicating a possible role of Cu in pollen development as well. However, whether COPT2, COPT6 or other Cu-related genes affect pollen development and what roles they play in this process remains to be investigated.

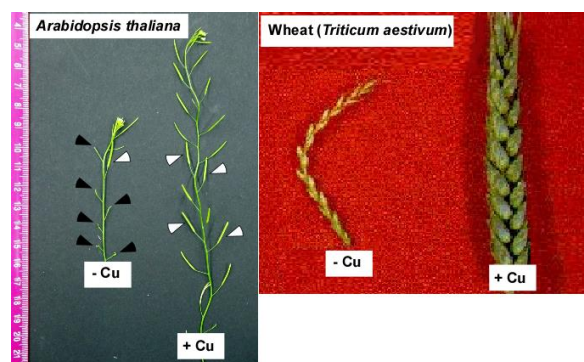


Figure 3. Cu deficiency leads to infertility in *A. thaliana* (Left, Yan et al in prep.) and wheat (right, from (Shorrocks and Alloway, 1988)). White and black arrows indicate fertile and infertile siliques, respectively in *A. thaliana*. Note that Cu deficiency results in total grain loss in wheat.

In addition to Cu transporters and a Cu chaperone, plantacyanins, which are classified as blue copper protein, have a conserved copper-binding site and are involved in pollen germination and pollen tube guidance

(Ryden and Hunt, 1993; Einsle et al., 2000). For example, chemocyanin, which is the plantacyanin in lily, is secreted from the pistil, and acts as an external signal to regulate *in vitro* pollen tube reorientation (Kim et al., 2003). It has been suggested, however that they might be involved in the ROS-induced calcium (Ca^{2+}) channel activation and Ca^{2+} gradient for pollen tube guidance (Malho et al., 2000; Chae and Lord, 2011). Plantacyanin in *Arabidopsis* showed abundant expression in stigma and style, overexpression of it resulted in the loss of directionality of pollen tube growth and a reduced seed set (Dong et al., 2005). However, the specific role of plantacyanins in pollen fertility and Cu in pollen tube guidance remains unclear.

Most recently, it has been suggested that a nuclear protein, KIN17, physically interacts with the central Cu regulator-SPL7, and plays an essential role in plant fertility together with SPL7 (Garcia-Molina et al., 2014). Under Cu starvation, the double mutant of *kin17-1* and *spl7-2* showed significantly reduced pollen viability and lower seed set, and this phenotype can be rescued by Cu application to soil (Garcia-Molina et al., 2014). During my PhD, I discovered that a novel regulator of Cu homeostasis, CCIT1 functions in the interactive SPL7-dependant pathway in regulating Cu homeostasis, and that the disruption of the SPL7-CCIT1 pathway is detrimental to plant viability and plant fertility even under Cu sufficient conditions (Chapter 2).

The publications in the recent decade also address the role of phyhormones-gibbrellin acid (GA), jamic acid (JA) and auxins in stamen development and plant fertility. The GA-deficient mutant, *ga1-3*, generates abortive anther caused by arrested microsporogenesis (Cheng et al., 2004). The mutation of *GID1a/b* (GA-INSENSITIVE DWARF 1a and b), which are the two receptors of GA, affect the stamen elongation (Iuchi et al., 2007). The GA-induced DELLA protein degradation is also reported to be involved in male gametophyte development (Hou et al., 2008). Auxin has been shown to be synthesized in anthers and plays a critical role in plant fertility (Cecchetti et al., 2008). The *tir1 afb* triple and quadruple auxin receptor mutants exhibits earlier anther dehiscence and pollen maturation which results in mature pollen release prior to the completion of filament elongation (Cecchetti et al., 2008). In addition, auxin transport also contributes to the regulation of the preanthesis filament elongation (Cecchetti et al., 2008). Jasmonic

acid (JA) biosynthesis in *Arabidopsis* has been long known to play an essential role in stamen development and male fertility. The mutant of several genes that are involved in JA biosynthesis and signaling, such as defective in anther dehiscence1 (*DAD1*), allene oxide synthase (*AOS*), lipoxygenase 3/4 (*LOX3/4*), were found to exhibit anther development/dehiscence defect, and male sterile phenotype (McConn and Browse, 1996; Stintzi and Browse, 2000; Ishiguro et al., 2001; Park et al., 2002; Caldelari et al., 2011). However, we do not yet know how the developmental cues interact with JA signaling, how the JA is perceived to regulate stamen development and whether Cu plays a role in this JA-dependent regulatory pathway of plant fertility. My data, discussed in Chapter 2 point to the crosstalk between CCIT1, SPL7, pollen fertility and jasmonic acid (JA) biosynthesis.

2. OVERVIEW OF CADMIUM AND ITS TOXICITY IN PLANTS

Cadmium (Cd), is a non-essential and highly toxic transition metal, which is a natural component of the Earth's crust, but is also increasingly emitted into the environment from various agricultural, mining and industrial activities, and the exhaustive gas of automobiles (Jarup, 2003; Waisberg et al., 2003). Exposure to Cd causes defect in root and shoot growth, chlorosis of leaves and brownish coloration of roots (Romero-Puertas et al., 1999; Sandalio et al., 2001; Mittler, 2002; Perfus-Barbeoch et al., 2002; Gichner, 2003; Morel et al., 2009). At the cellular level, Cd toxicity results from the displacement of endogenous co-factors from their cellular binding sites, Thiol-capping of essential proteins, inhibition of DNA repair processes, generation of reactive oxygen species (ROS) and interference with the antioxidant defense system (Hasan et al., 2009). Plants have developed several strategies for Cd detoxification, including binding of Cd within the cell wall, chelation with cellular ligands, compartmentation in the vacuole and enrichment in leaf trichomes (Clemens, 2006). Although significant progress has been made in understanding the mechanism of Cd resistance in plants, fundamental questions that remain in the field are: how Cd enters cells, how it is transported within the plant body, how it affects micronutrient homeostasis, and what signaling networks

underlie the basal Cd resistance. Below, I discuss the current knowledge of Cd uptake, Cd translocation, Cd detoxification and the interaction between the essential heavy metal Cu and Cd.

2.1 Cadmium uptake and translocation in plants

Studies to date have shown that uptake and transport of Cd is mediated by transporters for essential elements (*e.g.* Fe, Mn and Ca) due to either the broad substrate specificity of the transporter, or the similar ionic properties of essential and nonessential heavy metals (Figure 4). It has been reported that when *Iron-regulated transporter1 (IRT1)* is heterogeneously expressed in yeast, Cd inhibits the uptake of iron (Fe) by IRT1 (Eide et al., 1996b), and the expression of *IRT1* in yeast causes increased sensitivity to Cd (Rogers et al., 2000). In *A. thaliana*, *irt1-1* mutant plants were less sensitive to Cd than wild-type under limited iron condition, and the *irt1-1* roots contained five times less Cd than the wild-type (Vert et al., 2002b). *35S-IRT1*-expressing transgenic plants show enhanced sensitivity to Cd when they are grown on iron-deficient medium as a result of higher protein level of *IRT1* (Connolly et al., 2002b). These results together suggest that Cd is transported by IRT1 (Vert et al., 2002b). It was also noted that the expression of *IRT1* is induced by Cd, Cd inhibitS IRT1-dependent iron (II) uptake, and the *A. thaliana* overexpressing *IRT1* accumulates more Cd (Eide et al., 1996a; Connolly et al., 2002a). Therefore, it was suggested that Cd might compete with iron (II) for uptake in Cd-polluted soils, thus causing Fe deficiency (Vert et al., 2002a). Consistent with this suggestion, Cd exposure to the Cd/Zn hyperaccumulator, *Thlaspi caerulescens* (*Ganges* population), inhibited iron uptake (Kupper and Kochian, 2010).

It has also been found that heterogeneous expression of several members from **Natural Resistance Associated Macrophage Protein (Nramp)** family, such as *AtNramp1, 3 or 4* in yeast, increases Cd sensitivity and Cd accumulation (Thomine et al., 2000). The plasma membrane localization of AtNRAMP1 (Cailliatte et al., 2010) indicates that it can take Cd up into cells, whereas the vacuolar membrane localization of AtNRAMP3 and 4 (Molins et al., 2013) suggests that they may participate in the intracellular transport of Cd (Figure 4). The ability of *Nramp* genes of rice in Cd transport has been also investigated. Ectopic expression of *OsNRAMP1* in rice increases Cd accumulation in leaves (Takahashi et al., 2011), indicating

that *OsNRAMP1* is involved in root-to-shoot Cd translocation; whereas the suppression of another *Nramp* gene-*OsNRAMP5* promotes Cd translocation to shoots, suggesting that *OsNRAMP5* is involved in Cd redistribution from shoots to roots (Ishimaru et al., 2012). In addition, a short-term uptake experiment revealed that the knockout line of *OsNRAMP5* lost the ability to take up Cd (Sasaki et al., 2012).

The wheat (*Triticum aestivum*) calcium (Ca) transporter, Low-Affinity Cation Transporter 1 (TaLCT1), increases Cd toxicity when it is expressed in yeast (Clemens et al., 1998). However, overexpression of *TaLCT1* in tobacco resulted in greater tolerance to Cd and more efficient Ca uptake. Consistent with this observation, the transgenic plants overexpressing *TaLCT1* accumulate less Cd but more Ca in roots compared with the plants transformed with the empty vector (Antosiewicz and Hennig, 2004), indicating that discrepancy exists between the studies of TaLCT1 in yeast and plants.

Metallothioneins (MTs) are small metal-binding proteins that are involved in Zn and Cu homeostasis can function as Cd chelators (Zimeri et al., 2005). The simultaneous knock-down of *MT1a*, *b* and *c* in *A.thaliana* resulted in hypersensitivity to Cd and significant reduction of aboveground Cd accumulation, indicating MT1 is essential for Cd tolerance and may participate in root-to-shoot Cd translocation (Zimeri et al., 2005).

It has been found that a Zn-transporting P-type ATPase, AtHMA4, enhances the Cd tolerance of yeast, indication HMA4 is a Cd efflux transporter (Mills et al., 2003). Further, another Zn-transporting P-type ATPase, HMA2, was found to function together with HMA4 to contribute to root-to-shoot Cd translocation *via* xylem loading. The root-to-shoot Cd translocation was totally abolished due to the loss of function of HMA2 and HMA4 (Wong and Cobbett, 2009).

2.2 Cadmium detoxification

In the cytosol, Cd forms a bi-dentate complex with the ubiquitous thiol tripeptide glutathione GSH: Cd-GS2. This, in turn, promotes the synthesis of the principal metal-binding peptides, phytochelatins (PCs). PCs ([γ -Glu-Cys] n -Xaa, n=2-11) are synthesized enzymatically from free GSH and Cd-GS2 or related thiols by PC synthases (PCS), act as high-affinity Cd chelators, and play the major role in Cd detoxification

(Howden et al., 1995b; Howden et al., 1995a; Cobbett et al., 1998; Noctor and Foyer, 1998; Vatamaniuk et al., 1999). The Cd-sensitive mutant was unable to synthesize PCs (Howden and Cobbett, 1992; Howden et al., 1995b; Howden et al., 1995a), and was defective in the PC synthase gene, *PCS1* (Ha et al., 1999; Vatamaniuk et al., 1999). Cd-PC complexes and Cd ions are then either sequestered into the vacuole by ATP-binding cassette (ABC) transporters or cation exchangers (CAX), or travel radially from cell-to-cell towards the vasculature and loaded into the xylem (**Figure 4** and (Salt et al., 1995; Hirschi et al., 2000; Gong et al., 2003; Morel et al., 2009; Song et al., 2010; Park et al., 2012).

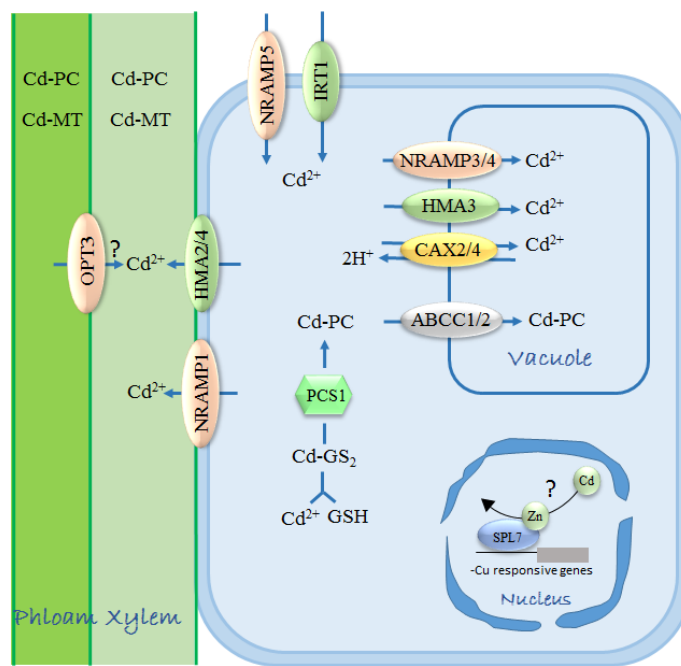


Figure 4. Overview of Cd transport in plants. The major entry route of Cd into *Arabidopsis* root epidermal cells is via IRT1. In rice, NRAMP5 was found to transport Cd into roots. Once in the cytosol, Cd forms a bi-dentate complex with the ubiquitous thiol tripeptide glutathione (GSH): Cd-GS2. This, in turn, promotes the synthesis of the principal metal-binding peptides, phytochelatins (PCs). PCs are synthesized enzymatically from free GSH and Cd-GS2 or related thiols by PC synthases (PCS). Cd-PC complex is then sequestered into vacuole via ABCC1/2, CAX2/4, HMA3 and NRAMP3/4 are also involved in Cd sequestration into vacuole. In *Arabidopsis*, Cd is loading into xylem by HMA2/4, whereas in rice, NRAMP1 may serve as a xylem loading transporter. OPT3, an iron transporter that is localized in phloem, can also transport Cd in the heterologous system. Its contribution to Cd transport *in planta* is unclear. Excess Cd in the cell may replace Zn from SPL7, mimic Cu deficiency response and result in upregulation of the SPL7-dependent Cu responsive genes.

Vascular heavy metals sequestration decreases the concentration of heavy metals in the cytosol and thus serves as an important detoxification mechanism. The mutants of the Cd-PC transporters, *abcc1* and

abcc1abcc2, showed hypersensitivity to Cd and impaired Cd sequestration into the vacuole, demonstrating that ABCC1 and ABCC2 play essential roles in sequestering Cd into vacuole (Figure 4; Park et al., 2012). A P-type ATPase, HMA3, localizes in the vacuolar membrane and can rescue the Cd-sensitive phenotype of yeast mutant which is lacking the Cd-GS₂ vacuolar transporter (Gravot et al., 2004). In planta, confocal imaging in the presence of the Zn/Cd fluorescent probe revealed that AtHMA3 participates in the vacuolar storage of Cd (Morel et al., 2009). A T-DNA insertional mutant of HMA3 was found more sensitive to Zn and Cd. Conversely, ectopic overexpression of AtHMA3 improved plant tolerance to Cd and Zn (Morel et al., 2009). The *Arabidopsis* antiporter, Calcium Exchanger 2 (CAX2), may also be a key player of Cd vacuolar sequestration. Tobacco (*Nicotiana tabacum*) plants expressing CAX2 accumulated more Ca, Cd, and Mn and the expression of CAX2 in tobacco increased Cd and Mn transport in isolated root tonoplast vesicles (Figure 4; Hirschi et al., 2000; Korenkov et al., 2007).

Recently, a phloem-specific iron transporter, Oligopeptide Transporter 3 (OPT3) was found to be involved in Cd partitioning. The Cd concentration in young leaves and the xylem sap of *opt3-3* mutant was significantly lower than it in wild-type, and the *opt3-3* shoots exhibited higher tolerance to Cd toxicity (Zhai et al., 2014). Consistently with the phenotype, the expression of several vacuolar heavy metal transporters was upregulated in roots of the *opt3-3* mutant (Zhai et al., 2014). These data suggest that increased abundance of the vacuolar heavy metal transporters is among the reasons for Cd retention in roots, decreased Cd loading into the xylem, and reduced accumulation in leaves of the *opt3-3* mutant compared to the wild-type, leading to Cd resistance phenotypes in shoots of the *opt3-3* mutant. In addition, *opt3* mutant allele, *opt3-2*, over-accumulates Cd in seeds and roots (Figure 4; Mendoza-Cozatl et al., 2014).

2.3 Crosstalk between Cd and essential metals in the cell.

There is also growing evidence indicating the crosstalk between micronutrient homeostasis and Cd resistance. A recent study on transcription regulation of Fe homeostasis suggested a crucial relationship between Fe homeostasis and Cd tolerance in *A. thaliana*. Expression of *FIT*, *AtbHLH38* and *39* is upregulated upon Cd toxicity. Co-overexpression of *FIT1* with *AtbHLH38* or *39* in *A.thaliana* increases Cd

tolerance probably due to increased expression of a subset heavy metal detoxification genes, including *HMA3*, *Metal tolerance protein 3 (MTP3)*, *Iron-regulated transporter 2 (IRT2)*, *Iron-regulated gene 2 (IREG2)* and *Nicotianamine synthetase 1 and 2 (NAS1, NAS2)*. The primary Fe transporter in *Arabidopsis*, IRT1 is transcriptionally upregulated by Cd and, as discussed above, is the main entry point of Cd into root epidermal cells. (Besson-Bard et al., 2009). It has also been shown that maintaining high Fe content in shoots can alleviate Cd toxicity (Wu et al., 2012). These results establish an important interaction between Cd detoxification and Fe homeostasis and suggest a crosstalk between micronutrients and toxic metals.

The recent studies in our lab have pointed to the essential role of Cu in basal Cd resistance in *A. thaliana* (Gayomba et al., 2013). Gayomba et al (2013) have found that Cd stimulates Cu accumulation in roots of *A. thaliana* and induces three plasma membrane-localized Cu uptake transporters, COPT1, COPT2 and COPT6. This response depends on SPL7 (Gayomba et al., 2013). Loss-of-function of *COPT5*, which translational product functions as Cu effluxer on the tonoplast, exhibits increased sensitivity to Cd, and this sensitivity can be reverted by adding extra Cu (Carrio-Segui et al., 2015). In addition, leaves of the *copt5* mutant accumulate less Cd. This finding and the fact that COPT5 is primarily expressed in the root vasculature, suggest that COPT5 is involved in Cd translocation from roots to shoots (Carrio-Segui et al., 2015). Further, Gayomba et al (2013) found that Cd mimics Cu deficiency response in *A. thaliana* by triggering the SPL7-dependant, miR398-mediated transcriptional pathway of Cu reallocation (Gayomba et al., 2013). It has been found that Zn binding is essential for CRR1 to target Cu-responsive elements (Kropat et al., 2005b; Sommer et al., 2010a), since SPL7 is a homolog of CRR1, it was proposed that Cd may replace Zn from SPL7, thereby activates it even under Cu replete condition (Gayomba et al., 2013). During my PhD work, I found that a novel regulator of Cu homeostasis, CCIT1 is also essential for basal Cd resistance in *A. thaliana*. Loss of the CCIT1 function results in hypersensitivity to Cd, higher accumulation of Cd in shoots and impaired Cu accumulation in roots. This CCIT1-dependent basal Cd resistance is achieved through controlling expression of Cu transporters such as COPT2 (Chapter 4).

Concluding Remarks: During my Ph.D. work, I discovered that a novel transcriptional regulator, CCIT1, is essential for the transcriptional regulation of Cu homeostasis, disruption of which results in hypersensitivity to Cu deficiency in *A. thaliana*. CCIT1 acts together with SPL7, play an important role in pollen viability and plant fertility, possibly *via* jasmonic acid signaling, providing the molecular evidence for the connection between Cu homeostasis, phytohormone signaling, and plant fertility.

REFERENCES

- Abdel-Ghany, S.E., and Pilon, M.** (2008). MicroRNA-mediated systemic down-regulation of copper protein expression in response to low copper availability in Arabidopsis. *The Journal of biological chemistry* **283**, 15932-15945.
- Abdel-Ghany, S.E., Muller-Moule, P., Niyogi, K.K., Pilon, M., and Shikanai, T.** (2005). Two P-type ATPases are required for copper delivery in *Arabidopsis thaliana* chloroplasts. *The Plant cell* **17**, 1233-1251.
- Andres-Colas, N., Sancenon, V., Rodriguez-Navarro, S., Mayo, S., Thiele, D.J., Ecker, J.R., Puig, S., and Penarrubia, L.** (2006). The *Arabidopsis* heavy metal P-type ATPase HMA5 interacts with metallochaperones and functions in copper detoxification of roots. *Plant J* **45**, 225-236.
- Antosiewicz, D.M., and Hennig, J.** (2004). Overexpression of LCT1 in tobacco enhances the protective action of calcium against cadmium toxicity. *Environmental pollution* **129**, 237-245.
- Arguello, J.M., Eren, E., and Gonzalez-Guerrero, M.** (2007). The structure and function of heavy metal transport P1B-ATPases. *Biometals : an international journal on the role of metal ions in biology, biochemistry, and medicine* **20**, 233-248.
- Attallah, C.V., Welchen, E., and Gonzalez, D.H.** (2007a). The promoters of *Arabidopsis thaliana* genes AtCOX17-1 and -2, encoding a copper chaperone involved in cytochrome c oxidase biogenesis, are preferentially active in roots and anthers and induced by biotic and abiotic stress. *Physiol Plantarum* **129**, 123-134.
- Attallah, C.V., Welchen, E., Pujol, C., Bonnard, G., and Gonzalez, D.H.** (2007b). Characterization of *Arabidopsis thaliana* genes encoding functional homologues of the yeast metal chaperone Cox19p, involved in cytochrome c oxidase biogenesis. *Plant Mol Biol* **65**, 343-355.
- Baxter, I., Tchieu, J., Sussman, M.R., Boutry, M., Palmgren, M.G., Grabskov, M., Harper, J.F., and Axelsen, K.B.** (2003). Genomic comparison of P-type ATPase ion pumps in *Arabidopsis* and rice. *Plant physiology* **132**, 618-628.
- Benatti, M.R., Yookongkaew, N., Meetam, M., Guo, W.J., Punyasuk, N., AbuQamar, S., and Goldsbrough, P.** (2014). Metallothionein deficiency impacts copper accumulation and redistribution in leaves and seeds of *Arabidopsis*. *New Phytologist* **202**, 940-951.
- Bernal, M., Casero, D., Singh, V., Wilson, G.T., Grande, A., Yang, H., Dodani, S.C., Pellegrini, M., Huijser, P., Connolly, E.L., Merchant, S.S., and Kramer, U.** (2012a). Transcriptome sequencing identifies SPL7-regulated copper acquisition genes FRO4/FRO5 and the copper dependence of iron homeostasis in *Arabidopsis*. *The Plant cell* **24**, 738-761.
- Bernal, M., Casero, D., Singh, V., Wilson, G.T., Grande, A., Yang, H., Dodani, S.C., Pellegrini, M., Huijser, P., Connolly, E.L., Merchant, S.S., and Krämer, U.** (2012b). Transcriptome Sequencing Identifies SPL7-Regulated Copper Acquisition Genes FRO4/FRO5 and the Copper Dependence of Iron Homeostasis in *Arabidopsis*. *The Plant Cell Online* **24**, 738-761.
- Besson-Bard, A., Gravot, A., Richaud, P., Auroy, P., Duc, C., Gaymard, F., Taconnat, L., Renou, J.P., Pugin, A., and Wendehenne, D.** (2009). Nitric oxide contributes to cadmium toxicity in *Arabidopsis* by promoting cadmium accumulation in roots and by up-regulating genes related to iron uptake. *Plant physiology* **149**, 1302-1315.
- Binder, B.M., Rodriguez, F.I., and Bleeker, A.B.** (2010). The copper transporter RAN1 is essential for biogenesis of ethylene receptors in *Arabidopsis*. *The Journal of biological chemistry* **285**, 37263-37270.
- Blaby-Haas, C.E., Padilla-Benavides, T., Stube, R., Arguello, J.M., and Merchant, S.S.** (2014). Evolution of a plant-specific copper chaperone family for chloroplast copper homeostasis. *Proc Natl Acad Sci U S A* **111**, E5480-5487.
- Bowler, C., Van Camp, W., Van Montagu, M., and Inze, D.** (1994). Superoxide Dismutase in Plants. *Crit Rev Plant Sci* **13**, 199 - 199.

- Burkhead, J., Reynolds, K., Abdel-Ghany, S., Cohu, C., and Pilon, M.** (2009a). Copper homeostasis. *The New phytologist* **182**, 799 - 816.
- Burkhead, J.L., Reynolds, K.A., Abdel-Ghany, S.E., Cohu, C.M., and Pilon, M.** (2009b). Copper homeostasis. *The New phytologist* **182**, 799-816.
- Cailliatte, R., Schikora, A., Briat, J.-F., Mari, S., and Curie, C.** (2010). High-Affinity Manganese Uptake by the Metal Transporter NRAMP1 Is Essential for *Arabidopsis* Growth in Low Manganese Conditions. *The Plant cell* **22**, 904-917.
- Caldelari, D., Wang, G., Farmer, E.E., and Dong, X.** (2011). *Arabidopsis* lox3 lox4 double mutants are male sterile and defective in global proliferative arrest. *Plant molecular biology* **75**, 25-33.
- Carrio-Segui, A., Garcia-Molina, A., Sanz, A., and Penarrubia, L.** (2015). Defective copper transport in the copt5 mutant affects cadmium tolerance. *Plant & cell physiology* **56**, 442-454.
- Casareno, R.L., Waggoner, D., and Gitlin, J.D.** (1998). The copper chaperone CCS directly interacts with copper/zinc superoxide dismutase. *The Journal of biological chemistry* **273**, 23625-23628.
- Cecchetti, V., Altamura, M.M., Falasca, G., Costantino, P., and Cardarelli, M.** (2008). Auxin regulates *Arabidopsis* anther dehiscence, pollen maturation, and filament elongation. *The Plant cell* **20**, 1760-1774.
- Chae, K., and Lord, E.M.** (2011). Pollen tube growth and guidance: roles of small, secreted proteins. *Ann Bot-London* **108**, 627-636.
- Cheng, H., Qin, L., Lee, S., Fu, X., Richards, D.E., Cao, D., Luo, D., Harberd, N.P., and Peng, J.** (2004). Gibberellin regulates *Arabidopsis* floral development via suppression of DELLA protein function. *Development* **131**, 1055-1064.
- Chu, C.C., Lee, W.C., Guo, W.Y., Pan, S.M., Chen, L.J., Li, H.M., and Jinn, T.L.** (2005). A copper chaperone for superoxide dismutase that confers three types of copper/zinc superoxide dismutase activity in *Arabidopsis*. *Plant physiology* **139**, 425-436.
- Clemens, S.** (2006). Toxic metal accumulation, responses to exposure and mechanisms of tolerance in plants. *Biochimie* **88**, 1707-1719.
- Clemens, S., Antosiewicz, D.M., Ward, J.M., Schachtman, D.P., and Schroeder, J.I.** (1998). The plant cDNA LCT1 mediates the uptake of calcium and cadmium in yeast. *Proceedings of the National Academy of Sciences of the United States of America* **95**, 12043-12048.
- Cobbett, C.S., May, M.J., Howden, R., and Rolls, B.** (1998). The glutathione-deficient, cadmium-sensitive mutant, cad2-1, of *Arabidopsis thaliana* is deficient in gamma-glutamylcysteine synthetase. *The Plant journal : for cell and molecular biology* **16**, 73-78.
- Cohu, C.M., Abdel-Ghany, S.E., Gogolin Reynolds, K.A., Onofrio, A.M., Bodecker, J.R., Kimbrel, J.A., Niyogi, K.K., and Pilon, M.** (2009). Copper Delivery by the Copper Chaperone for Chloroplast and Cytosolic Copper/Zinc-Superoxide Dismutases: Regulation and Unexpected Phenotypes in an *Arabidopsis* Mutant. *Mol Plant* **2**, 1336-1350.
- Connolly, E.L., Fett, J.P., and Guerinot, M.L.** (2002a). Expression of the IRT1 Metal Transporter Is Controlled by Metals at the Levels of Transcript and Protein Accumulation. *The Plant cell* **14**, 1347-1357.
- Connolly, E.L., Fett, J.P., and Guerinot, M.L.** (2002b). Expression of the IRT1 metal transporter is controlled by metals at the levels of transcript and protein accumulation. *The Plant cell* **14**, 1347-1357.
- Curie, C., Panaviene, Z., Loulergue, C., Dellaporta, S.L., Briat, J.F., and Walker, E.L.** (2001). Maize yellow stripe1 encodes a membrane protein directly involved in Fe(III) uptake. *Nature* **409**, 346-349.
- Deng, F., Yamaji, N., Xia, J., and Ma, J.F.** (2013). A member of the heavy metal P-type ATPase OsHMA5 is involved in xylem loading of copper in rice. *Plant physiology* **163**, 1353-1362.
- DiDonato, R.J., Jr., Roberts, L.A., Sanderson, T., Eisley, R.B., and Walker, E.L.** (2004). *Arabidopsis* Yellow Stripe-Like2 (YSL2): a metal-regulated gene encoding a plasma membrane transporter of nicotianamine-metal complexes. *The Plant journal : for cell and molecular biology* **39**, 403-414.

- Dong, J., Kim, S.T., and Lord, E.M.** (2005). Plantacyanin plays a role in reproduction in Arabidopsis. *Plant physiology* **138**, 778-789.
- Eide, D., Broderius, M., Fett, J., and Guerinot, M.L.** (1996a). A novel iron-regulated metal transporter from plants identified by functional expression in yeast. *Proceedings of the National Academy of Sciences of the United States of America* **93**, 5624-5628.
- Eide, D., Broderius, M., Fett, J., and Guerinot, M.L.** (1996b). A novel iron-regulated metal transporter from plants identified by functional expression in yeast. *Proc Natl Acad Sci U S A* **93**, 5624-5628.
- Einsle, O., Mehrabian, Z., Nalbandyan, R., and Messerschmidt, A.** (2000). Crystal structure of plantacyanin, a basic blue cupredoxin from spinach. *Journal of biological inorganic chemistry : JBIC : a publication of the Society of Biological Inorganic Chemistry* **5**, 666-672.
- Eriksson, M., Moseley, J.L., Tottey, S., Del Campo, J.A., Quinn, J., Kim, Y., and Merchant, S.** (2004). Genetic dissection of nutritional copper signaling in chlamydomonas distinguishes regulatory and target genes. *Genetics* **168**, 795-807.
- Feng, H., An, F., Zhang, S., Ji, Z., Ling, H.Q., and Zuo, J.** (2006). Light-regulated, tissue-specific, and cell differentiation-specific expression of the Arabidopsis Fe(III)-chelate reductase gene AtFRO6. *Plant physiology* **140**, 1345-1354.
- Flemming, C.A., and Trevors, J.T.** (1989). Copper toxicity and chemistry in the environment: a review. *Water, Air, and Soil Pollution* **44**, 143-158.
- Garcia-Molina, A., Xing, S.P., and Huijser, P.** (2014). A Conserved KIN17 Curved DNA-Binding Domain Protein Assembles with SQUAMOSA PROMOTER-BINDING PROTEIN-LIKE7 to Adapt Arabidopsis Growth and Development to Limiting Copper Availability. *Plant physiology* **164**, 828-840.
- Garcia-Molina, A., Andrés-Colás, N., Pereira-García, A., del Valle-Tascón, S., Peñarrubia, L., and Puig, S.** (2011a). The intracellular Arabidopsis COPT5 transport protein is required for photosynthetic electron transport under severe copper deficiency. *The Plant Journal* **65**, 848-860.
- Garcia-Molina, A., Andrés-Colás, N., Pereira-García, A., del Valle-Tascón, S., Peñarrubia, L., and Puig, S.** (2011b). The intracellular *Arabidopsis* COPT5 transport protein is required for photosynthetic electron transport under severe copper deficiency. *Plant J* **65**, 848-860.
- Garcia-Molina, A., Andres-Colas, N., Pereira-Garcia, A., Neumann, U., Dodani, S.C., Huijser, P., Penarrubia, L., and Puig, S.** (2013). The *Arabidopsis* COPT6 transport protein functions in copper distribution under copper-deficient conditions. *Plant Cell Physiol* **54**, 1378-1390.
- Gayomba, S.R., Jung, H.I., Yan, J., Danku, J., Rutzke, M.A., Bernal, M., Kramer, U., Kochian, L.V., Salt, D.E., and Vatamaniuk, O.K.** (2013). The CTR/COPT-dependent copper uptake and SPL7-dependent copper deficiency responses are required for basal cadmium tolerance in *A. thaliana*. *Metallomics* **5**, 1262-1275.
- Gichner, T.** (2003). DNA damage induced by indirect and direct acting mutagens in catalase-deficient transgenic tobacco. *Cellular and acellular Comet assays*. *Mutation research* **535**, 187-193.
- Glerum, D.M., Shtanko, A., and Tzagoloff, A.** (1996). Characterization of COX17, a yeast gene involved in copper metabolism and assembly of cytochrome oxidase. *The Journal of biological chemistry* **271**, 14504-14509.
- Gong, J.M., Lee, D.A., and Schroeder, J.I.** (2003). Long-distance root-to-shoot transport of phytochelatins and cadmium in Arabidopsis. *Proceedings of the National Academy of Sciences of the United States of America* **100**, 10118-10123.
- Gonzalez-Guerrero, M., and Arguello, J.M.** (2008). Mechanism of Cu+-transporting ATPases: soluble Cu+ chaperones directly transfer Cu+ to transmembrane transport sites. *Proc Natl Acad Sci U S A* **105**, 5992-5997.
- Gravot, A., Lieutaud, A., Verret, F., Auroy, P., Vavasseur, A., and Richaud, P.** (2004). AtHMA3, a plant P1B-ATPase, functions as a Cd/Pb transporter in yeast. *FEBS letters* **561**, 22-28.
- Gross, E.L.** (1993). Plastocyanin: Structure and function. *Photosynthesis research* **37**, 103-116.

- Guo, W.J., Meetam, M., and Goldsbrough, P.B.** (2008). Examining the specific contributions of individual *Arabidopsis* metallothioneins to copper distribution and metal tolerance. *Plant physiology* **146**, 1697-1706.
- Ha, S.B., Smith, A.P., Howden, R., Dietrich, W.M., Bugg, S., O'Connell, M.J., Goldsbrough, P.B., and Cobbett, C.S.** (1999). Phytochelatin synthase genes from *Arabidopsis* and the yeast *Schizosaccharomyces pombe*. *The Plant cell* **11**, 1153-1164.
- Halliwell, B., and Gutteridge, J.M.** (1984). Oxygen toxicity, oxygen radicals, transition metals and disease. *The Biochemical journal* **219**, 1-14.
- Hasan, S.A., Fariduddin, Q., Ali, B., Hayat, S., and Ahmad, A.** (2009). Cadmium: toxicity and tolerance in plants. *Journal of environmental biology / Academy of Environmental Biology, India* **30**, 165-174.
- Hill, K.L., and Merchant, S.** (1995). Coordinate expression of coproporphyrinogen oxidase and cytochrome c6 in the green alga *Chlamydomonas reinhardtii* in response to changes in copper availability. *The EMBO journal* **14**, 857-865.
- Himelblau, E., Mira, H., Lin, S.J., Culotta, V.C., Penarrubia, L., and Amasino, R.M.** (1998). Identification of a functional homolog of the yeast copper homeostasis gene ATX1 from *Arabidopsis*. *Plant physiology* **117**, 1227-1234.
- Hirayama, T., Kieber, J.J., Hirayama, N., Kogan, M., Guzman, P., Nourizadeh, S., Alonso, J.M., Dailey, W.P., Dancis, A., and Ecker, J.R.** (1999). RESPONSIVE-TO-ANTAGONIST1, a Menkes/Wilson disease-related copper transporter, is required for ethylene signaling in *Arabidopsis*. *Cell* **97**, 383-393.
- Hirschi, K.D., Korenkov, V.D., Wilganowski, N.L., and Wagner, G.J.** (2000). Expression of *arabidopsis* CAX2 in tobacco. Altered metal accumulation and increased manganese tolerance. *Plant physiology* **124**, 125-133.
- Hou, X., Hu, W.W., Shen, L., Lee, L.Y., Tao, Z., Han, J.H., and Yu, H.** (2008). Global identification of DELLA target genes during *Arabidopsis* flower development. *Plant physiology* **147**, 1126-1142.
- Howden, R., and Cobbett, C.S.** (1992). Cadmium-Sensitive Mutants of *Arabidopsis thaliana*. *Plant physiology* **100**, 100-107.
- Howden, R., Goldsbrough, P.B., Andersen, C.R., and Cobbett, C.S.** (1995a). Cadmium-sensitive, cad1 mutants of *Arabidopsis thaliana* are phytochelatin deficient. *Plant physiology* **107**, 1059-1066.
- Howden, R., Andersen, C.R., Goldsbrough, P.B., and Cobbett, C.S.** (1995b). A cadmium-sensitive, glutathione-deficient mutant of *Arabidopsis thaliana*. *Plant physiology* **107**, 1067-1073.
- Hussain, D., Haydon, M.J., Wang, Y., Wong, E., Sherson, S.M., Young, J., Camakaris, J., Harper, J.F., and Cobbett, C.S.** (2004). P-type ATPase heavy metal transporters with roles in essential zinc homeostasis in *Arabidopsis*. *The Plant cell* **16**, 1327-1339.
- Ishiguro, S., Kawai-Oda, A., Ueda, J., Nishida, I., and Okada, K.** (2001). The DEFECTIVE IN ANOTHER DEHISCENCE gene encodes a novel phospholipase A1 catalyzing the initial step of jasmonic acid biosynthesis, which synchronizes pollen maturation, anther dehiscence, and flower opening in *Arabidopsis*. *The Plant cell* **13**, 2191-2209.
- Ishimaru, Y., Takahashi, R., Bashir, K., Shimo, H., Senoura, T., Sugimoto, K., Ono, K., Yano, M., Ishikawa, S., Arao, T., Nakanishi, H., and Nishizawa, N.K.** (2012). Characterizing the role of rice NRAMP5 in Manganese, Iron and Cadmium Transport. *Scientific reports* **2**, 286.
- Iuchi, S., Suzuki, H., Kim, Y.C., Iuchi, A., Kuromori, T., Ueguchi-Tanaka, M., Asami, T., Yamaguchi, I., Matsuoka, M., Kobayashi, M., and Nakajima, M.** (2007). Multiple loss-of-function of *Arabidopsis* gibberellin receptor AtGID1s completely shuts down a gibberellin signal. *The Plant journal : for cell and molecular biology* **50**, 958-966.
- Jain, A., Wilson, G.T., and Connolly, E.L.** (2014). The diverse roles of FRO family metalloreductases in iron and copper homeostasis. *Frontiers in plant science* **5**, 100.
- Jarup, L.** (2003). Hazards of heavy metal contamination. *Br Med Bull* **68**, 167-182.

- Jeong, J., and Connolly, E.L.** (2009). Iron uptake mechanisms in plants: Functions of the FRO family of ferric reductases. *Plant Sci* **176**, 709-714.
- Jung, H.I., Gayomba, S.R., Yan, J., and Vatamaniuk, O.K.** (2014). Brachypodium distachyon as a model system for studies of copper transport in cereal crops. *Front Plant Sci* **5**, 236.
- Jung, H.I., Gayomba, S.R., Rutzke, M.A., Craft, E., Kochian, L.V., and Vatamaniuk, O.K.** (2012). COPT6 is a plasma membrane transporter that functions in copper homeostasis in *Arabidopsis* and is a novel target of SQUAMOSA promoter-binding protein-like 7. *J Biol Chem* **287**, 33252-33267.
- Kampfenkel, K., Kushnir, S., Babiychuk, E., Inze, D., and Van Montagu, M.** (1995). Molecular characterization of a putative *Arabidopsis thaliana* copper transporter and its yeast homologue. *The Journal of biological chemistry* **270**, 28479-28486.
- Kim, S., Mollet, J.C., Dong, J., Zhang, K., Park, S.Y., and Lord, E.M.** (2003). Chemocyanin, a small basic protein from the lily stigma, induces pollen tube chemotropism. *Proc Natl Acad Sci U S A* **100**, 16125-16130.
- Kim, Y.Y., Choi, H., Segami, S., Cho, H.T., Martinoia, E., Maeshima, M., and Lee, Y.** (2009). AtHMA1 contributes to the detoxification of excess Zn(II) in *Arabidopsis*. *The Plant journal : for cell and molecular biology* **58**, 737-753.
- Klaumann, S., Nickolaus, S.D., Fürst, S.H., Starck, S., Schneider, S., Ekkehard Neuhaus, H., and Trentmann, O.** (2011a). The tonoplast copper transporter COPT5 acts as an exporter and is required for interorgan allocation of copper in *Arabidopsis thaliana*. *New Phytol* **192**, 393-404.
- Klaumann, S., Nickolaus, S.D., Fürst, S.H., Starck, S., Schneider, S., Ekkehard Neuhaus, H., and Trentmann, O.** (2011b). The tonoplast copper transporter COPT5 acts as an exporter and is required for interorgan allocation of copper in *Arabidopsis thaliana*. *New Phytologist* **192**, 393-404.
- Kliebenstein, D.J., Monde, R.-A., and Last, R.L.** (1998). Superoxide Dismutase in *Arabidopsis*: An Eclectic Enzyme Family with Disparate Regulation and Protein Localization. *Plant Physiol.* **118**, 637-650.
- Kobayashi, Y., Kuroda, K., Kimura, K., Southron-Francis, J.L., Furuzawa, A., Kimura, K., Iuchi, S., Kobayashi, M., Taylor, G.J., and Koyama, H.** (2008). Amino acid polymorphisms in strictly conserved domains of a P-type ATPase HMA5 are involved in the mechanism of copper tolerance variation in *Arabidopsis*. *Plant physiology* **148**, 969-980.
- Korenkov, V., Hirschi, K., Crutchfield, J.D., and Wagner, G.J.** (2007). Enhancing tonoplast Cd/H antiport activity increases Cd, Zn, and Mn tolerance, and impacts root/shoot Cd partitioning in *Nicotiana tabacum* L. *Planta* **226**, 1379-1387.
- Kropat, J., Tottey, S., Birkenbihl, R.P., Depage, N., Huijser, P., and Merchant, S.** (2005a). A regulator of nutritional copper signaling in *Chlamydomonas* is an SBP domain protein that recognizes the GTAC core of copper response element. *Proceedings of the National Academy of Sciences of the United States of America* **102**, 18730-18735.
- Kropat, J., Tottey, S., Birkenbihl, R.P., Depege, N., Huijser, P., and Merchant, S.** (2005b). A regulator of nutritional copper signaling in *Chlamydomonas* is an SBP domain protein that recognizes the GTAC core of copper response element. *Proc Natl Acad Sci U S A* **102**, 18730-18735.
- Kuper, J., Llamas, A., Hecht, H.J., Mendel, R.R., and Schwarz, G.** (2004). Structure of the molybdopterin-bound Cnx1G domain links molybdenum and copper metabolism. *Nature* **430**, 803-806.
- Kupper, H., and Kochian, L.V.** (2010). Transcriptional regulation of metal transport genes and mineral nutrition during acclimatization to cadmium and zinc in the Cd/Zn hyperaccumulator, *Thlaspi caerulescens* (*Ganges* population). *The New phytologist* **185**, 114-129.
- Lee, S., Kim, Y.Y., Lee, Y., and An, G.** (2007). Rice P1B-type heavy-metal ATPase, OsHMA9, is a metal efflux protein. *Plant physiology* **145**, 831-842.

- Lin, S.J., Pufahl, R.A., Dancis, A., O'Halloran, T.V., and Culotta, V.C.** (1997). A role for the *Saccharomyces cerevisiae* ATX1 gene in copper trafficking and iron transport. *The Journal of biological chemistry* **272**, 9215-9220.
- Malho, R., Camacho, L., and Moutinho, A.** (2000). Signalling pathways in pollen tube growth and reorientation. *Ann Bot-London* **85**, 59-68.
- Marschner, H.** (1995a). Mineral nutrition of higher plants. (London; San Diego: Academic Press).
- Marschner, H.** (1995b). Mineral Nutrition of Higher Plants. (Elsevier Academic Press).
- McConn, M., and Browse, J.** (1996). The Critical Requirement for Linolenic Acid Is Pollen Development, Not Photosynthesis, in an *Arabidopsis* Mutant. *The Plant cell* **8**, 403-416.
- Mendoza-Cozatl, D.G., Xie, Q., Akmakjian, G.Z., Jobe, T.O., Patel, A., Stacey, M.G., Song, L., Demoin, D.W., Jurisson, S.S., Stacey, G., and Schroeder, J.I.** (2014). OPT3 is a component of the iron-signaling network between leaves and roots and misregulation of OPT3 leads to an over-accumulation of cadmium in seeds. *Molecular plant* **7**, 1455-1469.
- Merchant, S.S.** (2010). The elements of plant micronutrients. *Plant physiology* **154**, 512-515.
- Mills, R.F., Peaston, K.A., Runions, J., and Williams, L.E.** (2012). HvHMA2, a P(1B)-ATPase from barley, is highly conserved among cereals and functions in Zn and Cd transport. *PloS one* **7**, e42640.
- Mills, R.F., Krijger, G.C., Baccarini, P.J., Hall, J.L., and Williams, L.E.** (2003). Functional expression of AtHMA4, a P1B-type ATPase of the Zn/Co/Cd/Pb subclass. *The Plant journal : for cell and molecular biology* **35**, 164-176.
- Mills, R.F., Francini, A., Ferreira da Rocha, P.S., Baccarini, P.J., Aylett, M., Krijger, G.C., and Williams, L.E.** (2005). The plant P1B-type ATPase AtHMA4 transports Zn and Cd and plays a role in detoxification of transition metals supplied at elevated levels. *FEBS letters* **579**, 783-791.
- Mira, H., Martinez-Garcia, F., and Penarrubia, L.** (2001a). Evidence for the plant-specific intercellular transport of the *Arabidopsis* copper chaperone CCH. *The Plant journal : for cell and molecular biology* **25**, 521-528.
- Mira, H., Martinez, N., and Penarrubia, L.** (2002). Expression of a vegetative-storage-protein gene from *Arabidopsis* is regulated by copper, senescence and ozone. *Planta* **214**, 939-946.
- Mira, H., Vilar, M., Perez-Paya, E., and Penarrubia, L.** (2001b). Functional and conformational properties of the exclusive C-domain from the *Arabidopsis* copper chaperone (CCH). *The Biochemical journal* **357**, 545-549.
- Mittler, R.** (2002). Oxidative stress, antioxidants and stress tolerance. *Trends in plant science* **7**, 405-410.
- Molins, H., Michelet, L., Lanquar, V., Agorio, A., Giraudat, J., Roach, T., Krieger-Liszky, A., and Thomine, S.** (2013). Mutants impaired in vacuolar metal mobilization identify chloroplasts as a target for cadmium hypersensitivity in *Arabidopsis thaliana*. *Plant, cell & environment* **36**, 804-817.
- Morel, M., Crouzet, J., Gravot, A., Auroy, P., Leonhardt, N., Vavasseur, A., and Richaud, P.** (2009). AtHMA3, a P1B-ATPase allowing Cd/Zn/Co/Pb vacuolar storage in *Arabidopsis*. *Plant physiology* **149**, 894-904.
- Moreno, I., Norambuena, L., Maturana, D., Toro, M., Vergara, C., Orellana, A., Zurita-Silva, A., and Ordenes, V.R.** (2008). AtHMA1 is a thapsigargin-sensitive Ca²⁺/heavy metal pump. *The Journal of biological chemistry* **283**, 9633-9641.
- Mukherjee, I., Campbell, N.H., Ash, J.S., and Connolly, E.L.** (2006). Expression profiling of the *Arabidopsis* ferric chelate reductase (FRO) gene family reveals differential regulation by iron and copper. *Planta* **223**, 1178-1190.
- Nobrega, M.P., Bandeira, S.C., Beers, J., and Tzagoloff, A.** (2002). Characterization of COX19, a widely distributed gene required for expression of mitochondrial cytochrome oxidase. *The Journal of biological chemistry* **277**, 40206-40211.
- Noctor, G., and Foyer, C.H.** (1998). ASCORBATE AND GLUTATHIONE: Keeping Active Oxygen Under Control. *Annual review of plant physiology and plant molecular biology* **49**, 249-279.

- Park, J., Song, W.Y., Ko, D., Eom, Y., Hansen, T.H., Schiller, M., Lee, T.G., Martinoia, E., and Lee, Y.** (2012). The phytochelatin transporters AtABCC1 and AtABCC2 mediate tolerance to cadmium and mercury. *The Plant journal : for cell and molecular biology* **69**, 278-288.
- Park, J.H., Halitschke, R., Kim, H.B., Baldwin, I.T., Feldmann, K.A., and Feyereisen, R.** (2002). A knock-out mutation in allene oxide synthase results in male sterility and defective wound signal transduction in *Arabidopsis* due to a block in jasmonic acid biosynthesis. *The Plant journal : for cell and molecular biology* **31**, 1-12.
- Perea-Garcia, A., Garcia-Molina, A., Andres-Colas, N., Vera-Sirera, F., Perez-Amador, M.A., Puig, S., and Penarrubia, L.** (2013). *Arabidopsis* copper transport protein COPT2 participates in the cross talk between iron deficiency responses and low-phosphate signaling. *Plant physiology* **162**, 180-194.
- Perfus-Barbeoch, L., Leonhardt, N., Vavasseur, A., and Forestier, C.** (2002). Heavy metal toxicity: cadmium permeates through calcium channels and disturbs the plant water status. *The Plant journal : for cell and molecular biology* **32**, 539-548.
- Pich, A., Scholz, G.** (1996). Translocation of copper and other micronutrients in tomato plants (*Lycopersicon esculentum* Mill.): nicotianamine-stimulated copper transport in the xylem. *Journal of experimental botany* **47**, 41-47.
- Pich, A., Scholz, G., Stephan, U.W.** (1994). Iron-dependent changes of heavy metals, nicotianamine, and citrate in different plant organs and in the xylem exudate of two tomato genotypes: nicotianamine as possible copper translocator. *Plant and Soil* **165**, 189-196.
- Pilon, M., Abdel-Ghany, S.E., Cohu, C.M., Gogolin, K.A., and Ye, H.** (2006). Copper cofactor delivery in plant cells. *Curr Opin Plant Biol* **9**, 256-263.
- Puig, S., Andres-Colas, N., Garcia-Molina, A., and Peñarrubia, L.** (2007a). Copper and iron homeostasis in *Arabidopsis*: responses to metal deficiencies, interactions and biotechnological applications. *Plant Cell Environ* **30**, 271-290.
- Puig, S., Mira, H., Dorcey, E., Sancenon, V., Andres-Colas, N., Garcia-Molina, A., Burkhead, J.L., Gogolin, K.A., Abdel-Ghany, S.E., Thiele, D.J., Ecker, J.R., Pilon, M., and Penarrubia, L.** (2007b). Higher plants possess two different types of ATX1-like copper chaperones. *Biochemical and biophysical research communications* **354**, 385-390.
- Quinn, J.M., and Merchant, S.** (1995). Two copper-responsive elements associated with the *Chlamydomonas Cyc6* gene function as targets for transcriptional activators. *The Plant cell* **7**, 623-628.
- Quinn, J.M., Barraco, P., Eriksson, M., and Merchant, S.** (2000). Coordinate copper- and oxygen-responsive *Cyc6* and *Cpx1* expression in *Chlamydomonas* is mediated by the same element. *The Journal of biological chemistry* **275**, 6080-6089.
- Ravet, K., and Pilon, M.** (2013). Copper and Iron Homeostasis in Plants: The Challenges of Oxidative Stress. *Antioxid Redox Signal* **19**, 919-932.
- Robinson, N.J., Procter, C.M., Connolly, E.L., and Guerinot, M.L.** (1999). A ferric-chelate reductase for iron uptake from soils. *Nature* **397**, 694-697.
- Rogers, E.E., Eide, D.J., and Guerinot, M.L.** (2000). Altered selectivity in an *Arabidopsis* metal transporter. *Proc Natl Acad Sci U S A* **97**, 12356-12360.
- Romero-Puertas, M.C., McCarthy, I., Sandalio, L.M., Palma, J.M., Corpas, F.J., Gomez, M., and del Rio, L.A.** (1999). Cadmium toxicity and oxidative metabolism of pea leaf peroxisomes. *Free radical research* **31 Suppl**, S25-31.
- Ryden, L.G., and Hunt, L.T.** (1993). Evolution of protein complexity: the blue copper-containing oxidases and related proteins. *Journal of molecular evolution* **36**, 41-66.
- Salt, D.E., Prince, R.C., Pickering, I.J., and Raskin, I.** (1995). Mechanisms of Cadmium Mobility and Accumulation in Indian Mustard. *Plant physiology* **109**, 1427-1433.
- Sancenon, V., Puig, S., Mira, H., Thiele, D.J., and Peñarrubia, L.** (2003). Identification of a copper transporter family in *Arabidopsis thaliana*. *Plant molecular biology* **51**, 577-587.

- Sancenon, V., Puig, S., Mateu-Andres, I., Dorcey, E., Thiele, D.J., and Penarrubia, L.** (2004). The Arabidopsis copper transporter COPT1 functions in root elongation and pollen development. *J Biol Chem* **279**, 15348-15355.
- Sandalio, L.M., Dalurzo, H.C., Gomez, M., Romero-Puertas, M.C., and del Rio, L.A.** (2001). Cadmium-induced changes in the growth and oxidative metabolism of pea plants. *Journal of experimental botany* **52**, 2115-2126.
- Sasaki, A., Yamaji, N., Yokosho, K., and Ma, J.F.** (2012). Nramp5 is a major transporter responsible for manganese and cadmium uptake in rice. *The Plant cell* **24**, 2155-2167.
- Seigneurin-Berny, D., Gravot, A., Auroy, P., Mazard, C., Kraut, A., Finazzi, G., Grunwald, D., Rappaport, F., Vavasseur, A., Joyard, J., Richaud, P., and Rolland, N.** (2006). HMA1, a new Cu-ATPase of the chloroplast envelope, is essential for growth under adverse light conditions. *The Journal of biological chemistry* **281**, 2882-2892.
- Shikanai, T., Muller-Moule, P., Munekage, Y., Niyogi, K.K., and Pilon, M.** (2003). PAA1, a P-type ATPase of Arabidopsis, functions in copper transport in chloroplasts. *The Plant cell* **15**, 1333-1346.
- Shin, L.J., Lo, J.C., and Yeh, K.C.** (2012). Copper chaperone antioxidant protein1 is essential for copper homeostasis. *Plant physiology* **159**, 1099-1110.
- Shorrocks, V.M., and Alloway, B.J.** (1988). Copper in plant, animal and human nutrition. (Potters Bar, Hertfordshire: Copper Development Association).
- Solberg, E., Evans, I., and Penny, D.** (1999). Copper deficiency: Diagnosis and correction. Agri-facts. Soil Fertility/Crop Nutrition. Alberta Agriculture, Food and Rural Development, Agdex 532-3, pp. 1-9. (
- Sommer, F., Kropat, J., Malasarn, D., Grossoechme, N.E., Chen, X., Giedroc, D.P., and Merchant, S.S.** (2010a). The CRR1 nutritional copper sensor in Chlamydomonas contains two distinct metal-responsive domains. *Plant Cell* **22**, 4098-4113.
- Sommer, F., Kropat, J., Malasarn, D., Grossoechme, N.E., Chen, X., Giedroc, D.P., and Merchant, S.S.** (2010b). The CRR1 Nutritional Copper Sensor in Chlamydomonas Contains Two Distinct Metal-Responsive Domains. *The Plant Cell Online* **22**, 4098-4113.
- Song, W.Y., Park, J., Mendoza-Cozatl, D.G., Suter-Grottemeyer, M., Shim, D., Hortensteiner, S., Geisler, M., Weder, B., Rea, P.A., Rentsch, D., Schroeder, J.I., Lee, Y., and Martinoia, E.** (2010). Arsenic tolerance in Arabidopsis is mediated by two ABCC-type phytochelatin transporters. *Proceedings of the National Academy of Sciences of the United States of America* **107**, 21187-21192.
- Stintzi, A., and Browse, J.** (2000). The Arabidopsis male-sterile mutant, opr3, lacks the 12-oxophytodienoic acid reductase required for jasmonate synthesis. *Proceedings of the National Academy of Sciences of the United States of America* **97**, 10625-10630.
- Sunkar, R., Kapoor, A., and Zhu, J.-K.** (2006). Posttranscriptional Induction of Two Cu/Zn Superoxide Dismutase Genes in *Arabidopsis* Is Mediated by Downregulation of miR398 and Important for Oxidative Stress Tolerance. *The Plant cell* **18**, 2051-2065.
- Takahashi, R., Ishimaru, Y., Nakanishi, H., and Nishizawa, N.K.** (2011). Role of the iron transporter OsNRAMP1 in cadmium uptake and accumulation in rice. *Plant signaling & behavior* **6**, 1813-1816.
- Thomine, S., Wang, R., Ward, J.M., Crawford, N.M., and Schroeder, J.I.** (2000). Cadmium and iron transport by members of a plant metal transporter family in Arabidopsis with homology to Nramp genes. *Proc Natl Acad Sci U S A* **97**, 4991-4996.
- Vatamaniuk, O.K., Mari, S., Lu, Y.P., and Rea, P.A.** (1999). AtPCS1, a phytochelatin synthase from *Arabidopsis*: isolation and *in vitro* reconstitution. *Proceedings of the National Academy of Sciences of the United States of America* **96**, 7110-7115.
- Vert, G., Grotz, N., Dedaldechamp, F., Gaymard, F., Guerinot, M.L., Briat, J.-F., and Curie, C.** (2002a). IRT1, an *Arabidopsis* Transporter Essential for Iron Uptake from the Soil and for Plant Growth. *The Plant cell* **14**, 1223-1233.

- Vert, G., Grotz, N., Dedaldechamp, F., Gaymard, F., Guerinot, M.L., Briat, J.F., and Curie, C.** (2002b). IRT1, an *Arabidopsis* transporter essential for iron uptake from the soil and for plant growth. *The Plant cell* **14**, 1223-1233.
- Waisberg, M., Joseph, P., Hale, B., and Beyersmann, D.** (2003). Molecular and cellular mechanisms of cadmium carcinogenesis. *Toxicology* **192**, 95-117.
- Waters, B.M., Chu, H.H., Didonato, R.J., Roberts, L.A., Eisley, R.B., Lahner, B., Salt, D.E., and Walker, E.L.** (2006). Mutations in *Arabidopsis* yellow stripe-like1 and yellow stripe-like3 reveal their roles in metal ion homeostasis and loading of metal ions in seeds. *Plant physiology* **141**, 1446-1458.
- Williams, L.E., and Mills, R.F.** (2005). P(1B)-ATPases--an ancient family of transition metal pumps with diverse functions in plants. *Trends in plant science* **10**, 491-502.
- Wintz, H., Fox, T., Wu, Y.Y., Feng, V., Chen, W., Chang, H.S., Zhu, T., and Vulpe, C.** (2003). Expression profiles of *Arabidopsis thaliana* in mineral deficiencies reveal novel transporters involved in metal homeostasis. *The Journal of biological chemistry* **278**, 47644-47653.
- Woeste, K.E., and Kieber, J.J.** (2000). A strong loss-of-function mutation in RAN1 results in constitutive activation of the ethylene response pathway as well as a rosette-lethal phenotype. *The Plant cell* **12**, 443-455.
- Wong, C.K., and Cobbett, C.S.** (2009). HMA P-type ATPases are the major mechanism for root-to-shoot Cd translocation in *Arabidopsis thaliana*. *The New phytologist* **181**, 71-78.
- Wu, H., Chen, C., Du, J., Liu, H., Cui, Y., Zhang, Y., He, Y., Wang, Y., Chu, C., Feng, Z., Li, J., and Ling, H.Q.** (2012). Co-overexpression FIT with AtbHLH38 or AtbHLH39 in *Arabidopsis*-enhanced cadmium tolerance via increased cadmium sequestration in roots and improved iron homeostasis of shoots. *Plant physiology* **158**, 790-800.
- Wu, Q., Wang, X.Z., Tang, Y.Y., Yu, H.T., Ding, Y.F., De Yang, C., Cui, F.G., Zhang, J.C., and Wang, C.T.** (2014). Molecular cloning and characterization of NPR1 gene from *Arachis hypogaea*. *Molecular biology reports* **41**, 5247-5256.
- Yamasaki, H., Hayashi, M., Fukazawa, M., Kobayashi, Y., and Shikanai, T.** (2009a). SQUAMOSA Promoter Binding Protein-Like7 Is a Central Regulator for Copper Homeostasis in *Arabidopsis*. *The Plant cell* **21**, 347-361.
- Yamasaki, H., Hayashi, M., Fukazawa, M., Kobayashi, Y., and Shikanai, T.** (2009b). SQUAMOSA Promoter Binding Protein-Like7 Is a Central Regulator for Copper Homeostasis in *Arabidopsis*. *The Plant cell* **21**, 347-361.
- Yamasaki, H., Abdel-Ghany, S.E., Cohu, C.M., Kobayashi, Y., Shikanai, T., and Pilon, M.** (2007). Regulation of Copper Homeostasis by Micro-RNA in *Arabidopsis*. *Journal of Biological Chemistry* **282**, 16369-16378.
- Yuan, M., Li, X., Xiao, J., and Wang, S.** (2011). Molecular and functional analyses of COPT/Ctr-type copper transporter-like gene family in rice. *BMC plant biology* **11**, 69.
- Yuan, M., Chu, Z., Li, X., Xu, C., and Wang, S.** (2010). The bacterial pathogen *Xanthomonas oryzae* overcomes rice defenses by regulating host copper redistribution. *The Plant cell* **22**, 3164-3176.
- Zhai, Z., Gayomba, S.R., Jung, H.I., Vimalakumari, N.K., Pineros, M., Craft, E., Rutzke, M.A., Danku, J., Lahner, B., Punshon, T., Guerinot, M.L., Salt, D.E., Kochian, L.V., and Vatamaniuk, O.K.** (2014). OPT3 Is a Phloem-Specific Iron Transporter That Is Essential for Systemic Iron Signaling and Redistribution of Iron and Cadmium in *Arabidopsis*. *The Plant cell* **26**, 2249-2264.
- Zheng, L., Yamaji, N., Yokosho, K., and Ma, J.F.** (2012). YSL16 is a phloem-localized transporter of the copper-nicotianamine complex that is responsible for copper distribution in rice. *The Plant cell* **24**, 3767-3782.
- Zimeri, A.M., Dhankher, O.P., McCaig, B., and Meagher, R.B.** (2005). The plant MT1 metallothioneins are stabilized by binding cadmiums and are required for cadmium tolerance and accumulation. *Plant molecular biology* **58**, 839-855.

CHAPTER II

A Novel Transcription Factor, CCIT1, and a Member of the SPL Family, SPL7, Mediate Crosstalk between Copper Homeostasis, Pollen Fertility and Jasmonic Acid Synthesis in *Arabidopsis thaliana*.

ABSTRACT

Copper (Cu) is an essential heavy metal that is required for plant growth and development. However, when cellular Cu is in excess, it is also toxic, thus the concentration of Cu in plants needs to be tightly regulated. The sophisticated transcriptional regulatory network exist in plants to achieve this goal, in which SPL7 (SQUAMOSA promoter binding protein-like7) acts as the central regulator and is the only transcription factor with a documented role in Cu homeostasis in vascular plants. We have found recently that a member of the basic helix-loop-helix (bHLH) family of TFs, which we designated CCIT1, is transcriptionally regulated by Cu availability and localizes to the nucleus in *A. thaliana*. The *ccit1* T-DNA insertion mutants are hypersensitive to Cu deficiency and exhibit retarded growth under Cu limited condition, which can be rescued by introducing the genomic fragment of *CCIT1*. Previous transcriptome analyses have identified *CCIT1* among the downstream targets of *SPL7*. However, the *ccit1spl7* double mutant showed distinct phenotypes from the two single mutants, such as arrested growth, seed setting failure, pollen sterility and altered flower morphology even under Cu replete condition. Further, we found that the transcriptional response of *CCIT1* to Cu deficiency in roots and flowers is, in part, independent of *SPL7*, suggesting the existence of a more complex parallel interacting pathway of Cu homeostasis than previously thought. The transcriptome profile comparison between wild-type, *ccit1-1* and *spl7-1* in different tissues revealed that Cu homeostasis and jasmonic acid (JA) biosynthetic pathway are significantly changed in the mutants. JA has been known to play an essential role in male fertility in plants. Together, these data suggest that *CCIT1* and *SPL7* act in a parallel interacting Cu regulatory pathway and the JA biosynthetic pathway, to regulate plant fertility. This chapter addresses the more diverse role of Cu in plants, such as phytohormone signaling

and plant fertility, identifies novel regulators and other components in the transcriptional regulatory pathway furthering our understanding of the relationship between Cu homeostasis and plant fertility.

1. INTRODUCTION

Copper (Cu) is an essential micronutrient for all living organisms because it acts as a cofactor for enzymes participating in important biological processes such as respiration, photosynthesis, and scavenging of oxidative stress (Marschner, 1995; Ravet and Pilon, 2013a). In addition to these functions, plants require Cu for the perception of hormones, lignin synthesis, response to pathogens and reproduction (Shorrocks and Alloway, 1988; Marschner, 1995; Burkhead et al., 2009; Mendel and Kruse, 2012; Ravet and Pilon, 2013a). Among visible symptoms of Cu deficiency are stunted growth, distortion of young leaves, chlorosis/necrosis of leaves, compromised fertility and seed set, and, in acute cases, total crop failure (Shorrocks and Alloway, 1988; Marschner, 1995; Solberg et al., 1999). This remarkable array of physiological functions of Cu is attributed to its ability to change the oxidation state ($\text{Cu}^{2+} \leftrightarrow \text{Cu}^+$) (Marschner, 1995). However, the same property imposes toxicity when free Cu ions accumulate in cells in excess because they promote oxidative stress (Valko et al., 2005).

Cu homeostasis in plants is maintained mainly through the tight regulation of Cu uptake, root-to-shoot partitioning and accumulation in chloroplasts as well as by the redistribution of Cu between major Cu-containing enzymes and important Cu-requiring energy-related functions (Burkhead et al., 2009; Ravet and Pilon, 2013b). Based on studies in *Arabidopsis thaliana*, it has been suggested that Cu uptake from the soils into plant roots is achieved *via* a concerted action of Cu(II) to Cu(I) reductases and high-affinity Cu(I) transporters. Since Cu (II) is a dominant form of Cu in the majority of soils (Flemming and Trevors, 1989), it has been proposed that dicots and non-grass monocots reduce Cu(II) to Cu(I), so Cu(I) is the main form of Cu absorbed by plant roots (Burkhead et al., 2009). Further, it has been proposed that membrane-bound ferric reductases from the FRO family in *A. thaliana*, AtFRO4 and AtFRO5 reduce Cu(II) to Cu(I), and their activities are induced by Cu deficiency (Bernal et al., 2012a). Copper (I) then enters the cytosol of root epidermal cells *via* plasma membrane localized transporters of the CTR/COPT family, COPT1, COPT2

and COPT6, while Cu(II) is suggested to be taken up into roots via members of the ZIP (**ZRT-IRT-like Proteins**) family of transporters (Kampfenkel et al., 1995; Sancenon et al., 2003; Jung et al., 2012; Gayomba et al., 2013; Ravet and Pilon, 2013a). Based on tissue localization pattern, COPT2, as well as COPT6, were also suggested to function in Cu distribution in photosynthetic tissues (Jung et al., 2012; Garcia-Molina et al., 2013; Gayomba et al., 2013), while COPT5 is involved in Cu retrieval from the vacuole under Cu deficiency (Garcia-Molina et al., 2011; Klaumann et al., 2011). Xylem- and phloem-based long distance transport of Cu is also facilitated by members of the Yellow Stripe-Like (YSL) family, YSL1, YSL2 and YSL3 (DiDonato et al., 2004; Waters et al., 2006). The majority of these transport systems are subjected to transcriptional regulation in response to Cu availability (Yamasaki et al., 2009b; Jung et al., 2012).

Cu homeostasis is also maintained through the “Cu economy” (“metal-switch”) mechanism, which includes the re-allocation of Cu within the cell to meet the demands of Cu-essential functions (Ravet et al., 2011; Ravet and Pilon, 2013b). For example, plastocyanin is the major Cu-containing protein in higher plants and is essential for photosynthesis (Weigel et al., 2003). During Cu deficiency, the integrity and activity of plastocyanin in photosynthesis are maintained by the re-allocation of Cu from two Cu/Zn superoxide dismutases (SOD), CSD1 and CSD2, that are abundant Cu proteins located in the cytosol and plastids, respectively (Bowler et al., 1994; Kliebenstein et al., 1998; Cohu et al., 2009). As *CSD1* and *CSD2* transcripts and the activity of the encoded proteins decrease, their superoxide scavenging functions are replaced by an increase in gene expression and total enzyme activity of the Fe-containing SOD, FSD1 (Christopher and Marinus, 2007; Yamasaki et al., 2007).

It has been known for decades that Cu deficiency causes reduced grain set (Shorrocks and Alloway, 1988; Marschner, 1995; Solberg et al., 1999). However, our knowledge of the underlying molecular determinants that link Cu with plant reproduction, is surprisingly limited. From what is known, COPT1, COPT2 and COPT6 are highly expressed in pollen grains and COPT1 was noted to have a role in pollen development (Sancenon et al., 2004; Jung et al., 2012; Gayomba et al., 2013). *COPT1* antisense plants exhibit nutritional induced pollen abnormalities that were specifically reversed by Cu (Sancenon et al., 2004). In addition, a Cu chaperone, *AtCOX17*, is preferentially active in anthers (Attallah et al., 2007),

indicating a possible role of Cu in pollen development as well. However, the specific role of Cu in pollen development and fertility is unknown. In addition to Cu transporters, plantacyanins, which are classified as blue copper protein, have a conserved Cu-binding site and are involved in pollen germination and pollen tube guidance (Ryden and Hunt, 1993; Einsle et al., 2000). However, the specific role of plantacyanins in plant fertility is unknown as well. The publications in the recent decade also address the role of phytohormones-gibberellic acid (GA), jasmonic acid (JA) and auxins in stamen development and plant fertility. The GA-deficient and the GA receptor mutants, shows abortive anther (Cheng et al., 2004), and affect the stamen elongation (Iuchi et al., 2007), respectively. The GA-induced DELLA protein degradation is also reported to be involved in male gametophyte development (Hou et al., 2008). Auxin has been shown to be synthesized in anthers and is essential for plant fertility. The mutation of auxin receptors exhibits earlier anther dehiscence and pollen maturation which results in mature pollen release prior to the completion of filament elongation (Cecchetti et al., 2008). JA biosynthesis in *Arabidopsis* has also been known to play an essential role in stamen development and male fertility. Several genes that are involved in JA biosynthesis and signaling were found to exhibit anther development/dehiscence defect, and male sterile phenotype (McConn and Browse, 1996; Stintzi and Browse, 2000; Ishiguro et al., 2001a; Park et al., 2002; Caldelari et al., 2011).

Despite the importance of precise regulation of Cu homeostasis in plants for growth, development and fertility, our knowledge of Cu-related TFs and the hierarchy of their regulatory pathways in higher plants is limited. Thus far, *A. thaliana* SPL7, is the only identified TF with a role in Cu homeostasis in higher plants (Yamasaki et al., 2009b). SPL7 belongs to the Squamosa Promoter Binding Protein [SBP]-like transcription factors family, which in *A. thaliana* encounters 17 members, which have diverse functions in regulating fundamental aspects of plant growth and development, including seed germination and seedling development (Martin et al., 2010), leaf development (Wang et al., 2008), shoot development and floral transition (Cardon et al., 1997; Wu and Poethig, 2006; Gandikota et al., 2007; Schwarz et al., 2008; Shikata et al., 2009; Wang et al., 2009; Wu et al., 2009), trichome distribution (Yu et al., 2010), programmed cell death (Stone et al., 2005), grain production (Miura et al., 2010), as well as Cu homeostasis (Yamasaki

et al., 2009b; Bernal et al., 2012b). SPL7 is distinct from other SPL members, as evident by its separate clustering on the phylogenetic tree (Yamasaki et al., 2009a).

Based on homology to Copper Response Regulator1 (CRR1) in the green alga *Chlamydomonas reinhardtii*, SPL7 is suggested to act as a Cu sensor that regulates gene expression through binding to Cu-responsive elements (CuRE) in promoters of its targets in response to Cu deficiency (Yamasaki et al., 2009b; Sommer et al., 2010). Transcriptome analyses revealed that SPL7 is required for the expression of genes encoding several small RNAs, Cu chaperones, Fe/Cu-chelate reductases FRO4 and FRO5, Fe-superoxide dismutase (FSD1), and several Cu transporters including COPT1, COPT2, YSL2, and, in part, COPT6 (Yamasaki et al., 2009a; Bernal et al., 2012a; Jung et al., 2012; Gayomba et al., 2013). As a result of the important role of SPL7 in Cu homeostasis, *spl7* knockout and knockdown mutants accumulate less Cu and develop slower unless extra Cu is added to the growth medium (Yamasaki et al., 2009b; Bernal et al., 2012a; Gayomba et al., 2013). Most recently, it has been shown that a nuclear protein, KIN17, physically interacts with SPL7, and that the function of these proteins is essential for plant fertility under Cu deficiency (Garcia-Molina et al., 2014).

In addition to SPL7, mineral nutrient, primarily Fe homeostasis in plants is maintained by members of the basic-helix-loop-helix (bHLH) transcription factors. This family is defined by the bHLH signature domain, which consists of 60 amino acids with two functionally distinct regions. The basic region is located at the N-terminal end of the domain and consists of 15 amino acids with a high number of basic residues. The HLH region at the C-terminal end contains mainly hydrophobic residues that form two amphipathic-helices separated by a loop region of variable sequence and length (Nair and Burley, 2000). The basic region is involved in DNA binding, while the HLH region, functions as a dimerization domain (Murre et al., 1989). Outside of the conserved bHLH domain, these proteins exhibit considerable sequence divergence (Atchley et al., 1999). The core DNA sequence motif recognized by the bHLH proteins is a consensus hexanucleotide sequence known as the E-box (5-CANNTG-3). There are different types of E-boxes, depending on the identity of the two central bases. One of the most common is the palindromic G-box (5-CACGTG-3). Certain conserved amino acids within the basic region of the protein provide recognition of the core

consensus site, whereas other residues in the domain dictate specificity for a given type of E-box (Robinson et al., 2000). Several bHLH transcription factors have been shown to be involved in Fe homeostasis, including FIT1, POPEYE, bHLH38 and bHLH39 (Colangelo and Guerinot, 2004; Yuan et al., 2008; Long et al., 2010). The study of POPEYE suggests that POPEYE and its interaction with its homologs are important for transcriptional regulation of iron responsive factors (Long et al., 2010). AtbHLH38 and 39 were reported to form heterodimers with FIT, and act as complexes in transcriptional regulation for Fe homeostasis and Cd tolerance (Yuan et al., 2008; Wu et al., 2012a). However, the role of bHLH in Cu homeostasis has not been yet investigated.

Here I show that previously uncharacterized member of the bHLH family, CCIT1, (Cu, Cd-induced transcription factor1), is essential for the ability of plants to grow and develop under Cu-deficient conditions, and knock-out of *CCIT1* elicits molecular Cu deficiency response in flowers even under Cu sufficient condition. In addition, the genetic studies using the *spl7-1* and *ccit1-1* single mutants and the *ccit1spl7* double mutant show that SPL7 and CCIT1 act in a complex interacting pathway disruption of which is detrimental to the viability and male fertility of *A. thaliana* even under Cu sufficient condition. The genome-wide transcriptome analysis using RNA-seq have identified common and unique targets of CCIT1 and SPL7 in roots, shoots and flowers. The transcriptome analysis in floral buds and mature flowers identified enrichment in JA biosynthetic genes whose expression depends on CCIT1 and SPL7, and the significantly changed JA biosynthetic pathway in *ccit1* and *spl7* mutants. Consistent with these findings, concentration of JA was significantly lower in leaves of single *spl7* and *ccit1* mutants. Collectively, data presented in this Chapter demonstrate the existence of a complex SPL7-CCIT1 interactive transcriptional network that is essential for the maintaining Cu homeostasis and reproduction in *A. thaliana* and highlight the important of the crosstalk between Cu, JA and pollen fertility.

2. METHODS

2.1 Plant Material

All plant lines used in the study were in the *A. thaliana* Columbia (Col-0) background. Seeds of the *SPL7* (SALK_093849; alias *spl7-1*) mutant were obtained from Dr. Shikanai (Kyoto University, Japan) (Yamasaki et al., 2009a). Two *CCIT1* (AT1G71200) mutant alleles, SALK_073160 (alias *ccit1-1*), SAIL_711_B07 (alias *ccit1-2*) were obtained from the *Arabidopsis* Biological Resource Center (Alonso et al., 2003). Homozygous mutants bearing T-DNA insertions were selected by PCR using genomic DNA as a template and the LBb1.3 for SALK line and RP or LB1 for SAIL line and RP primer pairs indicated in Supplemental Table 1. To generate a double *ccit1spl7* mutant, the *ccit1-1* allele was crossed into *spl7-1* mutant (Yamasaki et al., 2009a), the homozygous double mutant was selected by PCR using the genomic DNA as a template and the LBb1.3 and RP primer pairs indicated in Supplemental Table 1. Transgenic plants ectopically expressing *CCIT1* cDNA in the wild-type background, or expressing the *CCIT1* genomic fragment in the *ccit1-1* mutant were produced using the floral dip method (Clough and Bent, 1998). Several one-copy-insertion homozygous lines expressing the genomic *CCIT1* fragment in the *ccit1-1* mutant were selected based on their segregation ratios on the selection plate. According to the expression level revealed by semi-quantitative RT-PCR, three one-copy-insertion homozygous lines with the similar expression level of *CCIT1* compared with wild-type are used in this chapter (from here on *CCIT1-1*, *CCIT1-2* and *CCIT1-3*). Three one-copy-insertion homozygous lines, ectopically expressing *CCIT1* in the wild-type background (from here on, 35S-*CCIT1-1*, 35S-*CCIT1-2* and 35S-*CCIT1-3*), were selected for subsequent experiments. Construction of plasmids is described below.

2.2 Growth Conditions and Experimental Treatments

Different *A. thaliana* plant lines were grown either on solid half-strength Murashige and Skoog (1/2 MS) medium (pH 5.7) (Murashige and Skoog, 1962) or in hydroponic solution (Zhai et al., 2014). For growing plants on solid medium, seeds of different plant lines were surface-sterilized in 75% (v/v) ethanol and a solution containing 1.8% sodium hypochlorite (made up by diluting a household Clorox solution), 0.1% (v/v) Tween-20. Sterilized seeds of uniform size were sown on 1/2 MS medium supplemented with 1% (w/v) sucrose and 0.7% agar (w/v, Sigma A1296). Depending on the experiment, 1/2 MS medium was

supplemented with the indicated concentrations of CuCl₂ or the specific Cu chelator, bathocuproine disulfonate (BCS) (w/v, Acros Organics, Inc. 164060010) (Rapisarda et al., 2002). After stratification at 4 °C for 2 days in darkness, seeds were germinated and grown vertically for 10 days at 22 °C, 14 h light/10 h dark photoperiod at a photon flux density of 110 $\mu\text{mol m}^{-2} \text{s}^{-1}$.

For growing plants hydroponically, seeds of different plant lines were surface-sterilized as described above. Seeds were sown in 10 μl pipette tips containing 0.7% agarose. The top of pipette tips was cut prior placing them into floats manually made of foam boards. This experimental set-up allowed roots to immerse into the hydroponic solution. Seeds were germinated and grown in hydroponic solution at 22 °C, 14 h light/10 h dark photoperiod and a photosynthetic photon flux density of 110 $\mu\text{mol m}^{-2} \text{s}^{-1}$. The solution was replaced every week. The standard solution contained 0.125 μM CuSO₄ (Zhai et al., 2014). For achieving Cu deficiency, Cu was omitted from the medium as indicated in each specific experiment. For example, Cu-deficiency phenotypes of the *ccit1* mutant alleles, *CCIT1* and 35S-*CCIT1* lines were evaluated after 5 weeks of growth in hydroponic medium with or without 0.125 μM CuSO₄. To support germination and growth of the *ccit1spl7* double mutant, all indicated lines were grown from the seed in hydroponic medium containing 0.5 μM CuCl₂. For global transcriptome analyses of root and shoot tissues using deep sequencing (RNA-seq) and qRT-PCR validation, indicated plant lines were grown for 6 weeks hydroponically with 0.25 μM CuSO₄ (to ensure the growth of the *spl7* mutant (Bernal et al., 2012a)). To achieve Cu deficiency, a subset of plants was grown without Cu for the final 3 weeks prior to harvesting. For RNA-seq analyses of flowers, plants were grown hydroponically for eight weeks under Cu-sufficient (0.25 μM CuSO₄) conditions. To achieve Cu deficiency, a subset of plants was grown without Cu for the last 3 weeks. For gene expression studies in flowers of different plant lines, including the *ccit1 spl7* double mutant, plants were grown hydroponically with 0.5 μM CuSO₄ (to ensure the growth of *ccit1 spl7* double mutant) continuously for 8 weeks and a subset of plants was grown without Cu for the last 3 weeks. In all cases plants were grown at 22 °C, 14 h light/10 h dark photoperiod and a photosynthetic photon flux density of 110 $\mu\text{mol m}^{-2} \text{s}^{-1}$,

2.3 RNA Extraction and cDNA Synthesis

Root, shoot and flower tissues, collected from plants grown under the indicated conditions, were separated and flash-frozen in liquid nitrogen before homogenization using a mortar and pestle. Samples were collected between 7 and 8 Zeitgeber time, where Zeitgeber hour 1 is defined as the first hour of light after the dark period. Total RNA was isolated using TRIzol reagent (Invitrogen), according to the manufacturer's instructions. One microgram of total RNA was digested with DNase I (New England Biolabs) prior to the first strand cDNA synthesis. The AffinityScript QPCR cDNA synthesis kit (Agilent Technologies) was used for producing cDNA for subsequent quantitative real-time (qRT)-PCR analyses.

2.4 Plasmid Construction

The *CCIT1* cDNA without the stop codon was amplified by RT-PCR from RNA isolated from *A. thaliana* roots. The genomic fragment of *CCIT1* was amplified by PCR from genomic DNA isolated from *A. thaliana* roots. Primers were designed to include attB sites on resulting PCR products. All cDNA inserts were introduced individually into the *DONR222* entry vector before recombination with the corresponding destination vector (Invitrogen). For complementation of the *ccit1-1* mutant, a 2.9-kb genomic region spanning the entire *CCIT1* locus was PCR-amplified from Col-0 and introduced by recombination cloning into *pRCS2-hpt* vector (Chung et al., 2005). The resulting construct was transformed into the *ccit1-1* mutant. To generate transgenic lines overexpressing *CCIT1*, the full-length *CCIT1* cDNA was cloned by recombination into *Earley-Gate102* and *201* destination vectors (Earley et al., 2006), to fuse *CCIT1* at the N-termini to genes encoding cyan fluorescent protein (CFP) or human influenza hemagglutinin (HA) epitope tags, respectively under the control of the 35S promoter. The resulting constructs were transformed into wild-type *A. thaliana*. To examine the pattern of *CCIT1* expression *in planta*, a 1,541-bp fragment of the genomic sequence upstream of the *CCIT1* start codon was amplified by PCR using primer pairs listed in Supplemental Table 1. The resulting PCR product was cloned by recombination into the *GUS1-Gate* vector upstream of *uidA*, encoding the β -glucuronidase (*GUS*) reporter gene. The *CCIT1_{pro}-GUS* construct

was transformed into wild-type *A. thaliana*. To study the subcellular localization of CCIT1 in *Arabidopsis* protoplasts, the full-length *CCIT1* cDNA without the stop codon was fused at the C-terminus with the modified green fluorescent protein (EGFP) of the *SAT6-N1-EGFP-Gate* vector (Jung et al., 2012) and expressed under the control of the cauliflower mosaic virus 35Spro.

2.5 Subcellular Localization and Fluorescent Microscopy

35S_{pro}-CCIT1-EGFP construct, or *SAT6-N1-Gate*, lacking the cDNA insert, was transfected into *A. thaliana* protoplasts isolated from leaf mesophyll cells using previously established procedures (Zhai et al., 2009). To visualize nuclei, protoplasts were incubated for 15 min with 5 µl 4',6' diamino-2-phenylindole 2HCl (DAPI, 10 mg/ml) at room temperature, and then were washed with W5 solution (Zhai et al., 2009) once before microscope observation. EGFP- and DAPI-mediated fluorescence and chlorophyll auto-fluorescence were visualized using FITC (for EGFP), DAPI and rhodamine (for chlorophyll) filter sets of the Axio Imager M2 microscope equipped with the motorized Z-drive (Zeiss). Images were collected with the high-resolution AxioCam MR Camera. Images were processed using the Adobe Photoshop software package, version 12.0.

2.6 Quantitative Real-time (qRT)-PCR and Data Analysis

Prior to qRT-PCR analysis, primer and cDNA concentrations were optimized to reach the target and normalizing gene amplification efficiency of 100 ± 10%. Two microliters of 15-fold-diluted cDNA was used as a template for qRT-PCR in a total volume of 15 µl containing a 500 nM concentration of each PCR primer, 50 mM KCl, 20 mM Tris-HCl, pH 8.4, 0.2 mM each dNTP, and 1.25 units of iTaq DNA polymerase in iQ SYBR Green Supermix (Bio-Rad). PCR was carried out using the CFX96 real-time PCR system (Bio-Rad). The thermal cycling parameters were as follows: denaturation at 95 °C for 3 min, followed by 39 cycles of 95 °C for 10 s and 55 °C for 30 s. Amplicon dissociation curves (i.e. melting curves) were recorded after cycle 39 by heating from 60 °C to 95 °C with 0.5 °C increments and an average ramp speed of 3.3 °C

s^{-1} . Real-time PCR experiments were conducted using three independent biological samples, each consisting of three technical replicates (Udvardi et al., 2008), unless indicated otherwise. Data were normalized to the expression of *ACTIN* 2. The -fold difference ($2^{\Delta\Delta Ct}$) was calculated using the CFX Manager Software, version 1.5 (Bio-Rad). Statistical analysis was performed using the Relative Expression Software Tool (REST; Qiagen).

2.7 Histochemical Analysis

Transgenic plants expressing the *CCIT1pro-GUS* construct were grown either on solid $\frac{1}{2}$ MS medium or in soils to visualize *CCIT1pro* activity. Histochemical staining was performed with 1 mM 5-bromo-4-chloro-3-indolyl- β -D-glucuronide as described (Jefferson et al., 1987) with an overnight incubation period at 37 °C. Staining patterns were analyzed using the Zeiss 2000 stereomicroscope. Images were collected using a Canon Power Shot S3 IS digital camera and a CS3IS camera adapter. Images were processed using the Adobe Photoshop software package, version 12.0.

2.8 Analyses of Cu Concentrations

For analyses of Cu concentrations in tissues of *A. thaliana*, seeds were set up and germinated on a standard hydroponic solution (Arteca and Arteca, 2000b). At indicated time points plants were transferred to a hydroponic solution without Cu and grown for addition for 4 weeks. Roots and shoots were harvested and roots were desorbed by washing with 10 mM EDTA for 5 min followed by washing in a solution of 0.3 mM BPS and 5.7 mM sodium dithionite for 10 min before rinsing with deionized water 3 times Elemental analysis was performed using inductively coupled plasma mass spectrometry (ICP-MS) as described (Zhai et al., 2014).

2.9 Synchrotron-based X-ray Fluorescence Microscopy (SXRF)

Leaves from the same position of the rosette from wild-type and *ccit1spl7* double mutant plants grown hydroponically with 0.5 μ M CuSO₄ for 5 weeks, and flowers from wild-type, *ccit1-1*, *spl7-1* and *ccit1spl7*

plants grown hydroponically for the first 3 weeks with 0.5 μM CuSO₄ and transferred to soil with 20 μM CuSO₄ for the subsequent 4 weeks, were used for SRXF analyses. Leaves and flowers were detached with forceps and mounted on 35 mm slide mounts across which Kapton™ metal-free tape was stretched. The distribution of elements in hydrated tissues was imaged *via* SRXF at the Cornell High Energy Synchrotron Source (CHESS) using F3 beam-line and a Vortex ME-4 Silicon Drift Detector (SDD). The source of CHESS F3 beamline is the radiation from 5.3 GeV positrons traveling through a bending magnet in Cornell Electron Storage Ring (CESR) about 20 m away from experiment hutch. A single bounce capillary made at CHESS was used to focus X-rays to a 20 μm FWHM microbeam, with focal distance of 55 mm measured from capillary exit end to focus. The SDD detector was positioned 90 degree to the incident beam to accept X-ray fluorescence emitted from sample. Such 90 degree geometry is used at synchrotron beamlines to minimize X-ray scattering from the sample when it is illuminated by the highly polarized synchrotron radiation. Samples were held on a XZ stage with X scanning direction 45 degree to both incident X-rays and SSD detector. X-ray monochromator with multilayers was used to provide monochromatic X-rays with energy bandwidth about 0.6%. X-ray energy was 12.2 keV for this experiment, which was enough to excite fluorescence of Fe, Cu, Zn, Mn, etc., but caused no discernible beam damage to hydrated plant samples. X-ray fluorescence data processing was handled with Praxes, a software package developed by CHESS staff scientist Darren Dale using PyMCA module, which was developed at European Synchrotron Research Facility (ESRF).

2.10 Pollen Viability Assays

Pollen viability was analyzed using the Alexander staining (Alexander, 1969). Briefly, floral buds (stage 12) (Alvarez-Buylla et al., 2010b) from wild-type, *ccit1-1*, *spl7-1* and *ccit1spl7* were fixed in 3:1 ethanol and acetic acid overnight, anthers were dissected on a slide and pollen was tapped out. A drop (about 15 μl) of the Alexander's stain was added and a coverslip was sealed with rubber cement. Slides were incubated on a hot plate for 1.5 h (Crismani and Mercier, 2013). Viable pollen grains were stained dark violet, while

nonviable pollen grains were pale turquoise. The numbers of viable and aborted pollens were counted and images were collected using the Axio Imager M2 microscope.

2.11 High-Throughput Sequencing of mRNA, Mapping Sequences and Differential Gene Expression Analysis

Total RNA was isolated using TRIzol reagent (Invitrogen), according to manufacturer's instructions. Three micrograms of total RNA of roots or shoot sample and five micrograms of total RNA of floral buds and mature flowers were used to construct the strand-specific RNA-Seq libraries as described (Zhong et al., 2011). RNA-seq was performed using the Illumina HiSeq 2500 system. Root and shoot samples were sequenced in 1 lane, flower samples were sequenced in 2 lanes. Three replicates, 72 samples in total that were generated in independently conducted biological experiments were run for each treatment and genotype. The Illumina raw reads were processed using Trimmomatic (Bolger et al., 2014) to remove adaptor and low-quality sequences. Reads shorter than 40 bp were discarded. The resulting reads were aligned to the ribosomal RNA database (Quast et al., 2013) using Bowtie (Langmead et al., 2009) allowing 3 mismatches, and those aligned were discarded. The final clean reads were aligned to the *Arabidopsis* genome sequence (TAIR 10) using TopHat (Trapnell et al., 2009) allowing 1 mismatch. Following alignment, for each gene model, the count of mapped reads from each sample was derived and normalized to RPKM (reads per kilobase of exon model per million mapped reads). Differentially expressed genes (DEGs) were identified using edgeR (Robinson et al., 2010) with the raw count data. Raw *p* values were corrected for multiple testing using the false discovery rate (FDR; Benjamini and Hochberg, 1995). Genes with an FDR less than 0.05 and fold-changes greater than or equal to 2 were regarded as DEGs.

The identification of significantly changed expression of pathways and Gene Ontology (GO) term analysis were performed using the Plant MetGenMap tool (<http://bioinfo.bti.cornell.edu/cgi-bin/MetGenMAP/home.cgi>), which is a web-based analysis and visualization package to identify significantly changed pathways and enriched GO terms from gene expression profile datasets. Biochemical pathways were delineated using the Plant MetGenMap server that extracts information from the BioCyc

database (<http://biocyc.org/>) and the Pathway Tools (<http://bioinformatics.ai.sri.com/ptools/>). The significance of a changed pathways was determined using the hypergeometric distribution: $p_value =$

$$\sum_{j=x}^n \frac{\binom{M}{j} \binom{N-M}{n-j}}{\binom{N}{n}},$$
 where N is the total number of genes in all the pathways, M is the total number of genes

in a particular pathway, n is the total number of significantly changed genes in all the pathways, and x is the total number of significantly changed genes in that particular pathway. The identification of over-represented (enriched) GO terms is implemented based on the CPAN (<http://search.cpan.org/dist/GOTermFinder/>) perl module (Boyle et al., 2004) which uses the hypergeometric distribution to calculate the significance of GO term enrichment. The gene functional classification was analyzed based on their GO annotations.

2.12 LC/MS Analysis of JA

Tissues were collected from five-week-old plants grown hydroponically with or without 0.5 μM CuSO₄, and flash-frozen in liquid N₂. Four to five hundred milligrams of frozen tissues were grounded into a fine powder using mortar and pestle. Free JA extraction and analyses were performed as described (Wang et al., 2007). Briefly, phytohormones were extracted with 1 ml of the solvent containing isopropanol: H₂O : HCl in 2 : 1 : 0.005 ratio. A hundred microliter of D₅–JA (80 pg/ μl) was added to each sample as an internal standard and samples were vortexed and centrifuged at 12000 g. The supernatant was collected, mixed with 1 ml of dichloromethane, and centrifuged for phase separation in an Eppendorf centrifuge 5424 at a speed of 12000 g. The aqueous and middle layers were discarded. The remaining solvent was air-dried in the fume hood. The dried residues were reconstituted in methanol and filtered through 0.45 μm nylon filter for subsequent analyses by liquid chromatography-mass spectrometry (LC-MS) using the triple quadrupole LC-MS system (Quantum Access; Thermo Scientific). The JA concentration was calculated by normalizing to the internal standard and was then converted to ng/g fresh weight.

2.13 Accession Numbers

Sequence data for genes used in this study can be found in the GenBank/EMBL libraries under the following accession numbers (accession numbers in parenthesis): *CCIT1* (AT1G71200), *SPL7* (AT5G18830), *COPT2* (AT3G46900), *FRO4* (AT5G23980), *FRO5* (AT5G23990), *NRT2.1* (AT1G08090), *NRT2.2* (AT1G08100), *LOX3* (AT1G17420), and *LOX4* (AT1G72520).

3. RESULTS

3.1 Identification and Domain Organization of CCIT1

Our microarray-based screen for metal-regulated transcription factors in roots and shoots of *A. thaliana* identified a gene with the accession number At1G71200 that was specifically upregulated by cadmium (Cd) but not by oxidative stress in roots and shoots (Yan et al in preparation and Chapter 4). At1G71200 has been also identified in microarray and RNA-seq screens as regulated by Cu deficiency in roots and shoot of *A. thaliana* and has been regarded among the downstream targets of SPL7 (Yamasaki et al., 2009b; Bernal et al., 2012a). The role of At1G71200 in Cu homeostasis or Cd resistance has not been yet investigated. This chapter discusses the role of At1G7200 in Cu homeostasis in *A. thaliana*, while its role in Cd resistance is discussed in Chapter 4. Given that At1G71200 is transcriptionally upregulated by Cu deficiency and Cd toxicity, we designated it as CCIT1.

CCIT1 (*alias* bHLH160) belongs to the bHLH family of transcription factors, which in *A. thaliana* encounters at least 162 members (Bailey et al., 2003; Heim et al., 2003). CCIT1 contains an N-terminal basic domain and a C-terminal helix-loop-helix domain, characteristic for the bHLH family members as evident from the *in silico* analyses using Predict Protein (<https://www.predictprotein.org/>) and Motif Scan (http://myhits.isb-sib.ch/cgi-bin/motif_scan) tools (Figure 1). Five helix motifs, 5 extended strand motifs from the beta sheet, one nuclear localization motif and several loop regions were found in CCIT1 protein (Figure 1). These software tools identified putative nucleotides binding and protein interacting sites in CCIT1 amino acid sequence (Figure 1), which is consistent with the functional requirement of bHLH members to form dimers in order to bind to DNA (Heim et al., 2003).

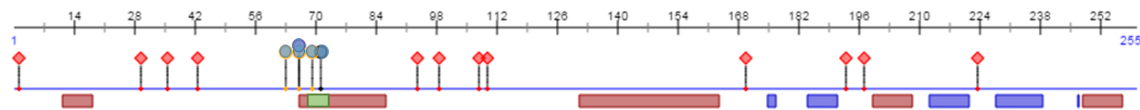


Figure 1. Protein motif prediction of the putative *A. thaliana* bHLH transcription factor, CCIT1. Schematic diagram showing predicted motifs in the amino acid sequence of CCIT1. CCIT1 consists 255 amino acids. The red, blue and green boxes represent helix, extended strand in beta-sheet conformation and bipartite nuclear localization signal, respectively. The rest of it is the loop motifs. The red diamonds and blue circles indicate the putative protein and nucleotides binding sites, respectively. The motif prediction is performed using the Predict Protein tool (<https://www.predictprotein.org/>) and the Motif Scan (http://myhits.isb-sib.ch/cgi-bin/motif_scan) tool (Rost et al., 2004; Ofran and Rost, 2007).

3.2 CCIT1 Localizes to the Nucleus in *A. thaliana* Protoplasts

To examine the subcellular localization of CCIT1, the coding sequence of CCIT1 was fused at the C-terminus to EGFP in the SAT6-EGFP-N1-Gate vector and transiently expressed under the control of the constitutive cauliflower mosaic virus 35S promoter in *A. thaliana* protoplasts. As a control, protoplasts were also transfected with the empty SAT6-EGFP-N1-Gate vector. EGFP-mediated fluorescence was present at the nucleus of CCIT1-EGFP-transfected protoplasts and did not overlap with chlorophyll auto-fluorescence (Figure 2A). To ascertain the nucleus localization of CCIT1-EGFP, transfected protoplasts were co-stained with a DNA dye, DAPI. After short-term incubation, DAPI stained the nucleus, and DAPI-mediated fluorescence overlapped with CCIT1-EGFP-mediated fluorescence but not with chlorophyll-mediated fluorescence (Figure 2A). In protoplasts transfected with the empty vector, EGFP was present as a soluble protein in the cytosol, and its fluorescence did not overlap with chlorophyll auto-fluorescence (Figure 2B). The subcellular localization assay reveals that CCIT1 localizes in the nucleus of *A. thaliana* protoplasts, which suggests that CCIT1 functions in regulating gene transcription as a transcription factor.

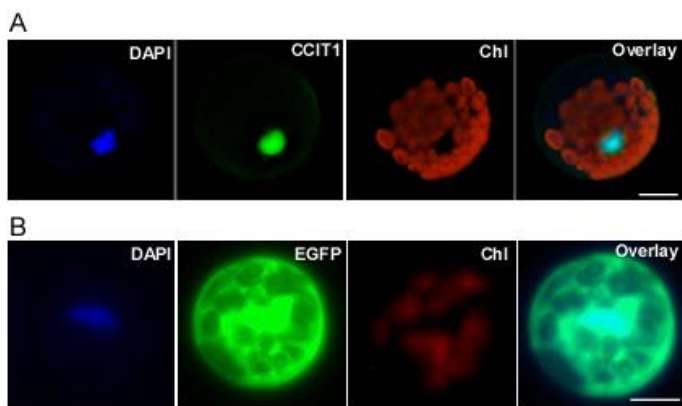


Figure 2. Subcellular localization of CCIT1 in *A. thaliana* protoplasts. *A. thaliana* leaf protoplasts were transfected with the vector expressing the *CCIT1-EGFP* fusion (A) or vector expressing *EGFP* without the *CCIT1* cDNA insert (B). To visualize the nucleus, *CCIT1-EGFP*-transfected protoplasts were co-stained with DAPI. EGFP-mediated fluorescence, derived from *CCIT1-EGFP* (CCIT1), EGFP (EGFP), DAPI-mediated fluorescence (DAPI) and chlorophyll auto-fluorescence (Chl) were visualized using FITC, DAPI and rhodamine filter sets. Superimposed images of *CCIT1-EGFP*- and DAPI-mediated fluorescence and chlorophyll auto-fluorescence (Overlay) were created to demonstrate that green fluorescence derived from *CCIT1-EGFP* co-localizes with DAPI. Scale bar=10 μ m.

3.3 Expression of *CCIT1* is Regulated by Cu Availability

Microarrays and RNA-seq data showed that *CCIT1* is up-regulated by Cu deficiency in roots and shoots and its transcriptional response to Cu deficiency depends on SPL7 (Yamasaki et al., 2009a; Bernal et al., 2012b). To validate these data in our experimental set-up, we analyzed the effect of Cu availability on the transcript abundance of *CCIT1* in roots and shoots of 10-day-old *A. thaliana* grown on solid $\frac{1}{2}$ MS medium. To achieve Cu deficiency, growth medium was supplemented with 500 μ M bathocuproine disulfonate (BCS), which is a specific Cu (I) chelator; to achieve Cu toxicity, we supplemented growth medium with 45 μ M CuCl₂ (Jung et al., 2012). We found that *CCIT1* was down-regulated by 45 μ M CuCl₂, whereas was significantly up-regulated by Cu deficiency in both, shoots and roots (Figure 3A). These data are consistent

with previous observations of Yamasaki et al (2009) and suggest that *CCIT1* might be involved in regulation of Cu homeostasis in *A. thaliana*.

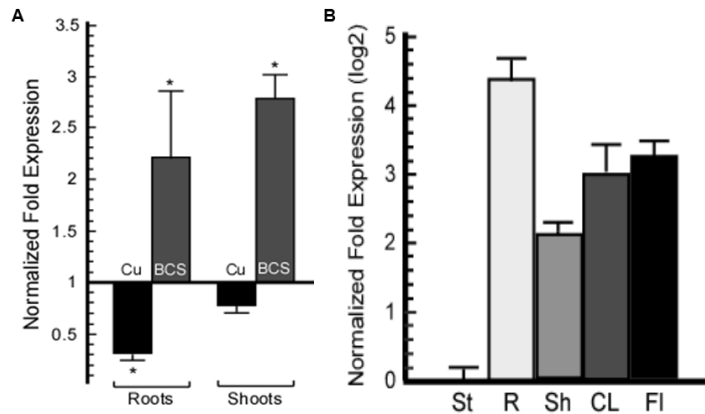


Figure 3. Expression of *CCIT1* is differentially regulated in response to Cu availability. **A**, Quantitative real-time PCR (qRT-PCR) analysis of the effect of 45 μ M CuSO₄ (Cu) and 500 μ M BCS (BCS) on the transcript abundance of *CCIT1* in both, shoots and roots of 10-day-old *A. thaliana*. Error bars indicate S.E. (n = 6). Results are presented relative to the expression of *CCIT1* in wild-type plants grown on $\frac{1}{2}$ MS agar media, which were designated as 1. Statistically significant differences of the mean values between control (untreated conditions) and treated plants are indicated as “*” ($p \leq 0.05$). **B**, Comparison of the transcript abundance of *CCIT1* in rosette leaves (Sh), roots (R), stems (St), flowers (Fl) and cauline leaves (CL) of wild-type plants. Error bars indicate S.E. (n = 6). Results are presented relative to the expression of *CCIT1* in the stem.

3.4 *CCIT1* is Expressed Mainly in Roots, Leaves and Anthers in *A. thaliana*

To investigate the sites of *CCIT1* action in *A. thaliana*, the expression level of *CCIT1* in different tissues was analyzed by qRT-PCR. The transcript level of *CCIT1* in roots (R), flowers (Fl) and cauline leaves (CL) was as 4.6, 2.1 and 1.8 fold higher than in rosette leaves (Sh), whereas in stems (St), it was 5 times lower than it in rosette leaves (Figure 3B). To validate the expression pattern of *CCIT1* revealed by qRT-PCR, the 1.5 kb genomic fragment upstream of the *CCIT1* open reading frame (*CCIT1pro*) was fused to the *uidA* reporter gene encoding β -glucuronidase (GUS), and the *CCIT1pro-GUS* construct was transformed into wild-type *A. thaliana*. Histochemical analysis of *CCIT1pro* activity in plants grown under standard hydroponic solution showed no GUS staining (Figure 4A). However, when the transgenic plants were exposed to a hydroponic solution without Cu, the expression of GUS was present in the main root but not in root tips of 2-week-old seedlings; lateral roots also exhibited a weak GUS staining (Figure 4B). Strong GUS staining was observed in roots, petioles and main veins of leaves of 4-week-old hydroponically grown

plants grown for 2 weeks in medium without Cu (Figure 4C and D). Analysis of the *CCIT1pro* activity in flowers revealed GUS staining in anthers of developing buds (Figure 4E). The expression pattern of *CCIT1* in different tissues suggests that *CCIT1* might play a role in Cu uptake from the soil, translocation to leaves and, perhaps in reproduction.

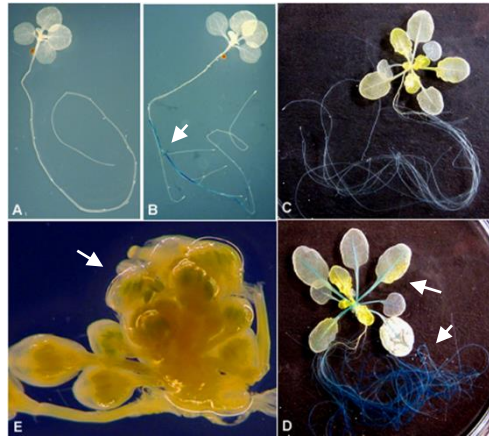


Figure 4. Histochemical analysis of the expression pattern of *CCIT1* in *A. thaliana* transformed with the *CCIT1pro*-GUS construct. **A**, Plants were grown for 14 days in standard hydroponic solution with 0.125 μ M CuSO₄. **B**, Plants were grown for 14 days in hydroponic solution without CuSO₄. **C**, Plants were grown for 4 weeks in standard hydroponic solution with 0.125 μ M CuSO₄. **D**, Plants were grown for the first 2 weeks in standard hydroponic solution with 0.125 μ M CuSO₄, and then transferred to a hydroponic solution lacking Cu. Tissues were collected after 2 weeks of growth under Cu-deficiency. **E**, To visualize the *CCIT1pro* activity in reproductive organs, plants were grown in hydroponic solution with 0.5 μ M CuSO₄ until bolt, and were then subjected to no Cu solution for the next 3 weeks. GUS expression was detected in anthers of developing buds. Note the absence of GUS staining in 14 day-old seedlings and 4-week-old mature plants of plants cultured in standard hydroponic solution (A and C), and intense GUS staining in roots (B and D) and petioles (D) when plants were grown under Cu-deficient condition. White arrows point to the location of GUS expression.

3.5 Isolation of the *ccit1-1* and *ccit1-2* mutant alleles and *CCIT1* complemented and overexpressing lines

To determine the role of *CCIT1* in Cu homeostasis, two *ccit1* T-DNA insertion lines, designated as *ccit1-1* and *ccit1-2*, were obtained from *Arabidopsis* Biological Resource Center (Alonso et al., 2003). In *ccit1-1* and *ccit1-2*, T-DNA is inserted in the 1st exon and 3'-UTR of the *CCIT1* gene, respectively (Figure 5A and Supplemental figure 1A). RT-PCR analyses revealed that the T-DNA insertion in the *ccit1-1* allele resulted

in a loss of the full-length *CCIT1* transcript and much lower levels in *ccit1-2* (Figure 5A and B, Supplemental Figure 1A and B).

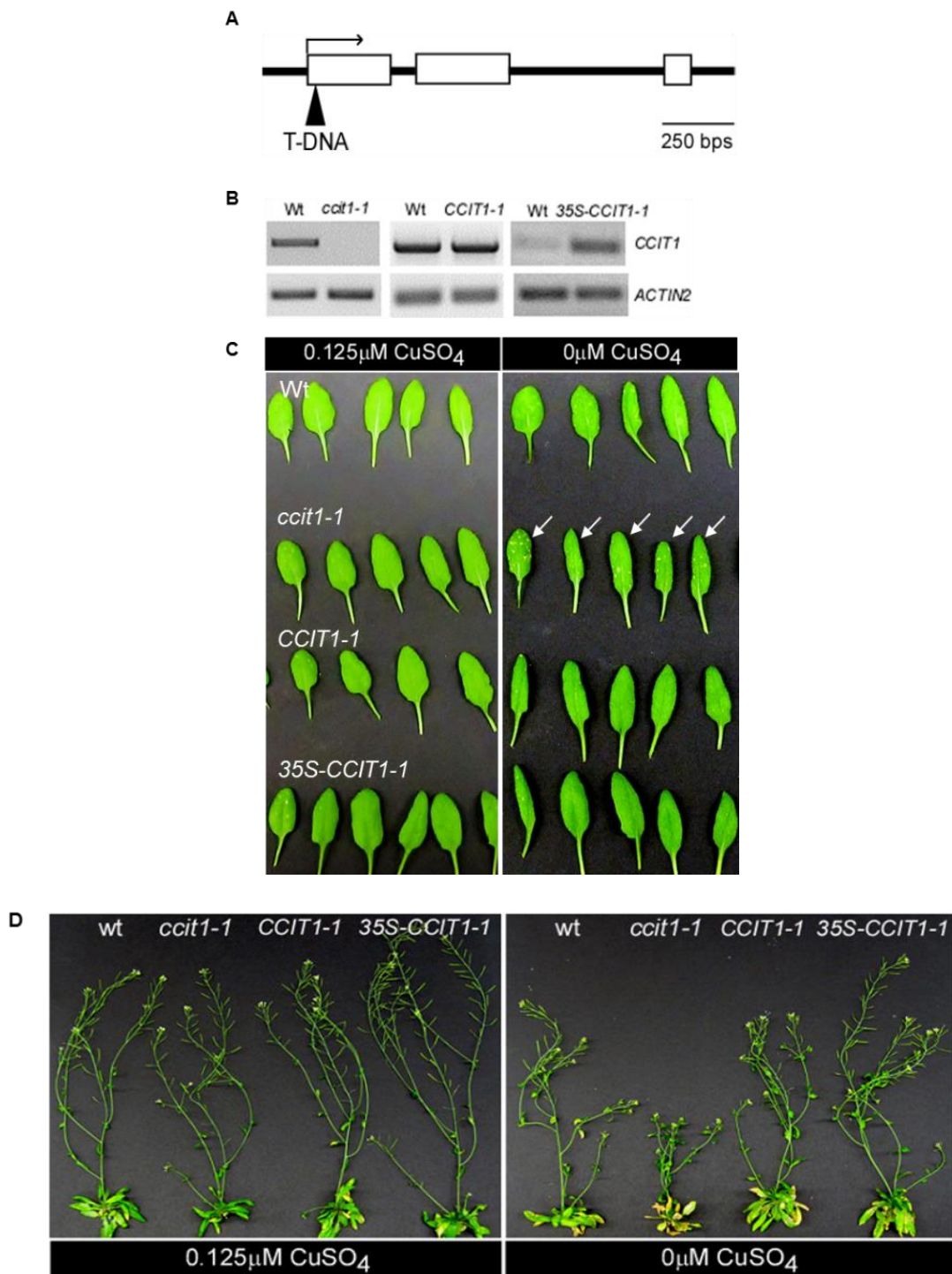


Figure 5. The *ccit1* mutant is hypersensitive to Cu deficiency. **A.** Shows an exon-intron structure of the *CCIT1* gene and the position of a T-DNA insertion site in *ccit1-1* allele. Black arrowheads indicate the T-DNA insertion, located 28 bps downstream from the start codon in the *ccit1-1* mutant allele respectively. Scale bar = 250 bps. **B.** Shows results of the semi-quantitative RT-PCR analysis of *CCIT1* expression in roots of 10-day-old wild-type (Wt),

the *ccit1-1* mutant, the *CCIT1* complemented line (*CCIT1-1*) and wild-type plants ectopically overexpressing 35S-*CCIT1* (35S-*CCIT1*). Wild-type, *ccit1-1* mutant and *CCIT1* plant lines were grown on ½ MS solid medium supplemented with 1000 µM BCS (to induce *CCIT1* expression and to show that *ccit1-1* is a knock-out plant line). 35S-*CCIT1-1* plants and corresponding wild-type were grown standard solid ½ MS medium. Twenty seven PCR cycles were performed to visualize *CCIT1* expression in roots of 35S-*CCIT1* transgenic plants and corresponding wild-type, while 30 cycles were performed to visualize *CCIT1* expression in the *ccit1-1* mutant and the *ccit1-1* mutant expressing the genomic *CCIT1* fragment. **C** and **D**, Wild-type, *ccit1-1*, *CCIT1-1* and 35S-*CCIT1-1* were grown hydroponically with 0.125 µM CuSO₄ or without CuSO₄ for 5 (**C**) or 8 (**D**) weeks. **C** shows 5th to 9th rosette leaves. Note the chlorotic spots between veins of rosette leaves in *ccit1-1*. The photo with all rosette leaves is presented in Supplemental Figure 2B. **D**, shows plant lines at the reproductive stage. Note the stunted growth of the *ccit1-1* mutant in response to low Cu status.

Because the *ccit1-1* mutant has fully lost the *CCIT1* transcript, it has been selected for more in-depth studies. To ascertain that phenotypes (if any) is associated with the *CCIT1* gene, I have also generated the *ccit1-1* mutant expressing the genomic *CCIT1* fragment encompassing the putative promoter region and the *CCIT1* open reading frame (ORF). In addition, I have generated wild-type transgenic plants ectopically expressing the *CCIT1* cDNA from the CaMV 35S promoter. Three independent one-copy-insertion lines for native promoter-*CCIT1* transgene (designated as *CCIT1-1*, *CCIT1-2* and *CCIT1-3*) and also for 35S promoter-*CCIT1* transgene (designated as 35S-*CCIT1-1*, 35S-*CCIT1-2* and 35S-*CCIT1-3*) were obtained for subsequent studies. Analyses of different transgenic lines by RT-PCR facilitated isolation of *ccit1-1* mutant plants expressing the genomic *CCIT1* fragment with similar *CCIT1* expression level as the wild-type (Figure 5B and Supplemental Figure 1B). I have also identified transgenic wild-type lines ectopically expressing *CCIT1* with an enhanced level of *CCIT1* expression compared to wild-type (Figure 5B and Supplemental Figure 1C).

3.6 The *ccit1* Knock-out Plants are Sensitive to Low Cu Condition

To test whether *CCIT1* function is essential for Cu homeostasis, wild-type, *ccit1-1*, *CCIT1-1* and 35S-*CCIT1* were grown hydroponically with or without Cu for 5 weeks until late vegetative (Figure 5C) or for 8 weeks until mid-reproductive stages (Figure 5D). I found that leaves of the *ccit1-1* mutant were indistinguishable from leaves of wild-type, both grown under Cu-sufficient conditions (Figure 5C). In contrast, leaves of *ccit1-1* plants started to exhibit Cu deficiency symptoms manifested by chlorotic spots

between veins of mature rosette leaves after 5 weeks of growth under Cu-deficient condition, while wild-type plants were still able to tolerate Cu deficiency at this stage (Figure 5C). Further growth under Cu deficiency has led to severe chlorotic spots in old leaves of the *ccit1-1* plants, which gradually appeared in young rosette leaves, whereas wild-type and *CCIT1* plants developed these symptoms significantly later (Figure 5C and Supplemental Figure 1E and I). When plants were grown to the reproductive stage under Cu deficiency, the *ccit1-1* mutant had severely stunted stem elongation, less branched stem, wilting cauline leaves and decreased seed set compared to wild-type, the complemented and overexpressing line (Figure 5D). Importantly, the genomic *CCIT1* fragment complemented *ccit1-1* sensitivity to Cu deficiency (Figure 5D), suggesting that the latter phenotype is due solely to the *ccit1-1* knockout. Further, wild-type plants ectopically expressing the 35S-*CCIT1* construct were significantly less sensitive to Cu deficiency than either of other plant lines (Figure 5D).

I also tested the sensitivity to Cu deficiency of the knockdown, *ccit1-2* allele. I found that although Cu deficiency phenotype was not as severe as in *ccit1-1* plants, the *ccit1-2* knockdown mutant still showed chlorotic symptoms in rosette leaves after 5-weeks of Cu deficiency and had decreased stem growth after 8-weeks of Cu deficiency compared to wild-type (Supplemental Figure 2D-I). Together these data indicate that *CCIT1* is a novel transcription regulator, which function is important for the ability of *A. thaliana* to grow under Cu deficiency.

3.7 *CCIT1* is Essential for Cu Accumulation in Roots and Shoots of *A. thaliana*

To test whether the increased sensitivity of the *ccit1-1* mutant to Cu deficiency is associated with altered ability of plants to uptake Cu into roots and/or translocation it into shoots, I compared Cu concentrations in roots, young and mature leaves of wild-type, *ccit1-1* mutant and *CCIT1* plants. Cu concentration in roots and mature leaves of the *ccit1-1* mutant are 38% and 21% lower, respectively than in corresponding tissues of wild-type, whereas Cu concentration in young leaves of the *ccit1-1* mutant was only about 10% lower compared to wild-type (Figure 6A and B). Interestingly, all tissues of the *CCIT1-1* complemented line accumulated more Cu than corresponding tissues of wild-type. Currently, I cannot explain this phenomenon. Nevertheless, data presented in Figure 6 indicate that *CCIT1* controls Cu uptake into roots and Cu translocation from roots to mature leaves in *A. thaliana*.

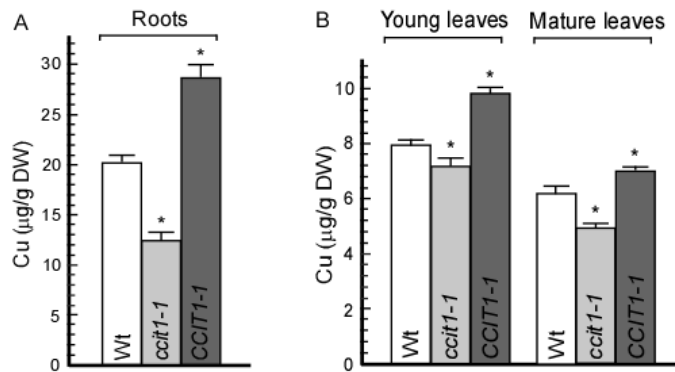


Figure 6. Cu concentration in roots and rosette leaves of 5-week-old wild-type, *ccit1-1* and *CCIT1-1* grown hydroponically. Asterisks (*, $p \leq 0.05$) indicate statistically significant differences in Cu concentration between wild-type (Wt), *ccit1-1* mutant, *CCIT1* (*CCIT1-1*) complemented plants. Error bars indicate S.E (n=5).

3.8 *CCIT1* and *SPL7* act in a parallel interacting pathway regulating Cu homeostasis

As indicated in Introduction, SPL7 was the only transcription regulator in vascular plants with the documented role in Cu homeostasis (Yamasaki et al., 2009b). To examine the relationship between *CCIT1*

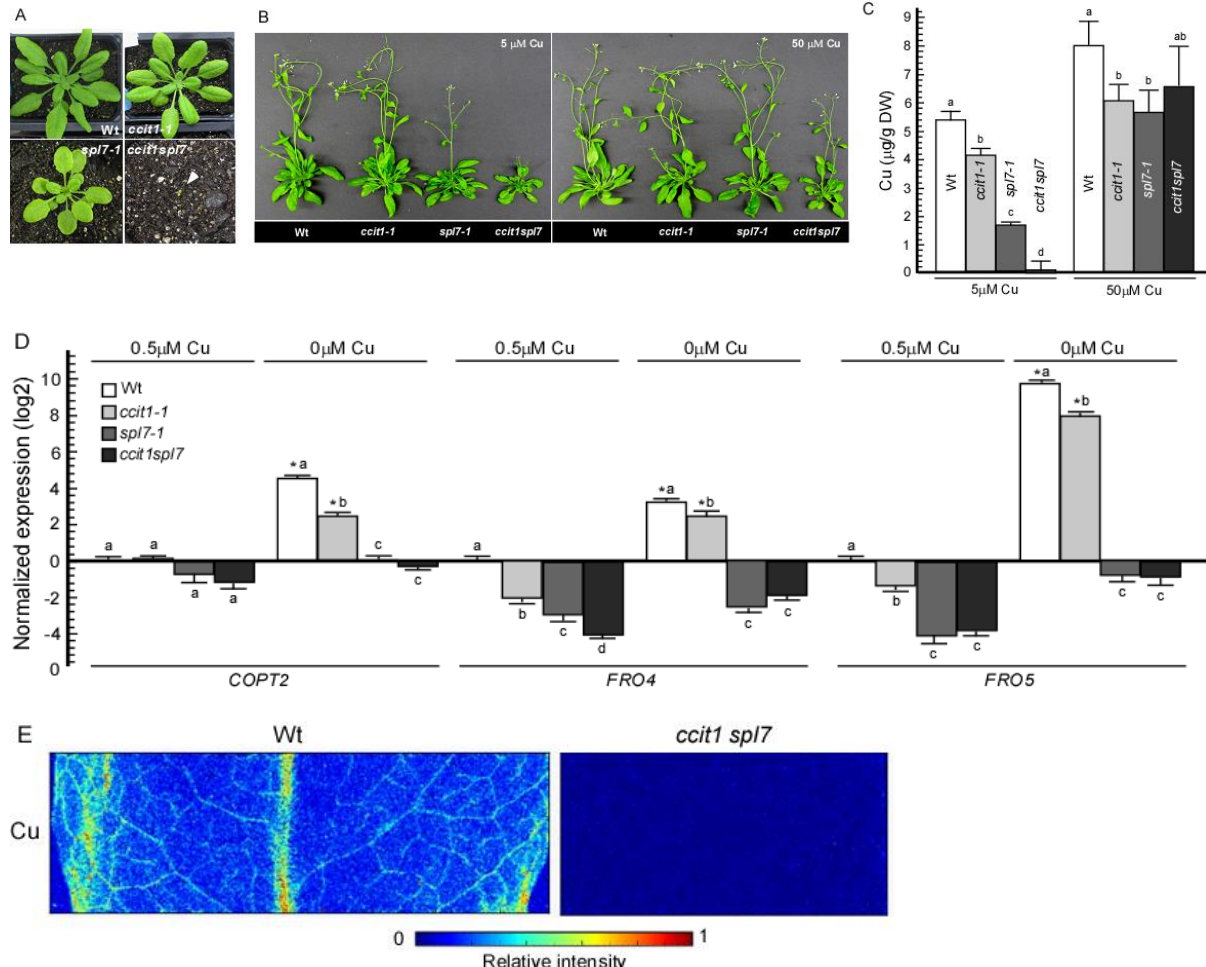


Figure 7. *CCIT1* and *SPL7* act in a parallel interacting pathways regulating Cu homeostasis. **A**, Seeds of the indicated plant lines were germinated and grown in soil fertilized with a standard nutrient solution containing 0.125 μM of CuSO_4 (Arteca and Arteca, 2000a). Note the retarded growth of the *ccit1spl7* double mutant (white arrowhead) that has eventually died. **B**, seeds were germinated hydroponically in medium supplemented with 0.5 μM CuSO_4 and transferred to soil with indicated concentrations of Cu. Different lower-case letters indicate the statistically-significant differences of Cu concentration between wild-type (Wt), *ccit1-1*, *spl7-1* and *ccit1spl7* ($p \leq 0.05$). Error bars indicate S.E (n=5). **C**, Cu concentration in 4 genotypes under indicated condition. Different letters ($p \leq 0.05$) indicate statistical significance in Cu concentration between wild-type (Wt), *ccit1-1*, *spl7-1* and *ccit1spl7*. Error bars indicate S.E (n=5). **D**, qRT-PCR comparison of the transcript abundance of *COPT2*, *FRO4* and *FRO5* in roots of 5-week-old wild-type, *ccit1-1*, *spl7-1* and *ccit1spl7* cultured in hydroponic system with 0.5 μM CuSO_4 for the first 3 weeks and transferred to hydroponic solution with or without CuSO_4 for another 2 weeks. Error bars indicate S.E. (n = 6). Results are presented relative to the gene expression in wild-type under 0.5 μM CuSO_4 , which was designated as 1. Asterisks (*, $p \leq 0.05$) indicate statistically significant differences in gene expression between control (0.5 μM CuSO_4) and treated (0 μM CuSO_4) plants, different letters indicate statistically significant differences in gene expression between different genotypes ($p \leq 0.05$). **E**, shows SXRF microphotographs from the preliminary analyses of Cu localization in rosette leaves of wild-type and *ccit1spl7* mutant.

and *SPL7*, we generated the *ccit1-1spl7-1* double mutant (from here on *ccit1spl7*). We then compared the growth and development of the double mutant with the growth and development of each of the single mutant

and wild-type, all grown under standard Cu-sufficient conditions. Consistent with our previous findings, the growth of wild-type and the *ccit1-1* mutant was indistinguishable under Cu-sufficient conditions (Figures 5C and 7A). The *spl7-1* mutant was somewhat smaller than the wild-type, which is consistent with observations of Yamasaki et al. (2009). In contrast, the growth of the *ccit1spl7* double mutant was arrested in the early seedling stage, and the double mutant eventually died (Figure 7A). These data suggest that *CCIT1* and *SPL7* act in the parallel interacting pathway and that the regulation of Cu homeostasis in *A. thaliana* is more complex than previously thought.

To test whether Cu can rescue the *ccit1spl7* double mutant, *ccit1spl7* were grown in soil fertilized with 5 μ M or 50 μ M CuSO₄. The growth of wild-type and the *ccit1-1* mutant was indistinguishable in soil supplemented with 5 μ M of Cu and both plant lines developed into fertile adults (Figure 7B). The *spl7-1* mutant also developed into the fertile adult under 5 μ M of Cu, although it was still smaller than wild-type or *ccit1-1* plants (Figure 7B). I also found that 5 μ M CuSO₄ rescued the seedling lethality of *ccit1spl7* double mutant, but its growth was arrested at very early reproductive stage (Figure 7B). Consistent with growth phenotypes, shoots of both, *ccit1-1* and *spl7-1* mutants accumulated significantly less Cu than wild-type plants, whereas Cu concentration in shoots of the double mutant was just at the minimal detection level (Figure 7C). Further, preliminary Synchrotron-based X-ray fluorescent microscopy (SXRF) experiments identified Cu accumulation in major and minor veins of wild-type rosette leaf, an almost disappearance in *ccit1 spl7* double mutant rosette leaf (Figure 7E). Soil fertilization with 50 μ M CuSO₄ fully rescued *spl7* mutant phenotype while did not affect the normal growth of wild-type and the *ccit1-1* mutant (Figure 7B). At this concentration of Cu, the *ccit1spl7* mutant reached and went through the reproductive stage (Figure 7B). Consistent with these phenotypes, all mutant lines accumulated about 6 μ g/g DW of Cu in shoots, which, although was less than the concentration of Cu in shoots of wild-type, but was within the range that is required for growth and development ((Marschner, 1995) and Figure 7C).

The transcript abundance analysis of the Cu uptake related genes revealed that the expression of *COPT2*, *FRO4* and *FRO5* were downregulated in *ccit1-1*, *spl7-1* mutants under Cu replete condition, loss of both *CCIT1* and *SPL7* function impaired the expression of *COPT2* and *FRO4* even further (Figure 7D),

which is consistent with the results of Cu concentration analysis (Figure 7C). Under Cu deficient conditions, the induction of *COPT2*, *FRO4* and *FRO5* was impaired in *ccit1-1* and *spl7-1* mutants, whereas in the *ccit1spl7* double mutant, the impair effect was similar to *spl7-1* single mutant (Figure 7D).

3.9 The *ccit1spl7* Double Mutant has Nonviable Pollens and Altered Gynoecium Morphology

Although Cu was able to rescue the growth and development of the *ccit1spl7* double mutant, the mutant has a thinner stem, longer internodes, fewer flowers in the panicle (Figure 8A), shorter siliques and no seeds compared with wild-type, *ccit1-1* and *spl7-1* single mutant (Figure 8B-D). I also noticed that pistils are longer than filaments in the *ccit1spl7* double mutant (Fig. 8D), which could create a barrier for pollen loading to the stigma. To examine whether the infertile phenotype resulted from a defect in androecium (the male part of the flower) or gynoecium (the female part of the flower), I hand pollinated the *ccit1 spl7* carpels with wild-type pollen and found that wild-type pollen was able to fertilize the *ccit1 spl7* plants (Supplemental Figure 3B). This result confirmed that female fertility of the double mutant was normal. In contrast, the pollen from the double mutant failed to fertilize wild-type carpels suggesting that the male fertility of the double mutant was compromised (Supplemental Figure 3B).

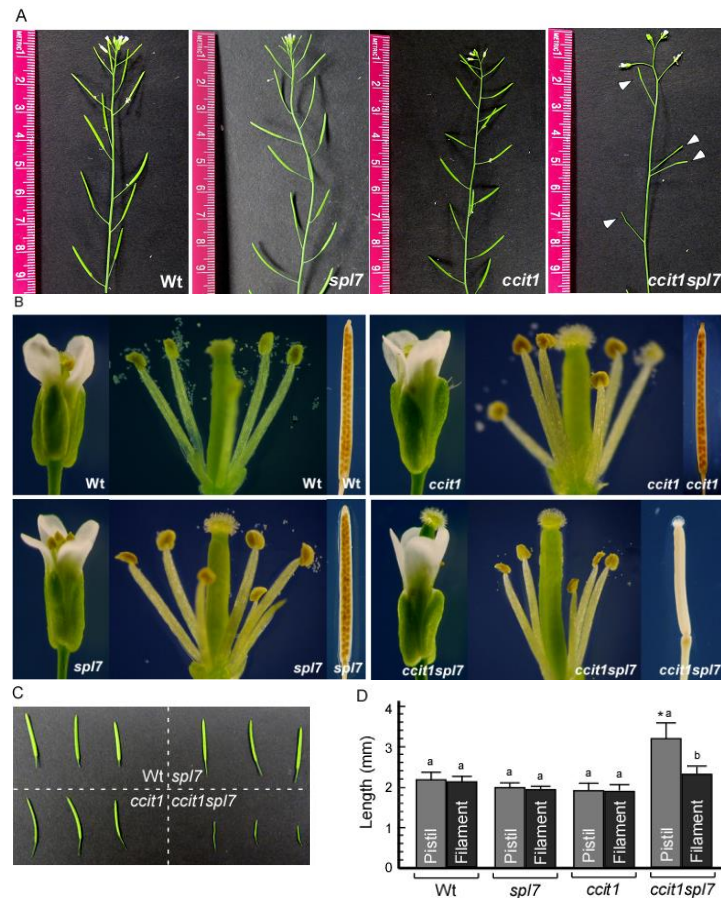


Figure 8. The altered morphology of the *ccit1spl7* double mutant. Wild-type (Wt), *ccit1-1* (*ccit1*), *spl7-1* (*spl7*), and *ccit1spl7* double mutant plants were grown hydroponically with 0.5 μM CuSO_4 . **A**, shows a comparison of stems and panicles between different lines. Note the thin stem, the long internode, infertile carpel and few flowers in *ccit1spl7*. **B** to **C**, Comparison of the flower and siliques between different lines. Note the longer pistil than filament of *ccit1spl7*. **D**, The length (mm) of pistil and filament in wild-type (Wt), *spl7-1* (*spl7*), *ccit1-1* (*ccit1*) and *ccit1spl7* double mutant. Error bars indicate S.D. (n = 10). Asterisks (*, p < 0.05) indicate statistically significant differences in length between pistil and filament of the same genotype, a letter “a” (p < 0.05) indicates statistically significant differences between wild-type and other plant lines.

In addition, there was a significant decrease in total pollen and viable pollen in *ccit1spl7* compared to wild-type or two single mutants (Figure 9A to C), demonstrating that the pollen yield and fertility is significantly altered in the *ccit1spl7* double mutant. These data provide an important molecular link between Cu homeostasis and plant fertility in *A. thaliana*. To examine whether Cu supplement can rescue pollen sterility of the *ccit1spl7* double mutant, 50 µM CuSO₄ was used once two week to fertilize *ccit1spl7* double mutant. After 3 weeks, a few siliques formed in *ccit1spl7* (Supplemental figure 3C), which indicates that additional Cu can partially rescue the pollen sterility of *ccit1spl7* double mutant.

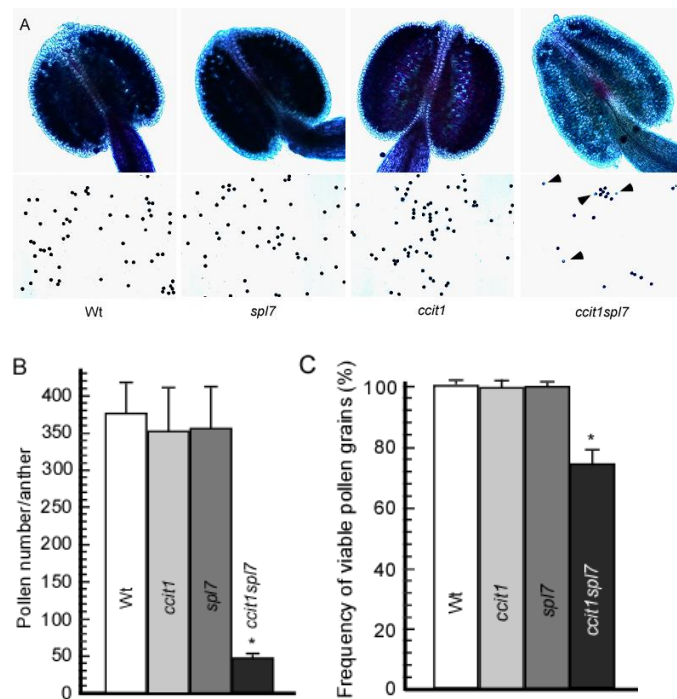


Figure 9. Pollen viability assay of wild-type, *spl7-1*, *ccit1-1* and *ccit1spl7* double mutant. **A**, Alexander staining of pollens in anther from different lines, showing that a significant number of pollen grains from *ccit1spl7* are nonviable. Viable pollen grains stained dark violet, while nonviable pollen grains were pale turquoise. Black arrow heads indicate the nonviable pollens. **B**, The total pollen production from different lines. **C**, The frequency of viable pollens from different lines. In **B** and **C**, error bars indicate S.D. (pollens from 5 anthers of different flowers). Asterisks (*, p < 0.05) indicate statistically significant differences between different genotypes.

3.10 Copper Localizes to Anthers in Flowers and is Essential for Plant Fertility

To investigate the role of Cu in plant fertility, wild-type plants were grown in hydroponic solution with or without Cu for 8 weeks and the reduction of seed setting was observed (Figure 10A). Pollen viability assay

revealed more than half of the pollen in the treatment with limited Cu supply were nonviable, which might be among reasons of the reduced seed set of *A. thaliana* under Cu deficiency (Figure 10C). Further, preliminary Synchrotron-based X-ray fluorescent microscopy (SXRF) experiments identified Cu in anthers of stamens, a reduction of Cu accumulation was observed in *ccit1-1*, and almost no Cu was found in *sp17* plants (Figure 10C).

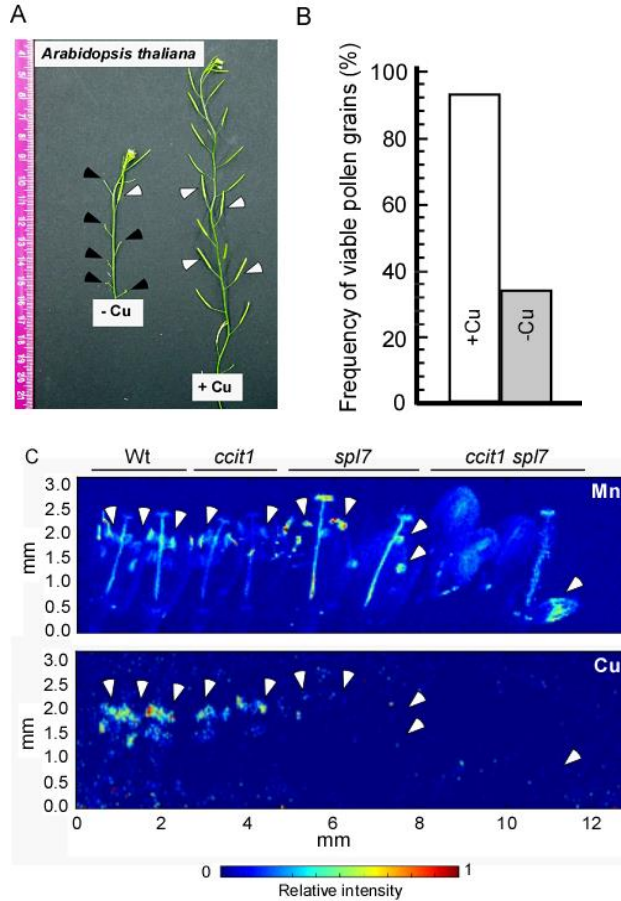


Figure 10. Cu deficiency significantly affects the seed setting and pollen viability. **A.** Wild-type plants were grown in hydroponic solution with or without 0.125 μM CuSO_4 (+Cu vs. -Cu) for 8 weeks. White arrowheads point to fertile siliques, and black arrowheads point to infertile siliques. **B.** Alexander staining of pollens in anther from wild-type plants grown in hydroponic solution with or without 0.125 μM CuSO_4 (+Cu vs. -Cu). The frequency of viable pollens under sufficient Cu (0.125 μM CuSO_4 ; +Cu) and limited Cu (0 μM CuSO_4 ; -Cu) conditions was counted. **C.** shows SXRF microphotographs from the preliminary analyses of Cu localization in different organs of flowers. Manganese (Mn) localization is shown for comparison and the location of anthers. White arrows indicate anthers.

Together, these data point to the important role of Cu in flower fertility, a phenomena that has been recognized for decades, but not comprehensively investigated.

3.11 Copper Deficiency Significantly Alters Transcriptome of *A. thaliana*

Despite the recognized role of Cu in plant fertility (Marschner, 1995; Burkhead et al., 2009), our knowledge of the molecular components regulating Cu homeostasis and responsive to Cu deficiency in the reproductive organs of plants is surprisingly limited. To fill this gap, RNA-seq was performed to identify Cu responsive genes in floral buds (a mix of developmental stages 10-12 as defined (Bowman et al., 1991; Alvarez-Buylla et al., 2010a)) and mature flowers (open and fertilized flowers at the developmental stage 14 as defined by (Bowman et al., 1991; Alvarez-Buylla et al., 2010a)) of *A. thaliana*. Plants were grown hydroponically for 7 weeks under Cu-sufficient conditions. To achieve Cu deficiency, half of plants were grown without Cu for the last one week. Inductively-coupled plasma mass spectrometry revealed that internal concentration of Cu was 8.85 or 1.53 µg/ g dry weight in flowers collected from plants under sufficient or Cu deficient conditions (Supplemental figure 5). These internal Cu concentrations are within the expected range for Cu sufficient or Cu deficient conditions (Marschner, 1995; Burkhead et al., 2009).

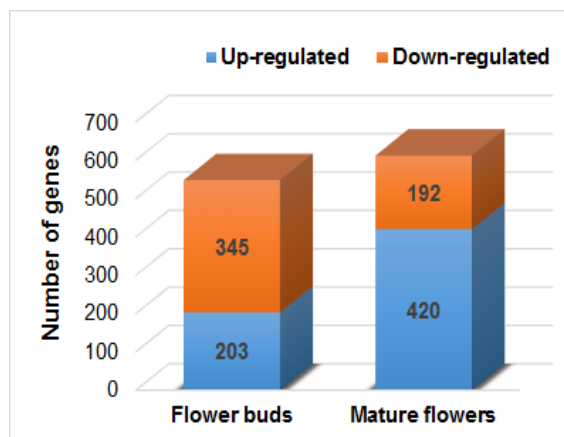


Figure 11. Cu deficiency significantly affects the transcriptome profile in flowers. Bars represent number of genes transcriptionally responding to Cu deficiency in flowers (ratio ≥ 2 or ratio ≤ 0.5 ; 0.05 false-discovery rate).

RNA-seq identified 353 million final clean reads in total (Supplemental table 5). I identified 548 and 612 genes that responded transcriptionally to Cu deficiency in young and mature flowers, respectively, a false-discovery rate (FDR) lower than 0.05 (Figure 11). Interestingly, the number Cu-responsive genes increased with the age (the developmental stage) of flowers. Further, the ratio between up-regulated and down-regulated genes has significantly changed (Figure 11). Specifically, the number of genes that were up-regulated by Cu deficiency was 2-fold higher, while down-regulated genes was 1.8-fold lower in mature

flowers in comparison with younger floral buds. These results indicate that Cu deficiency significantly alters the flower transcriptome in *A. thaliana*, and the alteration is different in floral buds from mature flowers. The transcriptional response of some genes to Cu deficiency was dynamic concerning the developmental stage of flowers. For example, the transcriptional response of *CCIT1* to Cu deficiency increased from 23-fold in younger to 148-fold in older flowers. Expression of genes encoding the Cu transporter, *COPT2* (Gayomba et al., 2013) was upregulated by Cu deficiency in young flowers (by 9.8-fold) but not in mature flowers. Expression of another Cu transporter, *YSL2* (DiDonato et al., 2004) increased with flower age in response to Cu deficiency from 2.5- to 4.9-fold in young and old flowers respectively. These findings suggest the existence of specific requirements for Cu at distinct developmental stages. Further, global functional analysis of Cu-responsive genes using the Plant MetGenMAP package (Joung et al., 2009) revealed an overrepresentation of genes involved in transcriptional regulation, response to biotic and abiotic stresses, metabolic processes and transport (Supplemental table 6-9). Many genes of unknown function were also recovered (not shown). We note that several genes that are involved in JA synthesis were downregulated by Cu deficiency in mature flowers. Among them was *DEFECTIVE ANTER DEHISCENCE 1 (DADI)* that plays an essential role in anther dehiscence, pollen maturation, and flower opening, suggesting a connection between Cu homeostasis, JA pathway and plant fertility (Peng et al., 2013).

These findings suggest that downregulation of the expression of genes that are essential could be among the contributing factors of Cu deficiency-promoted reduction in plant fertility.

3.12 Transcriptional Response of *CCIT1* to Cu Limitation in Flowers and Roots is Partially Independent of *SPL7*, Novel Transcriptional Regulator Exists to Control *CCIT1* Expression

Recent transcriptome analyzes have identified *CCIT1* among the downstream targets of *SPL7* in the shoot of *A. thaliana*, suggesting that *CCIT1* acts in a linear *SPL7*-dependant pathway (Yamasaki et al., 2009b; Bernal et al., 2012a). To reconcile our data with the transcriptome studies, we asked whether the

transcriptional response of *CCIT1* to Cu availability in other tissues, such as roots and flowers, depends on *SPL7* as well. Consistent with our previous findings, the expression of *CCIT1* in roots and leaves of wild-type plants was upregulated by Cu deficiency (Figure 12). *CCIT1* expression was also upregulated in flowers of wild-type plants in response to Cu deficiency (Figure 12). As we expected based on observations of Yamasaki et al. (2009) and Bernal et al. (2012), the transcriptional response of *CCIT1* in leaves fully depended on *SPL7* (Figure 12). In contrast, *CCIT1* expression in roots and flowers was still upregulated in the *spl7-1* mutant under Cu-deficiency (Figure 12). I concluded based on these findings that other TFs in addition to *SPL7* regulate the transcriptional response of *CCIT1* to Cu deficiency in roots and flowers. These results are also consistent with our suggestion that *CCIT1* and *SPL7* act in the parallel interacting pathway in regulating Cu homeostasis.

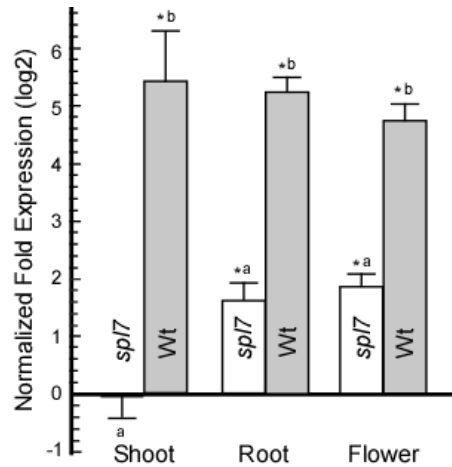


Figure 12. The transcriptional response of *CCIT1* to Cu limitation depends, in part, on *SPL7*. qRT-PCR comparison of the transcript abundance of *CCIT1* in shoots, roots of 5-week-old and flowers of 8-week-old wild-type (Wt) and *spl7-1* mutant (*spl7*) cultured in hydroponic system with 0.25 μ M CuSO₄ (control) for the first 3 (for shoots and roots) and then without Cu for subsequent 3 weeks prior collecting roots and shoot. To enable plants to grow to the reproductive stage, I grew plants with 0.5 μ M CuSO₄ (control) for the first 5 weeks, then transferred to a medium without Cu and continued to grow them for another 3 prior flower harvesting. Error bars indicate S.E. (n = 6). Results of wild-type are presented relative to wild-type plants grown under control conditions, which was designated as 0 (log2). Asterisks (*, p ≤ 0.05) indicate statistically significant differences in gene expression between control and Cu-deficient-treated plants, a letter “a” indicates statistically significant differences in gene expression between Wt and *spl7* mutant (p ≤ 0.05).

3.13 RNA-seq Identified Common and Unique Downstream Targets of *SPL7* and *CCIT1* in Flowers

Given the acute floral phenotype of the *ccit1spl7* double mutant (Figure 8 and 9) in flower development and male fertility, and partial independence of the *CCIT1* from *SPL7* in flowers (Figure 12), we next used RNA-seq analysis in flowers to identify the downstream *CCIT1* and *SPL7* targets and separate the *CCIT1*- and *SPL7*-dependent transcriptional networks regulating Cu homeostasis and plant fertility. Under control condition, among the downregulated target in the *ccit1-1 mutant*, 59.6% and 59.3% of them were also found to be *SPL7*-dependent in floral buds and mature flowers, respectively, whereas under Cu-deficient condition, the proportion of common targets was reduced to 16% and 25.6% in floral buds and mature flowers (Figure 13A and B), respectively, indicating that during Cu starvation, *CCIT1* plays a more independent role.

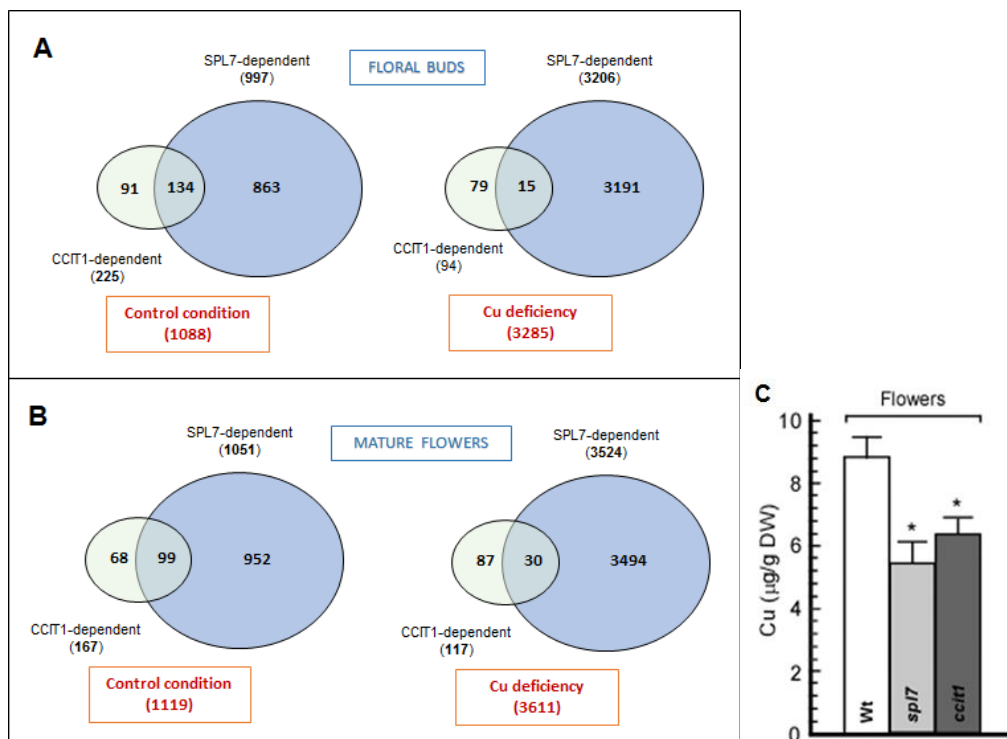


Figure 13. Comparison of the transcriptome profile in flowers from *ccit1* and *spl7*. A and B shows venn diagram of Cu deficiency-regulated genes unique to and shared between *SPL7* and *CCIT1* in young (flower buds [A]) and mature flowers (B). Genes that transcriptionally changed in *ccit1* mutant and their dependence on *SPL7* in roots and shoots under control (0.5 μM CuSO₄) and Cu deficient (0 μM CuSO₄) conditions. Ovals represent the number of genes for which transcript levels were changed in *ccit1-1* and *spl7-1* mutant under indicated conditions. (Ratio >=2 or ratio <=0.5, FDR<=0.05). C. Wild-type, *ccit1-1* and *spl7-1* plants were grown in hydroponic solution with 0.5 μM CuSO₄ for 8 weeks, the inflorescence heads were harvested for Cu concentration analysis by ICP-MS.

More interestingly, we also found the genes that are suppressed by Cu deficiency in wild-type plants, such as *CSD1*, *CSD2*, *LAC2* and *CCS* (Cu-economy model(Ravet and Pilon, 2013a), were also downregulated

in *ccit1-1* mutant, and the genes that are reported to be induced by limited Cu, such as *FSD1*, *COPT2* and *YSL2*, were also upregulated in *ccit1-1*, suggesting that the Cu-deficiency response was activated in *ccit1-1* mutant even under sufficient Cu condition (Table 1). These data also indicate that these genes are not among the downstream targets of CCIT1 in flowers. However, this transcriptional response to Cu deficiency was totally abolished in *spl7* (Table 1), suggesting that *CSD1*, *CSD2*, *LAC2*, *CCS*, *FSD1*, *COPT2* and *YSL2* are among the downstream targets of SPL7 in flowers. Cu concentration in flowers of wild-type, *ccit1-1*

Table 1. Transcripts that are involved in Cu deficiency response are also induced in *ccit1* mutant under Cu sufficient condition

Gene	Annotation	Ratio			Tissue
		(-Cu/+Cu) in Wt	<i>ccit1</i> /Wt in +Cu	<i>spl7</i> /Wt in +Cu	
<i>CSD1</i>	Copper/zinc superoxide dismutase 1	0.3*	0.4*	1.2	Mature flower
<i>CSD2</i>	Copper/zinc superoxide dismutase 2	0.3*	0.4*	1.1	Mature flower
<i>LAC2</i>	Laccase 2	0.3*	0.4*	0.8	Mature flower
<i>APRN</i>	Plantacyanin	0.3*	0.4*	1.1	Mature flower
<i>FSD1</i>	Iron superoxide dismutase 1	29.5*	26.6*	0.3*	Mature flower
<i>CCH</i>	Copper chaperone	2.1*	2*	1	Mature flower
<i>YSL2</i>	Yellow stripe like 2	4.9*	4.2*	0.8	Mature flower
<i>CSD1</i>	Copper/zinc superoxide dismutase 1	0.2*	0.3*	1	Floral bud
<i>CSD2</i>	Copper/zinc superoxide dismutase 2	0.3*	0.3*	1.1	Floral bud
<i>CCS</i>	Copper chaperone for SOD1	0.3*	0.4*	1.3	Floral bud
<i>FSD1</i>	Iron superoxide dismutase 1	55.2*	49.9*	0.1	Floral bud
<i>YSL2</i>	Yellow stripe like 2	2.5*	2.2*	0.05*	Floral bud
<i>COPT2</i>	Copper transporter 2	9.8*	5.7*	0.03	Floral bud

The genes that were reported previously to be responsive to Cu deficiency in roots or shoots are also found in our RNA-seq analysis in flowers. that were significantly up- or down-regulated by Cu deficiency (-Cu) compared to Cu replete condition (+Cu), and the genes that were significantly up- or down-regulated in *ccit1-1* (*ccit1*) or *spl7-1* (*spl7*) mutant compared to wild-type under Cu replete condition are summarized in this table (“*” indicates FDR≤0.05).

and *spl7-1* was then measured by ICP-MS. Consistent with the RNA-seq results, Cu concentration was significantly lower in flowers from *ccit1-1* and *spl7-1* compared with wild-type (Figure 13C).

By comparing the transcriptome profiles in mature flowers between wild-type and *ccit1-1* mutant under Cu replete and deficient conditions, we found significant enrichment of the genes that are involved in anther development, reproductive structure development, seed development and stamen development were downregulated in *ccit1-1* mutant, indicating an essential role of CCIT1 in plant fertility (Supplemental table 10 and 11).

3.14 Jasmonic acid biosynthetic pathway is significantly changed in *spl7* and *ccit1* mutants

By using the Plant MetGenMAP package [27], we identified enrichment of changes in jasmonic acid (JA) biosynthetic pathway in both *spl7-1* and *ccit1-1* mutant, such as lipoxygenase 3 and 4 (*LOX3* and *LOX4*), allene oxide synthase (*AOS* or *DDE2*), 12-oxophytodienoic acid reductase3 (*OPR3* or *DDE1*), which catalyzes different steps of JA biosynthesis and they are also the key components in male fertility (Figure 14). *LOX3* and *LOX4* are among the lipoxygenases which typically catalyze the oxygenation of fatty acid which serves as the precursor of jasmonate (Caldelari et al., 2011). Loss of function of both of them resulted in male sterility phenotype and a drastic reduction of seed set (Caldelari et al., 2011), which highly resembled the phenotype of *ccit1spl7* double mutant (Figure 8 and 9). Mutation of *AOS* or *OPR3* causes delayed anther dehiscence and male sterility (Stintzi and Browse, 2000; Park et al., 2002). In addition to genes shown in Figure 14, *DAD1* was also significantly downregulated in both *spl7* and *ccit1* mutants compared with wild-type and downregulated by Cu deficiency in mature flowers (not shown in figure 14). *DAD1* encodes a phospholipase A1 (PLA1) lipolytic enzyme that catalyzes the initial step of JA biosynthesis from phospholipids to linolenic acid, and is essential for anther dehiscence, pollen maturation, and flower bud development (Ishiguro et al., 2001a). Therefore, it is possible that impaired expression of genes from the JA biosynthetic pathway in *ccit1* and *spl7* mutants could be suggested among the reason of male sterility of the double mutant.

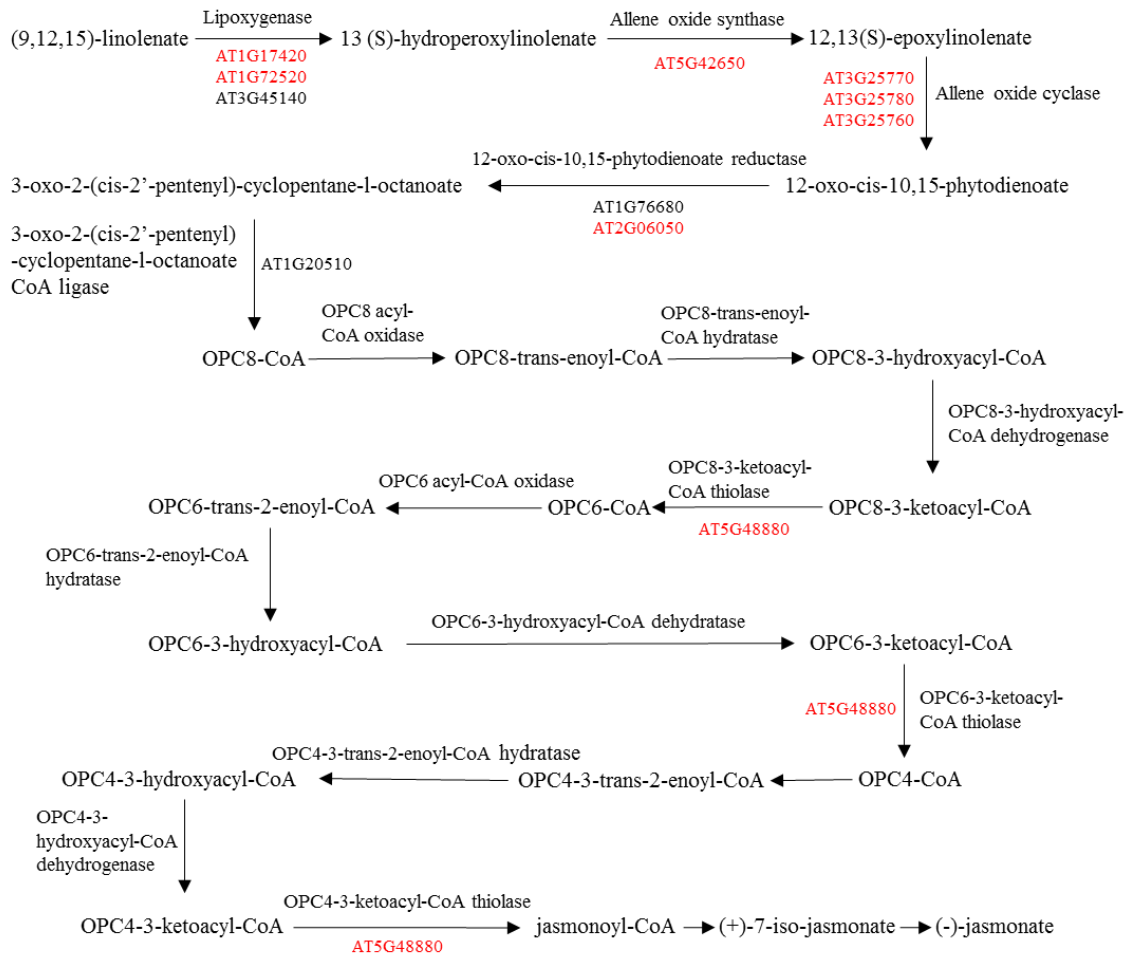


Figure 14. SPL7 and CCIT1 dependent genes that are involved in the JA biosynthetic pathway. The biosynthetic pathway of jasmonic acid is showing in this figure. The genes that were 1.5 fold significantly (FDR<0.05) up in flowers of wild-type than the *ccit1-1* mutant are included in this figure. Gene ID in red are the common targets of SPL7 and CCIT1, gene ID in black are the unique targets of SPL7.

3.15 RNA-seq Identified Common and Unique Downstream Targets of SPL7 and CCIT1 in Roots and Shoots

I then used RNA-seq to identify common and unique targets of CCIT1 and SPL7 in roots and shoots. I obtained a total of 136.8 million reads, which were mapped to the *Arabidopsis* genome and employed for the estimation of transcript abundance and differential expression (Supplemental Table 4). In doing so I have identified 126 and 21 in roots and shoots of wild-type that were upregulated and downregulated by

Cu deficiency, respectively. (Supplemental Figure 6). Smaller number of differentially expressed genes was identified in roots and shoots of the *ccit1* mutant under control condition than Cu deficient condition,

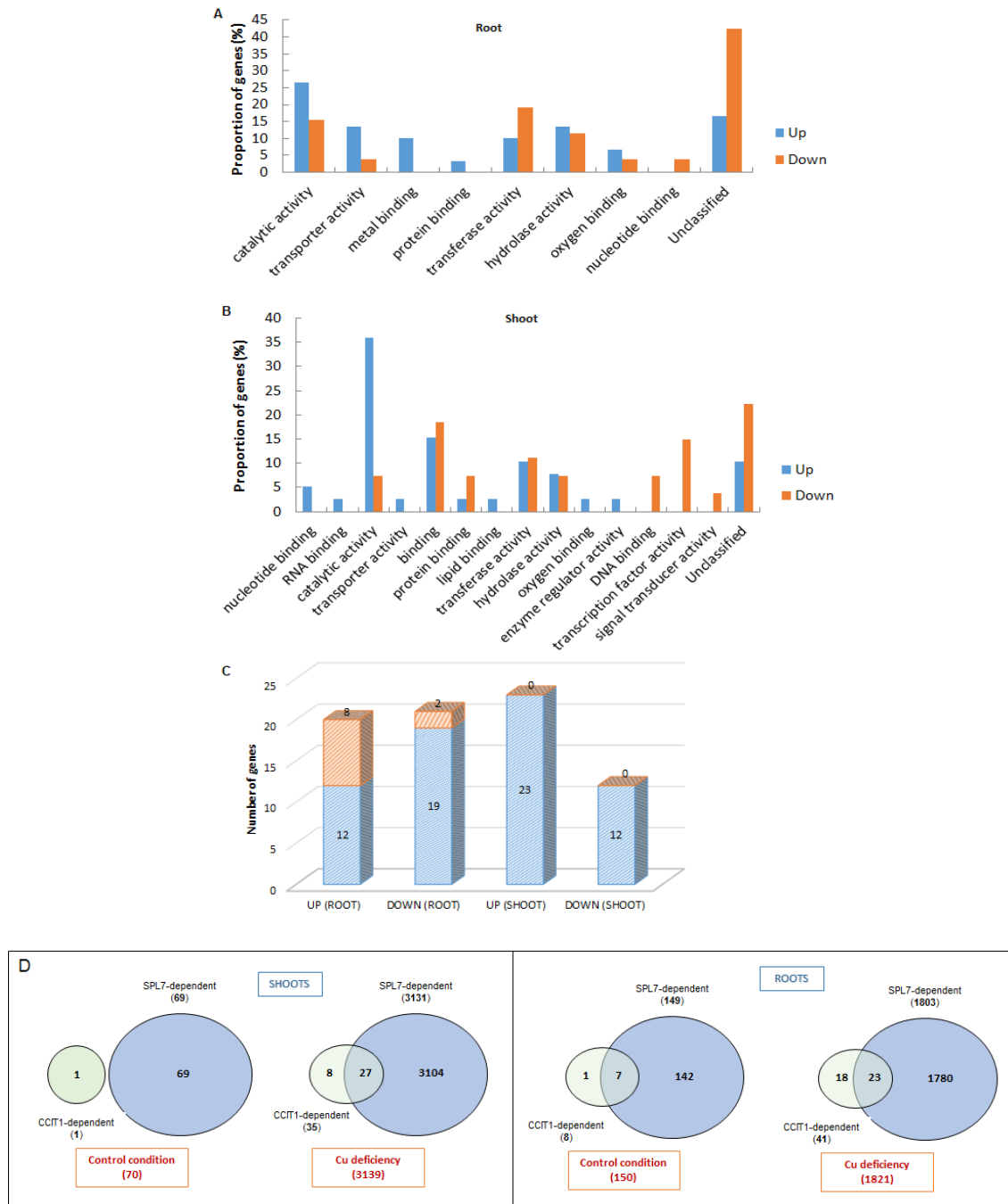


Figure 15. The CCIT1-dependent transcriptional profile and its comparison to wild-type and SPL7 according to RNAseq data. A-B. Functional categories represented by the CCIT1-dependent genes in roots (A) and shoots (B). Bars represent the proportion of genes for which transcript levels was changed in the *ccit1* mutant compared to wild-type in each category. Blue bars represent the genes that were up-regulated by CCIT1, and red bars represent the genes that were down-regulated by CCIT1. C. The number of genes that were downregulated (DOWN) or upregulated (UP) in roots and shoots by CCIT1 under Cu deficient condition, which also responded transcriptionally to Cu deficiency

according to RNA-Seq. The orange bars represent the CCIT1-dependent genes that were also responsive to Cu deficiency, the blue bars represent the CCIT1-dependent genes whose expression level were not significantly changed under limited Cu condition. **D**, Venn diagram shows number of CCIT1- and SPL7-specific and common targets. In **A** to **D**, transcript abundance was concluded to increase/decrease for a gene between 2 different conditions (control *vs.* Cu deficiency) or 2 genotypes (wild-type *vs.* *ccit1-1* or *spl7-1*) when arithmetic means of transcript abundances differed by a factor of at least 2 (FDR<0.05). 6-week-old plants were grown under control condition (0.25 μm CuSO₄) for the first 3 weeks and then continued to grow in control solution or transferred to Cu-deficient (0 μm CuSO₄) hydroponic solution for the last 3 weeks.

compared to wild-type (Figure 15D), which may results from the quite low expression of *CCIT1* under control condition, but highly induced under Cu starvation. Nevertheless, 20 genes were upregulated in roots by CCIT1, among which 8 genes were induced by Cu deficiency, indicating these genes are activated by CCIT1 in response to limited Cu; 21 genes were downregulated in roots by CCIT1, among which 2 genes were reduced by Cu deficiency, indicating these genes are suppressed by CCIT1 in response to limited Cu (Figure 15C). In shoots, 23 and 12 genes were upregulated or downregulated in by CCIT1, whereas they were not responsive to Cu deficiency (Figure 15C).

Analyses of gene expression profiles in roots under Cu-deficient condition between wild-type, *ccit1* and *spl7* mutants revealed that transcript levels of 41 and 1803 genes were changed in the *ccit1* and *spl7* mutant, respectively, among which 23 genes were common targets of CCIT1 and SPL7 (Figure 15D). In shoots, transcript level of 35 and 3131 genes were changed in *ccit1* and *spl7* mutants, respectively under Cu-deficient condition, of these, 27 genes showed to be regulated in CCIT1- and SPL7-dependent fashion (Figure 15D). Genes that were differentially expressed in roots and shoots of the *ccit1* mutant were grouped by GO functional classification analysis, indicating that they function in diverse biological processes including metal binding, protein binding, lipid binding, oxygen binding, nucleotide binding, RNA binding, DNA binding, transcription factor activity, enzyme regulator activity, catalytic activity, transporter activity, signal transducer activity, transferase activity and hydrolase activity (Figure 15A and B). RNA-seq data were validated by qRT-PCR analysis using RNA from the two biological replicates used for RNA-seq, as well as from an additional independent biological replicate. There was good quantitative agreement between RNA-seq and q RT-PCR data. Overall, there was a linear correlation between results from RNA-

seq and quantitative RT-PCR performed on the same RNA samples from two independent experiments (Figure 16A; $y = 0.7065x + 0.8882$ and $R^2 = 0.9078$ for differences between treatments; $y = 0.3845x + 1.2095$ and $R^2 = 0.661$ for differences between wild-type and *ccit1 mutant*; $y = 0.7777x - 0.071$ and $R^2 = 0.9463$ for differences between wild-type and *spl7 mutant*). Reproducibility between experiments was confirmed using RNA from a fourth, independent biological replicate for comparison by quantitative RT-PCR (Supplemental Figure 4).

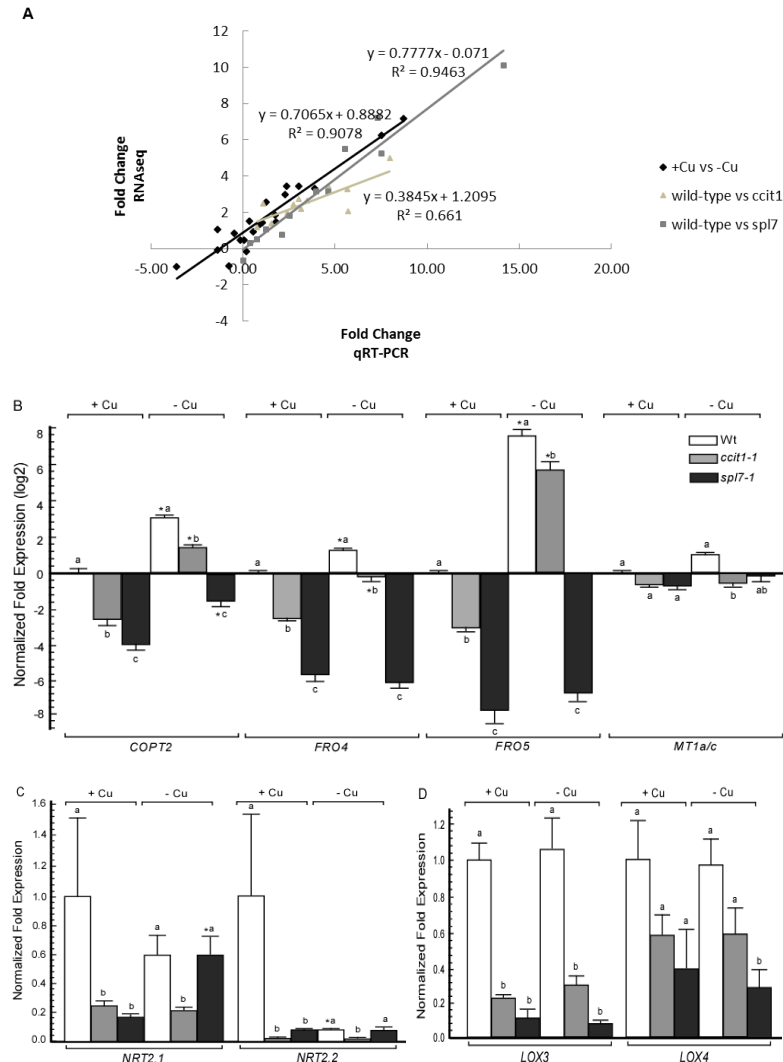


Figure 16. qRT-PCR-based validation of RNA-seq results. **A**, Correlation between RNA-seq and qRT-PCR data. Data points representing transcript level ratios of control condition (+Cu) versus Cu deficiency (-Cu) are shown in black, data points representing transcript level ratios of the wild type versus *ccit1-1* are shown in light gray, and data points representing transcript level ratios of the wild type versus *spl7-1* are shown in gray. Data of RNA-seq are from three independent biological experiments, and data of qRT-PCR are from two independent biological experiments. **B–D**, Relative transcript levels determined by qRT-PCR of *FRO4*, *FRO5*, *COPT2*, and *MT1a/c* genes in roots (B); *NRT2.1*, *NRT2.2* in roots (C); *LOX3* and *LOX4* (D) in shoots of 6-week-old wild-type (Wt), *ccit1-1* and *spl7-1* plants

cultivated continuously in a hydroponic solution containing the control concentrations of 0.25 μ M CuSO₄ or cultivated in a solution lacking added Cu for the final 3 weeks before harvest. Error bars indicate S.E. (n = 4). Results are presented relative to wild-type plants in 0.25 μ M CuSO₄, which was designated as 0 (log₂) in B, 1 in C and D. Asterisks (*, p ≤ 0.05) indicate statistically significant differences in gene expression between control (0.25 μ M CuSO₄) and treated (0 μ M CuSO₄) plants, different letters indicate statistically significant differences in gene expression between genotypes (p ≤ 0.05).

For the genes that showed to be responsive to Cu deficiency in CCIT1-dependent manner in RNA-seq, the expression of which also had the similar trend in quantitative RT-PCR analysis. *Copper Transporter 2 (COPT2)*, *Ferric Reduction Oxidase 4 (FRO4)* and *5 (FRO5)*, which were previously

Table 2. Transcripts Highly Responsive to Cu Deficiency in an CCIT1-Dependent Fashion

AGI ID	Gene	Annotation	Ratio					Tissue
			(-Cu/+Cu) in Wt	Wt/ccit1 in +Cu	Wt/ccit1 in -Cu	Wt/spl7 in +Cu	Wt/spl7 in -Cu	
AT5G23980	<i>FRO4</i>	ferric reduction oxidase 4	5.93*	3.28*	2.44*	45.14*	147.18*	Root
AT5G23990	<i>FRO5</i>	ferric reduction oxidase 5	75.35*	4.98	2.64*	37.91*	1106.62*	Root
AT3G46900	<i>COPT2</i>	copper transporter 2	10.78*	2.04	2.18*	8.98*	8.96*	Root
AT1G07600	<i>MT1a</i>	metallothionein 1A	2.73*	0.6	2.71*	1.44	2.07*	Root
AT5G56795	<i>MT1b</i>	metallothionein 1B	2.88*	1.29	2.48*	1.23	1.7*	Root
AT1G07610	<i>MT1c</i>	metallothionein 1C	2.73*	1.84	3.27*	1.54	1.93*	Root
AT1G14185	<i>Unknown</i>	Glucose-methanol-choline (GMC) oxidoreductase family protein	2.23*	1.15	2.14*	2.18	6.1*	Root

Genes are shown if transcript abundances were induced by Cu deficiency and were also significantly down in *ccit1-1 mutant* when compared to wild-type, and their dependence on *SPL7*. Plants of different lines were cultivated in hydroponic solutions for 6 weeks. Control plants were grown in hydroponic solution with 0.25 μ M CuSO₄ continuously, whereas Cu-deficiency treated plants were grown in 0 μ M CuSO₄ in the last 3 weeks. Asterisk “*” indicates significant difference between the comparison indicated (FDR≤0.05).

reported to highly respond to Cu deficiency in an SPL7-dependent manner (Yamasaki et al., 2009a; Bernal et al., 2012b), were also downstream targets of *CCIT1* (Table 2; Figure 16B). *METALLOTHIONEIN 1a*, encoding a Cu-binding chelator, which was showed to express in phloem and play a role in Cu accumulation in roots and Cu redistribution from senescent leaves to seeds (Guo et al., 2003; Guo et al., 2008; M et al., 2014), was also slightly induced by Cu limitation and down-regulated in the *ccit1* and *spl7* mutants (Table 2; Figure 16B). Together, my results suggest that SPL7-dependent Cu uptake through COPT2, FRO4 and FRO5 is partially under regulation of CCIT1 in response to Cu status in the environment.

In addition to Cu-responsive genes, the transcript level of *Nitrate transporter 2.1* (*NRT2.1*) and *2.2*

Table 3.Transcripts Related to Nitrate Uptake Specifically Depend on CCIT1

AGI ID	Gene	Anotation	Ratio				Tissue
			Wt/ccit1 in +Cu	Wt/ccit1 in -Cu	Wt/spl7 in +Cu	Wt/spl7 in -Cu	
AT1G08090	<i>NRT2.1</i>	nitrate transporter 2.1	3.43*	1.96*	4.53	0.64	Root
AT1G08100	<i>NRT2.2</i>	nitrate transporter 2.2	3.91*	2.03	3.5	0.62	Root

Genes are shown if transcript abundances were down-regulated in *ccit1-1* mutant but not in *spl7* mutant when compared to wild-type. Plants of different lines were cultivated as described in Table 1. Asterisk “*” indicates significant difference between the comparison indicated (FDR≤0.05).

(*NRT2.2*) significantly decreased in roots of *ccit1-1* in RNA-seq analysis, whereas in qRT-PCR assay, they were down-regulated in both *ccit1-1* and *spl7-1* mutant (Table 3; Figure 16C), suggesting that CCIT1 might be involved in regulating nitrate uptake and signaling and also indicating a crosstalk between nitrogen metabolism and Cu homeostasis.

Furthermore, two lipoxygenase genes, *LOX3* and *LOX4*, were also found to be downregulated in shoots of *ccit1-1* and *spl7-1* mutants in RNA-seq data, which was further validated by qRT-PCR (Table 4; Figure 16D). Interestingly, these two genes, *LOX3* and *LOX4* were also found to be downregulated in flowers of *ccit1-1* and *spl7-1* (Figure 14). The results from RNA-seq analysis of both flowers and shoots

Table 4.Transcripts Related to Jasmonic Acid Biosynthesis in a CCIT1- or SPL7-Dependent Fashion

AGI ID	Gene	Anotation	Ratio				Tissue
			Wt/ccit1 in +Cu	Wt/ccit1 in -Cu	Wt/spl7 in +Cu	Wt/spl7 in -Cu	
AT1G17420	<i>LOX3</i>	Lipoxygenase 3	3.39	4.47*	5.49*	8.33*	Shoot
AT1G72520	<i>LOX4</i>	Lipoxygenase 4	2.6	1.46	3.03	2.48*	Shoot

Genes that are involved in jasmonic acid biosynthesis are shown if their transcript abundances were down-regulated in *ccit1-1* mutant or *spl7-1* mutant when compared to wild-type. Plants of different lines were cultivated as described in Table 1. Asterisk “*” indicates significant difference between the comparison indicated (FDR≤0.05).

suggest an important transcriptional regulatory roles of CCIT1 and SPL7 in JA biosynthesis and further mediate plant fertility via JA signaling.

3.16 JA Synthesis is Impaired in Leaves of *spl7* and *ccit1* Mutants

To examine whether the downregulation of LOX3 and LOX4 in *ccit1* and *spl7* mutants impacts JA synthesis, I compared JA concentration in leaves of these mutants vs. wild-type, all grown either under Cu-sufficient or Cu-deficient conditions. I found that Cu deficiency significantly promoted JA biosynthesis in wild-type plants, suggesting a crosstalk between Cu homeostasis and JA signaling pathway (Figure 17). However, Cu-deficiency induced JA synthesis was partially impaired in the *ccit1-1*. The JA level decreased in *spl7-1* and *ccit1 spl7* mutants, regardless of Cu condition (Figure 17). This result is consistent with the gene expression changes and suggests a transcriptional regulatory function of SPL7 and CCIT1 in JA biosynthesis and signaling, and provides evidence for a connection between Cu nutrition, JA signaling and plant fertility.

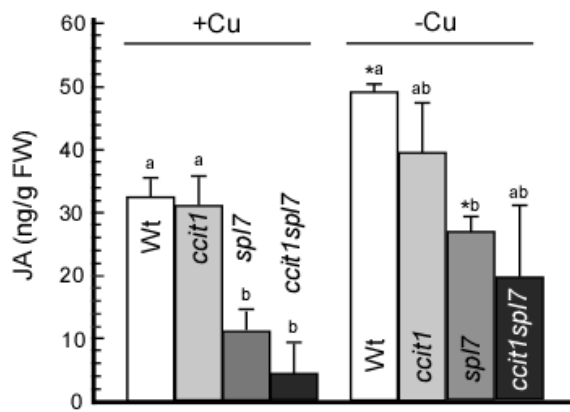


Figure 17. JA concentration in rosette leaves of 5-week-old wild-type (Wt), *ccit1-1* (*ccit1*), *spl7-1* (*spl7*) and *ccit1 spl7* grown hydroponically. Plants under 0.5 μ M CuSO₄ (+Cu) were cultivated in hydroponic system for 5 weeks, plants under Cu deficiency condition (-Cu) were subject to 0 μ M CuSO₄ for the last 2 weeks. Asterisks (*, $p \leq 0.05$) indicate statistically significant differences in JA concentration between control and Cu deficient condition, different letters ($p \leq 0.05$) indicates statistically significant differences between genotypes. Error bars indicate S.E (n=3).

4. DISCUSSION

4.1 CCIT1 is a Novel Cu-Responsive Transcription Factor in *A. thaliana* that is Mainly Expressed in Roots and Flowers and is Transcriptionally Upregulated During Cu Limitation in All Tissues

CCIT1 belongs to the bHLH transcription family, which is one of the largest gene families in *A. thaliana* and contains genes with regulatory functions in diverse biological processes. Consistent with the predicted function in the regulation of gene expression, transient expression studies of CCIT1-GFP in *A. thaliana* protoplasts identified CCIT1 in the nucleus (Figure 2). It has been shown that CCIT1 is highly upregulated

by Cu deficiency in a SPL7-dependent manner [12, 13]. I further investigated the transcript response of *CCIT1* to Cu availability. I found that *CCIT1* was induced by Cu deficiency in roots and shoots, which was consistent with the previous finding. I also found that *CCIT1* was upregulated by Cu deficiency in flowers (Figure 12) and was downregulated under high Cu concentration (Figure 3A). Together these data suggested that *CCIT1* may have a role in Cu homeostasis.

To investigate the sites of *CCIT1* action in *A. thaliana*, the expression pattern of *CCIT1* in different tissues was analyzed by qRT-PCR and histochemical assays. The transcript level of *CCIT1* in roots, flowers and cauline leaves, especially roots, was higher than it in other tissues (Figure 3B). To validate the expression pattern of *CCIT1* revealed by qRT-PCR, the promoter region of *CCIT1* was fused to the *uidA* reporter and was used for histochemical analysis. The seedlings and the mature hydroponic plants that were grown under Cu replete condition did not show expression of *CCIT1* (Figure 4A and C). However, when transgenic plants were exposed to Cu deficiency, the expression of *CCIT1* was highly induced in roots, and also slightly induced in petioles of leaves in mature plants (Figure 4B and D). Furthermore, analysis of the *CCIT1pro* activity in flowers revealed GUS staining in anthers of developing buds (Figure 4E), suggesting a possible role of *CCIT1* in reproduction during Cu limited condition.

4.2 *CCIT1* is Essential for Plant Growth and Development Under Low Cu Condition

To investigate the role of *CCIT1* in Cu homeostasis, two *ccit1* T-DNA insertion lines, designated as *ccit1-1* and *ccit1-2* were used for in depth analyses. In *ccit1-1* and *ccit1-2*, insertion of T-DNAs in the 1st exon and 3'-UTR of the *CCIT1* gene, respectively, result in a completely absence of the full-length *CCIT1* transcript or much lower *CCIT1* transcript, respectively (Figure 5A and B, Supplemental Figure 1A and B). *ccit1-1* was then used to generate the complemented lines (designated as *CCIT1-1*, *CCIT1-2* and *CCIT1-3*). The transgenic lines that ectopically express *CCIT1* were also established (designated as 35S-*CCIT1-1*, 35S-*CCIT1-2* and 35S-*CCIT1-3*). I then grew wild-type, *ccit1-1*, *CCIT1* and 35S-*CCIT1-1* plants hydroponically with or without Cu until they reached to late vegetative or reproductive stages. When grown in hydroponic solution with 0.125 μM CuSO₄ for 5 weeks, *ccit1-1* already started to exhibit chlorotic spots

between veins of mature rosette leaves (Supplemental Figure 2B), suggesting that Cu supply that is sufficient for wild-type plant growth may not be sufficient for maintaining the normal growth of the *ccit1-1* mutant. When grown in the hydroponic system without Cu, *ccit1-1* showed severe chlorotic symptom in its leaves, compared to wild-type, *CCIT1-1* and *35S-CCIT1-1* (Figure 5C and Supplemental Figure 2A and B). When plants were grown to the reproductive stage under Cu deficiency, the stem elongation of *ccit1-1* was decreased (Figure 5D). The second *ccit1* allele (*ccit1-2*) showed similar chlorotic symptoms, and a decrease in the stem growth, although not as pronounced as in the *ccit1-1* allele. These Cu deficiency symptoms were rescued by the genomic *CCIT1* fragment, suggesting that Cu deficiency phenotypes of the *ccit1-1* allele were due to the loss of the *CCIT1* function. The hypersensitive phenotype of *ccit1* mutants to Cu deficiency suggest that *CCIT1* is essential for plant growth and development under Cu limited condition.

4.3 *CCIT1* is Essential for Cu Accumulation in Roots and Shoots

To test whether the increased sensitivity to Cu deficiency of the *ccit1-1* mutant is associated with impaired ability of Cu uptake into roots, Cu translocation into shoots and Cu partitioning between mature and young leaves, I compared Cu concentrations in roots, young leaves and mature leaves of wild-type, *ccit1-1* mutant and *CCIT1-1* complemented plants. Cu concentration in roots and mature leaves of the *ccit1-1* mutant was significantly lower than it in wild-type and *CCIT1-1* plants, whereas in young leaves of the *ccit1-1* mutant, Cu concentration was slightly down compared to wild-type (Figure 6A and B). This observation suggests that Cu uptake in roots, Cu translocation from roots to shoots and Cu partitioning are impaired in the *ccit1-1* mutant. The *CCIT1-1* plants accumulates increased amount of Cu in both roots and shoots, which may be resulted from the position insertion effect.

4.4 *CCIT1*- and *SPL7*-dependent Cu Homeostasis is Indispensable for Plants Survival

CCIT1 was suggested to function downstream of the master regulator of Cu homeostasis, *SPL7* (Yamasaki et al., 2009b; Bernal et al., 2012b). To investigate the relationship between *CCIT1*- and *SPL7*-dependant pathways, I generated the *ccit1spl7* double mutant. I found that *ccit1 spl7*, cannot survive under standard

soil condition, whereas the *ccit1-1* single mutant grew as well as wild-type, and the *spl7-1* mutant had a reduced growth rate (Figure 7A). I was able to rescue the lethality of the *ccit1 spl7* double mutant by supplementing growth medium with 5 μ M CuSO₄. However, the growth of the double mutant was arrested at the early reproductive stage (Figure 7B). When CuSO₄ was supplied at 50 μ M, it rescued the reduced growth rate of *spl7-1* completely and also made the *ccit1spl7* double mutant reach and go through the reproductive stage (Figure 7B). The double mutant, however, had longer internodes between siliques and thinner stems (Figure 8A). The ICP-MS analysis of Cu concentrations in shoots of wild-type, single mutants and the double mutant uncovered a correlation between Cu accumulation in the above-ground part and the phenotype. Under 5 μ M CuSO₄, *ccit1-1* accumulated significantly less Cu, and *spl7-1* even less, whereas *ccit1spl7* double mutant had almost no detectable Cu in its leaves *vs.* wild-type (Figure 7C). Under 50 μ M CuSO₄ condition, the Cu concentration in all plant lines was in the sufficiency range (Figure 7C). These results correlate with qRT-PCR data (Figure 7D) showing a progressive reduction of the expression of *COPT2* and *FRO4* from wild-type to *ccit1spl7* double mutant, which explains the decrease of Cu in *ccit1-1*, *spl7-1* and *ccit1spl7* compared to wild-type.

CCIT1 has been considered to act downstream of SPL7 in the shoot of *A. thaliana*, since upregulation of *CCIT1* expression under Cu deficiency was abolished in shoots of the *spl7* mutant (Yamasaki et al., 2009b; Bernal et al., 2012a). To reconcile our data with data from Yamasaki et al 2009, we asked whether the transcriptional response of *CCIT1* to Cu availability in other tissues, such as roots and flowers, would depend on SPL7 as well. I found that while transcriptional response of *CCIT1* to Cu deficiency in shoots depended on SPL7, *CCIT1* was still upregulated by Cu deficiency in roots and flowers (Figure 12). These data indicate that other transcription regulators in addition to SPL7 control the transcriptional response of *CCIT1* to Cu deficiency in roots and flowers.

4.5 Simultaneous Knock-out of *CCIT1* and *SPL7* Results in male sterility and Seed Set Failure which can be Partially Reversed by Cu Application

In addition to stunted growth under limited Cu condition, the *ccit1 spl7* double mutant also showed a severe seed set failure (Figure 8A and C). I found that this infertility was due to drastic reduction of the total number of pollen grains and the proportion of viable pollen grains (Figure 9). Moreover, the morphology of the gynoecium was also altered by mutation of *CCIT1* and *SPL7*. The double mutant had longer length of pistil was also longer than the length of filament (Figure 8B and C), which may cause pollen loading difficulties. To examine whether Cu deficiency would result in a similar phenotype, wild-type plants were grown in hydroponic solution with or without Cu for 8 weeks, and the phenotype of the plants under the 2 different Cu conditions were compared. Interestingly, the plants that were grown under Cu deficient condition showed severe seed-set failure (Figure 9A), and the pollen viability assay revealed a significant reduction of the number of viable pollen grains (Figure 9B and C). Furthermore, our initial SXRF analyses of Cu localization in flower organs disclosed that Cu was associated with anthers (Figure 10C). Cu has been long known to be required for plant fertility, but the molecular mechanism behind this observation remains elusive (Shorrocks and Alloway, 1988; Marschner, 1995; Solberg et al., 1999). Recently, a reduced seed setting and pollen viability under Cu deficiency condition was found in the double mutant of *spl7* and *kin17*, which physically interact with each other (Garcia-Molina et al., 2014). In contrast to *spl7kin17*, *ccit1spl7* showed male sterility even under Cu- sufficient condition, which unraveled a new route for Cu regulatory pathway and its connection with plant fertility.

4.6 Cu Deficiency Significantly Alters Flower Transcriptome in *A. thaliana*

I next used deep transcriptome sequencing (RNA-seq) to initiate the comparison of the transcriptome response of different tissues of *ccit1-1*, *spl7-1* vs. wild-type to Cu deficiency. Given the acute floral phenotype of the *ccit1 spl7* double mutant and dramatic response of wild-type plant to Cu deficiency as well, I initially used flowers for RNA-seq. I collected flowers as flower buds (pre-anthesis) and at the anthesis (stage 13-14 (Yamasaki et al., 2009b)). This study has led to the following findings: 1) Cu deficiency significantly altered transcriptome of flowers: 548 and 612 genes were differentially expressed in response to Cu deficiency in floral buds and mature flowers, respectively (Figure 11). Interestingly, the

number of genes that were up-upregulated by Cu deficiency was 2-fold higher, while down-regulated genes was 1.8-fold lower in mature flowers in comparison with younger floral buds. (Figure 11). These results indicate that Cu deficiency significantly alters the flower transcriptome in *A. thaliana*, and the alteration is different in floral buds from mature flowers. I also found that *DAD1* (defective in anther dehiscence), encoding a phospholipase A1 that catalyzes the initial step of JA biosynthesis (Ishiguro et al., 2001b), and is essential for stamen filament extension and flower opening (Ishiguro et al., 2001b; Ito et al., 2007), was downregulated by Cu deficiency in the wild-type.

I also found that under control conditions, 59.6% and 59.3% of CCIT1-dependent genes were co-regulated by CCIT1 and SPL7 in floral buds and mature flowers, respectively. Whereas under limited Cu condition, the number of common targets was reduced to 16% and 25.6% in floral buds and mature flowers (Figure 13A and B), respectively, indicating that during Cu starvation, CCIT1 plays a more independent role. More interestingly, we also found the genes that are suppressed by Cu deficiency, such as *CSD1*, *CSD2*, *LAC2* and *CCS*, were also downregulated in *ccit1-1* mutant, whereas the genes that are reported to be induced by limited Cu, such as *FSD1*, *COPT2* and *YSL2*, were also upregulated in *ccit1-1*, suggesting that flowers of the *ccit1-1* mutant manifest transcriptional response to Cu deficiency even under sufficient Cu conditions (Table 1). This response was absent in the *spl7* mutant. Cu concentration in flowers of wild-type, *ccit1-1* and *spl7-1* measured by ICP-MS revealed a significant reduction of Cu in flowers from *ccit1-1* and *spl7-1* compared with wild-type (Figure 13C).

4.7 RNA-seq Analysis in Roots and Shoots Identified Targets of CCIT1 and SPL7 which are Involved in Cu Homeostasis and Plant Fertility

The whole-transcriptome analysis from Illumina (RNA-seq) was subsequently performed for a genome-wide analysis of mRNA abundance in roots and shoots of wild-type, *ccit1-1* and *spl7-1* mutant plants under Cu-sufficient and -deficient conditions. RNA-seq analysis identified 147 genes that transcriptionally responded to Cu deficiency in wild-type through an at least 2 fold upward or 0.5 fold downward (Supplemental Figure 6). The total number of differentially expressed genes in roots and shoots in my RNA-

seq data is less than the number of genes that were identified in previous genome-wide analyses of the response of *A. thaliana* transcriptome to Cu deficiency (Bernal et al., 2012b). This discrepancy could be because Bernal et al (2012) might have included differentially-expressed small RNAs, such as miRNAs, into their analyses, which have been found to be important regulators of Cu homeostasis. Moreover, 10 micrograms of total RNA and 16 lanes were used for sequencing in Bernal's manuscript, while 3 micrograms of total RNA and the samples were pooled in 2 lanes were used for our sequencing. Less total RNA and much more samples pooled in one lane resulted in less reads number obtained per sample. Nevertheless, a fair number of genes that were reported to be responsive to Cu availability were also found in our RNA-seq analysis. Interestingly, when comparing gene expression profiles of roots and shoots under Cu-deficient condition between wild-type, *ccit1* and *spl7* mutants, the change of the transcriptome profile was more pronounced during Cu deficiency (Figure 15D), which is consistent with the low expression of *CCIT1* under sufficient Cu condition and its significant upregulation in response of low Cu (Figure 3A and 4). The genes that were differentially expressed in roots and shoots of the *ccit1* mutant were grouped by GO functional classification analysis, and were found to function in diverse biological processes including metal binding, protein binding, lipid binding, oxygen binding, nucleotide binding, RNA binding, DNA binding, transcription factor activity, enzyme regulator activity, catalytic activity, transporter activity, signal transducer activity, transferase activity and hydrolase activity (Figure 15A and B). Specifically, several genes which was previously reported to highly respond to Cu deficiency in the SPL7-dependent manner in roots (Yamasaki et al., 2009a; Bernal et al., 2012b), such as *COPT2*, *FRO4* and *FRO5*, were also the targets of CCIT1 in roots (Table 1; Figure 16B). Metallothionein 1a, a Cu-binding chelator, which was shown to express in the phloem and to play a role in Cu accumulation in roots and Cu redistribution from senescent leaves to seeds (Guo et al., 2003; Guo et al., 2008; M et al., 2014), was also induced by Cu limitation via CCIT1 and SPL7 (Figure 15B). From the results in shoots, I found that 2 lipoxygenase genes, *LOX3* and *LOX4*, were downregulated in *ccit1-1* and *spl7-1* mutants (Table3 and Figure15D). LOX3 and LOX4 catalyze an early step of JA biosynthesis, loss of their function results in reduced pollen viability and seed setting (Caldelari et al., 2011). Similar phenotype was observed in the *ccit1spl7* double mutant,

suggesting that disruption of CCIT1 and SPL7 impairs the JA biosynthetic pathway which may cause the male sterility in the *ccit1spl7* double mutant.

4.8 SPL7 and CCIT1 Control Jasmonic Acid Pathway which Plays a Critical Role in Male Fertility

By using the Plant MetGenMAP package [27], I identified the significantly changed pathways in flowers of *ccit1-1* and *sp17-1* mutant. I found that the pathway controlling JA biosynthesis has been changed to a larger extent in both *ccit1-1* and *sp17-1* mutant (Figure 14). Genes that are involved in catalyzing production of JA precursors, such as *DAD1*, *AOS*, *OPR3*, *LOX3* and *LOX4*, were found to be downregulated in *sp17* and *ccit1* mutants, and mutants for these genes exhibit anther development/dehiscence defect, and male sterile phenotype (McConn and Browse, 1996; Stintzi and Browse, 2000; Ishiguro et al., 2001a; Park et al., 2002; Caldelari et al., 2011). JA production in the mutants and wild-type under different Cu conditions was analyzed by LC-MS. This analysis revealed that Cu deficiency significantly induced the JA biosynthesis in wild-type plants pointing to a connection of Cu to JA signaling (Figure 17). Since Cu was found to bind to the salicylic acid (SA) receptor, NPR1, which is also the essential factor in the crosstalk between SA and JA-dependent pathways (Leon-Reyes et al., 2009; Wu et al., 2012b), it's plausible to propose that Cu may be involved in the JA signaling pathway and/or the interaction between JA and SA signaling. In addition, this Cu-depletion-induced JA synthesis was partially impaired in *ccit1-1* mutant, and totally abolished in the *sp17-1* mutant (Figure 17). This result is consistent with the gene expression changes and suggests a transcriptional regulatory function of SPL7 and CCIT1 in JA biosynthesis and signaling, and provides evidence for a connection between mineral nutrition, phytohormone signaling and plant fertility.

Based on what I found in this chapter, I propose that CCIT1 and SPL7 act in a complex interacting pathway that is absolutely required for the ability of plant to uptake and partitioning Cu in plant tissues to ensure growth, development and fertility. My data also point to the existence of crosstalk between SPL7 and CCIT1-dependant Cu homeostasis, JA signaling and plant fertility. As summarized in Figure 18, Cu deficiency upregulates expression of *CCIT1*, in roots and flowers, in part independent of SPL7. These two interactive pathways upregulate the downstream Cu responsive genes, including *FRO4/5*, *COPT2*, *MT1*,

and further affects Cu uptake and translocation according to Cu status. In addition, CCIT1 and SPL7 regulates the JA biosynthetic pathway in leaves and flowers *via* regulation the expression of JA biosynthetic genes, such as *AOS*, *AOC1/2/3*, *OPR3*, *DAD1* and *LOX3/4*. The decreased JA biosynthesis or the disruption of JA signaling may contribute to pollen development and compromise male fertility (Figure 18). Although it's still not clear how Cu affects JA signaling and what the exact roles CCIT1 and SPL7 play in the

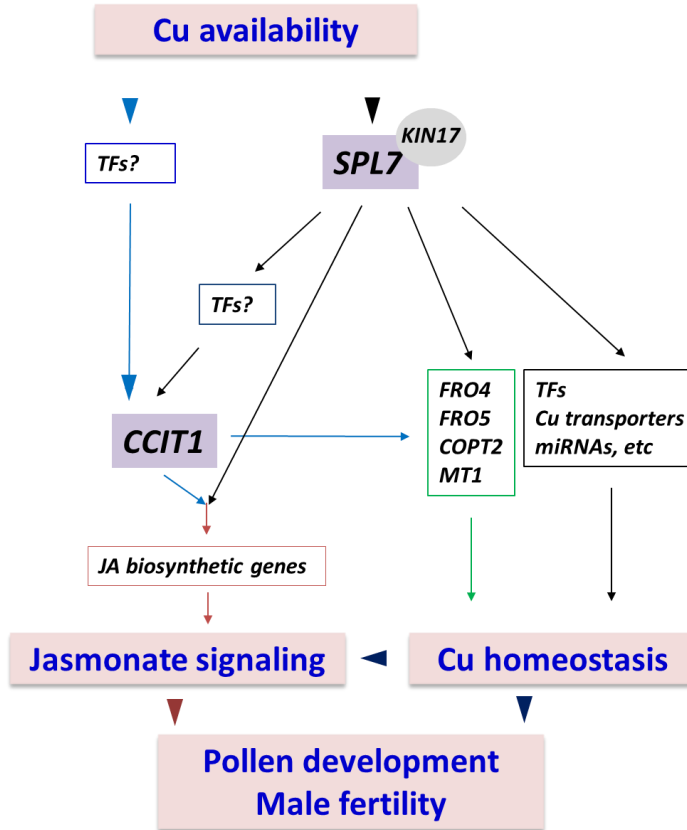
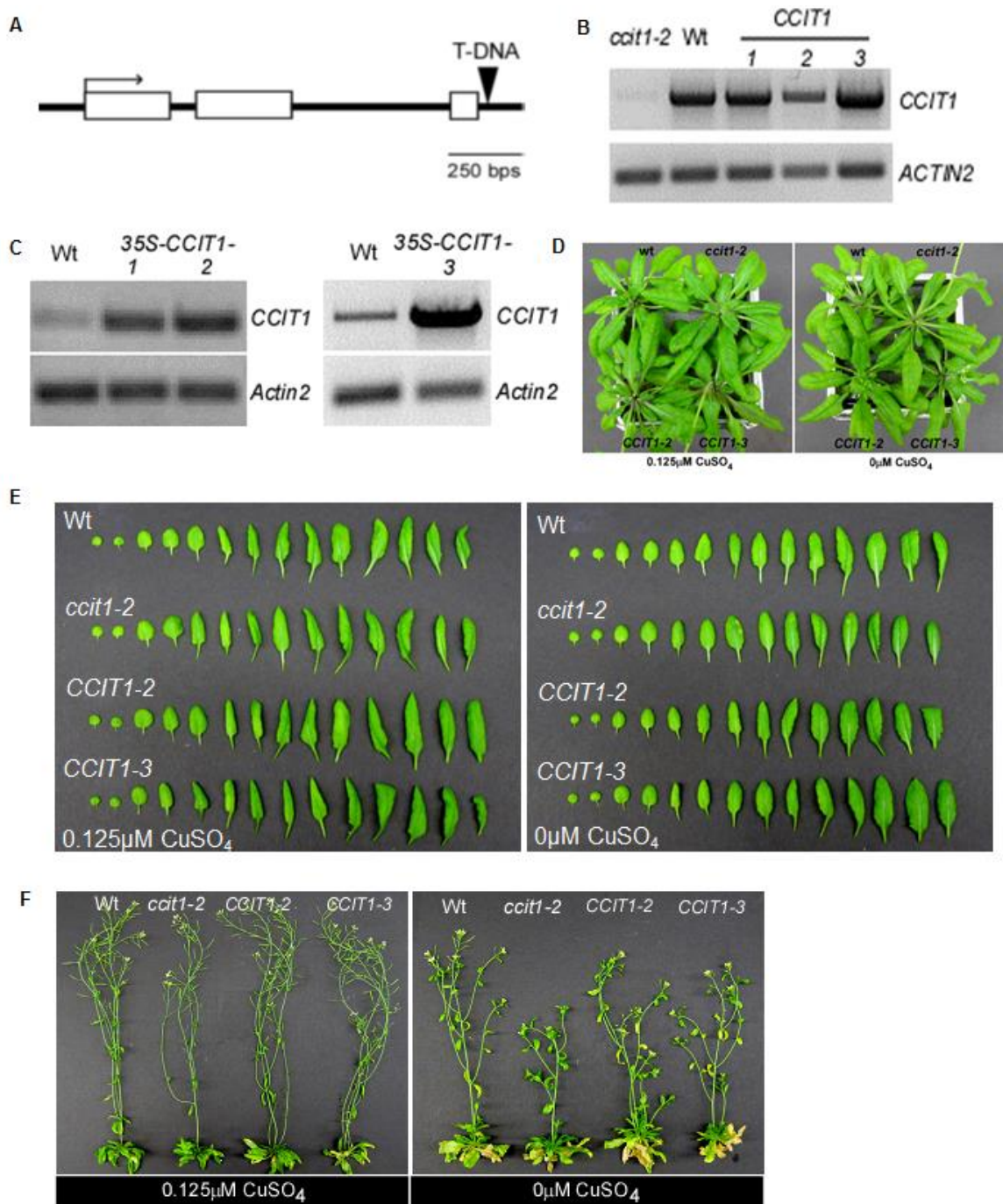


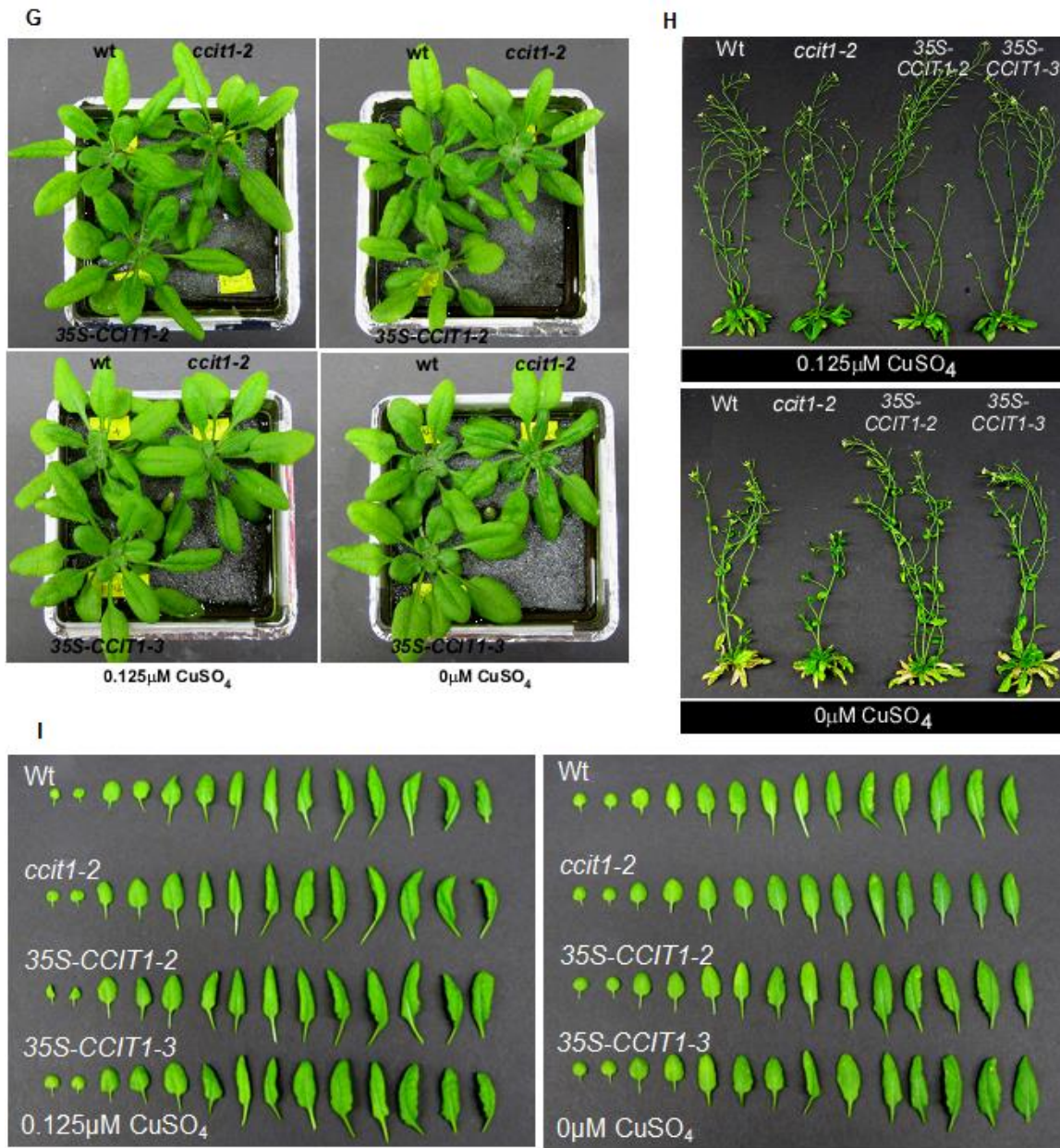
Figure 18. Model of the CCIT1- and SPL7-dependent pathway in response to Cu availability and their function in Cu homeostasis, JA signaling and plant fertility. CCIT1 and SPL7 operate in a complex interacting pathways that is essential for the ability of plants to uptake and partition Cu, stimulate JA synthases and maintain pollen fertility. SPL7 and CCIT1 regulate expression of Cu-responsive genes, including *FRO4/5*, *COPT2*, *MT1*, which further affects Cu uptake and translocation to flowers. In addition, Cu status can also affect JA biosynthesis and signaling via JA biosynthetic genes, such as *LOX3* and *LOX4* in leaves as well as *AOS*, *OPR3*, *AOC1/2/3* and *DADI* in flowers, which depend on SPL7 and CCIT1. The decreased JA biosynthesis or the disruption of JA signaling might contribute to a defect in pollen development and compromise male fertility. KIN17 has been found to physically interact with SPL7, and the double mutant of *spl7* and *kin17* exhibits reduced pollen viability and seed setting under limited Cu condition.

interaction between Cu, JA and pollen development, this chapter addresses the more diverse role of Cu in plants, such as phytohormone signaling and plant fertility, identifies novel regulators and other components

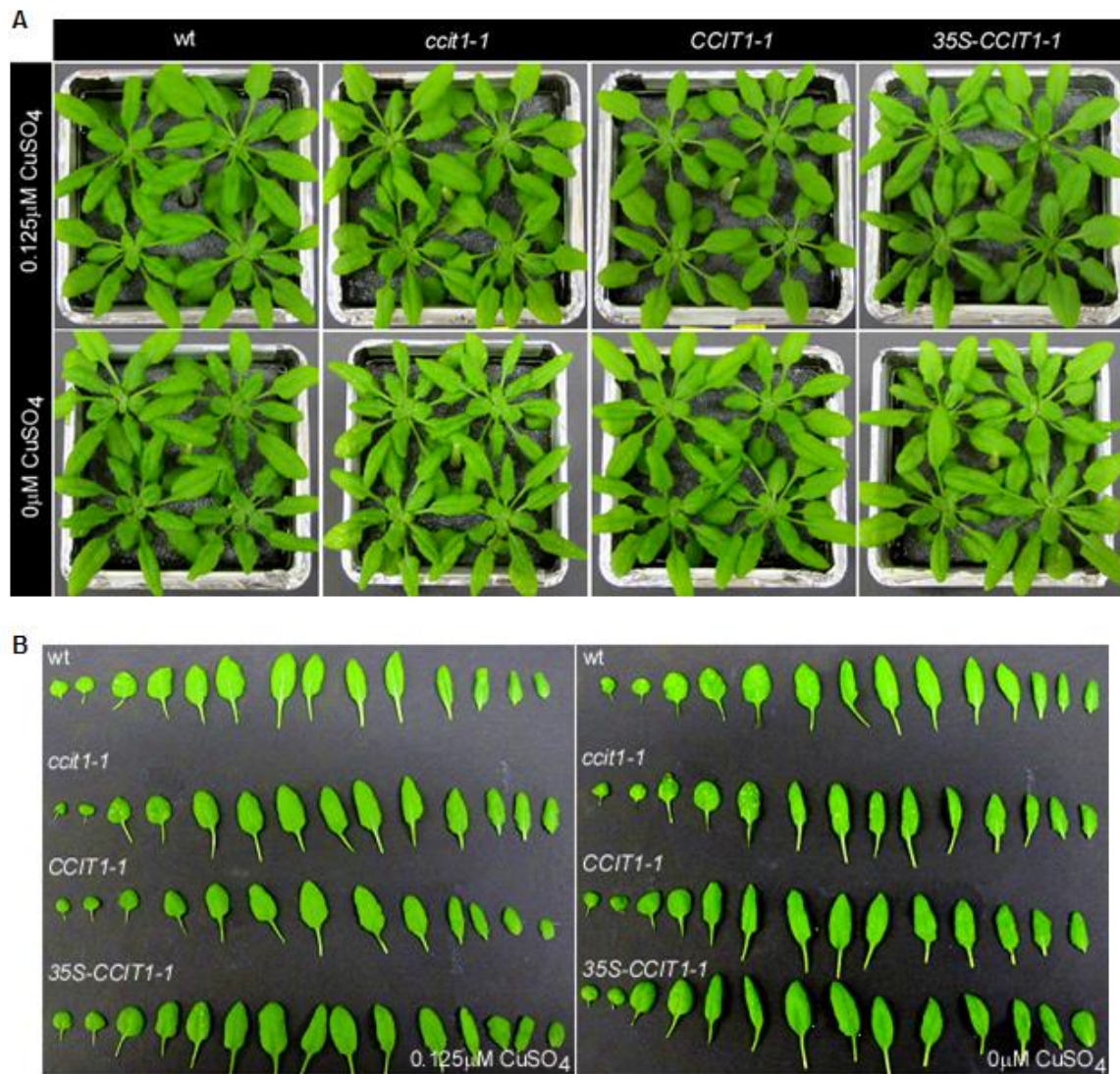
in the transcriptional regulatory pathway furthering our understanding of the relationship between Cu homeostasis and plant fertility.

5. SUPPLEMENTAL DATA





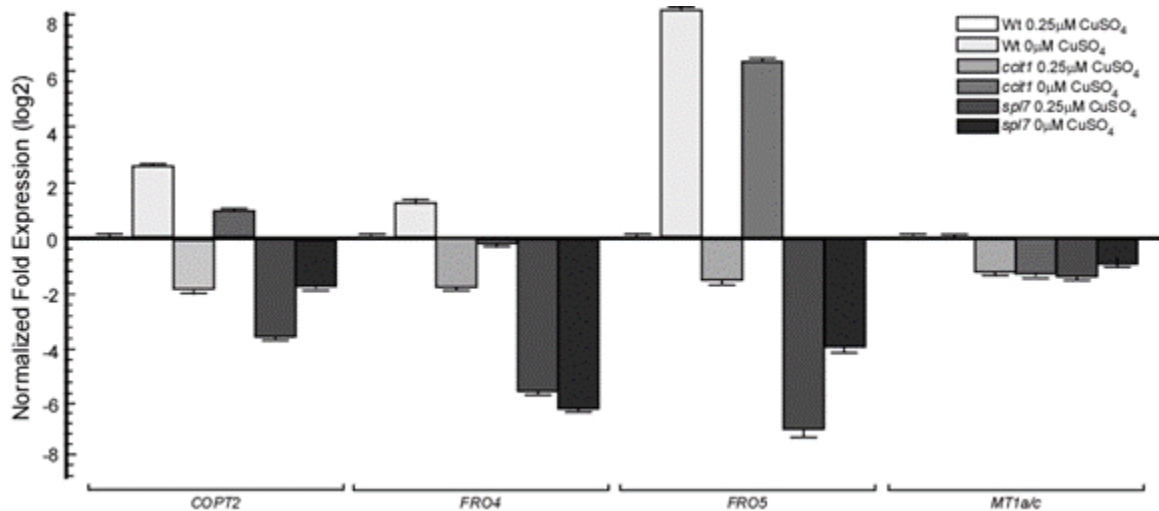
Supplemental Figure 1. CCIT1 transcript abundance of the second *ccit1* mutant allele (*ccit1-2*), 2 additional independent complemented and overexpressing lines and their phenotypes in response to Cu status. **A**, Exon-intron structure of *CCIT1* and the T-DNA insertion site of *ccit1-2*. Black arrowheads indicate T-DNA (black arrow head) insertion located 21 bps downstream from the stop codon in the *ccit1-2* mutant allele. Scale bar = 250 bps. **B and C**, Using *Actin2* (27 cycles) as reference, semi-quantitative PCR detection of full-length *CCIT1* transcripts (30 cycles in *ccit1-2* and complemented lines; 27 cycles in 35S-*CCIT1* lines) in roots of 10-day-old wild-type (Wt), *ccit1-2*, *CCIT1-1 to -3*, 35S-*CCIT1-1 to -3* seedlings (1000 μM BCS was added to induce *CCIT1* expression in *ccit1-2* and *CCIT1-1 to -3*). **D-I**, Wild-type (Wt), *ccit1-2*, *CCIT1-1 to -3*, 35S-*CCIT1-1 to -3* were grown in indicated hydroponic system until full-rosette and reproductive stages.



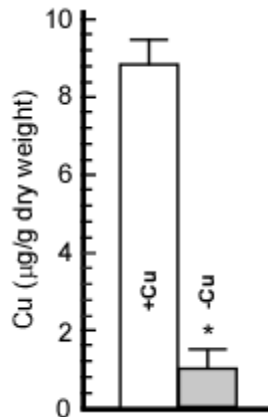
Supplemental Figure 2. The phenotype of full set of rosette leaves from wild-type, *ccit1-1*, *CCIT1-1* and *35S-CCIT1-1*. **A.** Wild-type, *ccit1-1*, *CCIT1-1* and *35S-CCIT1-1* were grown in hydroponic system with 0.125 μ M CuSO₄ or without CuSO₄ for 5 weeks. **B.** Rosette leaves from the plants in A were cut off and ordered from oldest to youngest to clearly show the development of chlorotic spots in response to low Cu status.



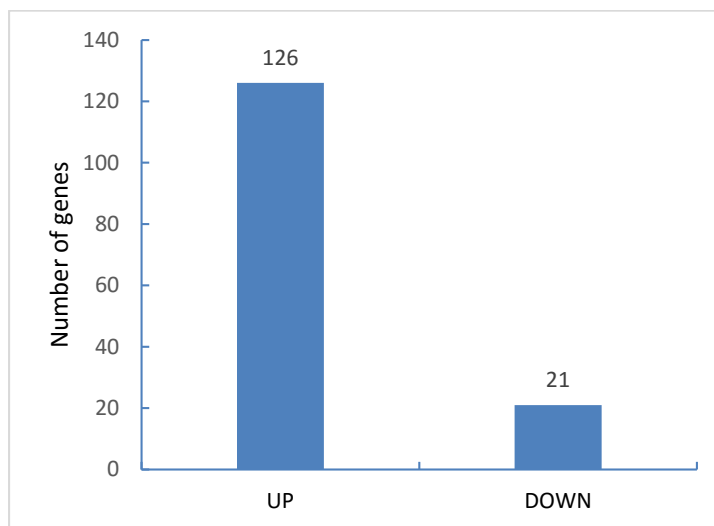
Supplemental figure 3. Using pollens from wild-type or floral dipping with Cu solution to rescue the infertility of the *ccit1 spl7* double mutant. A, *ccit1spl7* double mutant cannot survive when grown on compost soil mix with low Cu. **B.** Pollen from wild-type can rescue the infertility of *ccit1spl7*, whereas pollens from *ccit1spl7* was not able to fertilize wild-type carpel. **C.** Cu application to flowers can partially rescue the infertility of *ccit1spl7* double mutant. White arrows point to the siliques. 50 μ M CuSO₄ was used twice a week for flower dipping of *ccit1spl7*.



Supplemental figure 4. Validation by quantitative RT-PCR showing between-experiment reproducibility. Relative transcript levels determined by qRT-PCR of *FRO4*, *FRO5*, *COPT2*, and *MT1a/c* genes in roots from a fourth independent experiment are shown. Error bars represent the S.E. between 3 technique replicates (n=3).



Supplemental figure 5. Cu concentration in flowers of 8-week-old wild-type grown hydroponically. Wild-type plants were cultivated hydroponically at 0.5 µM CuSO₄ for the first 5 weeks, and then continued to stay in solution with 0.5 µM CuSO₄ (+Cu) or were transferred to solution with 0 µM CuSO₄ (-Cu) for the next 3 weeks. Asterisks (*, $p \leq 0.05$) indicate statistically significance between Cu sufficient and Cu deficient conditions. Error bars indicate S.E (n=5).



Supplemental figure 6. Number of genes that were changed in response to Cu deficiency. Plants were cultivated in hydroponic system with 0.25 µM CuSO₄ for the first 3 weeks and continued to grow under 0.25 µM CuSO₄ condition as control or were transferred to 0 µM CuSO₄ for the next 3 weeks as Cu deficient treatment. RNA-seq analysis revealed the differentially expressed genes by Cu deficient treatment. The numbers indicate how many genes were upregulated and downregulated by limited Cu, respectively.

Supplemental table 1. Primers used for genotyping		
Primer	Gene	Primer sequence (5' to 3')
LB 1.3 for sail line	<i>T-DNA</i>	ATTTTCCGATTCTCGAAC
LB 1 for sail line	<i>T-DNA</i>	GCCTTTCAGAAATGGATAAATAGCCTGCTTCC
SALK_073160 LP	<i>CCIT1</i>	GTTTAGGCCATTGTACTGC
SALK_073160 RP	<i>CCIT1</i>	CAATTCAAGAACCGAGATTGC
SAIL_711_B07 LP	<i>CCIT1</i>	TATTCTTGAGCCGTGTTG
SAIL_711_B07 RP	<i>CCIT1</i>	TGTTAGGGCCAAGTCATGG
SALK_093849 LP	<i>SPL7</i>	TTGGAAATTCAAGCTGATTG
SALK_093849 RP	<i>SPL7</i>	TCCACCTGTCAAAACCAAGAC

Supplemental table 2. Primers used for cloning		
Primer	Gene	Primer sequence (5' to 3')
attB1-CCIT1-F	<i>CCIT1</i>	ggggacaagttgtacaaaaaaggcaggcttaccATGTCTCTAACCGAATCATCAGAC
attB2-CCIT1-R (w/stop)	<i>CCIT1</i>	ggggaccacttgtacaaagaagctggtcTTGCACTTGTGTTGTCACGAAGC
attB2-CCIT1-R (w/o stop)	<i>CCIT1</i>	ggggaccacttgtacaaagaagctggtcTCATTGCACTTGTGTTGTCACGAAG
attB1-CCIT1pro-F	<i>CCIT1pro</i>	ggggacaagttgtacaaaaaaggcaggcttaccTGAAAAGTATGTCACAGAGAGGTCAG
attB2-CCIT1pro-R	<i>CCIT1pro</i>	ggggaccacttgtacaaagaagctggtcATATATACGACGGCAAGAGGAACAA

Supplemental table 3. Primers used in qRT-PCR		
Primer	Gene	Primer sequence (5' to 3')
Actin-F	<i>Actin</i>	GACCTTAACCTCCCCGCTA
Actin-R	<i>Actin</i>	GGAAGAGAGAAACCTCGTA
CCIT1-F	<i>CCIT1</i>	ACGAGGTCTCTATTGAGCA
CCIT1-R	<i>CCIT1</i>	ACCCTTGCTCTCGGCAAACCT
COPT2-F	<i>COPT2</i>	TGGTGATGCTCGCTGTTATGTCCT
COPT2-R	<i>COPT2</i>	TCTGGTCATCGGAGGGTTCTTGA
FRO4-F	<i>FRO4</i>	TTCCAGTGTAGTTTCTTA
FRO4-R	<i>FRO4</i>	TTGTACCTGATTCTTGAAC
FRO5-R	<i>FRO5</i>	TACCCAAAAGCAACCCCTCCC
FRO5-F	<i>FRO5</i>	ATCATCACCCCTCCCCATTCT
NRT2.1-F	<i>NRT2.1</i>	CATGTTCTGCCTCCTCCA
NRT2.1-R	<i>NRT2.1</i>	TTCTGCTTCTCCTGCTCATTC
NRT2.2-F	<i>NRT2.2</i>	GTAAGGAGGAGCAGCAGATTG
NRT2.2-R	<i>NRT2.2</i>	TGGTGCCTCCCTTGT
MT1a/c-F	<i>MT1a/c</i>	GGCAGATTCTAACTGTGGATGT
MT1a/c-R	<i>MT1a/c</i>	CCCACAGCTGCAGTTGAT
LOX3-F	<i>LOX3</i>	CTGCCGATCTAATCGCAGAGG
LOX3-R	<i>LOX3</i>	CGTCAACATAGGTTCGGACCC
LOX4-F	<i>LOX4</i>	CGTGGCAGCACAGACTTGATT
LOX4-R	<i>LOX4</i>	TGGTGTGTTGGTCTGGAACA

Supplemental table 4. The sample summary of RNA-seq analysis in roots and shoots. Wild-type (wt), *ccit1-1* (*ccit1*), *spl7-1* (*spl7*), 0.25 µM CuSO₄ (ctr), 0 µM CuSO₄ (0Cu), shoot (s), root (r), the number indicates the replicates.

Sample	Index	total reads	rRNA	clean reads (remove low quality, adaptor)		final clean reads	mapped	
				#	%raw		#	%
ccit1_0Cu_r_1	CACGAT	8,106,971	2,247,532	5,221,220	64.40	2,973,688	2,528,671	85.03
ccit1_0Cu_r_2	CACTCA	8,498,544	2,631,455	5,157,170	60.68	2,525,715	2,129,335	84.31
ccit1_0Cu_r_3	CAGGCG	10,110,091	1,778,284	6,486,466	64.16	4,708,182	3,927,120	83.41
ccit1_0Cu_s_1	ATGTCA	10,623,037	158,543	10,464,494	98.51	10,305,951	9,184,491	87.77
ccit1_0Cu_s_2	GAGTGG	9,411,773	4,663,512	6,333,615	67.29	1,670,103	1,445,571	86.56
ccit1_0Cu_s_3	GGTAGC	7,958,628	3,961,750	5,276,506	66.30	1,314,756	1,166,407	88.72
ccit1_ctr_r_1	AGTCAA	6,277,256	1,695,623	4,165,347	66.36	2,469,724	2,114,396	85.61
ccit1_ctr_r_2	AGTTCC	6,368,249	1,365,852	3,433,594	53.92	2,067,742	1,853,089	89.62
ccit1_ctr_r_3	ATGTCA	8,288,179	2,471,159	5,244,037	63.27	2,772,878	2,386,535	86.07
ccit1_ctr_s_1	TGACCA	7,571,458	3,933,012	5,056,161	66.78	1,123,149	976,785	86.97
ccit1_ctr_s_2	ACAGTG	8,079,249	4,139,590	5,335,296	66.04	1,195,706	1,043,133	87.24
ccit1_ctr_s_3	GCCAAT	7,635,989	3,832,846	5,025,294	65.81	1,192,448	1,023,463	85.83
spl7_0Cu_r_1	CATGGC	7,465,850	2,004,844	4,602,178	61.64	2,597,334	1,968,886	75.80
spl7_0Cu_r_2	CATTTT	11,046,835	2,232,361	7,090,583	64.19	4,858,222	3,529,615	72.65
spl7_0Cu_r_3	CCAACA	18,194,152	3,330,588	11,496,458	63.19	8,165,870	6,034,989	73.91
spl7_0Cu_s_1	ACTGAT	10,370,097	5,396,169	6,712,795	64.73	1,316,626	1,130,168	85.84
spl7_0Cu_s_2	ATGAGC	7,141,923	3,148,921	4,520,079	63.29	1,371,158	1,183,981	86.35
spl7_0Cu_s_3	ATT CCT	8,944,205	3,666,236	5,738,715	64.16	2,072,479	1,885,650	90.99
spl7_ctr_r_1	CCGTCC	9,995,248	2,903,976	6,488,613	64.92	3,584,637	3,067,503	85.57
spl7_ctr_r_2	GTAGAG	8,843,086	2,691,888	5,861,056	66.28	3,169,168	2,793,256	88.14
spl7_ctr_r_3	GTCCGC	8,083,128	2,257,725	5,245,228	64.89	2,987,503	2,519,091	84.32
spl7_ctr_s_1	AGTCAA	12,487,035	231,487	12,255,548	98.15	12,024,061	11,099,849	90.57
spl7_ctr_s_2	ACTTG A	10,295,849	5,050,989	6,691,249	64.99	1,640,260	1,474,202	89.88
spl7_ctr_s_3	AGTTCC	12,071,477	184,535	11,886,942	98.47	11,702,407	10,633,781	89.46
wt_0Cu_r_1	CAAAAG	7,753,318	2,232,457	4,950,774	63.85	2,718,317	2,373,502	87.32
wt_0Cu_r_2	CAACTA	9,914,964	3,250,237	6,441,073	64.96	3,190,836	2,856,767	89.53
wt_0Cu_r_3	CACCGG	8,257,856	2,097,377	5,235,576	63.40	3,138,199	2,757,834	87.88
wt_0Cu_s_1	CCGTCC	12,498,042	212,534	12,285,508	98.30	12,072,974	11,191,210	91.09
wt_0Cu_s_2	GTAGAG	12,340,297	185,480	12,154,817	98.50	11,969,337	10,273,936	84.53
wt_0Cu_s_3	GTT TCG	8,423,208	4,756,006	5,886,310	69.88	1,130,304	964,721	85.35
wt_ctr_r_1	TAGCTT	8,747,860	2,957,358	5,193,863	59.37	2,236,505	1,939,890	86.74
wt_ctr_r_2	GGCTAC	8,485,015	2,920,917	5,617,191	66.20	2,696,274	2,344,490	86.95
wt_ctr_r_3	CTTGTA	6,584,040	2,044,273	4,323,966	65.67	2,279,693	2,048,811	89.87
wt_ctr_s_1	ATCAC G	6,432,327	1,878,711	4,152,129	64.55	2,273,418	2,102,835	92.50
wt_ctr_s_2	CGATGT	6,550,052	3,216,258	4,394,177	67.09	1,177,919	982,923	83.45
wt_ctr_s_3	TTAGGC	7,633,073	3,929,977	5,049,147	66.15	1,119,170	999,106	89.27

Supplemental table 5. The sample summary of RNA-seq analysis in floral buds and mature flowers. Wild-type (wt), *ccit1-1* (*ccit1*), *spl7-1* (*spl7*), 0.5 µM CuSO₄ (0.5Cu), 0 µM CuSO₄ (0Cu), floral buds (yf), mature flowers (of), the number indicates the replicates.

Sample	Index	total reads	rRNA	clean reads		final clean reads	mapped	
				#	% raw reads		#	%
spl7_0Cu_of_1	CCGTC	9,881,623	156,244	9,725,379	98.42	9,569,135	9,089,486	93.46
spl7_0Cu_of_2	GTA	10,488,472	126,452	10,362,020	98.79	10,235,568	9,567,285	92.33
spl7_0Cu_of_3	GTC	12,310,834	255,930	12,054,904	97.92	11,798,974	10,996,115	91.22
wt_0.5_Cu_of_1	ATC	9,031,740	105,717	8,926,023	98.83	8,820,306	7,506,719	84.10
wt_0.5_Cu_of_2	CGA	8,872,964	433,251	8,439,713	95.12	8,006,462	7,597,445	90.02
wt_0.5_Cu_of_3	T	7,976,029	1,340,465	6,635,564	83.19	5,295,099	5,821,450	87.73
wt_0_Cu_of_1	TAG	13,840,064	263,046	13,577,018	98.10	13,313,972	10,737,784	79.09
wt_0_Cu_of_2	GGC	9,294,464	151,254	9,143,210	98.37	8,991,956	8,389,635	91.76
wt_0_Cu_of_3	CTT	11,234,019	156,120	11,077,899	98.61	10,921,779	10,039,127	90.62
ccit1_0.5Cu_of_1	TGA	9,972,289	164,957	9,807,332	98.35	9,642,375	8,801,736	89.75
ccit1_0.5Cu_of_2	ACAG	11,111,117	851,590	10,259,527	92.34	9,407,937	9,388,698	91.51
ccit1_0.5Cu_of_3	GCC	10,063,689	209,667	9,854,022	97.92	9,644,355	9,070,388	92.05
ccit1_0Cu_of_1	AGTC	10,203,754	134,643	10,069,111	98.68	9,934,468	8,957,916	88.96
ccit1_0Cu_of_2	AGTT	11,124,657	211,788	10,912,869	98.10	10,701,081	9,933,523	91.03
ccit1_0Cu_of_3	ATGT	10,368,725	366,487	10,002,238	96.47	9,635,751	8,723,719	87.22
spl7_0.5Cu_of_1	CAGAT	13,045,194	185,546	12,859,648	98.58	12,674,102	11,982,392	93.18
spl7_0.5Cu_of_2	ACTTG	10,442,527	173,363	10,269,164	98.34	10,095,801	9,521,200	92.72
spl7_0.5Cu_of_3	GATC	8,630,704	110,417	8,520,287	98.72	8,409,870	7,624,788	89.49
spl7_0Cu_yf_1	CATGG	10,101,402	180,530	9,920,872	98.21	9,740,342	8,736,001	88.06
spl7_0Cu_yf_2	CATT	9,572,989	162,418	9,410,571	98.30	9,248,153	8,395,359	89.21
spl7_0Cu_yf_3	CCAACA	13,925,145	384,483	13,540,662	97.24	13,156,179	11,658,776	86.10
wt_0.5_Cu_yf_1	GTGAA	11,835,514	189,369	11,646,145	98.40	11,456,776	10,701,844	91.89
wt_0.5_Cu_yf_2	GTGCC	8,882,478	92,334	8,790,144	98.96	8,697,810	7,682,083	87.39
wt_0.5_Cu_yf_3	GTTTC	8,979,832	104,234	8,875,598	98.84	8,771,364	8,045,239	90.64
wt_0_Cu_yf_1	CAAA	8,946,822	117,393	8,829,429	98.69	8,712,036	7,956,336	90.11
wt_0_Cu_yf_2	CAACT	8,811,656	101,547	8,710,109	98.85	8,608,562	7,879,644	90.47
wt_0_Cu_yf_3	CACCG	9,254,104	128,692	9,125,412	98.61	8,996,720	8,183,291	89.68
ccit1_0.5Cu_yf_1	CGTAG	8,644,885	96,955	8,547,930	98.88	8,450,975	7,803,862	91.30
ccit1_0.5Cu_yf_2	GAGTG	8,797,911	83,368	8,714,543	99.05	8,631,175	7,908,172	90.75
ccit1_0.5Cu_yf_3	GGTAG	9,424,061	99,607	9,324,454	98.94	9,224,847	8,429,116	90.40
ccit1_0Cu_yf_1	CACG	11,054,129	129,990	10,924,139	98.82	10,794,149	9,844,714	90.12
ccit1_0Cu_yf_2	CACT	10,036,500	147,218	9,889,282	98.53	9,742,064	8,574,110	86.70
ccit1_0Cu_yf_3	CAGGC	11,313,309	247,440	11,065,869	97.81	10,818,429	9,788,742	88.46
spl7_0.5Cu_yf_1	ACTG	9,232,238	105,210	9,127,028	98.86	9,021,818	8,373,354	91.74
spl7_0.5Cu_yf_2	ATGAG	13,243,065	355,375	12,887,690	97.32	12,532,315	11,273,996	87.48
spl7_0.5Cu_yf_3	ATTCC	9,772,944	235,554	9,537,390	97.59	9,301,836	8,392,373	87.99

Supplemental table 6. GO term enrichment analysis of the Cu deficiency upregulated genes in floral buds			
Gene Ontology term	Cluster frequency	Genome frequency of use	Corrected P-value
response to stimulus	48 out of 203 genes, 23.6%	2527 out of 27235 genes, 9.3%	0
biological regulation	51 out of 203 genes, 25.1%	3218 out of 27235 genes, 11.8%	0
response to hormone stimulus	18 out of 203 genes, 8.9%	620 out of 27235 genes, 2.3%	0
regulation of metabolic process	33 out of 203 genes, 16.3%	1802 out of 27235 genes, 6.6%	0
response to chemical stimulus	24 out of 203 genes, 11.8%	1112 out of 27235 genes, 4.1%	0
regulation of biological process	44 out of 203 genes, 21.7%	2903 out of 27235 genes, 10.7%	0
response to endogenous stimulus	18 out of 203 genes, 8.9%	681 out of 27235 genes, 2.5%	0
regulation of cellular metabolic process	31 out of 203 genes, 15.3%	1710 out of 27235 genes, 6.3%	0
regulation of macromolecule metabolic process	31 out of 203 genes, 15.3%	1740 out of 27235 genes, 6.4%	0
regulation of biosynthetic process	30 out of 203 genes, 14.8%	1654 out of 27235 genes, 6.1%	0
regulation of cellular biosynthetic process	30 out of 203 genes, 14.8%	1654 out of 27235 genes, 6.1%	0
response to abiotic stimulus	20 out of 203 genes, 9.9%	851 out of 27235 genes, 3.1%	0
regulation of transcription	29 out of 203 genes, 14.3%	1609 out of 27235 genes, 5.9%	0
regulation of nucleobase, nucleoside, nucleotide and nucleic acid metabolic process	29 out of 203 genes, 14.3%	1628 out of 27235 genes, 6.0%	0
regulation of macromolecule biosynthetic process	29 out of 203 genes, 14.3%	1636 out of 27235 genes, 6.0%	0
regulation of gene expression	29 out of 203 genes, 14.3%	1696 out of 27235 genes, 6.2%	0
regulation of cellular process	39 out of 203 genes, 19.2%	2712 out of 27235 genes, 10.0%	0
syncytium formation	3 out of 203 genes, 1.5%	10 out of 27235 genes, 0.0%	0
circadian rhythm	4 out of 203 genes, 2.0%	31 out of 27235 genes, 0.1%	0
rhythmic process	4 out of 203 genes, 2.0%	31 out of 27235 genes, 0.1%	0

plant-type cell wall loosening	4 out of 203 genes, 2.0%	34 out of 27235 genes, 0.1%	0
response to salt stress	8 out of 203 genes, 3.9%	199 out of 27235 genes, 0.7%	0
nitric oxide biosynthetic process	2 out of 203 genes, 1.0%	3 out of 27235 genes, 0.0%	0
nitric oxide metabolic process	2 out of 203 genes, 1.0%	3 out of 27235 genes, 0.0%	0
response to stress	25 out of 203 genes, 12.3%	1516 out of 27235 genes, 5.6%	0
response to abscisic acid stimulus	8 out of 203 genes, 3.9%	207 out of 27235 genes, 0.8%	0
plant-type cell wall modification	4 out of 203 genes, 2.0%	38 out of 27235 genes, 0.1%	0
response to light stimulus	10 out of 203 genes, 4.9%	339 out of 27235 genes, 1.2%	0.00143
response to osmotic stress	8 out of 203 genes, 3.9%	222 out of 27235 genes, 0.8%	0.00138
response to radiation	10 out of 203 genes, 4.9%	350 out of 27235 genes, 1.3%	0.00133
anatomical structure formation	4 out of 203 genes, 2.0%	52 out of 27235 genes, 0.2%	0.0071
response to auxin stimulus	8 out of 203 genes, 3.9%	256 out of 27235 genes, 0.9%	0.00688
nitrate assimilation	2 out of 203 genes, 1.0%	7 out of 27235 genes, 0.0%	0.01059
response to red or far red light	5 out of 203 genes, 2.5%	110 out of 27235 genes, 0.4%	0.012
response to red light	3 out of 203 genes, 1.5%	33 out of 27235 genes, 0.1%	0.02222
secondary metabolic process	8 out of 203 genes, 3.9%	301 out of 27235 genes, 1.1%	0.02595
hyperosmotic salinity response	3 out of 203 genes, 1.5%	34 out of 27235 genes, 0.1%	0.02789
hyperosmotic response	3 out of 203 genes, 1.5%	36 out of 27235 genes, 0.1%	0.03487
nitrogen compound biosynthetic process	6 out of 203 genes, 3.0%	186 out of 27235 genes, 0.7%	0.0405
phototransduction	2 out of 203 genes, 1.0%	12 out of 27235 genes, 0.0%	0.04909
detection of light stimulus	2 out of 203 genes, 1.0%	12 out of 27235 genes, 0.0%	0.048
detection of visible light	2 out of 203 genes, 1.0%	12 out of 27235 genes, 0.0%	0.04696
red, far-red light phototransduction	2 out of 203 genes, 1.0%	12 out of 27235 genes, 0.0%	0.04596

abscisic acid biosynthetic process	2 out of 203 genes, 1.0%	12 out of 27235 genes, 0.0%	0.045
apocarotenoid biosynthetic process	2 out of 203 genes, 1.0%	12 out of 27235 genes, 0.0%	0.04408
neurological system process	2 out of 203 genes, 1.0%	12 out of 27235 genes, 0.0%	0.0432
cognition	2 out of 203 genes, 1.0%	12 out of 27235 genes, 0.0%	0.04235
detection of stimulus involved in sensory perception	2 out of 203 genes, 1.0%	12 out of 27235 genes, 0.0%	0.04154
detection of light stimulus involved in visual perception	2 out of 203 genes, 1.0%	12 out of 27235 genes, 0.0%	0.04075
sensory perception of light stimulus	2 out of 203 genes, 1.0%	12 out of 27235 genes, 0.0%	0.04
detection of light stimulus involved in sensory perception	2 out of 203 genes, 1.0%	12 out of 27235 genes, 0.0%	0.03927
cellular nitrogen compound metabolic process	9 out of 203 genes, 4.4%	423 out of 27235 genes, 1.6%	0.04929

Supplemental table 7. GO term enrichment analysis of the Cu deficiency downregulated genes in floral buds			
Gene Ontology term	Cluster frequency	Genome frequency of use	Corrected P-value
sulfate assimilation	4 out of 345 genes, 1.2%	13 out of 27235 genes, 0.0%	0
sulfur utilization	4 out of 345 genes, 1.2%	14 out of 27235 genes, 0.1%	0

Supplemental table 8. GO term enrichment analysis of the Cu deficiency upregulated genes in mature flowers			
Gene Ontology term	Cluster frequency	Genome frequency of use	Corrected P-value
response to stimulus	107 out of 420 genes, 25.5%	2527 out of 27235 genes, 9.3%	0
response to chemical stimulus	66 out of 420 genes, 15.7%	1112 out of 27235 genes, 4.1%	0
response to hormone stimulus	45 out of 420 genes, 10.7%	620 out of 27235 genes, 2.3%	0
response to endogenous stimulus	45 out of 420 genes, 10.7%	681 out of 27235 genes, 2.5%	0

response to auxin stimulus	27 out of 420 genes, 6.4%	256 out of 27235 genes, 0.9%	0
response to stress	55 out of 420 genes, 13.1%	1516 out of 27235 genes, 5.6%	0
response to abiotic stimulus	38 out of 420 genes, 9.0%	851 out of 27235 genes, 3.1%	0
response to abscisic acid stimulus	17 out of 420 genes, 4.0%	207 out of 27235 genes, 0.8%	0
regulation of metabolic process	55 out of 420 genes, 13.1%	1802 out of 27235 genes, 6.6%	0
regulation of cellular metabolic process	53 out of 420 genes, 12.6%	1710 out of 27235 genes, 6.3%	0
response to osmotic stress	15 out of 420 genes, 3.6%	222 out of 27235 genes, 0.8%	0
abscisic acid metabolic process	5 out of 420 genes, 1.2%	17 out of 27235 genes, 0.1%	0
apocarotenoid metabolic process	5 out of 420 genes, 1.2%	17 out of 27235 genes, 0.1%	0
regulation of biosynthetic process	49 out of 420 genes, 11.7%	1654 out of 27235 genes, 6.1%	0
regulation of cellular biosynthetic process	49 out of 420 genes, 11.7%	1654 out of 27235 genes, 6.1%	0
regulation of transcription	48 out of 420 genes, 11.4%	1609 out of 27235 genes, 5.9%	0
regulation of nucleobase, nucleoside, nucleotide and nucleic acid metabolic process	48 out of 420 genes, 11.4%	1628 out of 27235 genes, 6.0%	0
response to salt stress	13 out of 420 genes, 3.1%	199 out of 27235 genes, 0.7%	0
regulation of macromolecule biosynthetic process	48 out of 420 genes, 11.4%	1636 out of 27235 genes, 6.0%	0
regulation of macromolecule metabolic process	50 out of 420 genes, 11.9%	1740 out of 27235 genes, 6.4%	0
biological regulation	79 out of 420 genes, 18.8%	3218 out of 27235 genes, 11.8%	0
response to water deprivation	10 out of 420 genes, 2.4%	127 out of 27235 genes, 0.5%	0
regulation of biological process	72 out of 420 genes, 17.1%	2903 out of 27235 genes, 10.7%	0

regulation of gene expression	48 out of 420 genes, 11.4%	1696 out of 27235 genes, 6.2%	0
regulation of cellular process	68 out of 420 genes, 16.2%	2712 out of 27235 genes, 10.0%	0
response to water	10 out of 420 genes, 2.4%	136 out of 27235 genes, 0.5%	0
response to light stimulus	16 out of 420 genes, 3.8%	339 out of 27235 genes, 1.2%	0.00296
response to temperature stimulus	15 out of 420 genes, 3.6%	308 out of 27235 genes, 1.1%	0.00286
defense response	22 out of 420 genes, 5.2%	576 out of 27235 genes, 2.1%	0.00276
circadian rhythm	5 out of 420 genes, 1.2%	31 out of 27235 genes, 0.1%	0.00267
rhythmic process	5 out of 420 genes, 1.2%	31 out of 27235 genes, 0.1%	0.00258
response to radiation	16 out of 420 genes, 3.8%	350 out of 27235 genes, 1.3%	0.0025
response to red light	5 out of 420 genes, 1.2%	33 out of 27235 genes, 0.1%	0.00242
response to bacterium	9 out of 420 genes, 2.1%	129 out of 27235 genes, 0.5%	0.00294
defense response to bacterium	7 out of 420 genes, 1.7%	79 out of 27235 genes, 0.3%	0.00343
response to red or far red light	8 out of 420 genes, 1.9%	110 out of 27235 genes, 0.4%	0.005
intracellular signaling cascade	18 out of 420 genes, 4.3%	469 out of 27235 genes, 1.7%	0.00486
regulation of defense response	5 out of 420 genes, 1.2%	45 out of 27235 genes, 0.2%	0.00632
abscisic acid biosynthetic process	3 out of 420 genes, 0.7%	12 out of 27235 genes, 0.0%	0.01077
apocarotenoid biosynthetic process	3 out of 420 genes, 0.7%	12 out of 27235 genes, 0.0%	0.0105
regulation of hydrogen peroxide metabolic process	2 out of 420 genes, 0.5%	4 out of 27235 genes, 0.0%	0.02293
regulation of transcription, DNA-dependent	27 out of 420 genes, 6.4%	934 out of 27235 genes, 3.4%	0.02286
response to inorganic substance	7 out of 420 genes, 1.7%	109 out of 27235 genes, 0.4%	0.02233
regulation of RNA metabolic process	27 out of 420 genes, 6.4%	940 out of 27235 genes, 3.5%	0.02273

response to light intensity	5 out of 420 genes, 1.2%	56 out of 27235 genes, 0.2%	0.02311
regulation of oxygen and reactive oxygen species metabolic process	2 out of 420 genes, 0.5%	5 out of 27235 genes, 0.0%	0.03957
terpenoid metabolic process	6 out of 420 genes, 1.4%	88 out of 27235 genes, 0.3%	0.03872
response to metal ion	6 out of 420 genes, 1.4%	88 out of 27235 genes, 0.3%	0.03792
abscisic acid mediated signaling	4 out of 420 genes, 1.0%	37 out of 27235 genes, 0.1%	0.03796
response to salicylic acid stimulus	7 out of 420 genes, 1.7%	119 out of 27235 genes, 0.4%	0.0388
secondary metabolic process	12 out of 420 genes, 2.9%	301 out of 27235 genes, 1.1%	0.03843
cold acclimation	3 out of 420 genes, 0.7%	19 out of 27235 genes, 0.1%	0.04115
isoprenoid metabolic process	7 out of 420 genes, 1.7%	124 out of 27235 genes, 0.5%	0.04151

Supplemental table 9. GO term enrichment analysis of the Cu deficiency downregulated genes in mature flowers

Gene Ontology term	Cluster frequency	Genome frequency of use	Corrected P-value
Response to wounding	8 out of 192 genes, 4.2%	111 out of 27235 genes, 0.4%	0
Sulfate assimilation	4 out of 192 genes, 2.1%	13 out of 27235 genes, 0.0%	0
Sulfur utilization	4 out of 192 genes, 2.1%	14 out of 27235 genes, 0.1%	0
Respiratory electron transport chain	17 out of 192 genes, 8.9%	630 out of 27235 genes, 2.3%	0
Electron transport chain	17 out of 192 genes, 8.9%	652 out of 27235 genes, 2.4%	0
Oxidation reduction	17 out of 192 genes, 8.9%	652 out of 27235 genes, 2.4%	0
Generation of precursor metabolites and energy	18 out of 192 genes, 9.4%	846 out of 27235 genes, 3.1%	0
Response to external stimulus	9 out of 192 genes, 4.7%	227 out of 27235 genes, 0.8%	0
Response to stress	24 out of 192 genes, 12.5%	1516 out of 27235 genes, 5.6%	0.00667

Unannotated	6 out of 192 genes, 3.1%	123 out of 27235 genes, 0.5%	0.006
Jasmonic acid biosynthetic process	3 out of 192 genes, 1.6%	23 out of 27235 genes, 0.1%	0.01667
Oxylipin biosynthetic process	3 out of 192 genes, 1.6%	24 out of 27235 genes, 0.1%	0.01429
Cytokinin catabolic process	2 out of 192 genes, 1.0%	7 out of 27235 genes, 0.0%	0.03333
Hormone catabolic process	2 out of 192 genes, 1.0%	7 out of 27235 genes, 0.0%	0.03125
Jasmonic acid and ethylene-dependent systemic resistance	3 out of 192 genes, 1.6%	32 out of 27235 genes, 0.1%	0.04118
Response to iron ion	2 out of 192 genes, 1.0%	9 out of 27235 genes, 0.0%	0.04444
Response to copper ion	2 out of 192 genes, 1.0%	9 out of 27235 genes, 0.0%	0.04211
Metabolic process	72 out of 192 genes, 37.5%	7531 out of 27235 genes, 27.7%	0.04
Removal of superoxide radicals	2 out of 192 genes, 1.0%	10 out of 27235 genes, 0.0%	0.04286
Superoxide metabolic process	2 out of 192 genes, 1.0%	11 out of 27235 genes, 0.0%	0.05

Supplemental table 10. GO term enrichment analysis of the downregulated genes in mature flowers of <i>ccitI-1</i> mutant compared to wild-type under Cu replete condition			
Gene Ontology term	Cluster frequency	Genome frequency of use	Corrected P-value
Response to stimulus	33 out of 91 genes, 36.3%	2527 out of 27235 genes, 9.3%	0
Response to stress	25 out of 91 genes, 27.5%	1516 out of 27235 genes, 5.6%	0
Response to chemical stimulus	20 out of 91 genes, 22.0%	1112 out of 27235 genes, 4.1%	0
Response to endogenous stimulus	16 out of 91 genes, 17.6%	681 out of 27235 genes, 2.5%	0
Jasmonic acid and ethylene-dependent systemic resistance	6 out of 91 genes, 6.6%	32 out of 27235 genes, 0.1%	0
Response to hormone stimulus	15 out of 91 genes, 16.5%	620 out of 27235 genes, 2.3%	0
Response to wounding	8 out of 91 genes, 8.8%	111 out of 27235 genes, 0.4%	0
Jasmonic acid biosynthetic process	5 out of 91 genes, 5.5%	23 out of 27235 genes, 0.1%	0

Oxylipin biosynthetic process	5 out of 91 genes, 5.5%	24 out of 27235 genes, 0.1%	0
Response to water	8 out of 91 genes, 8.8%	136 out of 27235 genes, 0.5%	0
Response to abiotic stimulus	16 out of 91 genes, 17.6%	851 out of 27235 genes, 3.1%	0
Defense response, incompatible interaction	7 out of 91 genes, 7.7%	94 out of 27235 genes, 0.3%	0
Response to external stimulus	9 out of 91 genes, 9.9%	227 out of 27235 genes, 0.8%	0
Cytokinin mediated signaling	5 out of 91 genes, 5.5%	38 out of 27235 genes, 0.1%	0
Response to water deprivation	7 out of 91 genes, 7.7%	127 out of 27235 genes, 0.5%	0
Innate immune response	7 out of 91 genes, 7.7%	135 out of 27235 genes, 0.5%	0
Immune response	7 out of 91 genes, 7.7%	147 out of 27235 genes, 0.5%	0
Hormone-mediated signaling	7 out of 91 genes, 7.7%	176 out of 27235 genes, 0.6%	0
Response to cytokinin stimulus	5 out of 91 genes, 5.5%	68 out of 27235 genes, 0.2%	0
Defense response	11 out of 91 genes, 12.1%	576 out of 27235 genes, 2.1%	0
Response to cold	7 out of 91 genes, 7.7%	203 out of 27235 genes, 0.7%	0
Response to abscisic acid stimulus	7 out of 91 genes, 7.7%	207 out of 27235 genes, 0.8%	0
Response to temperature stimulus	8 out of 91 genes, 8.8%	308 out of 27235 genes, 1.1%	0
Response to biotic stimulus	9 out of 91 genes, 9.9%	410 out of 27235 genes, 1.5%	0
Sulfate assimilation	3 out of 91 genes, 3.3%	13 out of 27235 genes, 0.0%	0
Sulfur utilization	3 out of 91 genes, 3.3%	14 out of 27235 genes, 0.1%	0
Fatty acid biosynthetic process	5 out of 91 genes, 5.5%	104 out of 27235 genes, 0.4%	0
Multi-organism process	9 out of 91 genes, 9.9%	469 out of 27235 genes, 1.7%	0
Response to desiccation	3 out of 91 genes, 3.3%	18 out of 27235 genes, 0.1%	0

Response to other organism	8 out of 91 genes, 8.8%	367 out of 27235 genes, 1.3%	0
Cell communication	12 out of 91 genes, 13.2%	963 out of 27235 genes, 3.5%	0.00235
Signal transduction	11 out of 91 genes, 12.1%	856 out of 27235 genes, 3.1%	0.004
Organic acid biosynthetic process	5 out of 91 genes, 5.5%	147 out of 27235 genes, 0.5%	0.00389
Carboxylic acid biosynthetic process	5 out of 91 genes, 5.5%	147 out of 27235 genes, 0.5%	0.00378
Oxygen and reactive oxygen species metabolic process	3 out of 91 genes, 3.3%	30 out of 27235 genes, 0.1%	0.00368
Intracellular signaling cascade	8 out of 91 genes, 8.8%	469 out of 27235 genes, 1.7%	0.00462
Fatty acid metabolic process	5 out of 91 genes, 5.5%	159 out of 27235 genes, 0.6%	0.0045
Cellular process	44 out of 91 genes, 48.4%	8326 out of 27235 genes, 30.6%	0.00537
Response to iron ion	2 out of 91 genes, 2.2%	9 out of 27235 genes, 0.0%	0.00619
Response to copper ion	2 out of 91 genes, 2.2%	9 out of 27235 genes, 0.0%	0.00605
Removal of superoxide radicals	2 out of 91 genes, 2.2%	10 out of 27235 genes, 0.0%	0.00682
Reproductive structure development	8 out of 91 genes, 8.8%	551 out of 27235 genes, 2.0%	0.00696
Superoxide metabolic process	2 out of 91 genes, 2.2%	11 out of 27235 genes, 0.0%	0.00681
Embryonic development ending in seed dormancy	6 out of 91 genes, 6.6%	342 out of 27235 genes, 1.3%	0.01042
Respiratory electron transport chain	8 out of 91 genes, 8.8%	630 out of 27235 genes, 2.3%	0.01388
Anther development	2 out of 91 genes, 2.2%	17 out of 27235 genes, 0.1%	0.018
Embryonic development	6 out of 91 genes, 6.6%	367 out of 27235 genes, 1.3%	0.01765
Electron transport chain	8 out of 91 genes, 8.8%	652 out of 27235 genes, 2.4%	0.01769

Oxidation reduction	8 out of 91 genes, 8.8%	652 out of 27235 genes, 2.4%	0.01736
Cold acclimation	2 out of 91 genes, 2.2%	19 out of 27235 genes, 0.1%	0.01782
Seed development	6 out of 91 genes, 6.6%	385 out of 27235 genes, 1.4%	0.01754
Monocarboxylic acid metabolic process	5 out of 91 genes, 5.5%	278 out of 27235 genes, 1.0%	0.02
Sulfur metabolic process	3 out of 91 genes, 3.3%	87 out of 27235 genes, 0.3%	0.02305
Systemic acquired resistance	2 out of 91 genes, 2.2%	25 out of 27235 genes, 0.1%	0.024
Lipid biosynthetic process	5 out of 91 genes, 5.5%	309 out of 27235 genes, 1.1%	0.03082
Developmental process	11 out of 91 genes, 12.1%	1292 out of 27235 genes, 4.7%	0.03032
Stamen development	2 out of 91 genes, 2.2%	28 out of 27235 genes, 0.1%	0.03238
Androecium development	2 out of 91 genes, 2.2%	28 out of 27235 genes, 0.1%	0.03188
Metabolic process	37 out of 91 genes, 40.7%	7531 out of 27235 genes, 27.7%	0.03723
Response to light stimulus	5 out of 91 genes, 5.5%	339 out of 27235 genes, 1.2%	0.03939
Hyperosmotic salinity response	2 out of 91 genes, 2.2%	34 out of 27235 genes, 0.1%	0.04
Cellular metabolic process	32 out of 91 genes, 35.2%	6294 out of 27235 genes, 23.1%	0.04059
Response to radiation	5 out of 91 genes, 5.5%	350 out of 27235 genes, 1.3%	0.04029
Hyperosmotic response	2 out of 91 genes, 2.2%	36 out of 27235 genes, 0.1%	0.03971
Response to osmotic stress	4 out of 91 genes, 4.4%	222 out of 27235 genes, 0.8%	0.03944
Abscisic acid mediated signaling	2 out of 91 genes, 2.2%	37 out of 27235 genes, 0.1%	0.03917
Generation of precursor metabolites and energy	8 out of 91 genes, 8.8%	846 out of 27235 genes, 3.1%	0.0411

Supplemental table 11. GO term enrichment analysis of the downregulated genes in mature flowers of <i>ccit1-1</i> mutant compared to wild-type under Cu deficient conditions			
Gene Ontology term	Cluster frequency	Genome frequency of use	Corrected P-value

Response to chemical stimulus	14 out of 77 genes, 18.2%	1112 out of 27235 genes, 4.1%	0
Response to stimulus	20 out of 77 genes, 26.0%	2527 out of 27235 genes, 9.3%	0
Secondary metabolic process	7 out of 77 genes, 9.1%	301 out of 27235 genes, 1.1%	0
Plant-type cell wall loosening	3 out of 77 genes, 3.9%	34 out of 27235 genes, 0.1%	0.005
Plant-type cell wall modification	3 out of 77 genes, 3.9%	38 out of 27235 genes, 0.1%	0.012
Response to iron ion	2 out of 77 genes, 2.6%	9 out of 27235 genes, 0.0%	0.01667
Response to copper ion	2 out of 77 genes, 2.6%	9 out of 27235 genes, 0.0%	0.01429
Toxin metabolic process	3 out of 77 genes, 3.9%	46 out of 27235 genes, 0.2%	0.0125
Toxin catabolic process	3 out of 77 genes, 3.9%	46 out of 27235 genes, 0.2%	0.01111
Removal of superoxide radicals	2 out of 77 genes, 2.6%	10 out of 27235 genes, 0.0%	0.01
Superoxide metabolic process	2 out of 77 genes, 2.6%	11 out of 27235 genes, 0.0%	0.01167
Reproductive process	8 out of 77 genes, 10.4%	656 out of 27235 genes, 2.4%	0.02154
Embryonic and seed development	6 out of 77 genes, 7.8%	367 out of 27235 genes, 1.3%	0.02286
Response to endogenous stimulus	8 out of 77 genes, 10.4%	681 out of 27235 genes, 2.5%	0.02
Response to toxin	3 out of 77 genes, 3.9%	65 out of 27235 genes, 0.2%	0.02222
Reproductive structure development	7 out of 77 genes, 9.1%	551 out of 27235 genes, 2.0%	0.021
Anatomical structure development	9 out of 77 genes, 11.7%	922 out of 27235 genes, 3.4%	0.02286
Response to hormone stimulus	7 out of 77 genes, 9.1%	620 out of 27235 genes, 2.3%	0.02727
Plant-type cell wall modification during multidimensional cell growth	2 out of 77 genes, 2.6%	25 out of 27235 genes, 0.1%	0.03478
Cell wall modification during multidimensional cell growth	2 out of 77 genes, 2.6%	27 out of 27235 genes, 0.1%	0.0425

REFERENCES

- Alexander, M.P.** (1969). Differential Staining of Aborted and Nonaborted Pollen. *Stain Technology* **44**, 117-122.
- Alonso, J.M., Stepanova, A.N., Leisse, T.J., Kim, C.J., Chen, H., Shinn, P., Stevenson, D.K., Zimmerman, J., Barajas, P., Cheuk, R., Gadrinab, C., Heller, C., Jeske, A., Koesema, E., Meyers, C.C., Parker, H., Prednis, L., Ansari, Y., Choy, N., Deen, H., Geralt, M., Hazari, N., Hom, E., Karnes, M., Mulholland, C., Ndubaku, R., Schmidt, I., Guzman, P., Aguilar-Henonin, L., Schmid, M., Weigel, D., Carter, D.E., Marchand, T., Risseeuw, E., Brogden, D., Zeko, A., Crosby, W.L., Berry, C.C., and Ecker, J.R.** (2003). Genome-wide insertional mutagenesis of *Arabidopsis thaliana*. *Science* **301**, 653-657.
- Alvarez-Buylla, E.R., Benítez, M., Corvera-Poiré, A., Chaos Cador, Á., de Folter, S., Gamboa de Buen, A., Garay-Arroyo, A., García-Ponce, B., Jaimes-Miranda, F., Pérez-Ruiz, R.V., Piñeyro-Nelson, A., and Sánchez-Corrales, Y.E.** (2010a). Flower Development. The *Arabidopsis Book / American Society of Plant Biologists* **8**, e0127.
- Alvarez-Buylla, E.R., Benítez, M., Corvera-Poiré, A., Chaos Cador, Á., de Folter, S., Gamboa de Buen, A., Garay-Arroyo, A., García-Ponce, B., Jaimes-Miranda, F., Pérez-Ruiz, R.V., Piñeyro-Nelson, A., and Sanchez-Corrales, Y.E.** (2010b). Flower development. The *Arabidopsis book / American Society of Plant Biologists* **8**, e0127.
- Arteca, R.N., and Arteca, J.M.** (2000a). A novel method for growing *Arabidopsis thaliana* plants hydroponically. *Physiol Plantarum* **108**, 188-193.
- Arteca, R.N., and Arteca, J.M.** (2000b). A novel method for growing *Arabidopsis thaliana* plants hydroponically. *Physiologia plantarum* **108**, 188-193.
- Atchley, W.R., Terhalle, W., and Dress, A.** (1999). Positional dependence, cliques, and predictive motifs in the bHLH protein domain. *Journal of molecular evolution* **48**, 501-516.
- Attallah, C.V., Welchen, E., and Gonzalez, D.H.** (2007). The promoters of *Arabidopsis thaliana* genes AtCOX17-1 and -2, encoding a copper chaperone involved in cytochrome c oxidase biogenesis, are preferentially active in roots and anthers and induced by biotic and abiotic stress. *Physiol Plantarum* **129**, 123-134.
- Bailey, P.C., Martin, C., Toledo-Ortiz, G., Quail, P.H., Huq, E., Heim, M.A., Jakoby, M., Werber, M., and Weisshaar, B.** (2003). Update on the basic helix-loop-helix transcription factor gene family in *Arabidopsis thaliana*. *The Plant cell* **15**, 2497-2502.
- Benjamini, Y., and Hochberg, Y.** (1995). Controlling the False Discovery Rate - a Practical and Powerful Approach to Multiple Testing. *J Roy Stat Soc B Met* **57**, 289-300.
- Bernal, M., Casero, D., Singh, V., Wilson, G.T., Grande, A., Yang, H., Dodani, S.C., Pellegrini, M., Huijser, P., Connolly, E.L., Merchant, S.S., and Krämer, U.** (2012a). Transcriptome Sequencing Identifies SPL7-Regulated Copper Acquisition Genes FRO4/FRO5 and the Copper Dependence of Iron Homeostasis in *Arabidopsis*. *The Plant Cell Online* **24**, 738-761.
- Bernal, M., Casero, D., Singh, V., Wilson, G.T., Grande, A., Yang, H., Dodani, S.C., Pellegrini, M., Huijser, P., Connolly, E.L., Merchant, S.S., and Kramer, U.** (2012b). Transcriptome sequencing identifies SPL7-regulated copper acquisition genes FRO4/FRO5 and the copper dependence of iron homeostasis in *Arabidopsis*. *The Plant cell* **24**, 738-761.
- Bolger, A.M., Lohse, M., and Usadel, B.** (2014). Trimmomatic: a flexible trimmer for Illumina sequence data. *Bioinformatics* **30**, 2114-2120.
- Bowler, C., Van Camp, W., Van Montagu, M., and Inze, D.** (1994). Superoxide Dismutase in Plants. *Crit Rev Plant Sci* **13**, 199 - 199.
- Bowman, J.L., Drews, G.N., and Meyerowitz, E.M.** (1991). Expression of the *Arabidopsis* floral homeotic gene AGAMOUS is restricted to specific cell types late in flower development. *Plant Cell* **3**, 749-758.

- Boyle, E.I., Weng, S., Gollub, J., Jin, H., Botstein, D., Cherry, J.M., and Sherlock, G.** (2004). GO::TermFinder--open source software for accessing Gene Ontology information and finding significantly enriched Gene Ontology terms associated with a list of genes. *Bioinformatics* **20**, 3710-3715.
- Burkhead, J., Reynolds, K., Abdel-Ghany, S., Cohu, C., and Pilon, M.** (2009). Copper homeostasis. *The New phytologist* **182**, 799 - 816.
- Caldelari, D., Wang, G., Farmer, E.E., and Dong, X.** (2011). Arabidopsis lox3 lox4 double mutants are male sterile and defective in global proliferative arrest. *Plant molecular biology* **75**, 25-33.
- Cardon, G.H., Hohmann, S., Nettesheim, K., Saedler, H., and Huijser, P.** (1997). Functional analysis of the Arabidopsis thaliana SBP-box gene SPL3: a novel gene involved in the floral transition. *The Plant journal : for cell and molecular biology* **12**, 367-377.
- Cecchetti, V., Altamura, M.M., Falasca, G., Costantino, P., and Cardarelli, M.** (2008). Auxin regulates Arabidopsis anther dehiscence, pollen maturation, and filament elongation. *The Plant cell* **20**, 1760-1774.
- Cheng, H., Qin, L., Lee, S., Fu, X., Richards, D.E., Cao, D., Luo, D., Harberd, N.P., and Peng, J.** (2004). Gibberellin regulates Arabidopsis floral development via suppression of DELLA protein function. *Development* **131**, 1055-1064.
- Christopher, M.C., and Marinus, P.** (2007). Regulation of superoxide dismutase expression by copper availability. *Physiologia Plantarum* **129**, 747-755.
- Chung, S.M., Frankman, E.L., and Tzfira, T.** (2005). A versatile vector system for multiple gene expression in plants. *Trends in plant science* **10**, 357-361.
- Clough, S.J., and Bent, A.F.** (1998). Floral dip: a simplified method for Agrobacterium-mediated transformation of Arabidopsis thaliana. *Plant Journal* **16**, 735-743.
- Cohu, C.M., Abdel-Ghany, S.E., Gogolin Reynolds, K.A., Onofrio, A.M., Bodecker, J.R., Kimbrel, J.A., Niyogi, K.K., and Pilon, M.** (2009). Copper Delivery by the Copper Chaperone for Chloroplast and Cytosolic Copper/Zinc-Superoxide Dismutases: Regulation and Unexpected Phenotypes in an Arabidopsis Mutant. *Mol Plant* **2**, 1336-1350.
- Colangelo, E.P., and Guerinot, M.L.** (2004). The essential basic helix-loop-helix protein FIT1 is required for the iron deficiency response. *The Plant cell* **16**, 3400-3412.
- Crismani, W., and Mercier, R.** (2013). Identifying meiotic mutants in Arabidopsis thaliana. *Methods in molecular biology* **990**, 227-234.
- DiDonato, R.J., Roberts, L.A., Sanderson, T., Eisley, R.B., and Walker, E.L.** (2004). Arabidopsis Yellow Stripe-Like2 (YSL2): a metal-regulated gene encoding a plasma membrane transporter of nicotianamine–metal complexes. *The Plant Journal* **39**, 403-414.
- Earley, K.W., Haag, J.R., Pontes, O., Opper, K., Juehne, T., Song, K.M., and Pikaard, C.S.** (2006). Gateway-compatible vectors for plant functional genomics and proteomics. *Plant Journal* **45**, 616-629.
- Einsle, O., Mehrabian, Z., Nalbandyan, R., and Messerschmidt, A.** (2000). Crystal structure of plantacyanin, a basic blue cupredoxin from spinach. *Journal of biological inorganic chemistry : JBIC : a publication of the Society of Biological Inorganic Chemistry* **5**, 666-672.
- Flemming, C.A., and Trevors, J.T.** (1989). Copper toxicity and chemistry in the environment: a review. *Water, Air, and Soil Pollution* **44**, 143-158.
- Gandikota, M., Birkenbihl, R.P., Hohmann, S., Cardon, G.H., Saedler, H., and Huijser, P.** (2007). The miRNA156/157 recognition element in the 3' UTR of the Arabidopsis SBP box gene SPL3 prevents early flowering by translational inhibition in seedlings. *The Plant journal : for cell and molecular biology* **49**, 683-693.
- Garcia-Molina, A., Xing, S.P., and Huijser, P.** (2014). A Conserved KIN17 Curved DNA-Binding Domain Protein Assembles with SQUAMOSA PROMOTER-BINDING PROTEIN-LIKE7 to Adapt Arabidopsis Growth and Development to Limiting Copper Availability. *Plant physiology* **164**, 828-840.

- Garcia-Molina, A., Andrés-Colás, N., Perea-García, A., del Valle-Tascón, S., Peñarrubia, L., and Puig, S.** (2011). The intracellular *Arabidopsis* COPT5 transport protein is required for photosynthetic electron transport under severe copper deficiency. *Plant J* **65**, 848-860.
- Garcia-Molina, A., Andres-Colas, N., Perea-Garcia, A., Neumann, U., Dodani, S.C., Huijser, P., Penarrubia, L., and Puig, S.** (2013). The *Arabidopsis* COPT6 transport protein functions in copper distribution under copper-deficient conditions. *Plant Cell Physiol* **54**, 1378-1390.
- Gayomba, S.R., Jung, H.I., Yan, J., Danku, J., Rutzke, M.A., Bernal, M., Kramer, U., Kochian, L.V., Salt, D.E., and Vatamaniuk, O.K.** (2013). The CTR/COPT-dependent copper uptake and SPL7-dependent copper deficiency responses are required for basal cadmium tolerance in *A. thaliana*. *Metallomics* **5**, 1262-1275.
- Guo, W.J., Bundithya, W., and Goldsbrough, P.B.** (2003). Characterization of the *Arabidopsis* metallothionein gene family: tissue-specific expression and induction during senescence and in response to copper. *New Phytologist* **159**, 369-381.
- Guo, W.J., Meetam, M., and Goldsbrough, P.B.** (2008). Examining the specific contributions of individual *Arabidopsis* metallothioneins to copper distribution and metal tolerance. *Plant physiology* **146**, 1697-1706.
- Heim, M.A., Jakoby, M., Werber, M., Martin, C., Weisshaar, B., and Bailey, P.C.** (2003). The basic helix-loop-helix transcription factor family in plants: a genome-wide study of protein structure and functional diversity. *Mol Biol Evol* **20**, 735-747.
- Hou, X., Hu, W.W., Shen, L., Lee, L.Y., Tao, Z., Han, J.H., and Yu, H.** (2008). Global identification of DELLA target genes during *Arabidopsis* flower development. *Plant physiology* **147**, 1126-1142.
- Ishiguro, S., Kawai-Oda, A., Ueda, J., Nishida, I., and Okada, K.** (2001a). The DEFECTIVE IN ANther DEHISCENCE gene encodes a novel phospholipase A1 catalyzing the initial step of jasmonic acid biosynthesis, which synchronizes pollen maturation, anther dehiscence, and flower opening in *Arabidopsis*. *The Plant cell* **13**, 2191-2209.
- Ishiguro, S., Kawai-Oda, A., Ueda, J., Nishida, I., and Okada, K.** (2001b). The DEFECTIVE IN ANther DEHISCENCE1 Gene Encodes a Novel Phospholipase A1 Catalyzing the Initial Step of Jasmonic Acid Biosynthesis, Which Synchronizes Pollen Maturation, Anther Dehiscence, and Flower Opening in *Arabidopsis*. *The Plant Cell* **13**, 2191-2209.
- Ito, T., Ng, K.H., Lim, T.S., Yu, H., and Meyerowitz, E.M.** (2007). The homeotic protein AGAMOUS controls late stamen development by regulating a jasmonate biosynthetic gene in *Arabidopsis*. *Plant Cell* **19**, 3516-3529.
- Iuchi, S., Suzuki, H., Kim, Y.C., Iuchi, A., Kuromori, T., Ueguchi-Tanaka, M., Asami, T., Yamaguchi, I., Matsuoka, M., Kobayashi, M., and Nakajima, M.** (2007). Multiple loss-of-function of *Arabidopsis* gibberellin receptor AtGID1s completely shuts down a gibberellin signal. *The Plant journal : for cell and molecular biology* **50**, 958-966.
- Jefferson, R.A., Kavanagh, T.A., and Bevan, M.W.** (1987). GUS fusions: beta-glucuronidase as a sensitive and versatile gene fusion marker in higher plants. *The EMBO journal* **6**, 3901-3907.
- Joung, J.-G., Corbett, A.M., Fellman, S.M., Tieman, D.M., Klee, H.J., Giovannoni, J.J., and Fei, Z.** (2009). Plant MetGenMAP: An Integrative Analysis System for Plant Systems Biology. *Plant Physiology* **151**, 1758-1768.
- Jung, H.I., Gayomba, S.R., Rutzke, M.A., Craft, E., Kochian, L.V., and Vatamaniuk, O.K.** (2012). COPT6 is a plasma membrane transporter that functions in copper homeostasis in *Arabidopsis* and is a novel target of SQUAMOSA promoter-binding protein-like 7. *J Biol Chem* **287**, 33252-33267.
- Kampfenkel, K., Kushnir, S., Babiychuk, E., Inzā, D., and Van Montagu, M.** (1995). Molecular Characterization of a Putative *Arabidopsis thaliana* Copper Transporter and Its Yeast Homologue. *Journal of Biological Chemistry* **270**, 28479-28486.

- Klaumann, S., Nickolaus, S.D., Fürst, S.H., Starck, S., Schneider, S., Ekkehard Neuhaus, H., and Trentmann, O.** (2011). The tonoplast copper transporter COPT5 acts as an exporter and is required for interorgan allocation of copper in *Arabidopsis thaliana*. *New Phytol* **192**, 393-404.
- Kliebenstein, D.J., Monde, R.-A., and Last, R.L.** (1998). Superoxide Dismutase in *Arabidopsis*: An Eclectic Enzyme Family with Disparate Regulation and Protein Localization. *Plant Physiol.* **118**, 637-650.
- Langmead, B., Trapnell, C., Pop, M., and Salzberg, S.L.** (2009). Ultrafast and memory-efficient alignment of short DNA sequences to the human genome. *Genome biology* **10**, R25.
- Leon-Reyes, A., Spoel, S.H., De Lange, E.S., Abe, H., Kobayashi, M., Tsuda, S., Millenaar, F.F., Welschen, R.A., Ritsema, T., and Pieterse, C.M.** (2009). Ethylene modulates the role of NONEXPRESSOR OF PATHOGENESIS-RELATED GENES1 in cross talk between salicylate and jasmonate signaling. *Plant physiology* **149**, 1797-1809.
- Long, T.A., Tsukagoshi, H., Busch, W., Lahner, B., Salt, D.E., and Benfey, P.N.** (2010). The bHLH transcription factor POPEYE regulates response to iron deficiency in *Arabidopsis* roots. *The Plant cell* **22**, 2219-2236.
- M, R.B., Yookongkaew, N., Meetam, M., Guo, W.J., Punyasuk, N., AbuQamar, S., and Goldsbrough, P.** (2014). Metallothionein deficiency impacts copper accumulation and redistribution in leaves and seeds of *Arabidopsis*. *The New phytologist* **202**, 940-951.
- Marschner, H.** (1995). Mineral nutrition of higher plants. (London; San Diego: Academic Press).
- Martin, R.C., Liu, P.P., Goloviznina, N.A., and Nonogaki, H.** (2010). microRNA, seeds, and Darwin?: diverse function of miRNA in seed biology and plant responses to stress. *Journal of experimental botany* **61**, 2229-2234.
- McConn, M., and Browse, J.** (1996). The Critical Requirement for Linolenic Acid Is Pollen Development, Not Photosynthesis, in an *Arabidopsis* Mutant. *The Plant cell* **8**, 403-416.
- Mendel, R.R., and Kruse, T.** (2012). Cell biology of molybdenum in plants and humans. *Biochim Biophys Acta* **1823**, 1568-1579.
- Miura, K., Ikeda, M., Matsubara, A., Song, X.J., Ito, M., Asano, K., Matsuoka, M., Kitano, H., and Ashikari, M.** (2010). OsSPL14 promotes panicle branching and higher grain productivity in rice. *Nature genetics* **42**, 545-549.
- Murashige, T., and Skoog, F.** (1962). A Revised Medium for Rapid Growth and Bio Assays with Tobacco Tissue Cultures. *Physiologia Plantarum* **15**, 473-497.
- Murre, C., McCaw, P.S., and Baltimore, D.** (1989). A new DNA binding and dimerization motif in immunoglobulin enhancer binding, daughterless, MyoD, and myc proteins. *Cell* **56**, 777-783.
- Nair, S.K., and Burley, S.K.** (2000). Recognizing DNA in the library. *Nature* **404**, 715, 717-718.
- Ofran, Y., and Rost, B.** (2007). ISIS: interaction sites identified from sequence. *Bioinformatics* **23**, E13-E16.
- Park, J.H., Halitschke, R., Kim, H.B., Baldwin, I.T., Feldmann, K.A., and Feyereisen, R.** (2002). A knock-out mutation in allene oxide synthase results in male sterility and defective wound signal transduction in *Arabidopsis* due to a block in jasmonic acid biosynthesis. *The Plant journal : for cell and molecular biology* **31**, 1-12.
- Peng, Y.J., Shih, C.F., Yang, J.Y., Tan, C.M., Hsu, W.H., Huang, Y.P., Liao, P.C., and Yang, C.H.** (2013). A RING-type E3 ligase controls anther dehiscence by activating the jasmonate biosynthetic pathway gene DEFECTIVE IN ANTER DEHISCENCE1 in *Arabidopsis*. *The Plant journal : for cell and molecular biology* **74**, 310-327.
- Quast, C., Pruesse, E., Yilmaz, P., Gerken, J., Schwerer, T., Yarza, P., Peplies, J., and Glockner, F.O.** (2013). The SILVA ribosomal RNA gene database project: improved data processing and web-based tools. *Nucleic acids research* **41**, D590-596.
- Rapisarda, V.A., Volentini, S.I., Farias, R.N., and Massa, E.M.** (2002). Quenching of bathocuproine disulfonate fluorescence by Cu(I) as a basis for copper quantification. *Anal Biochem* **307**, 105-109.

- Ravet, K., and Pilon, M.** (2013a). Copper and Iron Homeostasis in Plants: The Challenges of Oxidative Stress. *Antioxid Redox Signal* **19**, 919-932.
- Ravet, K., and Pilon, M.** (2013b). Copper and Iron Homeostasis in Plants: The Challenges of Oxidative Stress. *Antioxid Redox Signal*.
- Ravet, K., Danford, F.L., Dihle, A., Pittarello, M., and Pilon, M.** (2011). Spatiotemporal Analysis of Copper Homeostasis in *Populus trichocarpa* Reveals an Integrated Molecular Remodeling for a Preferential Allocation of Copper to Plastocyanin in the Chloroplasts of Developing Leaves. *Plant physiology* **157**, 1300-1312.
- Robinson, K.A., Koepke, J.I., Kharodawala, M., and Lopes, J.M.** (2000). A network of yeast basic helix-loop-helix interactions. *Nucleic acids research* **28**, 4460-4466.
- Robinson, M.D., McCarthy, D.J., and Smyth, G.K.** (2010). edgeR: a Bioconductor package for differential expression analysis of digital gene expression data. *Bioinformatics* **26**, 139-140.
- Rost, B., Yachdav, G., and Liu, J.F.** (2004). The PredictProtein server. *Nucleic acids research* **32**, W321-W326.
- Ryden, L.G., and Hunt, L.T.** (1993). Evolution of protein complexity: the blue copper-containing oxidases and related proteins. *Journal of molecular evolution* **36**, 41-66.
- Sancenon, V., Puig, S., Mira, H., Thiele, D.J., and Peñarrubia, L.** (2003). Identification of a copper transporter family in *Arabidopsis thaliana*. *Plant molecular biology* **51**, 577-587.
- Sancenon, V., Puig, S., Mateu-Andres, I., Dorsey, E., Thiele, D.J., and Penarrubia, L.** (2004). The *Arabidopsis* copper transporter COPT1 functions in root elongation and pollen development. *J Biol Chem* **279**, 15348-15355.
- Schwarz, S., Grande, A.V., Bujdoso, N., Saedler, H., and Huijser, P.** (2008). The microRNA regulated SBP-box genes SPL9 and SPL15 control shoot maturation in *Arabidopsis*. *Plant molecular biology* **67**, 183-195.
- Shikata, M., Koyama, T., Mitsuda, N., and Ohme-Takagi, M.** (2009). *Arabidopsis* SBP-box genes SPL10, SPL11 and SPL2 control morphological change in association with shoot maturation in the reproductive phase. *Plant & cell physiology* **50**, 2133-2145.
- Shorrocks, V.M., and Alloway, B.J.** (1988). Copper in plant, animal and human nutrition. (Potters Bar, Hertfordshire: Copper Development Association).
- Solberg, E., Evans, I., and Penny, D.** (1999). Copper deficiency: Diagnosis and correction. Agri-facts. Soil Fertility/Crop Nutrition. Alberta Agriculture, Food and Rural Development, Agdex 532-3, pp. 1-9. (
- Sommer, F., Kropat, J., Malasarn, D., Grossoehme, N.E., Chen, X., Giedroc, D.P., and Merchant, S.S.** (2010). The CRR1 nutritional copper sensor in *Chlamydomonas* contains two distinct metal-responsive domains. *Plant Cell* **22**, 4098-4113.
- Stintzi, A., and Browse, J.** (2000). The *Arabidopsis* male-sterile mutant, opr3, lacks the 12-oxophytodienoic acid reductase required for jasmonate synthesis. *Proceedings of the National Academy of Sciences of the United States of America* **97**, 10625-10630.
- Stone, J.M., Liang, X., Nekl, E.R., and Stiers, J.J.** (2005). *Arabidopsis* AtSPL14, a plant-specific SBP-domain transcription factor, participates in plant development and sensitivity to fumonisin B1. *The Plant journal : for cell and molecular biology* **41**, 744-754.
- Trapnell, C., Pachter, L., and Salzberg, S.L.** (2009). TopHat: discovering splice junctions with RNA-Seq. *Bioinformatics* **25**, 1105-1111.
- Udvardi, M.K., Czechowski, T., and Scheible, W.R.** (2008). Eleven golden rules of quantitative RT-PCR. *The Plant cell* **20**, 1736-1737.
- Valko, M., Morris, H., and Cronin, M.T.** (2005). Metals, toxicity and oxidative stress. *Curr Med Chem* **12**, 1161-1208.
- Wang, J.W., Czech, B., and Weigel, D.** (2009). miR156-regulated SPL transcription factors define an endogenous flowering pathway in *Arabidopsis thaliana*. *Cell* **138**, 738-749.

- Wang, J.W., Schwab, R., Czech, B., Mica, E., and Weigel, D.** (2008). Dual effects of miR156-targeted SPL genes and CYP78A5/KLUH on plastochron length and organ size in *Arabidopsis thaliana*. *The Plant cell* **20**, 1231-1243.
- Wang, L., Halitschke, R., Kang, J.H., Berg, A., Harnisch, F., and Baldwin, I.T.** (2007). Independently silencing two JAR family members impairs levels of trypsin proteinase inhibitors but not nicotine. *Planta* **226**, 159-167.
- Waters, B., Chu, H., Didonato, R., Roberts, L., Eisley, R., Lahner, B., Salt, D., and Walker, E.** (2006). Mutations in *Arabidopsis* yellow stripe-like 1 and yellow stripe-like 3 reveal their roles in metal ion homeostasis and loading of metal ions in seeds. *Plant physiology* **141**, 1446 - 1458.
- Weigel, M., Varotto, C., Pesaresi, P., Finazzi, G., Rappaport, F., Salamini, F., and Leister, D.** (2003). Plastocyanin is indispensable for photosynthetic electron flow in *Arabidopsis thaliana*. *J Biol Chem* **278**, 31286-31289.
- Wu, G., and Poethig, R.S.** (2006). Temporal regulation of shoot development in *Arabidopsis thaliana* by miR156 and its target SPL3. *Development* **133**, 3539-3547.
- Wu, G., Park, M.Y., Conway, S.R., Wang, J.W., Weigel, D., and Poethig, R.S.** (2009). The sequential action of miR156 and miR172 regulates developmental timing in *Arabidopsis*. *Cell* **138**, 750-759.
- Wu, H., Chen, C., Du, J., Liu, H., Cui, Y., Zhang, Y., He, Y., Wang, Y., Chu, C., Feng, Z., Li, J., and Ling, H.Q.** (2012a). Co-overexpression FIT with AtbHLH38 or AtbHLH39 in *Arabidopsis*-enhanced cadmium tolerance via increased cadmium sequestration in roots and improved iron homeostasis of shoots. *Plant physiology* **158**, 790-800.
- Wu, Y., Zhang, D., Chu, J.Y., Boyle, P., Wang, Y., Brindle, I.D., De Luca, V., and Despres, C.** (2012b). The *Arabidopsis* NPR1 protein is a receptor for the plant defense hormone salicylic acid. *Cell reports* **1**, 639-647.
- Yamasaki, H., Hayashi, M., Fukazawa, M., Kobayashi, Y., and Shikanai, T.** (2009a). SQUAMOSA Promoter Binding Protein-Like7 Is a Central Regulator for Copper Homeostasis in *Arabidopsis*. *The Plant cell* **21**, 347-361.
- Yamasaki, H., Hayashi, M., Fukazawa, M., Kobayashi, Y., and Shikanai, T.** (2009b). SQUAMOSA Promoter Binding Protein-Like7 Is a Central Regulator for Copper Homeostasis in *Arabidopsis*. *The Plant cell* **21**, 347-361.
- Yamasaki, H., Abdel-Ghany, S.E., Cohu, C.M., Kobayashi, Y., Shikanai, T., and Pilon, M.** (2007). Regulation of Copper Homeostasis by Micro-RNA in *Arabidopsis*. *Journal of Biological Chemistry* **282**, 16369-16378.
- Yu, N., Cai, W.J., Wang, S., Shan, C.M., Wang, L.J., and Chen, X.Y.** (2010). Temporal control of trichome distribution by microRNA156-targeted SPL genes in *Arabidopsis thaliana*. *The Plant cell* **22**, 2322-2335.
- Yuan, Y., Wu, H., Wang, N., Li, J., Zhao, W., Du, J., Wang, D., and Ling, H.Q.** (2008). FIT interacts with AtbHLH38 and AtbHLH39 in regulating iron uptake gene expression for iron homeostasis in *Arabidopsis*. *Cell research* **18**, 385-397.
- Zhai, Z., Jung, H.I., and Vatamaniuk, O.K.** (2009). Isolation of protoplasts from tissues of 14-day-old seedlings of *Arabidopsis thaliana*. *J Vis Exp*.
- Zhai, Z., Gayomba, S.R., Jung, H.I., Vimalakumari, N.K., Pineros, M., Craft, E., Rutzke, M.A., Danku, J., Lahner, B., Punshon, T., Guerinot, M.L., Salt, D.E., Kochian, L.V., and Vatamaniuk, O.K.** (2014). OPT3 Is a Phloem-Specific Iron Transporter That Is Essential for Systemic Iron Signaling and Redistribution of Iron and Cadmium in *Arabidopsis*. *The Plant cell* **26**, 2249-2264.
- Zhong, S., Joung, J.G., Zheng, Y., Chen, Y.R., Liu, B., Shao, Y., Xiang, J.Z., Fei, Z., and Giovannoni, J.J.** (2011). High-throughput illumina strand-specific RNA sequencing library preparation. *Cold Spring Harbor protocols* **2011**, 940-949.

CHAPTER III

AREB3, ATHB2 and bZIP53 are Upstream Regulators of *CCIT1* transcriptional response to Copper Deficiency in Reproductive Tissues of *A. thaliana*.

ABSTRACT

The transition metal copper (Cu) is among the most important mineral nutrients and is essential for plant growth, development and fertility. However, Cu is toxic if it is present in cells in excess. To maintain Cu homeostasis, plants have evolved sophisticated regulatory mechanisms, including transcriptional control of genes encoding proteins involved in Cu uptake, trafficking, tissue partitioning and reallocation among Cu requiring enzymes. SPL7 (**S**QUAMOSA **P**romoter binding protein–**L**ike7) has been shown to play a central role in this transcriptional regulatory network. We have found recently that a member of the bHLH (**b**asic **H**elix-**L**oop-**H**elix) family of transcription factors, CCIT1 (**Cu, Cd-Induced Transcription Factor 1**), responds transcriptionally to Cu availability and is essential for the growth and development of *A. thaliana* under Cu deficiency. *CCIT1* has been considered among the downstream targets of *SPL7*. However, our functional genetic studies of the relationship between CCIT1 and SPL7 pathways pointed to the existence of a complex SPL7-CCIT1-interactive pathway, disruption of which is detrimental to plant viability and pollen fertility. Further, our recent data suggested that other transcriptional regulators besides SPL7 mediate the transcriptional response of *CCIT1* to Cu availability in roots and flowers. Here, I present results from the screen for the upstream regulators of *CCIT1*. Yeast one-hybrid (Y1H) analyses and chromatin immunoprecipitation assays (ChIP) identified AREB3 (**ABA-R**esponsive **E**lement **B**inding protein 3), ATHB2 (**A**rabidopsis **T**haliana **H**omeobox protein 2) and bZIP53 (**b**asic region/**l**eucine **z**ipper motif 53) as upstream regulators of Cu-responsive *CCIT1* expression in flowers. Analyses of the subcellular localization of AREB3, ATHB2 and bZIP53 revealed that all three localize to the nucleus, which is consistent with their function in transcriptional regulation. I also found that SPL7 acts as a negative regulator of these transcription factors in flowers. Together, these data further our understanding of the complexity of CCIT1-SPL7 transcriptional regulatory networks controlling Cu homeostasis in *A. thaliana*.

1. INTRODUCTION

Copper (Cu) is a micronutrient that plays an essential role in photosynthesis, respiration, ethylene perception, reactive oxygen species (ROS) detoxification, pathogen response, cell wall remodeling, fertility and seed/grain set in plants (Marschner, 1995). The essential nature of Cu results from its ability to change the oxidation state (Marschner, 1995), and thus it functions as a cofactor that is required for structural and catalytic properties of a variety of important enzymes (Marschner, 1995; Pilon et al., 2006; Burkhead et al., 2009). The most abundant Cu-binding protein in higher plants is plastocyanin (PC), which acts as electron transfer agent in photosynthesis. Cytosolic and chloroplast-localized Cu/Zn superoxide dismutase (CSD), which functions in scavenging ROS, are two other major Cu-requiring enzymes (Yamasaki et al., 2009a). However, Cu can also be toxic when present in cells in excess. Redox cycling between Cu (I) and Cu (II) promotes the production of hydroxyl radicals, which cause damage to cells (Marschner, 1995). In addition, Cu has a high affinity for thiol groups and can thiol-cap and inactivate essential proteins as well as displace other essential elements from their cellular binding sites (Halliwell and Gutteridge, 1984; Burkhead et al., 2009). Therefore, Cu concentration within the cell must be tightly regulated to prevent deficiency while avoiding toxicity.

The transcriptional regulation of Cu homeostasis in plants has been investigated in the *Chlamydomonas* model (Hill and Merchant, 1995; Quinn and Merchant, 1995). **Cu-responsive regulator 1** (CRR1) is the key regulator that activates the Cu assimilatory mechanisms under Cu deficiency. SPL7 is an orthologue of CRR1 in *A. thaliana* and belongs to *SQUAMOSA* promoter binding protein-like family (SPL) (Kropat et al., 2005). Both, CRR1 and SPL7 activate gene expression by binding to **Copper-response elements** (CuREs) in promoters of their targets. The CuREs contain the GTAC core motifs (Quinn et al., 2000; Eriksson et al., 2004). SPL7 has been found to play a central role in regulating Cu homeostasis under limited Cu condition (Yamasaki et al., 2009b). The SPL7-dependent Cu regulatory pathway consists of at least two components. First, under Cu deficiency, SPL7 upregulates expression of genes encoding components of the Cu uptake system. These include Cu(II) to Cu(I) reductases *FRO3*, *FRO4* and *FRO5*, high-affinity Cu(I) transporters from the CTR/COPT family, such as *COPT1*, *COPT2* and *COPT6*, and

low-affinity Cu(II) transporters, ZIP2 and ZIP4. These transcriptional changes result in the increase of Cu acquisition from the soil and root-to-shoot translocation (Yamasaki et al., 2009a; Bernal et al., 2012). In addition, a Cu chaperone (CCH), which is involved in Cu trafficking, is also up-regulated under Cu starvation *via* SPL7 (Mira et al., 2002; Yamasaki et al., 2009a). The second SPL7-dependent component of Cu homeostasis includes the microRNA-dependent intracellular Cu reallocation. Under Cu limited condition, SPL7 upregulates several miRNAs, such as miR398 and miR408, which target the transcripts of abundant Cu-binding proteins, such as CSD1, CSD2, COPPER CHAPERONE FOR SOD (CCS), cytochrome c oxidase (COX-5b), PLANTACYANIN (ARPN) and LACCASES (LACs) in order to reallocate Cu to more essential Cu-binding protein, plastocyanin, to maintain its electron transfer capacity during photosynthesis. Function of CSDs can be replaced by FeSOD (Sunkar et al., 2006; Yamasaki et al., 2007; Abdel-Ghany and Pilon, 2008; Yamasaki et al., 2009b; Bernal et al., 2012). Recently, a nuclear protein, KIN17, was found to interact physically with SPL7 to mediate the expression of several genes, such as *COPT2*, *COPT6*, *CCH* and *FSD1*, in response to Cu deficiency in *Arabidopsis* (Garcia-Molina et al., 2014).

Previous microarray and RNA-seq studies identified a Cu-responsive gene from the **basic-helix-loop-helix** (bHLH) transcription factor family, whose transcriptional response to Cu deficiency in shoots depended on SPL7 (Yamasaki et al., 2009a; Bernal et al., 2012). As described in Chapter 2, the same bHLH family member has been identified in the microarray screen in the Vatamaniuk's lab as responsive to Cd toxicity, and thus was designated as *Cu, Cd-induced transcription factor 1 (CCIT1)*. The mutant alleles of *CCIT1* were hypersensitive to long-term Cu starvation, showed chlorotic spots in mature leaves and retarded growth during reproductive stage compared to wild-type and the complementary lines (Chapter 2). I also found that the double *ccit1 spl7* mutant was seedling lethal under standard growth conditions. As I described in Chapter 2, the seedling lethality of the *ccit1 spl7* double mutant could be rescued by Cu supplement. However, the double mutant was still largely infertile, suggesting that *CCIT1* is not an immediate downstream target of SPL7, and that both genes act in a complex interacting pathway that controls response to Cu deficiency. Further, I showed that other, not yet identified transcription regulators,

in addition to SPL7 control the transcriptional response of *CCIT1* to Cu deficiency in roots and flowers. This chapter describes the identification and initial characterization of putative upstream regulators of *CCIT1* in flowers, such as AREB3 (ABA-Responsive Element Binding protein 3), ATHB2 (Arabidopsis Thaliana Homeobox protein 2) and bZIP53 (Basic region/leucine zipper motif 53). My new data contribute to the fundamental understanding of transcriptional regulatory networks controlling Cu deficiency responses in *A. thaliana*.

2. METHODS

2.1 Plant Materials

All plant lines used in the study were in the *A. thaliana* Columbia (Col-0) background. Seeds of the *SPL7* (SALK_093849; *alias spl7-1*) mutant were obtained from Dr. Shikanai (Kyoto University, Japan) (Yamasaki et al., 2009a). *ATHB2* (SALK_106790; *alias athb2*), *AREB3* (SALK_020324; *alias areb3*) and *bZIP53* (SALK_004683; *alias bzip53*) mutant alleles were obtained from the *Arabidopsis* Biological Resource Center (Alonso et al., 2003). Mutants bearing homozygous T-DNA insertions were selected by PCR using genomic DNA as a template and the LBB1.3 (for SALK line) and RP primer pairs (Supplemental Table 1).

2.2 Growth Conditions and Experimental Treatments

Before growing *A. thaliana* on solid medium or in hydroponic system, seeds were surface-sterilized in 75% (v/v) ethanol and a solution containing 1.8% sodium hypochlorite (made up by diluting a household Clorox solution), 0.1% (v/v) Tween-20. Seeds were then sown on half-strength Murashige and Skoog ($\frac{1}{2}$ MS) medium (pH 5.7) (Murashige and Skoog, 1962). The medium was also supplemented with 1% (w/v) sucrose and 0.7% agar (w/v, Sigma A1296). After stratification at 4 °C for 2 days in darkness, seeds were germinated and grown horizontally on $\frac{1}{2}$ MS medium for 14 days. For transcript abundance analysis by qRT-PCR, wild-type, *spl7-1* (*spl7*), *areb3*, *athb2* and *bzip53* mutants were grown hydroponically in a

medium containing 0.5 μ M CuSO₄ to ensure growth and development of the *spl7* mutant. After 5 weeks, half of plants were transferred to a medium without Cu and plant were grown hydroponically for another 3 weeks before flowers were harvested. In all cases, plants were grown at 22 °C, 14 h light/10 h dark photoperiod at a photon flux density of 110 μ mol m⁻² s⁻¹.

2.3 Plasmid Construction

The vectors SAT6-N1-EGFP (Tzfira et al., 2005) were modified into Gateway destination vectors with the Gateway vector conversion system (Invitrogen). The cDNA without the stop codon was amplified by RT-PCR from RNA isolated from *A. thaliana*. The primers (Supplemental Table 2) added attB sites on resulting PCR products for subsequent cloning into SAT6-N1-EGFP-Gate by recombination (Invitrogen). The yeast-one-hybrid constructs were made according to (Mitsuda et al., 2010). The promoter regions were amplified from the genomic DNA isolated from *A. thaliana*. Primer pairs (Supplemental table 2) added attB sites on resulting PCR products, to facilitate cloning into R4L1pDEST_HISi_Gate (Mitsuda et al., 2010) by recombination (Invitrogen). The prey library with more than 1500 *Arabidopsis* transcription factors was a generous gift of Dr. Mitsuda (National Institute of Advanced Industrial Science and Technology, Japan, (Mitsuda et al., 2010).

2.4 Subcellular Localization and Fluorescent Microscopy

For studies of the subcellular localization of ATHB2, AREB3 and bZIP53 in *Arabidopsis* protoplasts, the corresponding full-length cDNAs without the stop codon were amplified by RT-PCR from RNA isolated from *A. thaliana*. The primer pairs are listed in Supplemental Table 2. PCR products were fused at the C-terminus with the modified green fluorescent protein (EGFP) of the SAT6-N1-EGFP-Gate vector and expressed under the control of the cauliflower mosaic virus 35S promoter. The resulting construct or SAT6-N1-Gate lacking the cDNA insert, were transfected into *A. thaliana* protoplasts isolated from leaf mesophyll tissue using previously established procedures (Zhai et al., 2009). Nuclei were stained with 10 mg/ml 4', 6'

diamino-2-phenylindole 2HCl (DAPI; Sigma D9542), and incubated for 15 min at room temperature prior imaging. EGFP- and DAPI-mediated fluorescence and chlorophyll auto-fluorescence were visualized using FITC (for EGFP), DAPI and rhodamine (for chlorophyll) filter sets of the Axio Imager M2 microscope equipped with the motorized Z-drive (Zeiss). Images were collected with the high resolution AxioCam MR Camera. Images were processed using the Windows live photo gallery.

2.5 RNA Extraction and cDNA Synthesis

Tissues from the plants grown under the indicated conditions were harvested and flash-frozen in liquid nitrogen before homogenization using a mortar and pestle. Total RNA was isolated using TRIzol reagent (Invitrogen), according to the manufacturer's instructions. One µg of total RNA was digested with DNase I (New England Biolabs) prior to first strand cDNA synthesis using the QPCR cDNA synthesis kit (Agilent Technologies).

2.6 Quantitative Real-Time (qRT)-PCR and Data Analysis

Prior to qRT-PCR analysis, primer and cDNA concentrations were optimized to reach the target and normalizing gene amplification efficiency of $100 \pm 10\%$. 2 µl of 15-fold-diluted cDNA was used as a template for qRT-PCR in a total volume of 15 µl containing a 500 nM concentration of each PCR primer, 50 mM KCl, 20 mM Tris-HCl, pH 8.4, 0.2 mM each dNTP, and 1.25 units of iTaq DNA polymerase in iQ SYBR Green Supermix (Bio-Rad). PCR was carried out using the CFX96 real-time PCR system (Bio-Rad). The thermal cycling parameters were as follows: denaturation at 95 °C for 3 min, followed by 39 cycles of 95 °C for 10 s and 55 °C for 30 s. Amplicon dissociation curves (i.e. melting curves) were recorded after cycle 39 by heating from 60 °C to 95 °C with 0.5 °C increments and an average ramp speed of 3.3 °C s⁻¹. Real-time PCR experiments were conducted using three independent biological samples, each consisting of three technical replicates (Udvardi et al., 2008), unless indicated otherwise. Data were normalized to the expression of *ACTIN 2*. The -fold difference ($2^{-\Delta\Delta Ct}$) was calculated using the CFX Manager Software,

version 1.5 (Bio-Rad). Statistical analysis was performed using the Relative Expression Software Tool (REST; Qiagen).

2.7 Yeast-one-hybrid Screen

The 0.7 kb *CCIT1* promoter fragment was fused to a reporter *HIS3* gene of the yeast-one-hybrid (Y1H) bait vector (Mitsuda et al., 2010) and integrated into the genome of the Y1H bait yeast strain YM4271 according to the manufacturer recommended procedures (Clontech). Briefly, the *CCIT1pro-R4L1pDEST_HISi* construct was digested by ApaI restriction enzyme, and was transformed into YM4271 yeast strain following lithium acetate transformation procedures as described in (Deplancke et al., 2006). The transformants were selected and grown on YNB medium (0.67% Yeast Nitrogen Base, 0.077% CSM-Ura, 0.05% NaCl, 2% glucose and 2% agar, pH6.0) without uracil. Transcription factor (TF)-only Y1H library with approximately 1500 TF (Mitsuda et al., 2010). The transformation of the TF library to the YM4271 yeast strain with *CCIT1pro-R4L1pDEST_HISi* bait construct was performed using lithium acetate transformation procedures. The transformants with both *bait* and *prey* were selected and grown on YNB medium without uracil and leucine. Interactions between prey and bait were selected by growing on YNB medium without uracil, leucine and histidine. Fifteen mM 3-Amino-1,2,4-triazole (3-AT) was also added to the YNB medium to inhibit the *HIS3* gene self-activation. The colonies were then subjected to yeast drop assay for validation. The 1 kb promoter fragment of *bHLH39* (AT3G56980) was fused to the R4L1pDEST_HISi yeast one hybrid bait vector as a negative control. *bHLH39* is a closely related gene to *CCIT1* which shares high sequence similarity with it. Plasmids which contain the putative *CCIT1* transcription regulators were isolated from yeast using Zymolase (Zymo Research) digestion method followed by alkaline lysis with SDS, and cDNA inserts were sequenced using primer (CTATTCGATGATGAAGATACCCC) located at GAL4AD to identify transcription regulators of CCIT1. Transformations were performed three times to obtain the full coverage.

2.8 Chromatin Immunoprecipitation

The coding region of genes that are subject to Chromatin immunoprecipitation (ChIP) were inserted into the SAT-N1-EGFP vector and were fused to the N-terminal of the EGFP protein. Protoplasts were isolated from 14-week-old *Arabidopsis* seedlings according to (Zhai et al., 2009), transfected with the EGFP constructs, and were then employed for ChIP following the procedures described in (He et al., 2013) and (Yamaguchi et al., 2014). The anti-GFP antibody (ThermoFisher Scientific, MA5-15256) was used to pull down the genomic DNA associated with the EGFP-tagged proteins. The untransfected protoplasts were used as negative control. The genomic DNA from the pull down was then purified by Invitrogen PureLink DNA purification kit (K3100-01). qRT-PCR was performed using iQ SYBR Green Supermix (Bio-Rad). To test AREB3, ATHB2 and bZIP53 occupancy on *CCIT1* genomic DNA, the ratio of ChIP over input DNA (%Input) was calculated by comparing the reaction threshold cycle for each ChIP sample to the corresponding input sample according to the instruction from Thermo Fisher Scientific (<https://www.thermofisher.com/us/en/home/life-science/epigenetics-noncoding-rna-research / chromatin-remodeling/chromatin immune precipitation-chip/chip-analysis.html>). Primers used for ChIP assays are summarized in Supplemental Table 3.

2.9 Accession Numbers

The accession numbers of the genes: *CCIT1* (At1g71200), *bHLH39* (AT3G56980), *ZFP622* (At4g31420), *ERF B4* (AT2G33710), *bHLH121* (AT3G19860), *NAC095* (AT5G41090), *TFIIA* (AT1G07470), *AGL72* (AT5G51860), *AGL14* (AT4G11880), *ATHB2* (AT4G16780), *EPR1* (AT1G18330), *INTEGRASE* (AT2G41710), *bZIP53* (AT3G62420), *TF-R* (AT4G17020), *BMIIA* (AT2G30580), *AREB3* (AT3G56850).

3. RESULTS

3.1 Y1H Screen of a Prey Library of *Arabidopsis* Transcription Factors Identified 14 Putative Regulators of *CCIT1*

CCIT1 expression has been shown to be responsive to Cu availability in a SPL7-dependent manner (Yamasaki et al., 2009a; Bernal et al., 2012), suggesting that SPL7 is the upstream regulator of *CCIT1*. However, my recent findings described in Chapter 2 suggested that other transcription regulators in addition to SPL7 might control the transcriptional response of *CCIT1* to Cu deficiency in roots and flowers. The transcription start site (TSS) has not been mapped for *CCIT1*. Therefore, here I define the *CCIT1* “promoter” as the intergenic sequence upstream of the *CCIT1* open reading frame (ORF). I have generated transgenic *A. thaliana* expressing *GUS* reporter under the control of the 1,541 bp genomic fragment upstream of the *CCIT1* ORF (*CCIT1_{pro}*). Histochemical analysis revealed weak GUS activity in the vasculature of different plant organs, including embryonic cotyledons, rosette leaves, roots, and anthers (Chapter 2). GUS staining became stronger in transgenic plants grown under Cu-limited conditions and disappeared in plants supplemented with higher concentrations of Cu (Chapter 2). This suggests that the 1,541 bp region upstream of the *CCIT1* ORF contains *cis*-elements required for the transcriptional response to Cu availability. Therefore, I designated these 1,541 bp as the *CCIT1* full promoter (*CCIT1_{pro full}*). Using the PLACE prediction software (Prestridge, 1991; Higo et al., 1999), I have identified 5 CuRE motifs within 0.7 kb from ORF that can be recognized by SPL7 (Figure 1A). I fused these 0.7 kb to the *GUS* reporter gene and expressed this construct in *A. thaliana*. I found that 0.7 kb were sufficient to upregulate *CCIT1* expression in response to Cu deficiency (Supplemental Figure 1). Therefore, I used 0.7 kb genomic region (*CCIT1_{pro}*) as a bait in subsequent screens for upstream regulators of *CCIT1*.

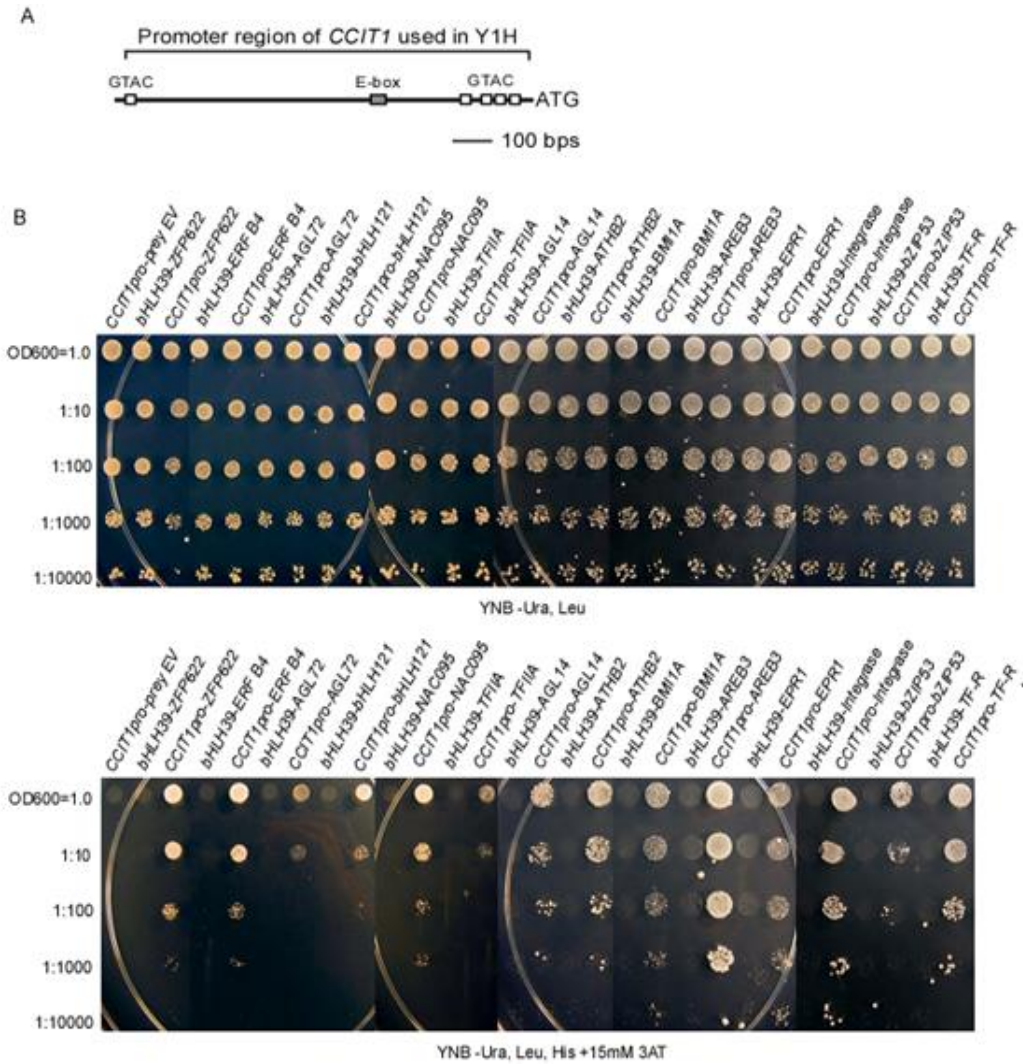


Figure 1. Putative regulators of CCIT1 that were identified in Y1H screens. **A**, Schematic representation of the *CCIT1* genomic fragment upstream of ORF that was used to make a bait construct for the Y1H screen. **B**, shows results of Y1H assays. Yeast transformed with *CCIT1pro*-His fusion and the empty prey vector (prey EV) and yeast transformed with *bHLH39pro*-His and indicated prey constructs were used as negative control. 3AT is added to the selection plates to inhibit self-activation of *HIS3*.

To examine whether SPL7 is a direct upstream regulator of *CCIT1*, the Y1H assay was performed between SPL7 and *CCIT1pro*. I found that SPL7 did not interact with *CCIT1pro* in Y1H (Chapter 4). Consistent with this finding, recent genome-wide ChIP-seq studies also did not detect CCIT1 among direct SPL7 targets (Zhang et al., 2014). Given that my studies described in Chapter 2 suggest that the transcriptional response of *CCIT1* to Cu limitation in flowers and roots is, in part, independent of SPL7, I used Y1H screen against a collection of approximately 1500 *A. thaliana* transcription factors (Mitsuda and Ohme-Takagi,

2009) to identify those that bind to the 0.7 kb *CCIT1* regulatory promoter regions (Figure 1A). This screen identified 14 transcription factors that bind to the *CCIT1pro* (Figure 1B).

3.2 SPL7 Negatively Regulates Expression of the Putative CCIT1 Regulators in Flowers of *A. thaliana* under Cu Deficiency

I then tested whether genes identified in Y1H as putative regulators of *CCIT1* would respond transcriptionally to Cu deficiency and whether this transcriptional response would depend on SPL7. These test were performed using flowers of *A. thaliana* wild-type plants and the *spl7-1* mutant grown with or without Cu as described in Methods. I found that none of the genes was differentially expressed in response to Cu deficiency in flowers of wild-type (Figure 2A and B).

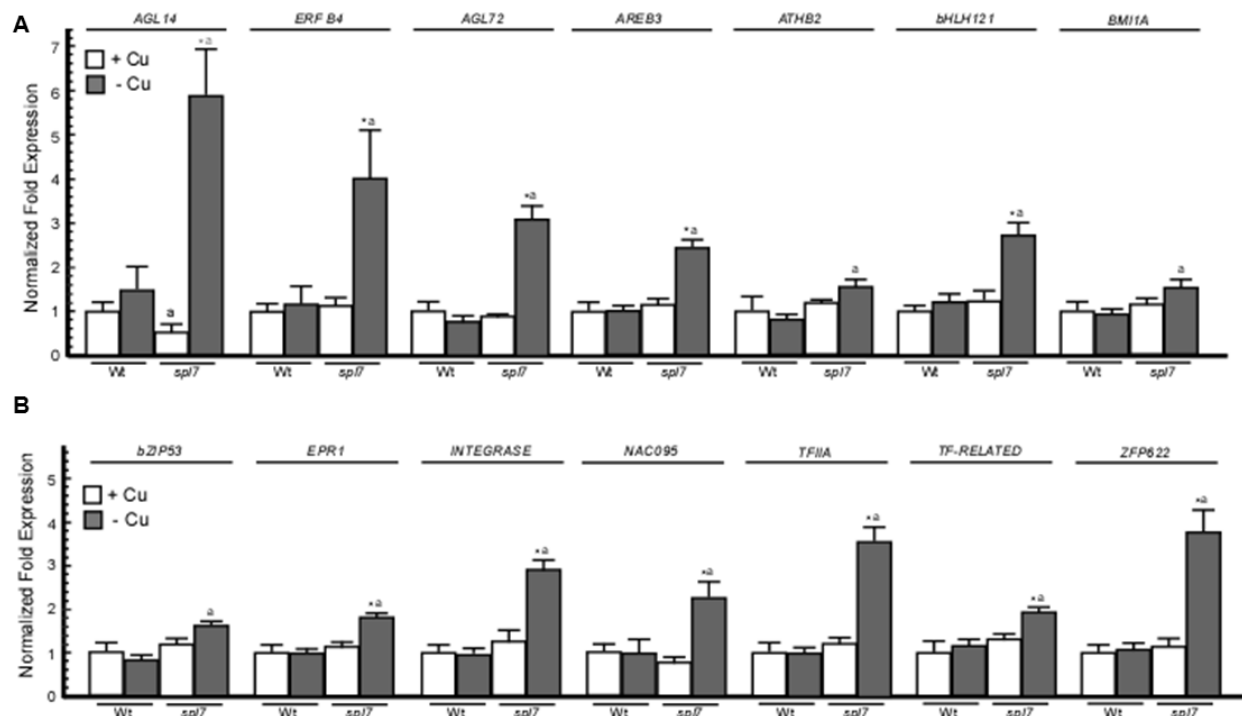


Figure 2. Transcript abundance of genes identified in Y1H is induced by Cu deficiency in flowers of the *spl7* mutant. A to B, The transcriptional response of genes identified in the Y1H screen to Cu limitation in flowers of wild-type (Wt) and the *spl7* mutant (*spl7*). Plants were grown in hydroponic solution with 0.5 μ M CuSO₄ for the first 5 weeks, and continue to grow for another 3 weeks in solution with or without CuSO₄. Results are presented relative to wild-type plants in 0.5 μ M CuSO₄, which was designated as 1. Asterisks (*, p < 0.05) indicate statistically significant differences in gene expression between control (0.5 μ M CuSO₄) and Cu-deficient-treated (0 μ M CuSO₄) plants, a letter "a" indicates statistically significant differences in gene expression between different genotypes (p < 0.05). Error bars indicate S.E. (n = 6).

Interestingly, of 14 genes that showed direct binding to *CCIT1pro* in Y1H assay, 12 were significantly up-regulated by Cu deficiency in flowers of the *spl7* mutant, and all of them exhibited increased transcriptional abundance in flowers of *spl7* mutant compared with wild-type (Figure 2A and B). This result shows that these genes are responsive to limited Cu in flowers when *SPL7* is absent and that *SPL7* can also act as a negative regulator of gene expression. This result also suggests a possibility of the compensatory mechanism for the event when *SPL7* function is compromised or in tissues where *SPL7* is not expressed.

3.3 Expression of *CCIT1* in Flowers, in Part Depends on AREB3, ATHB2 and bZIP53

I then searched for mutant alleles in the ABRC collection for each of 12 transcription regulators that showed binding to *CCIT1pro* (Figure 1) and which were transcriptionally upregulated in response to Cu availability in flowers of the *spl7-1* mutant. Homozygous plants were identified and knock-out alleles were identified. qRT-PCR analyses revealed that *homeobox protein 2* (*ATHB2*), *ABA-responsive element binding protein 3* (*AREB3*) and *basic region/leucine zipper motif 53* (*bZIP53*) exhibited reduced transcript abundance (Figure 3B) resulted from the T-DNA inserted at the 3' UTR, the first exon and the 3' UTR of *AREB3*, *ATHB2* and *bZIP53* (Figure 3A), respectively. I then studied the transcriptional response of *CCIT1* in flowers of each of these mutants. I predicted that the expression of *CCIT1* might not respond properly to Cu limitation if the function of its transcriptional regulator is compromised. The *athb2*, *areb3* and *bzip53* mutants showed decreased expression level of *CCIT1* (Figure 3C), indicating that these 3 genes are the functional regulator of *CCIT1* expression in Arabidopsis. When *SPL7*'s function is lost, their role can be partially replaced by *ATHB2*, *AREB3* and *bZIP53* to facilitate the *CCIT1*'s response to Cu limitation.

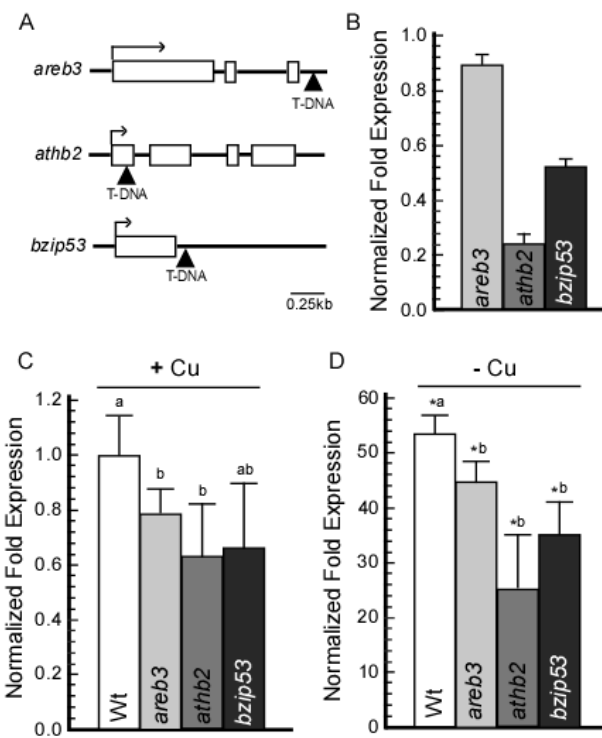


Figure 3. The transcriptional level of *CCIT1* to Cu deficiency depends, in part, on *AREB3*, *ATHB2* and *bZIP53*. **A**, Schematic representation of the T-DNA insertion sites in *areb3*, *athb2* and *bzip53* as predicted by TAIR (<https://www.arabidopsis.org>). **B**, qRT-PCR comparison of the transcript abundance of *AREB3*, *ATHB2*, *bZIP53* in flowers of 8-week-old wild-type and *areb3*, *athb2* and *bzip53* mutant plants. Gene expression of *AREB3*, *ATHB2*, *bZIP53* in flowers of *areb3*, *athb2* and *bzip53* mutant plants are presented relative to their expression in wild-type plant (designated as 1), respectively. Error bars indicate S.E. of 3 technique replicates. **C** and **D**, qRT-PCR comparison of the transcript abundance of *CCIT1* in flowers of 8-week-old wild-type (Wt), *areb3*, *athb2* and *bzip53* mutant plants. *CCIT1* expressions in the mutants are presented relative to wild-type plants in 0.5 μM CuSO₄, which was designated as 1. Asterisks (*, p ≤ 0.05) indicate statistically significant differences in gene expression between control (0.5 μM CuSO₄) and Cu-deficient-treated (0 μM CuSO₄) plants, different letters indicate statistically significant differences in gene expression between different genotypes (p ≤ 0.05). Error bars indicate S.E. (n = 6).

However, I didn't observe significantly different sensitivity of the mutants of *AREB3*, *ATHB2* and *bZIP53* in response to Cu limitation compared with wild-type plants (Supplemental Figure 2). I note that phenotypes were screened at the vegetative stage and my result does not preclude the possibility of increased sensitivity of mutants to Cu limitation at the reproductive stage.

3.4 AREB3, ATHB2 and bZIP53 Localize to the Nucleus in *A. thaliana* Protoplasts

The possible role of *AREB3*, *ATHB2* and *bZIP53* in regulation *CCIT1* expression prompted me to examine the subcellular localization of these 3 genes. Their coding sequence was fused at the C-terminus to EGFP in the SAT6-EGFP-N1-Gate vector and transiently expressed under the control of the constitutive

cauliflower mosaic virus 35S promoter in *A. thaliana* protoplasts. As a control, protoplasts were also transfected with the empty SAT6-EGFP-N1-Gate vector. EGFP-mediated fluorescence was present at the nucleus of AREB3-, ATHB2- or bZIP53-EGFP transfected protoplasts and did not overlap with chlorophyll auto-fluorescence (Figure 4A, B and C). To ascertain the nucleus localization of CCIT1-EGFP, transfected protoplasts were co-stained with a DNA dye, DAPI. After short term incubation, DAPI stained the nucleus, and DAPI-mediated fluorescence overlapped with CCIT1-EGFP-mediated fluorescence but not with chlorophyll-mediated fluorescence (Figure 4A, B and C). Whereas in protoplasts transfected with the empty vector, EGFP was present as a soluble protein in the cytosol (Figure 4D). The subcellular localization assay reveals that AREB3, ATHB2 and bZIP53 localize in the nucleus of *A. thaliana* protoplasts, which is consistent with their role as transcription factors.

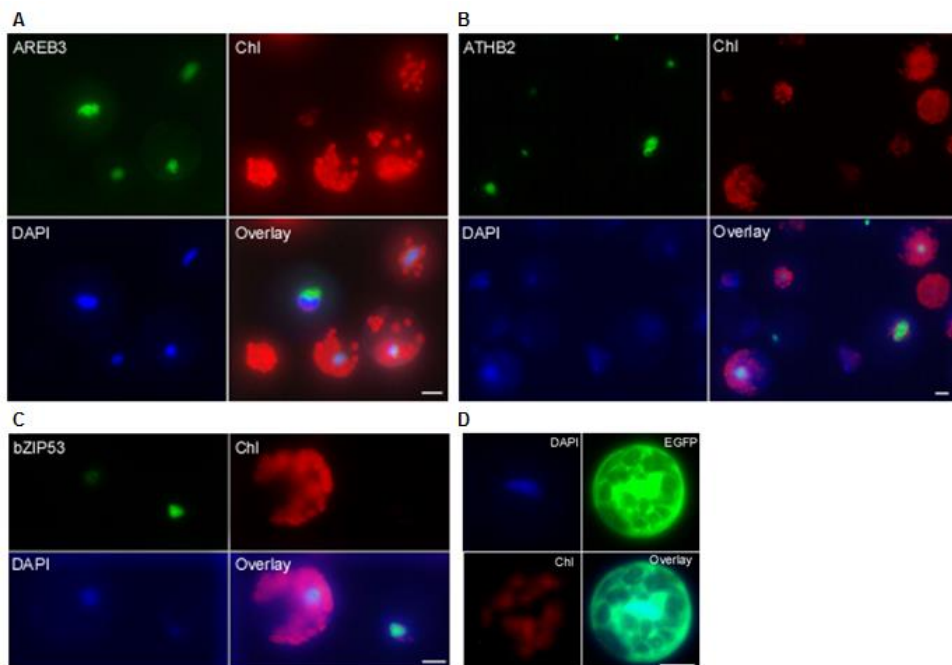


Figure 4. Subcellular localization of AREB3, ATHB2 and bZIP53 in *A. thaliana* protoplasts. *A. thaliana* leaf protoplasts were transfected with the vector expressing the *AREB3-EGFP* fusion (A), *ATHB2-EGFP* fusion (B), *bZIP53-EGFP* fusion (C), or vector expressing *EGFP* without the *CCIT1* cDNA insert (D). To visualize the nucleus, transfected protoplasts were co-stained with DAPI. EGFP-mediated fluorescence, derived from *AREB3-EGFP* (AREB3), *ATHB2-EGFP* (ATHB2), *bZIP53-EGFP* (bZIP53), *EGFP* (EGFP), DAPI-mediated fluorescence (DAPI) and chlorophyll auto-fluorescence (Chl) were visualized using FITC, DAPI and rhodamine filter sets. Superimposed images of *CCIT1-EGFP*- and DAPI-mediated fluorescence and chlorophyll auto-fluorescence (Overlay) were created to demonstrate that green fluorescence derived from *CCIT1-EGFP* co-localizes with DAPI. Scale bar=10 μ m.

3.5 AREB3, ATHB2 and bZIP53 Directly Regulate Expression of *CCIT1*

My findings suggest a possible role of AREB3, ATHB2 and bZIP53 in regulating *CCIT1* expression. To test whether these transcription regulators bind to the promoter of *CCIT1* *in vivo*, I used ChIP. *In silico* analyses using (<http://www.athamap.de/> and <http://www.dna.affrc.go.jp/PLACE/>) tools were used for the identification of the putative regulatory elements of *CCIT1* locus. Using these tools I identified 3 putative homeodomain binding elements within the *CCIT1* promoter region (Figure 5A; Sessa et al., 1993). Both AREB3 and bZIP53 contain a bZIP domain (Jakoby et al., 2002), and 4 bZIP binding elements were found in the *CCIT1* genomic locus (Figure 5A). To test whether the 3 genes which showed downregulation of *CCIT1* in their mutants directly regulates *CCIT1* gene expression by binding to any of these *cis* elements,

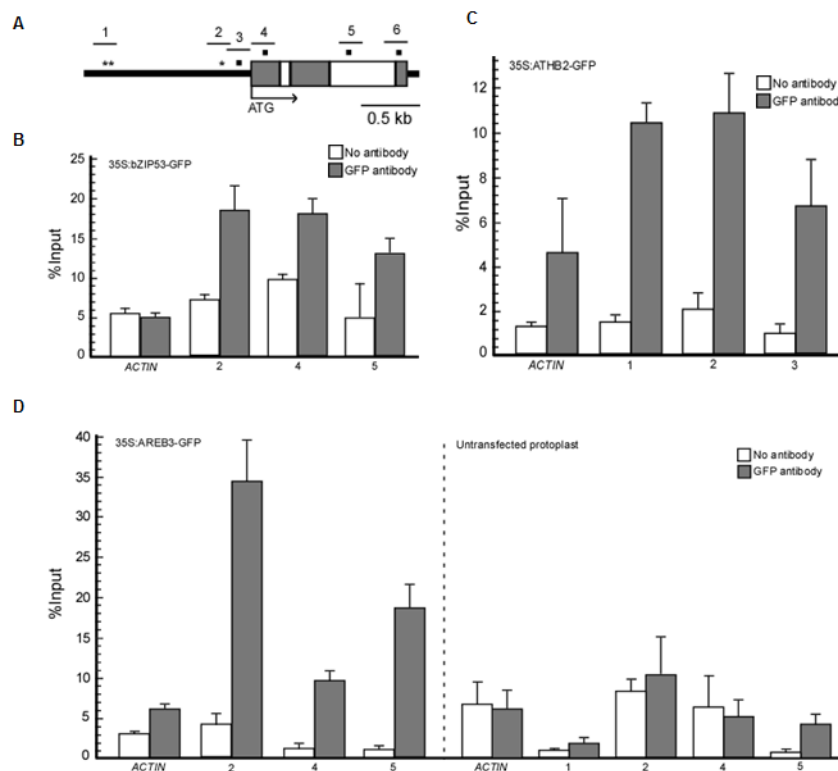


Figure 5. AREB3, ATHB2 and bZIP53 bind to regulatory regions of *CCIT1* chromatin *in vivo*. A. Schematic representation of the *CCIT1* locus. Gray and white boxes represent exons and introns, respectively. Asterisks and closed squares indicate homeodomain and bZIP domain binding motifs, respectively, predicted by AthaMap (<http://www.athamap.de/>) and PLACE (<http://www.dna.affrc.go.jp/PLACE/>). B to D, qRT-PCR of anti-GFP ChIP in *A. thaliana* leaf protoplasts transfected with 35S:bZIP53-GFP, 35S:ATHB2-GFP, 35S:AREB3-GFP or no plasmid (Untransformed protoplast), respectively. Immunoprecipitated DNA enrichment is presented as percent input DNA. Shown is the mean +/- SEM (n=4).

I probed their occupancy on the genomic DNA by ChIP. GFP-tagged constructs were generated and transiently expressed in *Arabidopsis* protoplasts. The genomic DNA that was bound to the GFP-tagged protein was pulled down by the GFP-antibody. Using qRT-PCR, I detected strong and selective occupancy of ATHB2 at the region 1 and 2 of the *CCIT1* promoter, which contains two and one consensus homeodomain binding motifs, respectively (Figure 5C). I also tested for AREB3-GFP and bZIP53-GFP occupancy at the *CCIT1* locus, and strong binding at region 2, 4 and 5 (Figure 5B and D). The protoplasts that were not transfected with GFP-tagged constructs didn't show significant enrichment (Figure 5D), indicating that the observed enrichments are specific. Since AREB3, ATHB2 and bZIP53 bind to regulatory regions in the *CCIT1* locus in protoplasts, our combined data of Y1H and ChIP assays demonstrate that *CCIT1* is the direct target of AREB3, ATHB2 and bZIP53 *in vivo*.

4. DISCUSSION

Cu is an essential micronutrient which is required for plant health, however, if it is present in cells in excess, Cu is toxic and causes damage to plants due to its ability of promoting ROS production. Therefore, plants have evolved sophisticated mechanisms to maintain Cu homeostasis in order to prevent Cu deficiency and meanwhile avoid toxicity. SPL7 has been shown to act as the central regulator during Cu limitation, and is also the only transcription factor in higher plants that has been studied to play a role in the transcriptional regulatory pathway of Cu homeostasis (Yamasaki et al., 2009b; Bernal et al., 2012). Recently, CCIT1, a bHLH transcription factor family member, has been found to be highly responsive to Cu limitation in a SPL7-dependent manner, however, our phenotypic and genetic studies indicate that CCIT1 is not simply a downstream target of SPL7, and a more complicated transcriptional regulatory network than what we previously thought may participate in mediating Cu homeostasis. To identify direct upstream regulators of *CCIT1*, I used the YIH screen of a library consisting of more than 1500 *Arabidopsis* transcription factors. Fourteen genes showed direct binding to *CCIT1* promoter region in Y1H (Figure 1).

To examine whether genes that were found in Y1H screen are responsive to Cu status and what their relationship is with SPL7, I performed qRT-PCR analyses of their expression in wild-type and *spl7* flowers

of plants grown under standard and Cu-limited conditions. The result revealed that most of these genes were upregulated by Cu deficiency in the *spl7* mutant (Figure 2), suggesting a compensatory mechanism when SPL7 function is lost. These data also suggest that SPL7 might act as a negative regulator of the expression of these genes.

To study whether genes identified in Y1H screen functionally regulate *CCIT1* expression, T-DNA insertion alleles for each of them has been identified and qRT-PCR was performed to analyze the expression level of *CCIT1* in these T-DNA insertion alleles (Figure 3A). From the result of the qRT-PCR, I learned that the transcript abundance of *CCIT1* is reduced in *areb3*, *athb2* and *bzip53* mutants (Figure 3C). Subcellular localization assays in *Arabidopsis* protoplasts revealed a nucleus-localization of proteins encoded by these 3 genes (Figure 4A, B and C). This result is consistent with their role as transcription factors. I then further examined the direct interaction of AREB3, ATHB2 and bZIP53 with the *CCIT1* genomic region by ChIP-qPCR assays in *Arabidopsis* protoplasts. Genomic region of *CCIT1* consists of 3 putative homeodomain binding elements and 4 bZIP domain binding motifs (Figure 5A). The results of ChIP-qPCR showed enrichment of *CCIT1* genomic regions in protoplasts transfected with all 3 constructs, AREB3-EGFP, ATHB2-EGFP and bZIP53-EGFP, respectively (Figure 5B, C and D), demonstrating AREB3, ATHB2 and bZIP53 are direct upstream regulator of *CCIT1*.

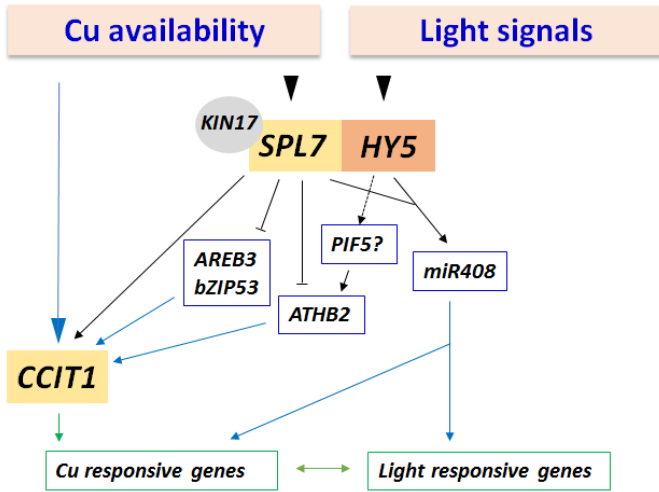
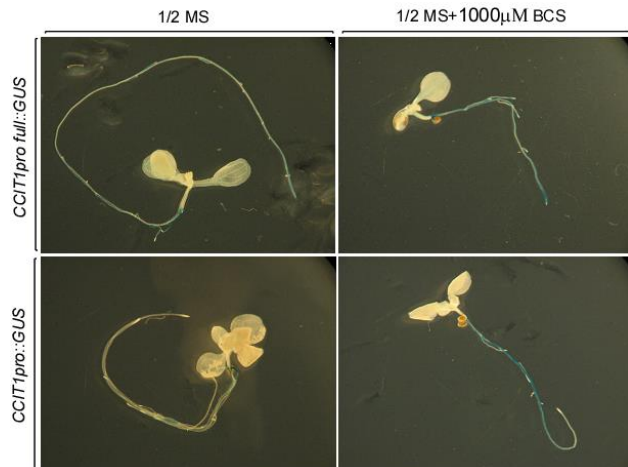


Figure 6. The model of the upstream transcriptional regulatory pathway of CCIT1. Cu availability induces SPL7 activity. During Cu deficiency, KIN17 is recruited to physically interact with SPL7, and activates the downstream Cu responsive genes via CuRE element. CCIT1 expression is also induced by SPL7, further regulates the expression of the Cu responsive genes, and mediates Cu homeostasis and plant development. When SPL7's function is lost, three transcription factors, ATHB2, AREB3 and bZIP53 are upregulated to induce CCIT1 expression, which further activates the downstream Cu responsive genes and regulates Cu homeostasis and plant development. SPL7 also physically interacts with ELONGATED HYPOCOTYL5 (HY5), and they act together to coordinate Cu and light responses via *miR408*. Since *ATHB2* is also a light responsive gene which is activated by PHYTOCHROME-INTERACTING FACTOR 5 (PIF5). It's prompting to propose that *ATHB2* may act as a coordinator between HY5-SPL7 and CCIT-SPL7 regulatory networks.

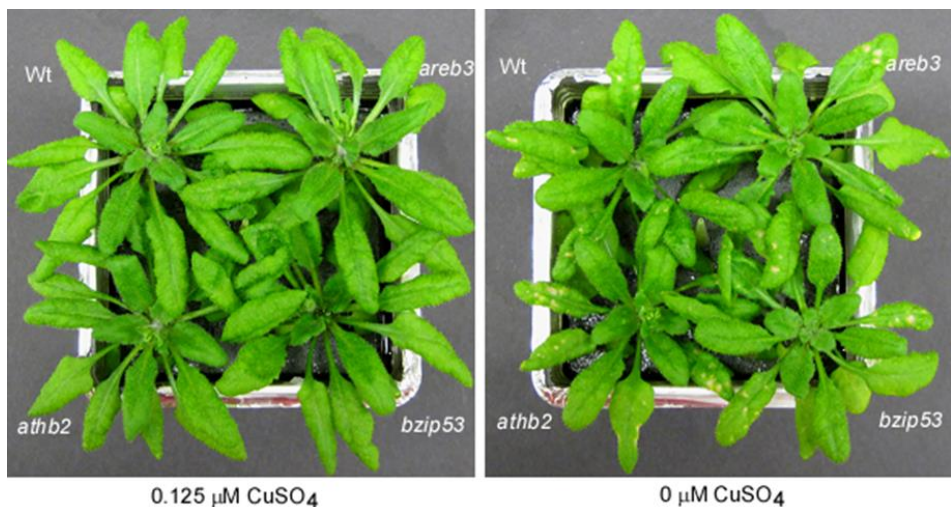
AREB3 and bZIP53 contain a bZIP domain (Jakoby et al., 2002), and ATHB2 is a homeodomain protein (Ruberti et al., 1991; Morelli et al., 1993). Past studies have shown that *AREB3* is expressed in maturing embryos (Bensmihen et al., 2002; Bensmihen et al., 2005), and is also expressed in pollens (Hoth et al., 2010), indicating that AREB3 functions at early developmental stages and may participate in regulating pollen development and germination. In this regard, I found that *CCIT1* is expressed in anthers. It is possible that AREB3 regulates *CCIT1* expression in case of Cu deficiency during pollen development. ATHB2 has been characterized, and its expression is rapidly and strongly upregulated by changes in red: far-red ratio, therefore functions as a positive regulator of shade avoidance and is directly involved in light-regulated growth phenomena throughout Arabidopsis development (Steindler et al., 1997; Steindler et al., 1999). More recently, it has been shown that progressive loss of HAT3, ATHB4 and ATHB2 activity causes developmental defects from embryogenesis onwards in white light, lacks an active shoot apical meristem as well and these defects correlate with changes in auxin distribution and response (Turchi et al., 2013),

suggesting a role of ATHB2 in the crosstalk between light response, auxin signaling and plant development. Recent studies of SPL7 identified its interaction with HY5 in coordination of light response and Cu homeostasis in *A. thaliana* (Zhang et al., 2014). It is possible that ATHB2 mediates a cross talk between HY5-SPL7 and CCIT-SPL7 regulatory networks. However this suggestion and the role of CCIT1 in coordinated response to light and Cu has to be further investigated. bZIP53 has been shown to positively regulate the biosynthetic genes of several amino acids, and thus is involved in energy homeostasis and seed maturation (Figure 6; Alonso et al., 2009; Dietrich et al., 2011). I propose that AREB3, ATHB2, bZIP53 and CCIT1 are the key regulators of the response to Cu deficiency and might play an essential role in tissues and cell types where *SPL7* is not expressed. Further genetic functional analysis of AREB3, ATHB2, bZIP53 in Cu homeostasis and plant fertility is required to demonstrate this hypothesis.

5. SUPPLEMENTAL DATA



Supplemental figure 1. Histochemical analysis of Cu-deficiency induced CCIT1 expression using 1.5 kb full length (*CCIT1pro full*) and 0.7 kb promoter region (*CCIT1pro*). Plants were grown on $\frac{1}{2}$ MS medium with or without 1000 μM bathocuproinedisulfonic acid (BCS), which was used as a Cu chelator to make it unavailable for plants.



Supplemental figure 2. The phenotype of *areb3*, *athb2* and *bzip53* mutants under Cu deficient conditions. Plants were grown in hydroponic system for 6 weeks with or without 0.125 μM CuSO_4 . Chlorotic spots were exhibited in the mature leaves of all lines grown.

Supplemental table 1. Primers used for genotyping

Primer	Gene	Primer sequence (5' to 3')
LB 1.3 for salk line	T-DNA	ATTTGCCGATTTCGGAAC
SALK_093849 LP	SPL7	TTGGAAATTCAAGCTGATTG
SALK_093849 RP	SPL7	TCCACCTGTAAAACCAAGAC
SALK_106790 LP	ATHB2	CTCACGACTCAACGATCTAAC
SALK_106790 RP	ATHB2	CGTCACTGATTCCTCTTGAGC
SALK_004683 LP	bZIP53	TGGGTCAAGAACAACTAACCG
SALK_004683 RP	bZIP53	GGAGGTCAAGGATGAGGAAAC
SALK_020324 LP	AREB3	AGCAGGCTTACACTCATGAGC
SALK_020324 RP	AREB3	TCTTGTGTGTTCTGATGCAG

Supplemental table 2. Primers used for cloning

Primer	Gene	Primer sequence (5' to 3')
attB1r-CCIT1pro-F	CCIT1pro	ggggacaactttgtatagaaaagtgtGAGAGGAGAGATTACGGTTACA
attB4-CCIT1pro-R	CCIT1pro	ggggactgctttttgtacaaacttgATATATACGACGGCAAGAGGAACAA
attB1r-bHLH39pro-F	bHLH39	ggggacaactttgtatagaaaagtgtTTTGACCTGGTCTCAATCAGC
attB4-bHLH39pro-R	bHLH39	ggggactgctttttgtacaaacttgTTTGCTTACTAAGGACAAGTATTGAG
attB1-ATHB2-F	ATHB2	ggggacaagtgtacaaaaaagcaggcttcaccATGATGTTCGAGAAAGACGATCTG
attB2-ATHB2-R (w/stop)	ATHB2	ggggaccactttgtacaaaaaagctggtcGGACCTAGGACGAAGAGCGT
attB1-bZIP53-F	bZIP53	ggggacaagtgtacaaaaaagcaggcttcaccATGGGGTCGGCAAATGCA
attB2-bZIP53-R (w/stop)	bZIP53	ggggaccactttgtacaaaaaagctggtcGCAATCAAACATATCAGCAGAAC
attB1-AREB3-F	AREB3	ggggacaagtgtacaaaaaagcaggcttcaccATGGATTCTCAGAGGGTATTGTTG
attB2-AREB3-R (w/stop)	AREB3	ggggaccactttgtacaaaaaagctggtcGAAAGGAGCCGAGCTGTCC

Supplemental table 3. Primers used in qRT-PCR		
Primer	Gene	Primer sequence (5' to 3')
Actin-F	Actin	GACCTTAACTCTCCCGCTA
Actin-R	Actin	GGAAGAGAGAACCTCGTA
CCIT1-F	CCIT1	ACGAGGTCTTCTATTGAGCA
CCIT1-R	CCIT1	ACCCTTGCTCTGGCAAACCT
ZFP622-F	ZFP622	GAAGACAGTACCGTCGAAAGAG
ZFP622-R	ZFP622	GACATTACTCTCACTCCGATCTT
ERF B4-F	ERF B4	CATTATCGTGCACACCACCTAGTC
ERF B4-R	ERF B4	AGTTGGCACTGGAATCACTAC
bHLH121-F	bHLH121	GCCCTACATGCCTCTAATAC
bHLH121-R	bHLH121	GCTTCTCAGATCTGCTCTCTC
NAC095-F	NAC095	CGGCGAATTAGTCGGTATCAAG
NAC095-R	NAC095	CTGTCATGGGAGGCTGATT
TFIIA-F	TFIIA	CCTTCAAATGTCGGATGTCTTC
TFIIA-R	TFIIA	AGCCAACCAGAGTACATATTCC
AGL72-F	AGL72	CTTATGCCAGGTTGGAGAAAGA
AGL72-R	AGL72	GGTCGGTTCTCAGAAATCCA
AGL14-F	AGL14	GTGAGATGCAAGGAAGAGGAATA
AGL14-R	AGL14	AGTCTCAGGAGGTCCAATGA
ATHB2-F	ATHB2	CTGGGAGAACTAACCGGAAGAG
ATHB2-R	ATHB2	AGGGCACATGGTCAAAGTAG
EPR1-F	EPR1	TTTCGGGAAGATTGCTTGT
EPR1-R	EPR1	CAACTAGCATCCCTGAGTAGTG
INTEGRASE-F	INTEGRASE	TGTACCCACTTACCTCTCTCTT
INTEGRASE-R	INTEGRASE	GTCTCTGTCTTGTACCTCTG
bZIP53-F	bZIP53	GCTTCGGAGTTGACGGATAG
bZIP53-R	bZIP53	GCCAAGGGTTCTGCATAGAT
TF-R F	TF-R	GCTGATCGAGTCCCATCTATT
TF-R R	TF-R	GCCTGGGTATCTCAATTCT
AREB3-F	AREB3	GTCTCTTGATGGGTGGTTG
AREB3-R	AREB3	TCTCTCTGCCTCTCTCTAC
BMI1A-F	BMI1A	GCAGCTTCACAGCTTAGTAGAC
BMI1A-R	BMI1A	CAGGGAGCTTCCOGAGAATAAAC
ChIP 1-F	CCIT1	GTCGCCACCTTGTTCGAAA
ChIP 1-R	CCIT1	TGAAGACGAATTAGATGAAATACTAAAGTACTTAATG
ChIP 2-F	CCIT1	GTACTGCAGATATACGACCATTTCTC
ChIP 2-R	CCIT1	GTCAACCCCTGACCGAGTAATAT
ChIP 3-F	CCIT1	CTGCAGCTCATTGCATTGTGC
ChIP 3-R	CCIT1	CTACCAACGATGGCTCTAAGTT
ChIP 4-F	CCIT1	CATCAGACTCAATATCAAGTTACTCCATG
ChIP 4-R	CCIT1	CCTCATGCAAAACTGGTTCTTCC
ChIP 5-F	CCIT1	GGGAGGATTGTGTTAACTTAGCTAAC
ChIP 5-R	CCIT1	CGAACAGTCTCTCCCACCAATAG
ChIP 6-F	CCIT1	GTATATGGGAAAGTAGATGGATGAGAAC
ChIP 6-R	CCIT1	GCACTTGTGTTGTCACGAAGCGA

REFERENCES

- Abdel-Ghany, S.E., and Pilon, M.** (2008). MicroRNA-mediated systemic down-regulation of copper protein expression in response to low copper availability in Arabidopsis. *J Biol Chem* **283**, 15932-15945.
- Alonso, J.M., Steanova, A.N., Leisse, T.J., Kim, C.J., Chen, H., Shinn, P., Stevenson, D.K., Zimmerman, J., Barajas, P., Cheuk, R., Gadrinab, C., Heller, C., Jeske, A., Koesema, E., Meyers, C.C., Parker, H., Prednis, L., Ansari, Y., Choy, N., Deen, H., Geralt, M., Hazari, N., Hom, E., Karnes, M., Mulholland, C., Ndubaku, R., Schmidt, I., Guzman, P., Aguilar-Henonin, L., Schmid, M., Weigel, D., Carter, D.E., Marchand, T., Risseeuw, E., Brogden, D., Zeko, A., Crosby, W.L., Berry, C.C., and Ecker, J.R.** (2003). Genome-wide insertional mutagenesis of *Arabidopsis thaliana*. *Science* **301**, 653-657.
- Alonso, R., Onate-Sanchez, L., Weltmeier, F., Ehlert, A., Diaz, I., Dietrich, K., Vicente-Carbajosa, J., and Droege-Laser, W.** (2009). A pivotal role of the basic leucine zipper transcription factor bZIP53 in the regulation of *Arabidopsis* seed maturation gene expression based on heterodimerization and protein complex formation. *The Plant cell* **21**, 1747-1761.
- Bensmihen, S., Giraudat, J., and Parcy, F.** (2005). Characterization of three homologous basic leucine zipper transcription factors (bZIP) of the ABI5 family during *Arabidopsis thaliana* embryo maturation. *Journal of experimental botany* **56**, 597-603.
- Bensmihen, S., Rippa, S., Lambert, G., Jublot, D., Pautot, V., Granier, F., Giraudat, J., and Parcy, F.** (2002). The homologous ABI5 and EEL transcription factors function antagonistically to fine-tune gene expression during late embryogenesis. *The Plant cell* **14**, 1391-1403.
- Bernal, M., Casero, D., Singh, V., Wilson, G.T., Grande, A., Yang, H., Dodani, S.C., Pellegrini, M., Huijser, P., Connolly, E.L., Merchant, S.S., and Kramer, U.** (2012). Transcriptome sequencing identifies SPL7-regulated copper acquisition genes FRO4/FRO5 and the copper dependence of iron homeostasis in *Arabidopsis*. *The Plant cell* **24**, 738-761.
- Burkhead, J.L., Reynolds, K.A., Abdel-Ghany, S.E., Cohu, C.M., and Pilon, M.** (2009). Copper homeostasis. *The New phytologist* **182**, 799-816.
- Deplancke, B., Vermeirssen, V., Arda, H.E., Martinez, N.J., and Walhout, A.J.** (2006). Gateway-compatible yeast one-hybrid screens. *CSH protocols* **2006**.
- Dietrich, K., Weltmeier, F., Ehlert, A., Weiste, C., Stahl, M., Harter, K., and Droege-Laser, W.** (2011). Heterodimers of the *Arabidopsis* transcription factors bZIP1 and bZIP53 reprogram amino acid metabolism during low energy stress. *The Plant cell* **23**, 381-395.
- Eriksson, M., Moseley, J.L., Tottey, S., Del Campo, J.A., Quinn, J., Kim, Y., and Merchant, S.** (2004). Genetic dissection of nutritional copper signaling in chlamydomonas distinguishes regulatory and target genes. *Genetics* **168**, 795-807.
- Garcia-Molina, A., Xing, S.P., and Huijser, P.** (2014). A Conserved KIN17 Curved DNA-Binding Domain Protein Assembles with SQUAMOSA PROMOTER-BINDING PROTEIN-LIKE7 to Adapt *Arabidopsis* Growth and Development to Limiting Copper Availability. *Plant physiology* **164**, 828-840.
- Halliwell, B., and Gutteridge, J.M.** (1984). Oxygen toxicity, oxygen radicals, transition metals and disease. *The Biochemical journal* **219**, 1-14.
- He, Y., Sidhu, G., and Pawlowski, W.P.** (2013). Chromatin immunoprecipitation for studying chromosomal localization of meiotic proteins in maize. *Methods in molecular biology* **990**, 191-201.
- Higo, K., Ugawa, Y., Iwamoto, M., and Korenaga, T.** (1999). Plant *cis*-acting regulatory DNA elements (PLACE) database: 1999. *Nucleic Acids Res* **27**, 297-300.
- Hill, K.L., and Merchant, S.** (1995). Coordinate expression of coproporphyrinogen oxidase and cytochrome c6 in the green alga *Chlamydomonas reinhardtii* in response to changes in copper availability. *The EMBO journal* **14**, 857-865.

- Hoth, S., Niedermeier, M., Feuerstein, A., Hornig, J., and Sauer, N.** (2010). An ABA-responsive element in the AtSUC1 promoter is involved in the regulation of AtSUC1 expression. *Planta* **232**, 911-923.
- Jakoby, M., Weisshaar, B., Droege-Laser, W., Vicente-Carbajosa, J., Tiedemann, J., Kroj, T., Parcy, F., and b, Z.I.P.R.G.** (2002). bZIP transcription factors in Arabidopsis. *Trends in plant science* **7**, 106-111.
- Kropat, J., Tottey, S., Birkenbihl, R.P., Depege, N., Huijser, P., and Merchant, S.** (2005). A regulator of nutritional copper signaling in Chlamydomonas is an SBP domain protein that recognizes the GTAC core of copper response element. *Proc Natl Acad Sci U S A* **102**, 18730-18735.
- Marschner, H.** (1995). Mineral Nutrition of Higher Plants. (Elsevier Academic Press).
- Mira, H., Martinez, N., and Penarrubia, L.** (2002). Expression of a vegetative-storage-protein gene from Arabidopsis is regulated by copper, senescence and ozone. *Planta* **214**, 939-946.
- Mitsuda, N., and Ohme-Takagi, M.** (2009). Functional analysis of transcription factors in Arabidopsis. *Plant & cell physiology* **50**, 1232-1248.
- Mitsuda, N., Ikeda, M., Takada, S., Takiguchi, Y., Kondou, Y., Yoshizumi, T., Fujita, M., Shinozaki, K., Matsui, M., and Ohme-Takagi, M.** (2010). Efficient yeast one-/two-hybrid screening using a library composed only of transcription factors in Arabidopsis thaliana. *Plant & cell physiology* **51**, 2145-2151.
- Morelli, G., Baima, S., Carabelli, M., Lucchetti, S., Nobill, F., Sessa, G., and Ruberti, I.** (1993). Identification of Distinct Families of Hd-Zip Proteins in Arabidopsis-Thaliana. *J Cell Biochem*, 43-43.
- Murashige, T., and Skoog, F.** (1962). A Revised Medium for Rapid Growth and Bio Assays with Tobacco Tissue Cultures. *Physiologia plantarum* **15**, 473-497.
- Pilon, M., Abdel-Ghany, S.E., Cohu, C.M., Gogolin, K.A., and Ye, H.** (2006). Copper cofactor delivery in plant cells. *Current opinion in plant biology* **9**, 256-263.
- Prestridge, D.S.** (1991). SIGNAL SCAN: a computer program that scans DNA sequences for eukaryotic transcriptional elements. *Comput Appl Biosci* **7**, 203-206.
- Quinn, J.M., and Merchant, S.** (1995). Two copper-responsive elements associated with the Chlamydomonas Cyc6 gene function as targets for transcriptional activators. *The Plant cell* **7**, 623-628.
- Quinn, J.M., Barraco, P., Eriksson, M., and Merchant, S.** (2000). Coordinate copper- and oxygen-responsive Cyc6 and Cpx1 expression in Chlamydomonas is mediated by the same element. *The Journal of biological chemistry* **275**, 6080-6089.
- Ruberti, I., Sessa, G., Lucchetti, S., and Morelli, G.** (1991). A novel class of plant proteins containing a homeodomain with a closely linked leucine zipper motif. *The EMBO journal* **10**, 1787-1791.
- Sessa, G., Morelli, G., and Ruberti, I.** (1993). The Athb-1 and Athb-2 Hd-Zip Domains Homodimerize Forming Complexes of Different DNA-Binding Specificities. *Embo Journal* **12**, 3507-3517.
- Steindler, C., Carabelli, M., Borello, U., Morelli, G., and Ruberti, I.** (1997). Phytochrome A, phytochrome B and other phytochrome(s) regulate ATHB-2 gene expression in etiolated and green Arabidopsis plants. *Plant Cell and Environment* **20**, 759-763.
- Steindler, C., Matteucci, A., Sessa, G., Weimar, T., Ohgishi, M., Aoyama, T., Morelli, G., and Ruberti, I.** (1999). Shade avoidance responses are mediated by the ATHB-2 HD-Zip protein, a negative regulator of gene expression. *Development* **126**, 4235-4245.
- Sunkar, R., Kapoor, A., and Zhu, J.K.** (2006). Posttranscriptional induction of two Cu/Zn superoxide dismutase genes in Arabidopsis is mediated by downregulation of miR398 and important for oxidative stress tolerance. *The Plant cell* **18**, 2051-2065.
- Turchi, L., Carabelli, M., Ruzza, V., Possenti, M., Sassi, M., Penalosa, A., Sessa, G., Salvi, S., Forte, V., Morelli, G., and Ruberti, I.** (2013). Arabidopsis HD-Zip II transcription factors control apical embryo development and meristem function. *Development* **140**, 2118-2129.
- Tzfira, T., Tian, G.W., Lacroix, B., Vyas, S., Li, J., Leitner-Dagan, Y., Krichevsky, A., Taylor, T., Vainstein, A., and Citovsky, V.** (2005). pSAT vectors: a modular series of plasmids for

- autofluorescent protein tagging and expression of multiple genes in plants. Plant molecular biology **57**, 503-516.
- Udvardi, M.K., Czechowski, T., and Scheible, W.R.** (2008). Eleven golden rules of quantitative RT-PCR. *The Plant cell* **20**, 1736-1737.
- Yamaguchi, N., Winter, C.M., Wu, M.F., Kwon, C.S., William, D.A., and Wagner, D.** (2014). PROTOCOLS: Chromatin Immunoprecipitation from Arabidopsis Tissues. *The Arabidopsis book / American Society of Plant Biologists* **12**, e0170.
- Yamasaki, H., Hayashi, M., Fukazawa, M., Kobayashi, Y., and Shikanai, T.** (2009a). SQUAMOSA Promoter Binding Protein-Like7 Is a Central Regulator for Copper Homeostasis in Arabidopsis. *The Plant cell* **21**, 347-361.
- Yamasaki, H., Hayashi, M., Fukazawa, M., Kobayashi, Y., and Shikanai, T.** (2009b). SQUAMOSA Promoter Binding Protein-Like7 Is a Central Regulator for Copper Homeostasis in *Arabidopsis*. *The Plant cell* **21**, 347-361.
- Yamasaki, H., Abdel-Ghany, S.E., Cohu, C.M., Kobayashi, Y., Shikanai, T., and Pilon, M.** (2007). Regulation of Copper Homeostasis by Micro-RNA in *Arabidopsis*. *Journal of Biological Chemistry* **282**, 16369-16378.
- Zhai, Z., Jung, H.I., and Vatamaniuk, O.K.** (2009). Isolation of protoplasts from tissues of 14-day-old seedlings of *Arabidopsis thaliana*. *J Vis Exp*.
- Zhang, H., Zhao, X., Li, J., Cai, H., Deng, X.W., and Li, L.** (2014). MicroRNA408 is critical for the HY5-SPL7 gene network that mediates the coordinated response to light and copper. *The Plant cell* **26**, 4933-4953.

CHAPTER IV

A Member of the bHLH Family of Transcription Factors, CCIT1, Contributes to the Crosstalk between Cu Homeostasis and Basal Cd Resistance in *A. thaliana*

ABSTRACT

Cadmium (Cd) is a non-essential and toxic metal that causes growth retardation and interferes with vital biochemical processes including photosynthesis and redox balance in plants. Among the cellular mechanisms of Cd toxicity is the disruption of the homeostasis of micronutrients. We have found recently that the central regulator of copper (Cu) homeostasis in *A. thaliana*, SPL7 (*SQUAMOSA* promoter binding protein-like7), is important for Cd resistance. Here we show that an SPL7 downstream target, a putative transcription factor designated as CCIT1 (Cu-Cd-induced transcription factor 1), which belongs to the bHLH (basic helix-loop-helix) family, is induced by Cd toxicity and Cu deficiency. Analyses of two independent T-DNA insertion alleles (*ccit1-1* and *ccit1-2*) and transgenic plants expressing the genomic *CCIT1* fragment showed that loss of CCIT1 function increases the sensitivity of plants to Cd toxicity and increases Cd accumulation in shoots. The genomic fragment of *CCIT1* partially rescues the hypersensitivity of the *ccit1-1* mutant to Cd and reduces Cd concentration in shoots compared to the *ccit1-1* mutant. Analysis of Cu concentration in the *ccit1* mutants revealed that CCIT1 plays an important role in Cu accumulation in roots in response to Cd toxicity. I also showed that upregulation of expression of Cu(I) transporters from the CTR/COPT family by Cd is impaired in the *ccit1-1* mutant. Collectively, results presented in this chapter suggest that CCIT1 functions in the SPL7-dependent regulatory network in basal Cd resistance and plays an essential role in the crosstalk between Cd and Cu homeostasis.

1. INTRODUCTION

Cadmium (Cd) is a highly toxic transition metal of considerable biological and environmental concerns. Cd reduces plant growth, causes chlorosis of leaves and brownish coloration of roots, decreases root length, and affects major biochemical processes including redox balance, photosynthesis, and water status (Das et

al., 1997; Hasan et al., 2009). At the cellular level, Cd toxicity results from the displacement of endogenous co-factors from their cellular binding sites, thiol-capping of essential proteins, inhibition of DNA repair processes, interference with the antioxidant defense system, and the generation of reactive oxygen species (ROS) (Stadtman, 1990; Valko et al., 2005; Clemens, 2006a).

Studies to date have shown that uptake of Cd from the soils into the root epidermal cells is mediated by transporters for essential elements (*e.g.* iron [Fe], and zinc [Zn], calcium [Ca] and manganese [Mn]) due to either the broad substrate specificity of the transporter, or the similar ionic properties of essential and nonessential heavy metals (Eide et al., 1996a; Clemens et al., 1998; Cohen et al., 1998; Sasaki et al., 2012). For example, a high-affinity Fe transporter, IRT1 (**I**ron-**r**egulated **t**ransporter1), plays a major role in Cd uptake into the root of *A. thaliana* (Eide et al., 1996a). Plants have developed several strategies for Cd detoxification, including binding of Cd within the cell wall, chelation with cellular ligands, compartmentation in the vacuole and enrichment in leaf trichomes (Clemens, 2006b). In the cytosol, Cd forms a bi-dentate complex with the ubiquitous thiol tripeptide glutathione GSH, Cd-GS₂. This, in turn, promotes the synthesis of the principal metal-binding peptides, phytochelatins (PCs) (Vatamaniuk et al., 2000). PCs ([γ-Glu-Cys]_n-Xaa, n=2-11) are synthesized enzymatically from free GSH and Cd-GS2 or related thiols by PC synthases (PCS), act as high-affinity Cd chelators, and play the major role in Cd detoxification (Vatamaniuk et al., 2000; Vert et al., 2002; Vatamaniuk et al., 2004; Clemens, 2006a). Cd-PC complexes and Cd ions are then either sequestered into the vacuole in the roots by **ATP-*b*inding cassette** (ABC) transporters or **cation exchangers** (CAX), or travel radially via plasmodesmata towards the vasculature, are loaded into the xylem vessels in the root and move into shoots with the transpiration stream (Gong et al., 2003; Song et al., 2010). Metallothioneins (MTs) are small metal-binding proteins that were found to be stabilized by binding with Cd, suggesting that they can function as Cd chelators (Zimeri et al., 2005). Additionally, the simultaneous knock-down of *MT1a*, *b* and *c* in *A.thaliana* resulted in increased sensitivity to Cd and significant reduction of aboveground Cd accumulation, indicating MT1 is essential for Cd tolerance and may participate in root-to-shoot Cd translocation (Zimeri et al., 2005).

There is growing evidence indicating the crosstalk between micronutrient homeostasis and Cd resistance. Competition of Cd with essential metals for cellular uptake sites as well as binding sites in metalloenzymes disrupts homeostasis of essential elements. In this regard, effects of Cd on the Fe status in plants is the best understood. In *A. thaliana*, Cd upregulates the mRNA expression of the Fe uptake system including the root ferric chelate reductase, *FRO2*, and a plasma membrane-localized Fe(II) transporter, *IRT1* (Eide et al., 1996b; Robinson et al., 1999). In addition, transgenic *A. thaliana* plants overexpressing *IRT1* accumulate more Cd (Eide et al., 1996b; Connolly et al., 2002). Therefore, it is suggested that Cd might compete with Fe(II) for uptake in Cd-polluted soils, thus causing Fe deficiency (Vert et al., 2002). Consistent with this suggestion, exposure of the Cd/Zn hyperaccumulator, *Thlaspi caerulescens* (*Ganges* population) to Cd inhibited Fe uptake (Kupper and Kochian, 2010). The expression of the master regulator of Fe homeostasis in *A. thaliana*, a member of the bHLH family of transcription factors, FIT (AtbHLH29), and two other bHLH family members, AtbHLH38 and AtbHLH39, which are involved in Fe homeostasis, are also upregulated upon Cd toxicity. A recent study showed that co-expression of FIT with AtbHLH38 and bHLH39 confer Cd tolerance *via* increased Cd sequestration in the root and improved Fe homeostasis in the shoot (Wu et al., 2012). Studies in our lab have recently shown that a phloem-specific Fe transporter, Oligopeptide Transporter 3 (OPT3) is involved in Cd partitioning. The Cd concentration in young leaves and the xylem sap of *opt3-3* mutant was significantly lower than it in wild-type, and the *opt3-3* shoots exhibited higher tolerance to Cd toxicity (Zhai et al., 2014). Zhai et al., 2014 also showed that OPT3 mediates Cd uptake in a heterologous system, however, contributes to Cd partitioning *in planta* indirectly via functioning in Fe homeostasis. These results establish an important interaction between Cd detoxification and Fe homeostasis and suggest a crosstalk between micronutrients and toxic metals.

Our recent studies have also shown that Cd stimulates Cu accumulation in roots of *A. thaliana* and mimics transcriptional Cu deficiency responses by inducing Cu-uptake and reallocation system. Indeed, expression of high-affinity Cu transporters, *COPT1*, *COPT2* and *COPT6*, are upregulated and these transcriptional responses depend on the master regulator of Cu homeostasis in *A. thaliana*, SPL7 (Gayomba et al., 2013). We also found that the triple *cop1copt2copt6* mutant is sensitive to Cd (Gayomba et al., 2013).

Another member of the COPT family, COPT5, which effluxes Cu from the vacuole in case of Cu deficiency, plays a role in Cd resistance as well (Carrio-Segui et al., 2015). In addition, Cd triggers miR398-mediated Cu reallocation between Cu/Zn superoxide dismutase (Cu/ZnSOD) and FeSOD to provide Cu to essential Cu-requiring cellular functions and this response also depends on SPL7 (Gayomba et al., 2013). Finally, we found that Cd-triggered Cu accumulation in roots is impaired in the *spl7-1* mutant, suggesting that at a minimum both the SPL7-dependent Cu uptake and intracellular Cu reallocation are important for basal Cd resistance in *A. thaliana* (Gayomba et al., 2013).

Results in this chapter showed that a member of the bHLH transcription factor family in *A. thaliana*, CCIT1 facilitates Cu-dependant basal Cd resistance. The described data substantiate our previous finding of the important role of Cu in basal Cd resistance in *A. thaliana*.

2. METHODS

2.1 Plant Materials

All plant lines used in the study were in the *A. thaliana* Columbia (Col-0) background. Seeds of the *SPL7* (SALK_093849; *alias spl7-1*) mutant were obtained from Dr. Shikanai (Kyoto University, Japan) (Yamasaki et al., 2009). Two *CCIT1* (AT1G71200) mutant alleles, SALK_073160 (*alias ccit1-1*), SAIL_711_B07 (*alias ccit1-2*) mutant alleles were obtained from the *Arabidopsis* Biological Resource Center (Alonso et al., 2003). Mutants bearing homozygous T-DNA insertions were selected by PCR using genomic DNA as a template and the LBb1.3 for SALK line and RP or LB1 for SAIL line and RP primer pairs (Supplemental Table 1) to select plant homozygous. For complementation of the *ccit1-1* mutant, a 2.9-kb genomic region spanning the entire *CCIT1* locus was PCR-amplified from Col-0 and introduced by recombination cloning into pRCS2-hpt. The resulting constructs were transformed into *ccit1-1* via the floral dip method (Clough and Bent, 1998). To generate the transgenic lines overexpressing *CCIT1*, full-length *CCIT1* cDNA was introduced by Gateway cloning into Earley-Gate102 and 201 destination vector (Earley et al., 2006b), where *CCIT1* was fused at the N-termini to the cyan fluorescent protein and human influenza hemagglutinin (HA) epitope tag under the control of the 35S promoter. The resulting constructs were

transformed into wild-type *A. thaliana* (Col-0) via the floral dip method (Clough and Bent, 1998). Based on results of semi-quantitative RT-PCR analyses of T2 transgenic lines, three one-copy-insertion homozygous lines complemented to *ccit1-1* (designated as *CCIT1-1*, *CCIT1-2* and *CCIT1-3*), and overexpressing *CCIT1* (designated as 35S-*CCIT1-1*, 35S-*CCIT1-2* and 35S-*CCIT1-3*) were selected for subsequent experiments.

2.2 Growth Conditions and Experimental Treatments

Before growing different *A. thaliana* lines on solid medium, seeds were surface-sterilized in 75% (v/v) ethanol and a solution containing 1.8% sodium hypochlorite (made up by diluting a household Clorox solution), 0.1% (v/v) Tween-20, and seeds of uniform size were sown on half-strength Murashige and Skoog (½ MS) medium (pH 5.7) (Murashige and Skoog, 1962) containing 1% (w/v) sucrose and 0.7% agar (w/v, Sigma A1296), and indicated concentrations of CdCl₂, CuCl₂ and BCS (w/v, Acros 164060010). After stratification at 4 °C for 2 days in darkness, seeds were germinated and grown vertically for 10 days or horizontally for 14 days. For plants that were cultivated hydroponically, plants were grown in hydroponically with 0.125 µM CuSO₄ continuously for 4 weeks, and then subject to 25 µM CdCl₂ for indicated time. In all cases plants were grown at 22 °C, 14 h light/10 h dark photoperiod and a photosynthetic photon flux density of 110 µmol m⁻² s⁻¹.

2.3 Plasmid Construction

Vectors *EarleyGate102* and *201* (Earley et al., 2006a) were used for generating transgenic plants ectopically expressing *CCIT1*. The vector *RCS2-hpt* was used for *ccit1-1* mutant complementation (Chung et al., 2005). The *CCIT1* cDNA was amplified by RT-PCR from RNA isolated from *A. thaliana*. The genomic fragment of *CCIT1* was amplified by PCR from genomic DNA isolated from *A. thaliana*. The primers (Supplemental table 1) added attB sites on resulting PCR products, which were then introduced into corresponding vectors by recombination cloning (Invitrogen). To make the *CCIT1pro-GUS* and *CCIT1pro-GFP* construct, a 1.5kb fragment of the genomic sequence upstream of the *CCIT1* start codon was amplified by PCR using primer

pairs listed in Supplemental Table 1. The resulting PCR product was cloned by recombination into the *GUS1-Gate* vector upstream of *uidA*, encoding the β-glucuronidase (GUS) reporter gene and the *YXT2-GFP-Gate* vector upstream of the green fluorescent protein (GFP). The *CCIT1pro-GUS* or *CCIT1pro-GFP* construct was transformed into wild-type *A. thaliana* (Clough and Bent, 1998).

2.4 RNA Extraction and cDNA Synthesis

Roots and shoots from plants grown under the indicated conditions were separated and flash-frozen in liquid nitrogen before homogenization using a mortar and a pestle. Total RNA was isolated using TRIzol reagent (Invitrogen), according to the manufacturer's instructions. One µg of total RNA samples were digested with DNase I (New England Biolabs) prior to first strand cDNA synthesis using the QPCR cDNA synthesis kit (Agilent Technologies).

2.5 Quantitative Real-Time (qRT)-PCR and Data Analysis

Prior to qRT-PCR analysis, primer and cDNA concentrations were optimized to reach the target and normalizing gene amplification efficiency of $100 \pm 10\%$. Two µl of 15-fold-diluted cDNA was used as a template for qRT-PCR in a total volume of 15 µl containing a 500 nM concentration of each PCR primer, 50 mM KCl, 20 mM Tris-HCl, pH 8.4, 0.2 mM each dNTP, and 1.25 units of iTaq DNA polymerase in iQ SYBR Green Supermix (Bio-Rad). PCR was carried out using the CFX96 real-time PCR system (Bio-Rad). The thermal cycling parameters were as follows: denaturation at 95 °C for 3 min, followed by 39 cycles of 95 °C for 10 s and 55 °C for 30 s. Amplicon dissociation curves (i.e. melting curves) were recorded after cycle 39 by heating from 60 °C to 95 °C with 0.5 °C increments and an average ramp speed of 3.3 °C s⁻¹. Real-time PCR experiments were conducted using three independent biological samples, each consisting of three technical replicates (Udvardi et al., 2008), unless indicated otherwise. Data were normalized to the expression of *ACTIN 2*. The -fold difference ($2^{-\Delta\Delta Ct}$) was calculated using the CFX Manager Software, version 1.5 (Bio-Rad). Statistical analysis was performed using the Relative Expression Software Tool (REST; Qiagen).

2.6 Histochemical Analysis

Histochemical staining was performed with *A. thaliana* transgenic plants expressing *CCIT1pro-GUS1* construct. Staining was performed as detailed in Chapter 2 and (Jefferson et al., 1987). Incubation of transgenic plants with the GUS substrate was overnight at 37 °C. Staining patterns were analyzed using the Zeiss 2000 stereomicroscope. Images were collected using a Canon Power Shot S3 IS digital camera and a CS3IS camera adapter.

2.7 Fluorescent Microscopy

Three one-copy insertion transgenic lines that were transformed with *CCIT1pro-GFP* were used for the fluorescent microscopy. EGFP-mediated fluorescence and brightfield view were visualized using FITC (for EGFP) filter set and DIC set of the Axio Imager M2 microscope equipped with the motorized Z-drive (Zeiss), respectively. Images were collected with the high-resolution AxioCam MR Camera.

2.8 Analyses of Cadmium and Copper Concentrations

For analyses of Cd and Cu concentration, seeds of indicated *A. thaliana* plant lines, were germinated and grown hydroponically using medium described in (Arteca and Arteca, 2000). After 4 weeks of growth, plants were transferred to a fresh hydroponic solution supplemented with or without 25 µM CdCl₂. Roots and shoots were harvested after 2 days. Roots were desorbed from ions associated with the cell wall by washing with 10 mM EDTA for 5 min followed by washing with a solution containing 0.3 mM BPS and 5.7 mM sodium dithionite for 10 min before rinsing with deionized water 3 times. Plant tissues were then dried, subjected to acid digestion with nitric acid prior to analyses of Cd and Cu concentrations by inductively coupled plasma mass spectroscopy (ICP-MS; Agilent 7500).

2.9 Yeast-one-hybrid Assay

The 0.7 kb *CCIT1* promoter fragment and 1 kb *COPT2* promoter fragment were fused individually to a reporter *HIS3* gene of the yeast one-hybrid (Y1H) *bait* vector (Mitsuda et al., 2010) by homologous recombination. After linearization of the plasmid with ApaI restriction enzyme, constructs were integrated into the genome of the yeast Y1H strain, YM4271 using the manufacturer recommended procedures (Clontech) and (Deplancke et al., 2006). The transformants were selected and grown on YNB medium without Uracil but with 0.67% Yeast Nitrogen Base, 0.077% CSM-Ura, 0.05% NaCl, 2% glucose and 2% agar, pH6.0. The coding region of *CCIT1* and *SPL7* were fused with the prey vector *pGAD424* bearing the activation domain that is able to activate the expression of *HIS3* gene (Mitsuda et al., 2010). The transformation of the *prey* construct into the YM4271 yeast strain with bait construct was performed following lithium acetate transformation procedures. The transformants with both bait and prey constructs were selected and grown on YNB medium without uracil and leucine. Interactions between prey and bait were selected by growing on YNB medium without uracil, leucine and histidine. 15 mM 3-Amino-1,2,4-triazole (3-AT) was also added to the YNB medium to inhibit the *HIS3* gene self-activation. Colonies were then subjected to yeast drop assay for validation.

2.10 Accession Numbers

SPL7 (AT5G18830), *CCIT1* (AT1G71200), *COPT1* (AT5G59030), *COPT2* (AT3G46900), *COPT6* (AT2G26975).

3. RESULTS

3.1 Cadmium Increases the Transcript Abundance of *CCIT1* in Roots of *A. thaliana* in the Partial *SPL7*-Dependent Manner

CCIT1 was identified in the microarray-based screen for transcription factors and transport proteins that are differentially regulated in *A. thaliana* roots and shoots by Cd but not by oxidative stress that is a by-product of Cd toxicity. Verification of the microarray data by qRT-PCR showed that the expression of *CCIT1* in roots but not in shoots of 10-day-old plants is significantly up-regulated by Cd (Figure 1A). Consistent with microarray data, *CCIT1* expression was not significantly altered in roots by H₂O₂ (Figure 1B).

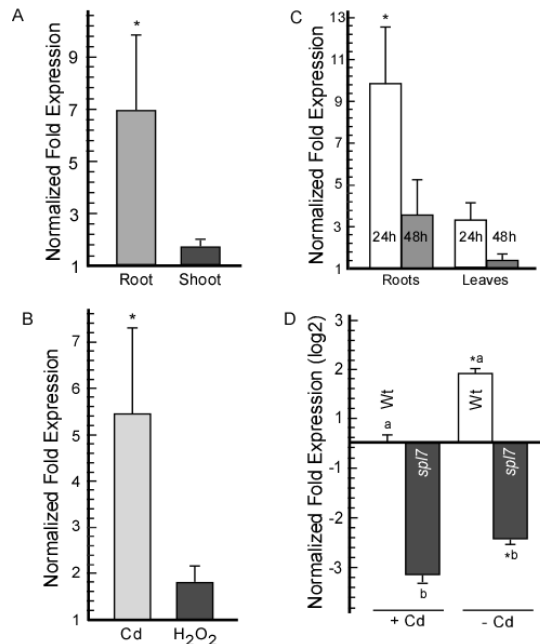


Figure 1. Expression of *CCIT1* is regulated by cadmium (Cd) in the *SPL7*-dependent manner. **A.** Quantitative real-time PCR (qRT-PCR) analysis of the effect of Cd on the expression of *CCIT1* in roots and shoots of *A. thaliana*. Error bars indicate S.E. (n = 4). **B.** qRT-PCR analysis of the effect of Cd and H₂O₂ on the expression of *CCIT1* in roots of *A. thaliana*. Error bars indicate S.E. (n = 4). **C.** qRT-PCR analysis of the effects of Cd on transcript levels of *CCIT1* in roots and rosette leaves of 24-day-old hydroponically-grown plants with vs without 25 µM CdCl₂. Error bars show S.E. (n = 4). **D.** qRT-PCR comparison of the transcript abundance of *CCIT1* in roots of wild-type (Wt) and *spl7-1* (*spl7*) mutant seedlings cultured at control conditions vs. cultured with Cd. Error bars indicate S.E. (n = 4). In A, B and D, plants were germinated and grown vertically for 10 days on 1/2 MS plates under control (0 µM CdCl₂), cadmium-treated (50 µM CdCl₂) or H₂O₂-treated (500 µM H₂O₂) as indicated. Significant statistical differences of the mean values between control (no added Cd or H₂O₂) and treated plants are indicated as * (p ≤ 0.05), different letters indicate significant statistical differences between wild-type and *spl7-1*. Results are presented relative to the expression of genes under control conditions, designated as 1.

I then analyzed the effect of Cd on *CCIT1* expression in mature *A. thaliana*. To do so, I grew plants hydroponically for 24 days and analyzed *CCIT1* transcript abundance in rosette leaves and roots after short-term (24h, 48h) Cd exposure. After 24h Cd treatment, slight chlorosis of leaves was observed; after 48h Cd treatment, leaf veins showed yellowish color and leaves were wilting (Supplemental Figure 1). The qRT-

PCR result showed that *CCIT1* expression was significantly up-regulated in roots and rosette leaves after 24h Cd exposure (Figure 1C). The transcript level of *CCIT1* decreased in both, roots and shoot after 48h of Cd treatment (Figure 1C). The decreased induction might have been resulted from the severe stress caused by prolonged Cd treatment, which overwhelms cell's intrinsic defense system.

It has been shown that increased expression of *CCIT1* in response to copper deficiency in shoots depends on *SPL7* (Yamasaki et al., 2009; Bernal et al., 2012), while in roots and flowers, in part on other transcription regulators (Chapter 2). Here, I sought to determine whether its transcriptional response to Cd toxicity in roots depends on *SPL7* as well. I compared the transcript abundance of *CCIT1* in roots of 10-day-old seedlings of wild-type (Wt) and a T-DNA insertion allele of *SPL7* (*spl7-1*) (Yamasaki et al., 2009), grown under control conditions vs. 50 µM CdCl₂. I found that expression of *CCIT1* was significantly down-regulated in the *spl7-1* mutant grown under standard conditions but its expression was still induced in *spl7* grown with Cd (Figure 1D). These results suggest that *CCIT1* is transcriptionally induced by Cd, which in part depends on *SPL7*.

3.2 *ccit1* Knock-out Alleles are Sensitive to Cadmium Toxicity

To test the role of *CCIT1* in Cd resistance I used two *ccit1* T-DNA insertion lines, designated as *ccit1-1* and *ccit1-2* (Chapter 2). Briefly, T-DNA was inserted in the 1st exon and 3'-UTR of the *CCIT1* gene in *ccit1-1* and *ccit1-2*, respectively. As detailed in Chapter 2, the *ccit1-1* is a null allele since it lacks the detectable *CCIT1* transcript (Chapter 2), and *ccit1-2* is a knock-down allele (Chapter 2). Wild-type and the *ccit1* mutant plants germinated and grew vertically on ½ MS plates with or without Cd for 10 days, root lengths were measured and shoot phenotype was observed. When cultured on ½ MS plates without Cd, the root length of the *ccit1-1* and *ccit1-2* mutants was 1.2 and 1.6 fold shorter than the root length of the wild-type, respectively. When grown on ½ MS plates with Cd, the root length significantly decreased, the root length of the *ccit1-1* and *ccit1-2* mutants are 4 fold shorter than the root length of wild-type (Figure 2A to D), suggesting that *CCIT1* function is essential for root growth under Cd toxicity. In addition to the root elongation defect, shoots from *ccit1-1* and *ccit1-2* were smaller and showed more visually chlorotic

phenotype when compared to shoots of Cd-grown wild-type (Figure 2E). Collectively, the hypersensitivity of *ccit1* mutant to Cd toxicity suggests CCIT1 function is essential for basal Cd resistance in *A. thaliana*.

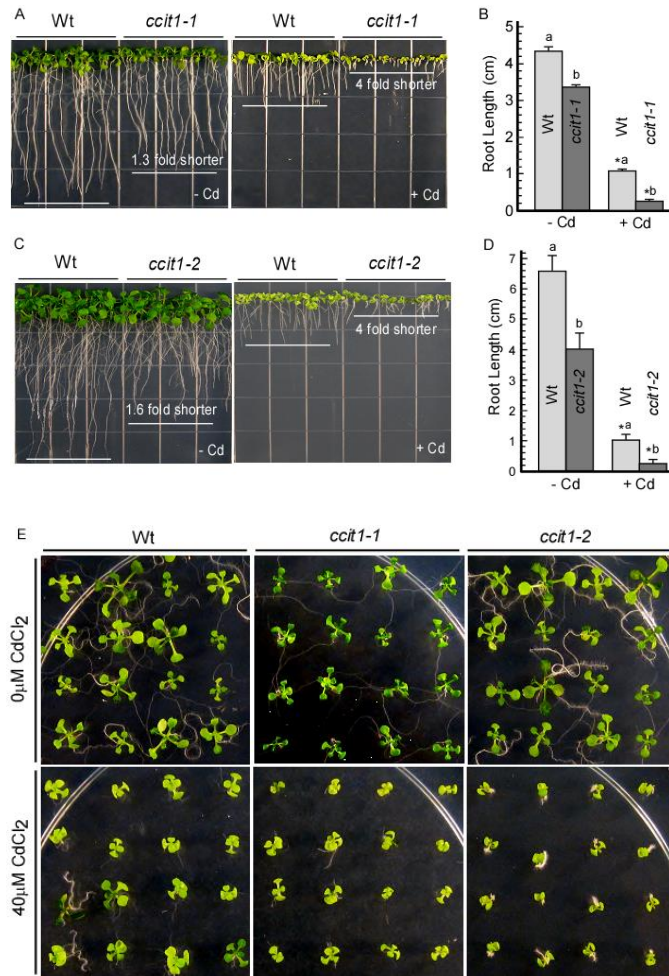


Figure 2. *ccit1* mutant is hypersensitive to Cd toxicity. **A.** Comparison of wild-type (Wt) and the *ccit1-1* seedlings germinated and grown vertically for 10 days on 1/2 MS plates under control (0 μM CdCl₂) and Cd-treated conditions (50 μM CdCl₂). Representative results of at least three biological replicates are shown. **B.** Root length of Wt and *ccit1-1* mutant of plants shown in **A**. **C.** Comparison of wild-type (Wt) and the *ccit1-2* seedlings germinated and grown vertically for 10 days on 1/2 MS plates under control (0 μM CdCl₂) and Cd-treated conditions (50 μM CdCl₂). **D.** Root length of Wt and *ccit1-2* mutant of plants shown in **C**. In **B** and **D**, asterisks (*, $p \leq 0.05$) indicate statistically significant differences in root length between control and Cd-treated condition. Different letters ($p \leq 0.05$) indicate statistically significant difference in root length between wild-type and mutants. **E.** Comparison of Wt, *ccit1-1* and *ccit1-2* seedlings germinated and grown horizontally for 14 days on 1/2 MS plates under control (0 μM CdCl₂) and Cd-treated conditions (40 μM CdCl₂). Representative results of at least three biological replicates are shown.

3.3 The Genomic Fragment of CCIT1 Partially Complements the Hypersensitivity of the *ccit1-1* Mutant to Cd

To examine whether the hypersensitive phenotype of the *ccit1-1* mutant is solely due to the loss of *CCIT1* function, the construct containing the genomic *CCIT1* fragment, encompassing the 1.5 kb region upstream of *CCIT1* and the *CCIT1* gene was transformed into the *ccit1-1* mutant. Three independent one-copy-insertion lines (designated as *CCIT1-1*, *CCIT1-2* and *CCIT1-3*) with similar expression level of *CCIT1* in wild-type (Chapter 2) were selected and subjected to further phenotype analysis. Wild-type and *CCIT1* complementary lines germinated and grew vertically on $\frac{1}{2}$ MS plates with or without Cd for 10 days, and root length and shoot phenotype were observed. When grown on $\frac{1}{2}$ MS plates without Cd, the roots from the *CCIT1-1*, *CCIT1-2* and *CCIT1-3* were at the similar length with the roots from wild-type (Figure 3A-C, E-G). When cultured on Cd-containing medium, the root length from all lines significantly decreased compared to plants grown on plates without Cd, the root length from 3 complemented lines were slightly shorter than the root length of wild-type but longer than the *ccit1-1* mutant under Cd-treated condition (Figure 3A-C, E-G). When grown horizontally on Cd plates to observe the shoot phenotype, *CCIT1-1* showed similar shoot size with wild-type, whereas the other two complementary lines exhibited slightly smaller shoot size (Figure 3D). All of these results indicated that the genomic *CCIT1* fragment partially complements the Cd sensitive phenotype of the *ccit1-1* mutant. The transgenic plants which are ectopically expressing *CCIT1* were also generated, and the expression level of *CCIT1* is higher in these transgenic plants compared to it in wild-type, suggesting they are *CCIT1* overexpression lines (Chapter 2). However, I did not find difference in Cd tolerance between wild-type and overexpression lines (Supplemental figure 2). bHLH family members function as homo- or heterodimers. Whether bHLH heterodimerizes is not known , however inability of overexpressed *CCIT1* to increase Cd tolerance of wild-type plants suggest that it interacting partner is not expressed to the same level as *CCIT1* and so, *CCIT1* is not fully functional.

In this regard it has been shown that overexpression of the regulator of Fe homeostasis, FIT does not produce phenotype unless FIT is co-expressed with its interacting partners (Wu et al., 2012).

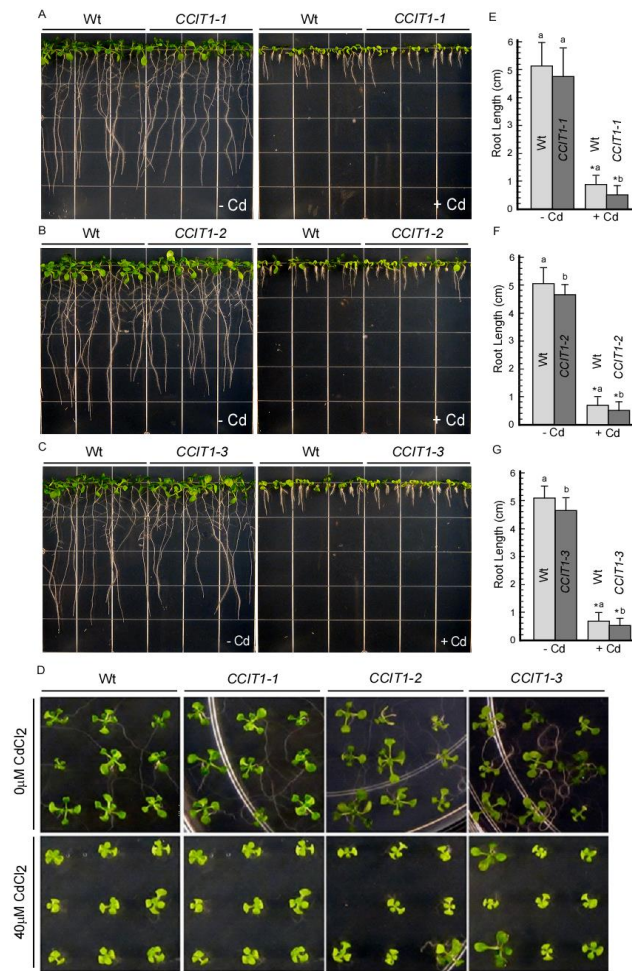


Figure 3. Genomic CCIT1 fragment partially complement the hypersensitivity of the *ccit1-1* mutant to Cd. **A** to **C**. Root length comparison of wild-type (Wt) and 3 complementary lines, designated as *CCIT1-1*, *CCIT1-2* and *CCIT1-3*. Plants were grown vertically for 10 days on 1/2 MS plates under control (0 μ M CdCl₂) or Cd-treated conditions (50 μ M CdCl₂). **D**. Shoot phenotypes of Wt and the *CCIT1* complementary lines. Plants were grown horizontally for 14 days on 1/2 MS plates under control (0 μ M CdCl₂) or Cd-treated conditions (40 μ M CdCl₂). **E** to **G**. Root length measurements for Wt and *CCIT1-1* to -3 plants shown in **A** to **C**. Asterisks (*, $p \leq 0.05$) indicate statistically significant differences in root length between control and Cd-treated condition. Different letters ($p \leq 0.05$) indicate statistically significant difference in root length between wild-type and the complemented lines.

3.4 *ccit1* Mutant Accumulates High Cd in Shoots and has Defect in Cu Accumulation

To examine whether the hypersensitivity of the *ccit1* mutant allele to Cd is associated with altered Cd accumulation, Cd concentration was measured in shoots of wild-type, *ccit1-1* and the *CCIT1* complemented line (*CCIT1-1*) which were grown hydroponically with 25 μ M CdCl₂. The result showed that *ccit1* mutant

accumulates significantly higher Cd in its shoots, compared to wild-type and *CCIT1-1* (Figure 4A), suggesting the hypersensitivity of *ccit1-1* is resulted from more Cd accumulated in its shoots. The recent studies from our lab have shown that Cd stimulates Cu

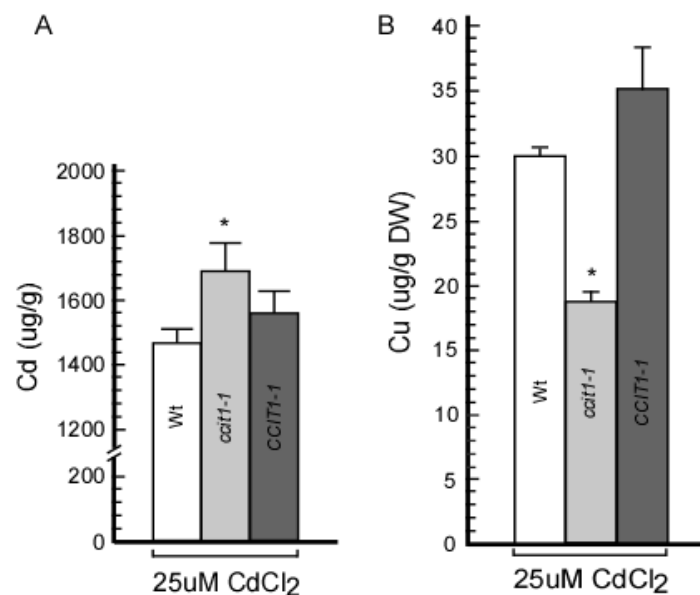


Figure 4. *ccit1-1* contains higher Cd in shoots and lower Cu in roots compared to wild-type. Wild-type (Wt), the *ccit1-1* mutant, *CCIT1* complemented line (*CCIT1-1*) were grown in standard hydroponic solution (0 μM CdCl₂) for 4 weeks, and subject to 25 μM CdCl₂ treatment for 2 days, roots and shoots were harvested for ICP-MS analysis of Cu and Cd concentration, respectively. Asterisks (*, $p \leq 0.05$) indicate statistically significant differences from wild-type (Wt). Error bars indicate S.E (n=5).

uptake in roots in a SPL7-dependant manner and that the SPL7-dependant Cu uptake and reallocation among Cu-requiring functions are essential for basal Cd resistance in *A. thaliana* (Gayomba et al., 2013). My studies described in Chapter 2 show that CCIT1 functions in the interactive pathway with SPL7 in mediating Cu uptake under Cu deficient conditions. Further, I found that Cd promotes CCIT1 expression in part via SPL7 (Figure 1D). To further investigate whether CCIT1- mediated Cu uptake is involved in the response of *A. thaliana* to Cd toxicity, I measured Cu concentrations in roots of wild-type, the *ccit1-1* mutant, the *CCIT1* complemented line which grown in hydroponic solution with 25 μM CdCl₂. I found that Cu concentrations in roots of the *ccit1-1* mutant were much lower than in corresponding tissues of the wild-type and *CCIT1-1* (Figure 4B). Given that Cu is essential for basal Cd resistance, it is possible that the decreased ability of the *ccit1-1* in Cu accumulation results in compromised Cd tolerance in the *ccit1* mutant.

3.5 Cadmium Toxicity Affects the Expression Pattern of *CCIT1* in *A. thaliana*

As I described in Chapter 2, analyses of the tissue-specificity of *CCIT1* expression using transgenic plants expressing *CCIT1pro-GUS* construct identified *CCIT1pro* activity mainly in roots, leaves and anthers of flowers in response to Cu deficiency (Chapter 2). Here I analyzed the effect of Cd on tissues-localization of *CCIT1*. To do so, I used three transgenic lines that exhibited a similar pattern of GUS activity (Figure 5A). Consistent with observations presented in Chapter 2, histochemical analysis of *CCIT1pro* activity in 10-day-old plants grown under standard $\frac{1}{2}$ MS medium revealed almost no GUS staining (Figure 5A). The intensity of staining dramatically increased in root-to-hypocotyl junction, primary and secondary roots but not in roots tips of seedlings grown on Cd (Figure 5A). Consistent with qRT-PCR analyses (Figure 1A), shoots of 10-day old seedlings did not exhibit obvious GUS activity under these conditions (Figure 5A). These results suggest that roots of young seedlings are the primary sites of *CCIT1* activity. Increased *CCIT1pro* activity in roots of Cd-treated plants was also observed in transgenic plants expressing the *CCIT1pro-GFP* construct (Figure 5B). The GFP signal was significantly induced by Cd treatment in root meristem and elongation zone from all 3 independent transgenic lines (Figure 5B). Given that Cu deficiency and Cd toxicity induce *CCIT1* expression in the root (Figure 1 A and C), Cd toxicity induced Cu accumulation is impaired in *ccit1* mutant (Figure 4B), and that CCIT1 localizes to the nucleus (Chapter 2), it is possible that CCIT1 is primarily involved in regulating Cu uptake transporters in roots under Cd toxicity.

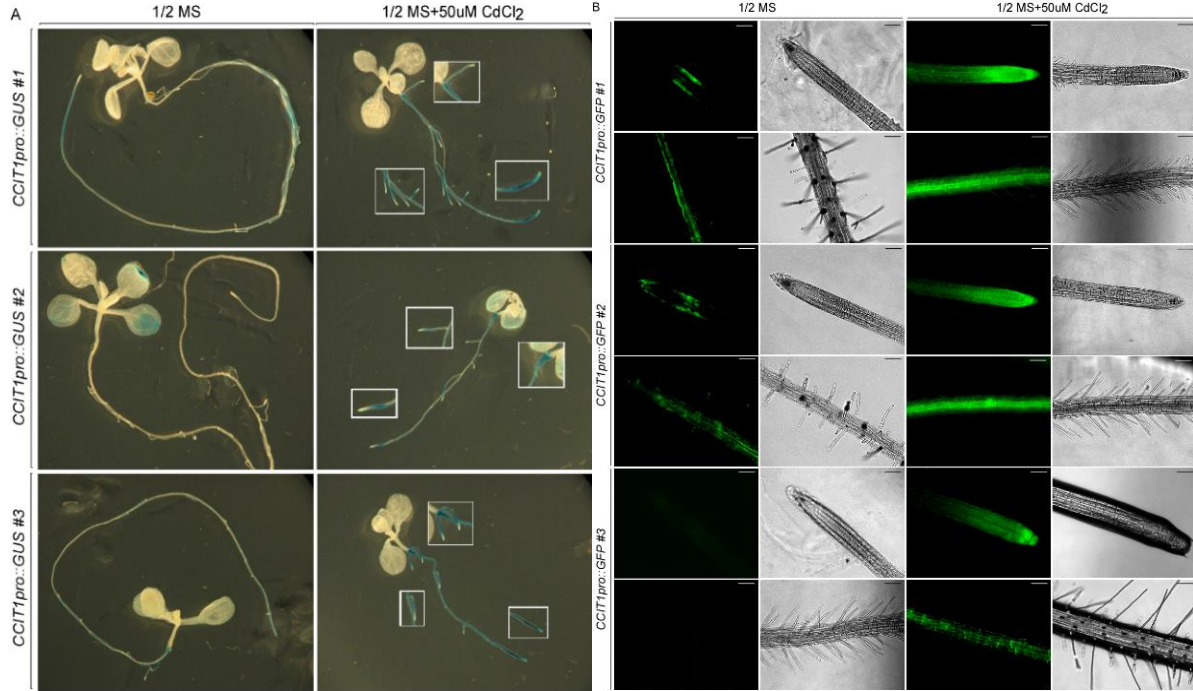


Figure 5. The expression pattern of CCIT1 in *A. thaliana*. **A.** Histochemical analysis of the expression pattern of CCIT1 in 10-day-old *A. thaliana* seedlings with the CCIT1pro-GUS construct grown on 1/2 MS with or without 50 μM Cd. Three independent lines transformed with CCIT1pro-GUS construct are showed in this figure. GUS activity was low under 0 μM CdCl₂, however, was significantly induced by 50 μM CdCl₂ treatment, and mainly exhibited at primary and lateral roots, whereas was not observed at root tips. **B.** Expression pattern of CCIT1 in 10-day-old *A. thaliana* roots with the CCIT1pro-GFP construct grown on 1/2 MS with or without 50 μM Cd. 3 independent lines transformed with CCIT1pro-GFP construct are showed in this figure. GFP under control of CCIT1pro was low under 0 μM CdCl₂, however, was significantly induced by 50 μM CdCl₂ treatment. Scale bar = 20 μm.

3.6 The Effect of Cadmium on the Expression of COPT2 Depends, in part, on CCIT1

Studies by Gayomba et al 2013 have shown that Cd upregulates expression of genes encoding Cu transporters, *COPT1*, *COPT2* and *COPT6* and that this result depends mainly on SPL7. Here, I tested whether the effect of Cd on their expression also depends on CCIT1. I found that although expression of *COPT6* was not altered in the *ccit1-1* mutant, the transcriptional response of *COPT1* to Cd was fully dependent of CCIT1 (Figure 6). I also found that *COPT2* was still upregulated by Cd toxicity in the *ccit1-1* mutant, although its transcript level was significantly lower in *ccit1-1* regardless of Cd treatment (Figure 6). Taken together these results suggest that the transcriptional response of *COPT1* and *COPT2* elicited by Cd, in part, depends on CCIT1.

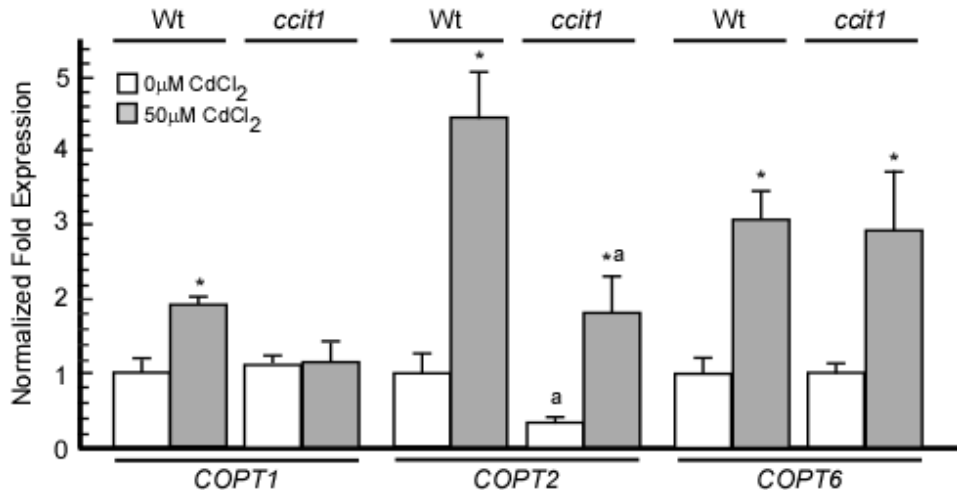


Figure 6. The transcriptional response of *COPT2* to Cd toxicity depends, in part, on CCIT1. qRT-PCR comparison of the transcript abundance of *COPT1*, *COPT2* and *COPT6* in roots of wild-type (Wt) and *ccit1-1* (*ccit1*) seedlings grown on solid ½ MS media for 10 days without (white bar) vs. with 50 μ M CdCl₂ (gray bar). Error bars indicate S.E. (n = 6). Results are presented relative to the expression of genes in Wt plants grown on solid ½MS media without Cd, which were designated as 1. Asterisks (*, p < 0.05) indicate statistically significant differences in gene expression between control and Cd-treated plants, a letter “a” indicates statistically significant differences in gene expression between Wt and *ccit1-1* plants.

4. DISCUSSION

This chapter addresses the function of CCIT1, a transcription factor from the bHLH family that I identified during my PhD as being transcriptionally upregulated by Cd toxicity and Cu deficiency. I found that the expression level of *CCIT1* is upregulated by Cd in roots but not in shoots of 10-day-old seedling and 4-week-old mature plants grown hydroponically (Figure 1A and C), suggesting that CCIT1 functions specifically in roots. In addition, we found that Cd, but not H₂O₂, induces the transcript abundance of *CCIT1* in roots (Figure 1B), indicating that the induction of *CCIT1* is specific to Cd toxicity but not to the oxidative stress triggered by Cd. The histochemical analysis of *CCIT1pro-GUS* and the microscopic observation of *CCIT1pro-GFP* revealed that the expression of *CCIT1* in roots significantly increases under Cd treatment (Figure 5), which validated the results of qRT-PCR presented in Figure 1. Further, it showed in our qRT-PCR result that the increased transcript abundance of *CCIT1* in response to Cd partially depends on SPL7 (Figure 1D). Therefore, it's prompting to hypothesize that other transcription factors may also be involved in the transcriptional response of *CCIT1* to Cd, such as AREB3, ATHB2 and bZIP53 that have been found

in chapter 3 to function as upstream regulators for CCIT1. However, the roles of these three genes in Cd detoxification needs to be further investigated.

SPL7 has been previously shown to regulate the Cu uptake and reallocation in response to Cd (Gayomba et al., 2013). Given that, CCIT1 could function as a second transcription factor that acts downstream to SPL7 in Cu uptake and reallocation triggered by Cd. According to the RNA-seq analysis in chapter 2, it's likely that the components in Cu uptake system are under regulation of CCIT1 in response to Cd, since several genes were downregulated in *ccit1-1* mutant (Chapter 2). However, it's unlikely that CCIT1 regulates the genes that are involved in Cu reallocation, such as *CSD1/2* and *FSD1*, since they were not found as targets in RNA-seq analysis (Chapter 2). We later examine whether *miR398*, *CSD1/2* and *FSD1* are targets of CCIT1 by qRT-PCR, and the result is consistent with our hypothesis that the expression of these genes did not change in the *ccit1-1* mutant (data not shown).

The phenotypic analysis using *ccit1-1*, *ccit1-2* mutants and the complemented lines showed that the *ccit1* mutants are more sensitive to Cd toxicity compared to wild-type and show significantly shorter root length and smaller shoot size (Figure 2A to E). The transgenic lines bearing the genomic fragment of *CCIT1* partially complemented the hypersensitivity of the mutant to Cd (Figure 3A to G), indicating that loss of *CCIT1* function impairs Cd resistance in *A. thaliana*. Ectopically expressed *CCIT1* did not improve Cd tolerance. It is noteworthy that members of the bHLH family must homo- or heterodimerise in order to bind to DNA to regulate gene expression. Whether bHLH heterodimerizes is not known, however inability of overexpressed *CCIT1* to increase Cd tolerance of wild-type plants suggest that its interacting partner is not expressed to the same level as *CCIT1* and so, CCIT1 cannot fully realize its capability to regulate gene expression. Similar phenomenon was observed in studies of one of the key regulator of Fe homeostasis, FIT (Wu et al., 2012). It has been shown that overexpression of the regulator of Fe homeostasis, FIT does not produce phenotype unless FIT is co-expressed with its interacting partners (Wu et al., 2012).

Metal concentration analysis revealed that the Cd accumulated in shoots of the *ccit1* mutant plants are significantly higher than wild-type (Figure 4) provides evidence for the connection between the hypersensitivity to Cd that was observed in the *ccit1-1* mutant and indicates that CCIT1 may be involved

in Cd sequestration in roots. The *CCIT1-1* complemented line completely reverts the increased Cd accumulation in shoots, indicating the higher Cd in the *ccit1-1* mutant is solely due to loss of CCIT1 function (Figure 4).

I also found that the concentration of Cu in roots of the *ccit1* mutant is significantly reduced compared to wild-type, the *CCIT1-1* complemented line (Figure 4), indicating that *ccit1-1* mutant has a defect in Cu uptake and accumulation, which has been reported as an essential basal Cd tolerance response (Gayomba et al., 2013; Carrio-Segui et al., 2015). We have shown previously that Cd stimulates Cu uptake into *A. thaliana* roots and increases mRNA abundance of genes encoding plasma membrane-localized Cu uptake transporters of the CTR-COPT family, *COPT1*, *COPT2* and *COPT6*, suggesting that Cu accumulation through these transporters might be an essential component of Cd resistance (Gayomba et al., 2013). Gayomba et al 2013 showed that this transcriptional response depends on SPL7. Here, I also describe the upregulation of *COPT1*, 2 and 6 by Cd toxicity (Figure 6). In contrast, recent findings by Carrio-Segui et al. 2015 show that transcript abundance of *COPT1* and 2 is reduced under Cd treatment, and of *COPT6* remains unaffected (Carrio-Segui et al., 2015). I note that Carrio-Segui et al 2015 did not separate root and shoot tissues but instead used the whole 7-day-old seedlings. Our data clearly indicate the transcriptional response of these genes to Cd is mainly in root tissues. Further, increased transcript abundance of genes encoding Cu transporters also explains enhanced Cu accumulation of roots of Cd-treated plants.

Further analyses of transcript abundance of *COPT* genes in the *ccit1-1* mutant showed that *COPT2* is downregulated in the *ccit1-1* mutant under both control and Cd-treated conditions, and the induction of *COPT1* under Cd treated condition was impaired in the *ccit1-1* mutant (Figure 6). This result suggests that *CCIT1* is also an upstream regulator of *COPT1* and *COPT2* in addition to SPL7, and the reduced Cu accumulation in roots of the *ccit1-1* mutant may result from the decreased transcript abundance of *COPT1* and *COPT2*. Their loss of function might be compensated by *COPT6* in the *ccit1-1* mutant (Figure 6).

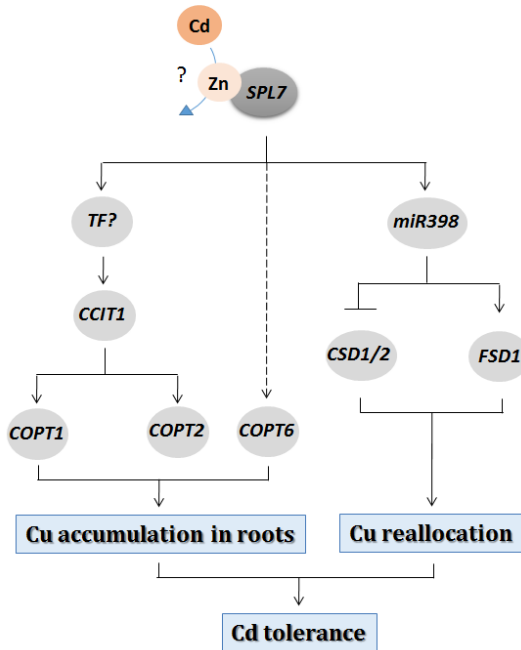


Figure 7. The model depicting the role of CCIT1 in Cd induced transcriptional regulation. Cd elicits SPL7-dependent transcriptional upregulation of Cu transporters, and this response partially depend on CCIT1. Under Cd toxicity, it's possible that Cd displaces the putative metal cofactor of SPL7, Zn, therefore mimics the Cu deficiency response. Zn is a cofactor of SBP domain of the SPL7 orthologue in *Chlamydomonas*, CRR1 (Cu Responsive Regulator), and its function is essential for the binding capacity of SBP domain to Cu responsive elements (Kropat et al., 2005; Sommer et al., 2010). This displacement of Zn by Cd then results in *miR398*-mediated Cu reallocation, upregulation of *COPT1* and *COPT2* via CCIT1 and induction of *COPT6*. Cu uptake from roots is induced to promote Cu uptake possibly to protect essential Cu-proteins. In addition to this scenario, it is also possible that Cd displaced Cu from its binding sites and is sensed as Cu deficiency, which in turn activates SPL7-dependent Cu responsive pathway, including the upregulation of Cu transporters, in which partially depends on CCIT1. This model is modified from (Gayomba et al., 2013) to reflect new findings described in this section.

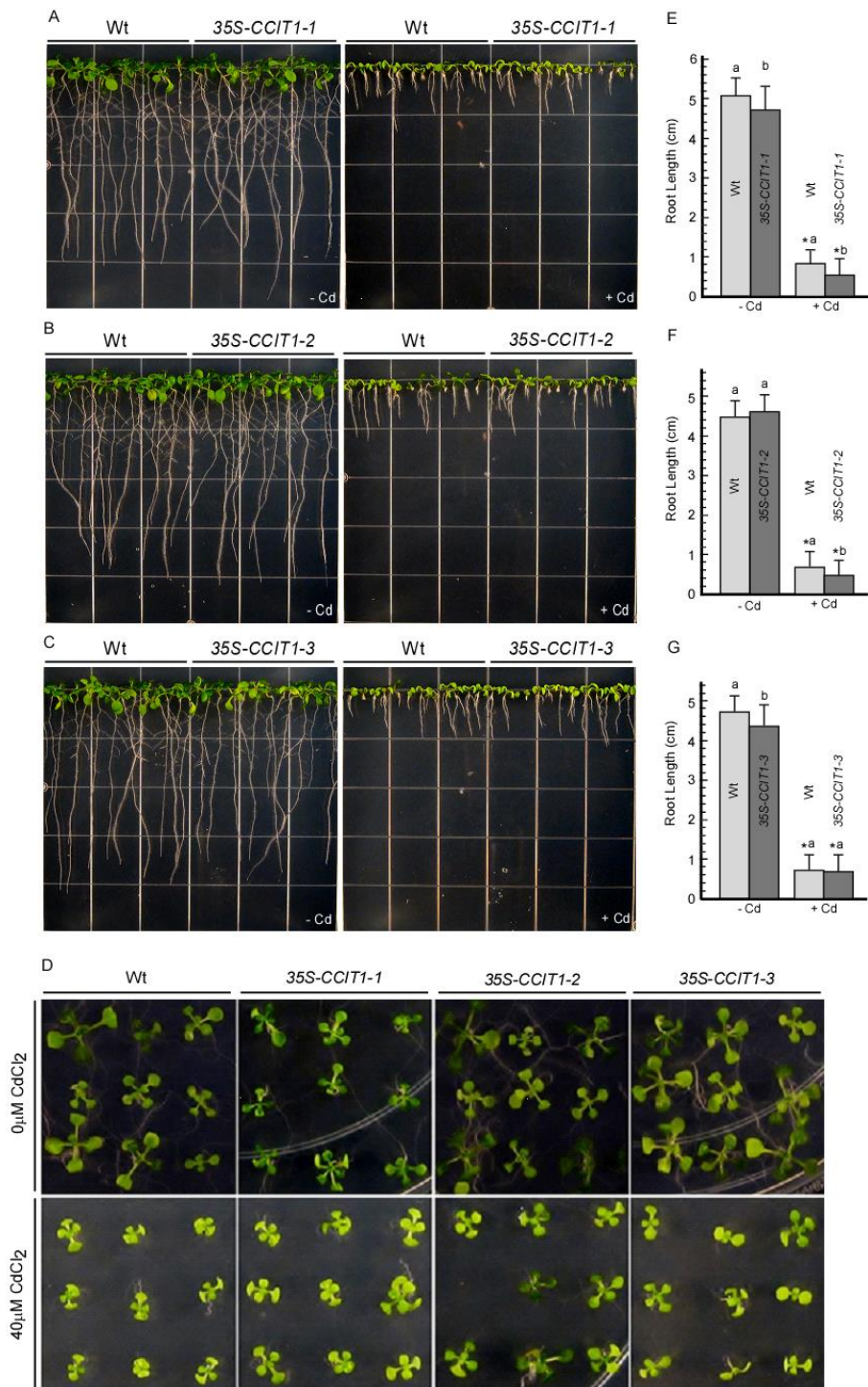
To conclude, data presented in this chapter expand our previous findings of the requirements of Cu homeostasis for Cd resistance by including a novel regulator, CCIT1. Based on the presented data, I propose, that Cd induces the SPL7-CCIT1 interactive pathway to stimulate Cu uptake for conferring basal Cd resistance in *A. thaliana* (Figure 7). As we proposed previously (Gayomba et al., 2013), Cd stimulates the SPL7-dependent components of Cu homeostasis either by interacting directly with SPL7 or by displacing Cu from its binding sites which in turn mimics Cu deficiency (Figure 7). SPL7 then upregulates Cu transporters directly or indirectly to trigger Cu uptake and accumulation in roots. CCIT1 regulates *COPT1* and *COPT2* expression, in part acting as a downstream target of SPL7. Given that transcriptional response

of *CCIT1* to Cd in roots, in part is independent on SPL7 (Figure 1D), it is also possible that other factors regulate the response of *CCIT1* to Cd toxicity to initiate the CCIT1-dependant components of basal Cd resistance in *A. thaliana*.

5. SUPPLEMENTAL DATA



Supplemental Figure 1. The phenotype of wild-type plants after Cd treatment. Wild-type plants were grown in standard hydroponic solution for 4 weeks before subject to Cd treatment. After 4 weeks, 25 μM CdCl_2 was added to the solution, and the plants were grown for another one or two days. After 2 days Cd treatment, plants showed an overall yellowish color in rosette leaves and started to wilt.



Supplemental Figure 2. Ectopic expression of *CCIT1* does not improve Cd tolerance of wild-type *A. thaliana*. **A** to **C**. Indicated plant lines were grown vertically for 10 days on 1/2 MS plates under control (0 μ M CdCl₂) or Cd-treated conditions (50 μ M CdCl₂). **D**. Shoot phenotype comparison of wild-type (Wt) and overexpression lines. Plants were grown horizontally for 14 days on 1/2 MS plates under control (0 μ M CdCl₂) or Cd-treated conditions (40 μ M CdCl₂). **E** to **G**. Root length of Wt and 35S-CCIT1-1 to -3 plants shown in **A** to **C**. Asterisks (*, $p \leq 0.05$) indicate statistically significant differences in root length between control and Cd-treated condition. Different letters ($p \leq 0.05$) indicate statistically significant difference in root length between wild-type and the overexpression lines.

Supplemental table 1. Primers used in this study		
Primers used for genotyping		
Primer	Gene	Primer sequence (5' to 3')
LB_1.3 for sail line	<i>T-DNA</i>	ATTTGCCGATTCGGAAC
LB_1 for sail line	<i>T-DNA</i>	GCCTTTCAGAAATGGATAAAATGCCTGCTCC
SALK_073160 LP	<i>CCIT1</i>	GTTAGCGCCATTGTACTGC
SALK_073160 RP	<i>CCIT1</i>	CAATTCAAGAACCGAGATTGC
SAIL_711_B07 LP	<i>CCIT1</i>	TATTCTTTGGAGCCGTGTTG
SAIL_711_B07 RP	<i>CCIT1</i>	TGTTAGGGTCCAAGTCATGG
SALK_093849 LP	<i>SPL7</i>	TTGAAATTCAAGCTGATTG
SALK_093849 RP	<i>SPL7</i>	TCCACCTGTCAAAACCAAGAC
Primers used for cloning		
Primer	Gene	Primer sequence (5' to 3')
attB1-CCIT1-F	<i>CCIT1</i>	ggggacaagttgtacaaaaaaggcggcttaccATGTCTCTAACCGAATCATCAGAC
attB2-CCIT1-R (w/stop)	<i>CCIT1</i>	ggggaccacttgtacagaaggctgggtcTTTGCACTTGTGTTGTCACGAAGC
attB2-CCIT1-R (w/o stop)	<i>CCIT1</i>	ggggaccacttgtacaaaggctgggtcTCATTGCACTTGTGTTGTCACGAAG
attB1-CCIT1pro-F	<i>CCIT1pro</i>	ggggacaagttgtacaaaaaaggcggcttaccTGAAGAGTATGTCACAGAGAGGTAG
attB2-CCIT1pro-R	<i>CCIT1pro</i>	ggggaccacttgtacagaaggctgggtcATATATACGACGGCAAGAGGAACAA
Primers used in qRT-PCR		
Primer	Gene	Primer sequence (5' to 3')
Actin-F	<i>Actin</i>	GACCTTAACCTCCCGCTA
Actin-R	<i>Actin</i>	GGAAGAGAGAACCCCTCGTA
CCIT1-F	<i>CCIT1</i>	ACGAGGTCTCTATTGAGCA
CCIT1-R	<i>CCIT1</i>	ACCCTTGCTCTCGGCAAACCT
COPT1-F	<i>COPT1</i>	CATGTCGTTAACGCCGGTGTGTT
COPT1-R	<i>COPT1</i>	CCGGAAAGTTGGCTTCCGAACAA
COPT2-F	<i>COPT2</i>	TGGTGATGCTCGCTGTTATGTCCT
COPT2-R	<i>COPT2</i>	TCTGGTCATCGGAGGGTTCTGA
COPT6-F	<i>COPT6</i>	ACACTCAAGACAGGCCCT
COPT6-R	<i>COPT6</i>	CGAAGAGCATGAAACCCAC

REFERENCE

- Alonso, J.M., Stepanova, A.N., Leisse, T.J., Kim, C.J., Chen, H., Shinn, P., Stevenson, D.K., Zimmerman, J., Barajas, P., Cheuk, R., Gadrinab, C., Heller, C., Jeske, A., Koesema, E., Meyers, C.C., Parker, H., Prednis, L., Ansari, Y., Choy, N., Deen, H., Geralt, M., Hazari, N., Hom, E., Karnes, M., Mulholland, C., Ndubaku, R., Schmidt, I., Guzman, P., Aguilar-Henonin, L., Schmid, M., Weigel, D., Carter, D.E., Marchand, T., Risseeuw, E., Brogden, D., Zeko, A., Crosby, W.L., Berry, C.C., and Ecker, J.R.** (2003). Genome-wide insertional mutagenesis of *Arabidopsis thaliana*. *Science* **301**, 653-657.
- Arteca, R.N., and Arteca, J.M.** (2000). A novel method for growing *Arabidopsis thaliana* plants hydroponically. *Physiol Plantarum* **108**, 188-193.
- Bernal, M., Casero, D., Singh, V., Wilson, G.T., Grande, A., Yang, H., Dodani, S.C., Pellegrini, M., Huijser, P., Connolly, E.L., Merchant, S.S., and Kramer, U.** (2012). Transcriptome sequencing identifies SPL7-regulated copper acquisition genes FRO4/FRO5 and the copper dependence of iron homeostasis in *Arabidopsis*. *The Plant cell* **24**, 738-761.
- Carrio-Segui, A., Garcia-Molina, A., Sanz, A., and Penarrubia, L.** (2015). Defective copper transport in the copt5 mutant affects cadmium tolerance. *Plant & cell physiology* **56**, 442-454.
- Chung, S.M., Frankman, E.L., and Tzfira, T.** (2005). A versatile vector system for multiple gene expression in plants. *Trends in plant science* **10**, 357-361.
- Clemens, S.** (2006a). Toxic metal accumulation, responses to exposure and mechanisms of tolerance in plants. *Biochimie* **88**, 1707-1719.
- Clemens, S.** (2006b). Toxic metal accumulation, responses to exposure and mechanisms of tolerance in plants. *Biochimie* **88**, 1707-1719.
- Clemens, S., Antosiewicz, D.M., Ward, J.M., Schachtman, D.P., and Schroeder, J.I.** (1998). The plant cDNA LCT1 mediates the uptake of calcium and cadmium in yeast. *Proceedings of the National Academy of Sciences of the United States of America* **95**, 12043-12048.
- Clough, S.J., and Bent, A.F.** (1998). Floral dip: a simplified method for Agrobacterium-mediated transformation of *Arabidopsis thaliana*. *Plant Journal* **16**, 735-743.
- Cohen, C.K., Fox, T.C., Garvin, D.F., and Kochian, L.V.** (1998). The role of iron-deficiency stress responses in stimulating heavy-metal transport in plants. *Plant Physiol* **116**, 1063-1072.
- Connolly, E.L., Fett, J.P., and Guerinot, M.L.** (2002). Expression of the IRT1 Metal Transporter Is Controlled by Metals at the Levels of Transcript and Protein Accumulation. *The Plant cell* **14**, 1347-1357.
- Das, P., Samantaray, S., and Rout, G.R.** (1997). Studies on cadmium toxicity in plants: a review. *Environmental pollution* **98**, 29-36.
- Deplancke, B., Vermeirssen, V., Arda, H.E., Martinez, N.J., and Walhout, A.J.** (2006). Gateway-compatible yeast one-hybrid screens. *CSH protocols* **2006**.
- Earley, K.W., Haag, J.R., Pontes, O., Opper, K., Juehne, T., Song, K., and Pikaard, C.S.** (2006a). Gateway-compatible vectors for plant functional genomics and proteomics. *The Plant Journal* **45**, 616-629.
- Earley, K.W., Haag, J.R., Pontes, O., Opper, K., Juehne, T., Song, K.M., and Pikaard, C.S.** (2006b). Gateway-compatible vectors for plant functional genomics and proteomics. *Plant Journal* **45**, 616-629.
- Eide, D., Broderius, M., Fett, J., and Guerinot, M.** (1996a). A novel iron regulated metal transporter from plants identified by functional expression in yeast. *Proc Natl Acad Sci USA* **93**, 5624 - 5628.
- Eide, D., Broderius, M., Fett, J., and Guerinot, M.L.** (1996b). A novel iron-regulated metal transporter from plants identified by functional expression in yeast. *Proceedings of the National Academy of Sciences of the United States of America* **93**, 5624-5628.
- Gayomba, S.R., Jung, H.I., Yan, J., Danku, J., Rutzke, M.A., Bernal, M., Kramer, U., Kochian, L.V., Salt, D.E., and Vatamaniuk, O.K.** (2013). The CTR/COPT-dependent copper uptake and SPL7-

- dependent copper deficiency responses are required for basal cadmium tolerance in *A. thaliana*. *Metalomics* **5**, 1262-1275.
- Gong, J.M., Lee, D.A., and Schroeder, J.I.** (2003). Long-distance root-to-shoot transport of phytochelatins and cadmium in *Arabidopsis*. *Proc Natl Acad Sci U S A* **100**, 10118-10123.
- Hasan, S.A., Fariduddin, Q., Ali, B., Hayat, S., and Ahmad, A.** (2009). Cadmium: toxicity and tolerance in plants. *Journal of environmental biology / Academy of Environmental Biology, India* **30**, 165-174.
- Jefferson, R.A., Kavanagh, T.A., and Bevan, M.W.** (1987). GUS fusions: beta-glucuronidase as a sensitive and versatile gene fusion marker in higher plants. *The EMBO journal* **6**, 3901-3907.
- Kropat, J., Tottey, S., Birkenbihl, R.P., Depage, N., Huijser, P., and Merchant, S.** (2005). A regulator of nutritional copper signaling in *Chlamydomonas* is an SBP domain protein that recognizes the GTAC core of copper response element. *Proceedings of the National Academy of Sciences of the United States of America* **102**, 18730-18735.
- Kupper, H., and Kochian, L.V.** (2010). Transcriptional regulation of metal transport genes and mineral nutrition during acclimatization to cadmium and zinc in the Cd/Zn hyperaccumulator, *Thlaspi caerulescens* (*Ganges* population). *The New phytologist* **185**, 114-129.
- Mitsuda, N., Ikeda, M., Takada, S., Takiguchi, Y., Kondou, Y., Yoshizumi, T., Fujita, M., Shinozaki, K., Matsui, M., and Ohme-Takagi, M.** (2010). Efficient yeast one-/two-hybrid screening using a library composed only of transcription factors in *Arabidopsis thaliana*. *Plant & cell physiology* **51**, 2145-2151.
- Murashige, T., and Skoog, F.** (1962). A Revised Medium for Rapid Growth and Bio Assays with Tobacco Tissue Cultures. *Physiol Plantarum* **15**, 473-497.
- Robinson, N.J., Procter, C.M., Connolly, E.L., and Guerinot, M.L.** (1999). A ferric-chelate reductase for iron uptake from soils. *Nature* **397**, 694-697.
- Sasaki, A., Yamaji, N., Yokosho, K., and Ma, J.F.** (2012). Nramp5 Is a Major Transporter Responsible for Manganese and Cadmium Uptake in Rice. *The Plant Cell Online* **24**, 2155-2167.
- Sommer, F., Kropat, J., Malasarn, D., Grossoehm, N.E., Chen, X., Giedroc, D.P., and Merchant, S.S.** (2010). The CRR1 Nutritional Copper Sensor in *Chlamydomonas* Contains Two Distinct Metal-Responsive Domains. *The Plant Cell Online* **22**, 4098-4113.
- Song, W.Y., Park, J., Mendoza-Cozatl, D.G., Suter-Grottemeyer, M., Shim, D., Hortensteiner, S., Geisler, M., Weder, B., Rea, P.A., Rentsch, D., Schroeder, J.I., Lee, Y., and Martinoia, E.** (2010). Arsenic tolerance in *Arabidopsis* is mediated by two ABCC-type phytochelatin transporters. *Proc Natl Acad Sci U S A* **107**, 21187-21192.
- Stadtman, E.R.** (1990). Metal ion-catalyzed oxidation of proteins: biochemical mechanism and biological consequences. *Free Radic Biol Med* **9**, 315-325.
- Udvardi, M.K., Czechowski, T., and Scheible, W.R.** (2008). Eleven golden rules of quantitative RT-PCR. *Plant Cell* **20**, 1736-1737.
- Valko, M., Morris, H., and Cronin, M.T.** (2005). Metals, toxicity and oxidative stress. *Curr Med Chem* **12**, 1161-1208.
- Vatamaniuk, O.K., Mari, S., Lu, Y.P., and Rea, P.A.** (2000). Mechanism of heavy metal ion activation of phytochelatin (PC) synthase: blocked thiols are sufficient for PC synthase-catalyzed transpeptidation of glutathione and related thiol peptides. *The Journal of biological chemistry* **275**, 31451-31459.
- Vatamaniuk, O.K., Mari, S., Lang, A., Chalasani, S., Demkiv, L.O., and Rea, P.A.** (2004). Phytochelatin synthase, a dipeptidyltransferase that undergoes multisite acylation with gamma-glutamylcysteine during catalysis: stoichiometric and site-directed mutagenic analysis of *arabidopsis thaliana* PCS1-catalyzed phytochelatin synthesis. *The Journal of biological chemistry* **279**, 22449-22460.
- Vert, G., Grotz, N., Dedaldechamp, F., Gaymard, F., Guerinot, M.L., Briat, J.-F., and Curie, C.** (2002). IRT1, an *Arabidopsis* Transporter Essential for Iron Uptake from the Soil and for Plant Growth. *The Plant cell* **14**, 1223-1233.

- Wu, H., Chen, C., Du, J., Liu, H., Cui, Y., Zhang, Y., He, Y., Wang, Y., Chu, C., Feng, Z., Li, J., and Ling, H.-Q.** (2012). Co-Overexpression FIT with AtbHLH38 or AtbHLH39 in Arabidopsis-Enhanced Cadmium Tolerance via Increased Cadmium Sequestration in Roots and Improved Iron Homeostasis of Shoots. *Plant physiology* **158**, 790-800.
- Yamasaki, H., Hayashi, M., Fukazawa, M., Kobayashi, Y., and Shikanai, T.** (2009). SQUAMOSA Promoter Binding Protein-Like7 Is a Central Regulator for Copper Homeostasis in Arabidopsis. *Plant Cell* **21**, 347-361.
- Zhai, Z., Gayomba, S.R., Jung, H.I., Vimalakumari, N.K., Pineros, M., Craft, E., Rutzke, M.A., Danku, J., Lahner, B., Punshon, T., Guerinot, M.L., Salt, D.E., Kochian, L.V., and Vatamaniuk, O.K.** (2014). OPT3 Is a Phloem-Specific Iron Transporter That Is Essential for Systemic Iron Signaling and Redistribution of Iron and Cadmium in Arabidopsis. *The Plant cell* **26**, 2249-2264.
- Zimeri, A.M., Dhankher, O.P., McCaig, B., and Meagher, R.B.** (2005). The plant MT1 metallothioneins are stabilized by binding cadmiums and are required for cadmium tolerance and accumulation. *Plant molecular biology* **58**, 839-855.

CONCLUSIONS

The knowledge of Cu uptake, intracellular trafficking, root-to-shoot translocation, miRNA-dependent intracellular Cu reallocation has widely expanded in recent years, however, SPL7 so far is still the only transcription factor with a documented role in regulating the transcriptional network in response to Cu availability. The work described herein identifies a novel transcription factor, CCIT1 that is essential for the transcriptional regulatory network of Cu homeostasis. Disruption of CCIT1 leads to hypersensitivity to Cu deficiency, reduced Cu accumulation in roots and shoots and impaired transcriptional response to low Cu. Loss of function of both SPL7 and CCIT1 causes seedling lethal which can be rescued by Cu. However, the double *ccit1spl7* mutant still shows severe male sterility and seed setting failure. The transcriptome comparison between wild-type, *ccit1* and *spl7* in roots revealed that genes that are induced by low Cu and involved in Cu uptake and partitioning is impaired in *ccit1* mutant. In addition, the transcriptome comparison in shoots and flowers found the enrichment of the transcriptional changes in the genes involved in jasmonic acid biosynthetic pathway caused by mutation of either *SPL7* and *CCIT1*. And this finding provides essential molecular evidence for the connection between Cu and plant fertility, since JA is critical for male fertility. It has been known for decades that Cu is required for seed setting, however, the mechanism underlying this observation remains elusive. The findings in this dissertation expands our knowledge of the diverse roles of Cu in plant growth and development and fills the gaps between the observed seed set reduction by low Cu and the underlying molecular mechanism. Further work of examine the exact roles of CCIT1, SPL7 and their targets in the interaction between Cu, JA and pollen viability will be essential for connecting the metal homeostasis, phytohormone signaling and plant fertility.

CCIT1 has been reported as a downstream target of SPL7. However, the distinguish phenotype of *ccit1spl7* from the single mutants and the induction of CCIT1 in response to low Cu in *spl7* mutant suggests that CCIT1 is not simply a downstream target of SPL7, and points to the existence of a more complex parallel interactive pathway than previously thought. The Y1H screen of direct upstream regulators of CCIT1 identifies AREB3, ATHB2 and bZIP53, disruption of each results in compromised CCIT1

expression. Interestingly, all of them are upregulated by Cu deficiency in *spl7* mutant but not in wild-type, suggesting a compensatory mechanism including AREB3, ATHB2, bZIP53 and CCIT1, which may participate in Cu deficiency responses when SPL7's function is lost. These findings expand the knowledge of the components involved in the transcriptional network of Cu homeostasis, further work focus on unraveling the function of these three CCIT1 regulators in response to Cu availability, JA signaling and plant fertility will facilitate a deeper understanding of this interactive transcriptional pathway.

There's growing knowledge of the interaction of essential heavy metals and toxic heavy metals. The generation of Cd free crop can be achieved by manipulating the components that function in maintaining the essential mineral nutrition while reducing Cd uptake. The work described herein identifies a novel gene, *CCIT1*, as an essential regulator that is involved in the basal Cd resistant mechanism. Knock out of *CCIT1* leads to increased sensitivity to Cd and impaired Cu accumulation which has been found to play an important role in Cd tolerance. Furthermore, the induced expression of COPT1 and COPT2 are found to be compromised in *ccit1* mutant, indicating *CCIT1* participates in the Cu-mediated basal Cd resistance *via* regulating the expression of Cu transporters. Future investigation of identifying the components that is involved in this transcriptional pathway will expand the understanding of the interaction between the essential heavy metal-Cu and the toxic heavy metal-Cd, which will ultimately provide molecular knowledge of making Cd free crops.